Western Graduate&PostdoctoralStudies

Western University
Scholarship@Western

Electronic Thesis and Dissertation Repository

4-13-2015 12:00 AM

Exploring the Structural and Functional Organization of the Dorsal Zone of Auditory Cortex in Hearing and Deafness

Melanie A. Kok
The University of Western Ontario

Supervisor
Dr. Stephen Lomber
The University of Western Ontario

Graduate Program in Neuroscience
A thesis submitted in partial fulfillment of the requirements for the degree in Doctor of Philosophy
© Melanie A. Kok 2015

Follow this and additional works at: https://ir.lib.uwo.ca/etd

Part of the Neurosciences Commons

Recommended Citation

Kok, Melanie A., "Exploring the Structural and Functional Organization of the Dorsal Zone of Auditory Cortex in Hearing and Deafness" (2015). *Electronic Thesis and Dissertation Repository*. 2735.
https://ir.lib.uwo.ca/etd/2735

This Dissertation/Thesis is brought to you for free and open access by Scholarship@Western. It has been accepted for inclusion in Electronic Thesis and Dissertation Repository by an authorized administrator of Scholarship@Western. For more information, please contact wlswadmin@uwo.ca.

EXPLORING THE STRUCTURAL AND FUNCTIONAL ORGANIZATION OF THE DORSAL ZONE OF AUDITORY CORTEX IN HEARING AND DEAFNESS

(Thesis format: Integrated Article)

by

Melanie A. Kok

Graduate Program in Neuroscience

A thesis submitted in partial fulfillment
of the requirements for the degree of
Doctor of Philosophy

The School of Graduate and Postdoctoral Studies
The University of Western Ontario
London, Ontario, Canada

© Melanie A. Kok 2015

Abstract

Recent neuroscientific research has focused on cortical plasticity, which refers to the ability of the cerebral cortex to adapt as a consequence of experience. Over the past decade, an increasing number of studies have convincingly shown that the brain can adapt to the loss or impairment of a sensory system, resulting in the expansion or heightened ability of the remaining senses. A particular region in cat auditory cortex, the dorsal zone (DZ), has been shown to mediate enhanced visual motion detection in deaf animals. The purpose of this thesis is to further our understanding of the structure and function of DZ in both hearing and deaf animals, in order to better understand how the brain compensates following insult or injury to a sensory system, with the ultimate goal of improving the utility of sensory prostheses.

First, I demonstrate that the brain connectivity profile of animals with early- and late-onset deafness is similar to that of hearing animals, but the projection strength to visual brain regions involved in motion processing increases as a consequence of deafness. Second, I specifically evaluate the functional impact of the strongest auditory connections to area DZ using reversible deactivation and electrophysiological recordings. I show that projections that ultimately originate in primary auditory cortex (A1) form much of the basis of the response of DZ neurons to auditory stimulation. Third, I show that almost half of the neurons in DZ are influenced by visual or somatosensory information. I further demonstrate that this modulation by other sensory systems can have effects that are opposite in direction during different portions of the auditory response. I also show that techniques that incorporate the responses of multiple neurons, such as multi-unit and local field potential recordings, may vastly overestimate the degree to which multisensory processing occurs in a given brain region. Finally, I confirm that individual neurons in DZ become responsive mainly to visual stimulation following deafness.

Together, these results shed light on the function and structural organization of area DZ in both hearing and deaf animals, and will contribute to the development of a comprehensive model of cross-modal plasticity.

Keywords: Hearing, deafness, multisensory, neuroplasticity, auditory cortex, electrophysiology, reversible deactivation, cat

Statement of Co-Authorship

All data collection, analysis and writing of the manuscripts that comprise this doctoral thesis dissertation were primarily conducted by the author of this thesis, Melanie Kok. Dr. Nicole Chabot assisted with experimental design and data analysis, as well as editing of the manuscript for Chapter 2. Dr. Daniel Stolzberg provided assistance with the experimental design for Chapter 3, and in addition, assisted with data collection and edited the manuscript for this chapter, along with Dr. Trecia Brown. Drs. M. Alex Meredith and Andres Carrasco assisted with the experimental design and edited the manuscript for Chapters 4 and 5. Dr. Stephen Lomber provided expert advice and supervision during all phases of this work, including experimental design and manuscript edits for all chapters.

Acknowledgements

First and foremost, I would like to thank my supervisor, Dr. Stephen Lomber, for quite simply, everything. I feel incredibly fortunate to have been able to mentor under someone who is not only a world-class scientist, but a world-class person. I truly couldn't have ended up in a better lab.

I would also like to thank the members of my advisory committee, Dr. Scott MacDougall-Shackleton and Dr. David Sherry for always providing thoughtful insight and constructive criticism throughout my graduate career.

Words can't adequately express the gratitude I feel towards all of the members of the Lomber lab, past and present (Dr. Trecia Brown, Dr. Blake Butler, Dr. Andres Carrasco, Dr. Nicole Chabot, Amee Hall, Pam Nixon, Dr. Daniel Stolzberg, and Carmen Wong). Whether providing serious scientific feedback during all aspects of every project I undertook, or sharing a laugh (by which I mean tolerantly listening to me as I spout off about something), I quite literally could not have done this without you. Special thanks to Pam Nixon for making sure that I always had healthy and happy participants for my experiments.

Finally, I would like to thank my friends and family, who have never wavered in their support for me. Special mention to my close friends and fellow (now former) doctoral students, Drs. Sara Lippa, Chrissie Monaghan, and Amanda Therrien, thanks for lending an ear anytime I needed to talk to someone who understands the rigors of grad school (and life in general). To my parents, Richard and Donna, and my siblings, Renee, Jon, Jennifer, Chad and Matthew, thank you for always being there for me on the biggest days of my life (…and all of the others in between!). To my beautiful nieces, Emily and Lauren, thank you for brightening many days. And to Chris, thank you for being so supportive, for making sure my life had some balance and for keeping me sane.

Table of contents

Abstract ii
Statement of Co-Authorship iv
Acknowledgements v
Table of contents. vi
List of Figures xi
List of Abbreviations and Symbols xiv
Chapter 1: General Introduction 1
1.1 Overview 1
1.2 The auditory system 2
1.2.1 Acquisition of auditory information by the nervous system 2
1.2.2 Interpretation of auditory information by the nervous system 3
1.3 Sensory loss and the cerebral cortex 5
1.3.1 Short-term removal of sensory input 6
1.3.2 Blindness and visual deprivation 7
1.3.3 Deafness and auditory deprivation 10
1.3.4 General principles of cross-modal plasticity 13
1.3.5 Developmental considerations 14
1.4 Thesis overview 15
1.5 References 17
Chapter 2: Cross-modal reorganization of cortical afferents to dorsal auditory cortex following early- and late-onset deafness 27
2.1 Abstract. 27
2.2 Introduction 28
2.3 Materials and Methods 30
2.3.1 Deafening Procedures 33
2.3.2 Tracer injections. 35

2.3.3 Histological processing 36
2.3.4 Areal border delimitation 37
2.3.5 Data analysis. 39
2.4 Results 40
2.4.1 Tracer deposits 40
2.4.2 Labeling of cortical afferents 42
2.4.3 Comparisons between modalities 49
2.4.4 Auditory cortical projections 51
2.4.5 Visual cortical projections 52
2.5 Discussion 53
2.5.1 Spatial processing in DZ 53
2.5.2 Localization of injection sites 53
2.5.3 Auditory cortical projections to DZ in hearing animals 54
2.5.4 Comparison to late- and early-deafened animals 55
2.5.5 Visual cortical projections to DZ in hearing animals 56
2.5.6 Comparison to late- and early-deafened animals 58
2.5.7 Other considerations 62
2.5.8 Summary and conclusions 64
2.6 References 67
Chapter 3: Dissociable influences of primary auditory cortex and the posterior auditory field on neuronal responses in the dorsal zone of auditory cortex 75
3.1 Abstract. 75
3.2 Introduction 76
3.3 Materials and Methods 78

3.3.1 Overview. 78
3.3.2 Surgical procedures 79
3.3.3 Stimulus generation and presentation. 80
3.3.4 Data acquisition. 81
3.3.5 Histological procedures 84
3.3.6 Data analysis. 85
3.4 Results 87
3.4.1 Comparison of DZ responses to A1 and AAF responses 87
3.4.2 Noise burst responses during cooling deactivation 88
3.4.3 Noise RIF responses during cortical cooling 91
3.4.4 Responses to tones during reversible deactivation 91
3.4.5 Results summary 101
3.5 Discussion 101
3.5.1 Comparison of DZ responses to previously published findings 101
3.5.2 Effects of reversible deactivation in DZ 103
3.6 References 107
Chapter 4: Diametric modulation of early and late components of acoustically-evoked activity in the dorsal zone of auditory cortex by visual and tactile stimulation 110
4.1 Abstract 110
4.2 Introduction 111
4.3 Materials and Methods 112
4.3.1 Overview 112
4.3.2 Surgical Preparation 113
4.3.3 Surgical Procedures 113

4.3.4 Preparation for recording 114
4.3.5 Stimulus generation and presentation 116
4.3.6 Data acquisition 118
4.3.7 Histological Procedures 118
4.3.8 Data Analysis 119
4.4 Results 123
4.4.1 Overview 123
4.4.2 Multisensory integration in DZ neurons 124
4.4.3 Response characteristics of single units in DZ 130
4.4.4 Timing of the visual stimulus 135
4.4.5 Comparison of SU data with MU and LFP activity 138
4.4.6 Summary of findings 141
4.5 Discussion 141
4.6 References 146
Chapter 5: Visual and somatosensory cross-modal reorganization in the dorsal zone of auditory cortex following perinatal deafness 152
5.1 Abstract 152
5.2 Introduction 153
5.3 Materials and methods 154
5.3.1 Deafening procedures 154
5.3.2 Electrophysiological recordings 156
5.3.3 Data acquisition and stimulus presentation 158
5.3.4 Histological procedures 159
5.3.5 Data analysis 159
5.4 Results 161

5.4.1 Area DZ identification. 161
5.4.2 Single unit responses 162
5.4.3 Comparison to multiunit responses and LFP activity 165
5.5 Discussion 167
5.6 References 170
Chapter 6: General Discussion 174
6.1 Main findings and conclusions 174
6.1.1 DZ receives strong projections from visual cortex in hearing animals 174
6.1.2 The strength of visual cortical projections to DZ is increased in deaf animals 174
6.1.3 DZ neurons rely on input from A1, whereas PAF may modulate DZ responses 175
6.1.4 Almost half of DZ neurons are multisensory 175
6.1.5 Population-based measures of neural activity may overestimate the degree of multisensory processing in a cortical area 176
6.1.6 DZ neurons in deaf animals respond mainly to visual stimulation 176
6.2 Conclusions 177
6.2.1 DZ may be homologous to caudal auditory fields in the primate 177
6.2.2 DZ is the most extensively-documented model of cross-modal plasticity in mammalian cortex to date 180
6.3 Future directions 181
6.4 References 182
Appendix A 187
Curriculum Vitae 188

List of Figures

Figure 2.1 The auditory and visual cortices and sub-fields of the cat. 31

Figure 2.2 Timeline of deafening and other procedures performed on each group. 32

Figure 2.3 Pre- and post-deafening auditory brainstem responses. 34

Figure 2.2.4 Cortical border delimitation. 38

Figure 2.5 BDA-labeled neurons in DZ. 41

Figure 2.6 Injection sites and labeling in a hearing animal. 42

Figure 2.7 Labeled neurons and injection sites from a late-deafened animal (L4). 44

Figure 2.8 Labeled neurons and injection sites from an early-deaf animal (E2). 45

Figure 2.9 Injection sites and neuronal labeling for a hearing animal. 46

Figure 2.10 Standardized injection sites and neuronal labeling for a late-deafened animal. 47

Figure 2.11 Injection sites and labeled neurons on std. sections. 48

Figure 2.12 Proportion of projections by cortical area. 50

Figure 2.13 Pattern of labeling within the middle suprasylvian sulcus. 59

Figure 2.14 Projections present in hearing animals and change in projection strength following late- and early-deafness. 65

Figure 3.1 Organization and hierarchical connections of cat auditory cortex. 77

Figure 3.2 Position of cryoloops and extent of cortical deactivation. 82

Figure 3.3 Population level effects of reversible deactivation on DZ responses to 65 dB noise bursts. 89

Figure 3.4 Effects of reversible deactivation during noise burst presentation on individual sites. 90

Figure 3.5 Noise Rate-intensity functions and monotonicity ratios. 92

Figure 3.6 Population level effects of reversible deactivation on DZ responses to tones. 93

Figure 3.7 Effects of reversible deactivation during tone presentations on individual sites. 95

Figure 3.8 Representative example of tuning curves recorded in fields A1, AAF and DZ. 97

Figure 3.9 Summary of changes in DZ receptive field properties as a function of reversible deactivation. 98

Figure 3.10 Summary of changes in threshold and CF at individual sites in DZ. 100

Figure 3.11 Representative example of a recording site in DZ in response to various stimuli. 102

Figure 4.1 Location of recording sites within DZ. 115

Figure 4.2 Waveforms and typical profile of single unit and multiunit activity at a representative site following auditory noise burst stimulation 120

Figure 4.3 Representative examples of rasters, PSTHs and bar graphs of single unit responses for the four classes of neurons recorded in DZ. 125

Figure 4.4 Summary of multisensory integration for individual single units. 127

Figure 4.5 Summary of multisensory integration across the population of single units. 129

Figure 4.6 Location of bimodal and integrative neurons in DZ. 131

Figure 4.7 Summary of differences in response characteristics among classes of neurons in DZ. 132

Figure 4.8 Distributions showing the enhancement and additivity indices for responses to combined-modality stimulation for each class of neuron encountered 134

Figure 4.9 Analysis of visual onset asynchronies. 136

Figure 4.10 Representative site showing neuronal responses at different scales of activity 137

Figure 4.11 Summary of results for single unit (SU), multiunit (MU) and local field potential (LFP) responses 139

Figure 5.1 Photomicrographs of the craniotomy, electrode penetrations and SMI-32 stained sections in hearing and deafened animals 155

Figure 5.2 Auditory brainstem responses (ABRs) for a hearing and a deaf animal. 157

Figure 5.3 Single unit and multiunit waveforms for a representative site in DZ following visual flash stimulation. 160

Figure 5.4 Representative examples of sensory neurons recorded in DZ of hearing and deaf animals. 163

Figure 5.5 Organization of bimodal versus unimodal neurons in DZ of deaf animals 164

Figure 5.6 Comparison of single unit, multiunit and LFP responses in DZ of hearing and deafened animals 166

List of Abbreviations and Symbols

A1	primary auditory cortex
A2	second auditory cortex
AAF	anterior auditory field
ABR	auditory brainstem response
AES	anterior ectosylvian sulcus
AEV	anterior ectosylvian visual area
ALLS	anterolateral lateral suprasylvian area
AMLS	anteromedial lateral suprasylvian area
ANOVA	analysis of variance
BDA	biotinylated dextran amine
CF	characteristic frequency
dB SPL	decibels sound pressure level
df	degrees of freedom
DLS	dorsal lateral suprasylvian area
dPE	dorsal posterior ectosylvian area of auditory cortex
DZ	dorsal zone of auditory cortex
EEG	electroencephalogram
EPp	posterior part of the posterior ectosylvian gyrus
fAES	field of the anterior ectosylvian sulcus
fMRI	functional magnetic resonance imaging
GABA	gamma-aminobutyric acid
Hz	hertz
i.m.	intramuscular
i.v.	intravenous
IN	insular cortex
iPE	intermediate posterior ectosylvian area of auditory cortex
kg	kilograms
kHz	kilohertz
L	litres
LFP	local field potential
MEG	magnetoencephelogram
mg	milligrams
MGN	medial geniculate nucleus

mm	millimeters
ms	milliseconds
MT	middle temporal area
MU	multiunit
MW	molecular weight
PAF	posterior auditory field
PLLS	posterolateral lateral suprasylvian area
PMLS	posteromedial lateral suprasylvian area
PS	posterior suprasylvian area
PSTH	peri-stimulus time histogram
R	rostral field of auditory cortex
RIF	rate-intensity function
s.c.	subcutaneous
SU	single unit
T	temporal cortex
V1	primary visual cortex (area 17)
VAF	ventral auditory field
VLS	ventral lateral suprasylvian area
VPAF	ventral posterior auditory field
vPE	ventral posterior ectosylvian area of auditory cortex
ºC	degrees Celsius
%	percent

*Note: regions of the brain denoted by a number (e.g. area 7) refer to Brodmann areas.

Chapter 1: General Introduction

1.1 Overview

Until relatively recently, it was thought that the structure of the brain was largely immutable following the closure of developmental critical periods (Gross, 2001). This was based largely on the knowledge that outside of specialized regions of the hippocampus and olfactory system, neurons do not regenerate once lost, and damage to the brain, whether degenerative or traumatic, is for the most part, irreversible. However, multiple avenues of research over the last quarter-century have demonstrated that the brain adapts to environmental input throughout life, and that its connectivity can be both structurally and functionally altered as a consequence of experience. This phenomenon is referred to as plasticity.

While much research on cortical plasticity has focused on normal adaptation to environmental input (e.g. development and maturation, learning), a growing body of research is focused on understanding the conditions under which the cerebrum is capable of rewiring itself following the loss or impairment of a sensory system. This rewiring is a compensatory mechanism that has been shown to take place across sensory modalities, and is therefore referred to as cross-modal plasticity. It is generally understood that this process not only helps to compensate for the lost sensory modality, but additionally results in enhanced behavioral performance in the remaining sensory modalities. This plasticity has important consequences for the use of sensory prostheses (i.e. cochlear implants), as it is thought that cross-modal reorganization may limit the reintroduction of missing sensory information by colonizing the deprived region of cortex for the processing of other sensory functions (Lee et al., 2001).

As such, a complete framework for understanding how and why the brain is able to reorganize following sensory loss must include both an understanding of how the brain functions in basic sensory perception, as well as

characterization of the changes that occur under conditions of sensory loss or impairment. Because the body of work that comprises this thesis was conducted in auditory cortex, I first review what is known about the sense of hearing and how sound is processed by the auditory system. I then go on to discuss the consequences of the removal of sensory input on sensory systems in the brain.

1.2 The auditory system

1.2.1 Acquisition of auditory information by the nervous system

The basic mechanisms underlying how the nervous system acquires auditory information from the environment are relatively well known at this point. Sound waves in the environment are detected as mechanical pressure by the tympanic membrane or eardrum, and these vibrations are passed along by middle ear structures to the cochlea. The cochlea is a specialized structure within the inner ear containing the basilar membrane, whose properties change as a function of length. Because of this, the basilar membrane responds differently based on the spectral information of the incoming sound wave. Sounds of high frequency do not propagate far along the basilar membrane, reaching a peak displacement at the base, while sounds of low frequency travel further along the membrane and reach a peak displacement at the apex. Sounds of intermediate frequency are represented orderly and continuously along the length of the basilar membrane on a logarithmic scale. The local movement of the basilar membrane is converted to electrical impulses by specialized sensory hair cells, which synapse with auditory nerve fibers. In this way, hair cells and auditory nerve fibers from a particular location along the basilar membrane fire in response to sound of a particular frequency. This position-based spectral organization is referred to as a tonotopic map, and the place theory states that it is this tonotopic organization of the basilar membrane that gives rise to pitch perception. Sound intensity is also coded by the firing rate of auditory nerve fibers, i.e. maximal displacement of the basilar membrane is represented by a saturated neuronal response. Thus, the frequency of the incoming sound is represented by *which* auditory nerve fibers are activated, while the intensity is

represented by the *firing rate* of those fibers. This information is then propagated along the auditory pathway to the brainstem (cochlear nuclei and superior olivary nuclei), then to the midbrain (nuclei of the lateral lemniscus and inferior colliculus), to the thalamus (medial geniculate nucleus; MGN) and finally, to auditory cortex. It should be noted that the tonotopic map previously discussed is preserved throughout these subcortical stations and in some regions of auditory cortex.

1.2.2 Interpretation of auditory information by the nervous system

Unlike the visual system, acoustical information is processed in parallel at the subcortical level, and significant auditory processing occurs before information reaches primary auditory cortex (A1). Specifically, while the spectral content of incoming sound is represented in the auditory system, the location of it is not, and must be reconstructed in order to decipher the source of the sound in space. This reconstruction is done in the superior olivary nuclei by comparing the input arriving from each ear. Neurons in the medial superior olive code for the difference in sound arrival time at each ear, referred to as the interaural time difference. Neurons in the lateral superior olive code for the difference in sound intensity arriving at each ear, or the interaural level difference.

Beyond the level of the superior olivary nuclei, specific functional designations for structures in the auditory pathway are less clear-cut. For example, a portion of the inferior colliculus receives both auditory and somatosensory inputs, and a putative role in sound localization has also been suggested based on the high numbers of neurons sensitive to interaural timing and level differences. It should be noted that there is no homolog of the inferior colliculus in any of the other sensory systems (Winer et al., 2005). At the level of the thalamus, clear structural and functional differences exist between the ventral, dorsal and medial subregions of MGN (Banks and Smith, 2011) and the current opinion is that auditory thalamus is not a simple relay station, but rather provides important modification of incoming information based on the state of the organism (Winer et al., 2005).

The ascending auditory pathway terminates in auditory cortex, which consists of central core areas, surrounded by belt and para-belt regions in mammals. The core includes A1, which is a cytoarchitectonically distinct region that is tonotopically organized and has been described in detail in many species. Core auditory cortical fields share a number of characteristics. Core fields receive strong projections from ventral MGN (Kaas et al., 1999), are densely interconnected with one another, are characterized by robust, short latency responses to pure tones with sharp frequency tuning curves, and function in parallel with one another (i.e. lesions of one core region do not abolish responses to pure tones in the remaining core regions). Core regions outside of A1 include the rostral (R) and rostrotemporal fields in the primate and the anterior auditory field (AAF) in the cat, ferret, gerbil, and rat (Hackett, 2011).

The core is surrounded by several other regions, which vary in number based on the species under study, as well as in terms of the response properties of the neurons located there. Some of these fields maintain tonotopic organization while others do not. These fields may also show response specificity for more complex sounds compared to pure tones (such as conspecific vocalizations or the rate or direction of frequency-modulated sweeps), or may display more complex receptive field tuning. While significant subcortical processing of interaural timing and level differences is known to occur, sound localization behavior is dependent on an intact auditory cortex, as ablation and reversible deactivation studies have conclusively demonstrated. From these studies, a number of non-primary fields have been identified as playing a role in the spatial processing of sound in the cat, namely, the dorsal zone (DZ), the auditory field of the anterior ectosylvian sulcus (fAES), the posterior auditory field (PAF). Similarly, caudal fields in the monkey also show more spatial sensitivity than do rostral fields.

In conjuction with these findings, as well as emerging structural and functional investigations from multiple species, a dual-stream model of auditory processing has been proposed, involving parallel streams for the identification of

auditory objects and the guidance of movement in space, namely the ‘what’ and ‘where’ pathways, similar to those that exist in the visual system (Romanski et al., 1999; Rauschecker and Tian, 2000; Lomber and Malhotra, 2008). Hierarchical models of auditory cortical processing incorporating these features, in conjuction with known connectivity have been introduced for both the primate and the cat.

Overall, the neuroanatomy and connectivity of auditory cortical and subcortical structures have been fairly well-documented in a number of species (de la Mothe et al., 2006 a, b; Lee and Winer, 2008 a, b). However, our understanding of the organization of function in auditory cortex seems comparatively lacking, especially when compared to the serial, hierarchical organization of the visual system, in which visual features of increasing complexity are processed in an orderly fashion. While the basic perceptual features of sound (i.e. loudness, pitch, duration, timbre) have been investigated in auditory cortex, no one region has been identified as being specialized for the processing of that particular function to the exclusivity of other regions. Rather, representations of auditory features appear to be distributed across auditory cortex, and many of these features are present in subcortical regions as well. From these observations, it seems clear that although many parallels can be drawn between the processing of auditory and visual information, important differences also exist.

1.3 Sensory loss and the cerebral cortex

Neuroscientists have long used loss-of-function techniques in order to evaluate which structures in the brain are responsible for the mediation of particular behaviors or functions. For more than a century, researchers have evaluated case studies of individuals who had either had naturally occurring lesions of the brain (e.g. due to stroke) or experimentally induced permanent damage to the brain via the ablation or aspiration of tissue in animal models. More recently, methodological advancements have paved the way for the short-

term, reversible removal of input using pharmacological or cryogenic reversible deactivation. With respect to sensory loss, both short-term deactivation, as well as investigations of long-term removal of sensory input (i.e. blindness, deafness), have been used to probe sensory function in the brain. Because investigations of sensory removal in the somatosensory system have largely resulted in changes in local cortical maps, but not cross-modal plasticity (Merzenich et al., 1984; Chen et al., 2002), I focus my review on the effects of sensory loss on the auditory and visual systems.

1.3.1 Short-term removal of sensory input

Short-term sensory deprivation has been a method of choice for investigations of local plasticity and assessment of function within sensory systems for decades. In fact, investigations of the effects of early visual deprivation on cat visual cortex (Wiesel and Hubel 1963, 1965 a, b) were critical in establishing a role for experience in the development of sensory systems and directly shaped our understanding of critical periods for sensory input (Hubel and Wiesel 1970). There are a number of advantages associated with reversible deactivation of sensory areas, including the use of within-subject comparisons and the ability to experimentally control regions of deactivation with a high degree of precision (Lomber, 1999). Reversible deactivation techniques have directly led to the localization of functions to regions of visual cortex (e.g. Girard et al., 2002), assessments of the role played by feedback connections to visual cortical regions (e.g. Bullier et al, 2001), and functional evaluation of visual cortical hierarchical organization (e.g. Girard et al., 1991). Similarly, pharmacological (e.g. Nodal et al., 2012) and cryogenic (e.g. Lomber and Malhotra, 2008) deactivation of specific regions in auditory cortex have been shown to impair localization behavior in ferrets and cats, and have allowed for direct assessment of the dependence of higher-order fields of auditory cortex on core fields (e.g. Carrasco and Lomber, 2009). Hierarchical assessments of somatosensory regions of the brain have also been evaluated using reversible deactivation (Zhang et al., 2001).

1.3.2 Blindness and visual deprivation

The first neuronal evidence of cross-modal compensation following visual deprivation was shown in the superior colliculus, a multimodal midbrain structure that contains spatial maps of auditory, tactile, and visual space in register with one another. These studies showed a decrease in the number of visually responsive neurons, with a corresponding increase in auditory- and somatosensory-responsive neurons in dark-reared rats (Vidyasagar 1978) and binocularly deprived cats (Rauschecker and Harris, 1983). Similar reorganization was shown in area 7 of parietal cortex in binocularly deprived monkeys (Hyvarinen 1981). More recently, a series of behavioral and electrophysiological investigations showed auditory and somatosensory reorganization of a normally visually-responsive region in the multimodal anterior ectosylvian area (AES) of binocularly deprived cats (Rauschecker and Korte, 1993). These animals also showed concomitant improvements in auditory localization behavior (Rauschecker and Kniepert, 1994) and auditory spatial tuning of neurons in that area (Korte and Rauschecker, 1993). Together, these observations provide cellular evidence of cross-modal reorganization in polymodal areas that are part of the same cerebral network responsible for multimodal processing in non-deprived animals.

But what happens to the brain regions that are primarily involved in processing the missing sense? Do these regions of the brain effectively lie dormant or are they reorganized for some other purpose? While anecdotal reports of enhanced sensory abilities in blind individuals have been circulating for more than a century, only recently has concrete behavioral evidence attesting to this arisen. Blind subjects have been shown to outperform sighted individuals on selected tactile discrimination tasks (Stevens et al. 1996; Van Boven et al. 2000; Goldreich and Kanics 2003; Alary et al. 2008, 2009; Legge et al. 2008; Wong et al. 2011), as well as auditory spatial (Lessard 1998; Röder et al. 1999; Voss et al. 2004) and pitch discrimination tasks (Gougoux et al. 2004; Wan et al., 2010). These findings have even been extended to the chemical senses (Cuevas et al.,

2009), suggesting that these compensatory behaviors are not restricted to auditory and tactile functions.

However, this raises the question of whether these enhanced abilities are mediated by supra-normal processing within the auditory and somatosensory cortices themselves, or potentially in polymodal or other cortical regions. Early investigations showed corresponding changes in somatosensory (Pascual-Leone and Torres 1993, Sterr et al., 1998 a,b) and auditory (Elbert et al., 2002, Stevens and Weaver, 2009) cortices in the blind, but also showed evidence of posterior activation in blind subjects performing sound localization (Kujala et al., 1992) and discrimination (Alho et al, 1993) tasks, suggesting that regions of the brain involved in visual processing in sighted individuals may be recruited for the processing of stimuli from other sensory modalities. Since then, a host of functional imaging studies has confirmed the latter (Sadato et al., 1996, 1998; Büchel et al., 1998; Weeks et al., 2000; Burton et al, 2002, 2004; Gougoux et al., 2005; Ptito et al., 2005; Poirier et al., 2006; Voss et al., 2008), and further evidence has shown that transcranial magnetic stimulation-induced disruptions to occipital cortex interfere with Braille reading in blind individuals (Cohen et al., 1997; Hamilton and Pascual-Leone, 1998; Kupers et al., 2007), directly demonstrating a functional role for occipital cortex in the performance of compensatory behaviors in the blind. While a range of visual cortical areas were activated in these studies, it is important to note that many of these investigations demonstrated V1 activation in congenitally or early-blind individuals.

Electrophysiological investigations in animal models largely corroborate these findings. Auditory evoked potentials have been found in visual cortex of mice lacking photoreceptors (Bonaventure and Karli, 1968), bilaterally enucleated hamsters (Izraeli et al., 2002), and dark-reared cats (Sanchez-Vives et al., 2006). Multiunit responses during active tactile object manipulation have been observed in area 19 of monkeys following one year of binocular deprivation (Hyvarinen et al., 1981). Auditory, but not somatosensory, single unit responses have been observed in the visual cortex of bilaterally enucleated hamsters

(Izraeli et al., 2002). An increase in the number of neurons responding to auditory stimulation was found in the anterior lateral suprasylvian areas of both binocularly deprived and enucleated cats compared to hearing controls (Yaka et al., 1999). Primary visual cortex (V1) itself has been shown to respond to auditory and somatosensory stimuli in bilaterally enucleated mice and opossums (Kahn and Krubitzer, 2002; Karlen et al., 2006), and to auditory stimulation in binocularly enucleated (Yaka et al., 2000) and dark-reared cats (Sanchez-Vivez et al., 2006). Finally, auditory responses in visual cortex (Heil et al., 1991), including V1 (Bronchti et al, 1992), have been observed in the congenitally blind mole rat, although it should be noted that drawing meaningful conclusions from these two studies is constrained by the lack of an appropriate sighted control, as was present in all of the previously cited studies.

Interestingly, despite the plethora of electrophysiological, behavioral and functional imaging evidence of cross-modal plasticity following blindness or visual deprivation, the anatomical substrates of these plastic changes have remained largely uninvestigated. While a number of conflicting volumetric, metabolic, and morphological changes in visual cortex of blind humans have been reported (reviewed in Noppeney, 2007), only one study has evaluated changes in connectivity of the blind human brain using dynamic causal modeling, which suggested that cortico-cortical multimodal feedback projections may constitute the main input to blind V1 (Fujii et al., 2009). In animal models of blindness, projections from auditory, somatosensory, and multimodal regions of thalamus and cortex are present in visual cortex of the bilaterally enucleated opossum, but not in sighted controls (Karlen et al., 2006). Two separate studies in the congenitally blind mole rat (Doron and Wollberg, 1994) and the binocularly enucleated hamster (Izraeli et al., 2002) have found no evidence of cortico-cortical connectional changes, but have documented novel inferior colliculus projections to visual thalamus.

It has been suggested that regions of the brain that are known to receive input from more than one sensory modality may be the most likely to undergo

cross-modal reorganization following the loss of one sense (Rauschecker and Korte, 1993). For this reason, anatomical and electrophysiological studies of multisensory processing in non-deprived animals also provide information pertinent to the investigation of the mechanisms underlying cross-modal plasticity. Consistent with this hypothesis, a growing number of studies have shown that even primary sensory areas receive multimodal projections – V1 receives direct projections from auditory cortex in the primate (e.g. Falchier et al., 2002), cat (e.g. Hall and Lomber, 2008), prairie vole (e.g. Campi et al., 2010), rat (e.g. Miller and Vogt, 1984) and mouse (e.g. Charbonneau et al., 2012). Although electrophysiological investigations of multisensory processing in visual cortex are generally lacking, modulation of visually responsive neurons by auditory stimulation has been demonstrated in cat extrastriate cortex (Allman and Meredith, 2007).

While important progress has been made by studying visual deprivation, some important caveats should be noted. For example, in many of the imaging studies cited above, a range of visual cortical areas are activated in blind compared to sighted individuals. Additionally, there are two problems with the two most commonly studied animal models of visual deprivation. First, binocular deprivation is accomplished by suturing the eyelids shut, which still allows for some light penetration through the eyelids, resulting in an incomplete impairment. Second, while binocular enucleation ensures that the animal receives no light exposure, the enucleation itself is traumatic, resulting in widespread atrophy of the retinocortical pathway, including complete degeneration of the optic nerve and optic chiasm (e.g. Yaka et al., 1999). This trauma could have unintended consequences for spontaneous activity in visual cortex, which may affect subsequent reorganization, and which may not be generalizable to congenital blindness in humans.

1.3.3 Deafness and auditory deprivation

In comparison to the fairly extensive documentation of enhanced auditory and tactile abilities in the blind, the corollary in the deaf has been less well

documented. Like blind individuals, the early deaf have shown enhanced tactile sensitivity (Levanen and Hamdorf, 2001), and deaf individuals have been shown to respond faster and more accurately to visual motion than hearing controls (Hauthal et al., 2013). Converging evidence from a number of studies has also suggested enhanced peripheral visual processing in deaf individuals (reviewed in Bavelier et al., 2006).

As with cross-modal visual cortical activation in the blind, the activation of hearing-related areas of the brain by other sensory modalities has been documented in the deaf. Activation of deaf auditory cortex has been shown in response to vibrotactile (Levanen et al., 1998; Auer et al., 2007), and visual (Finney et al., 2001, 2003) stimulation. Sign language has also been shown to activate auditory cortex (Nishimura et al., 1999; Lambertz et al., 2005), as well as speech-related areas (Petitto et al., 2000) of deaf individuals. Visual motion stimuli also evoke responses in the auditory cortex of deaf signers, whereas hearing signers or non-signers do not show auditory cortical activation (Fine et al., 2005), suggesting that this cross-modal activation is not the consequence of sign language use.

Electrophysiological evidence of cross-modal reorganization following deafness has also been documented in the animal literature. With respect to A1 itself, there are conflicting reports. An early study by Rebillard and colleagues (1977) showed visually-evoked activity in A1 of congenitally deaf and cochleotomized cats. However, more recent studies have found no visually-evoked potentials or spiking activity in A1 of congenitally deaf cats (Kral et al., 2003), while core auditory areas A1 and AAF in the congenitally deaf mouse showed both visual and tactile responses (Hunt et al., 2006). This finding has been confirmed for AAF of early-deafened cats (Meredith et al., 2011), while late-deafened ferrets or animals with early hearing impairment only show tactile reorganization of A1 and AAF (Allman and Meredith, 2009; Meredith and Allman, 2012). Beyond core auditory cortex, only one non-primary region of auditory cortex has been electrophysiologically investigated for cross-modal

reorganization: fAES becomes responsive mainly to visual stimulation in early deaf animals, but also responds extensively to tactile and bimodal visual-tactile stimulation (Meredith et al., 2011).

Importantly, the neural loci of enhanced visual motion detection and peripheral localization abilities in deaf cats have recently been determined. Reversible deactivation of auditory cortical area DZ abolishes enhanced visual motion detection behavior, whereas deactivation of PAF abolishes enhanced peripheral localization behavior (Lomber et al., 2010). Similarly, deficits in contralateral visual orienting behavior were shown when fAES was reversibly deactivated, confirming a functional role for the visual reorganization previously mentioned (Meredith et al., 2011). As all three of these areas are involved in auditory spatial localization, these findings suggest that original function of these reorganized cortical areas may be maintained following sensory deprivation, even though the sensory modality that mediates the function has changed. As such, the spatially-related functionality of these areas appears to be supramodal – although the sensory modality of the input changes, these areas remain dedicated to the spatial processing of environmental stimuli.

As with visual deprivation, structural investigations of the changes in auditory cortical connectivity that subserve these plastic changes are lacking. Ferrets deafened late in life showed no evidence of structural changes in connectivity that could account for the tactile cross-modal changes that were electrophysiologically observed (Allman and Meredith, 2009). Similarly, evidence of weak novel projections to DZ in deaf animals from visual areas 19 and 20, as well as from somatosensory area IV (Barone et al., 2013) are unlikely to account for the enhanced visual motion detection mentioned above (Lomber et al., 2010). Novel projections from the retina to regions of auditory thalamus and the superior colliculus have been documented in congenitally deaf mice (Hunt et al., 2005), however, whether these findings are generalizable to other phylogenetically higher mammals remains to be determined.

Multisensory processing in auditory cortex of animal models has been better documented than it has in visual cortex. Evidence of auditory-somatosensory and auditory-visual processing have been demonstrated in the primate using functional imaging, multiunit and field potential activity (Schroeder et al., 2001; Schroeder and Foxe, 2002; Kayser et al., 2007; Lakatos et al., 2007). Single unit studies have shown auditory-visual integration in both primary and higher-order regions of ferret (Bizley et al., 2007; Bizley and King, 2008, 2009) and macaque (Kayser et al., 2008) auditory cortex, as well as overt somatosensory responses in non-primary regions of macaque auditory cortex (Fu et al., 2003).

1.3.4 General principles of cross-modal plasticity

As with comparisons between the processing of visual and auditory information in the brain, similarities and differences between cross-modal reorganization in visually- and auditory-deprived cortices exist. Taken together, similarities between these studies can hint at generalized principles of cross-modal plasticity in cerebral cortex. For example, both deaf and blind individuals show enhanced abilities for the performance of specific sensory tasks, suggesting that the brain develops compensatory mechanisms following the loss of a sense. These enhanced abilities do not appear to be related to superior perception, since sensory thresholds are not altered in deaf individuals (reviewed in Bavelier et al., 2006). In both the blind and deaf, as well as in humans and animals, the deprived sensory cortices are recruited by the remaining senses, and furthermore, the deprived region may maintain its characteristic functional specialization following deprivation (reviewed in Dormal and Collignon, 2011).

Evidence of multisensory processing in higher-order regions of cortex that have traditionally been considered unimodal is mounting for auditory and visual cortices alike (e.g. see review of Macaluso, 2006). Furthermore, evidence of extra-modal responses is being documented at increasingly earlier stages of sensory processing in unimodal areas, even as early as primary fields (e.g. see review of Ghazanfar and Schroeder, 2006). These findings suggest a substrate

for cross-modal influences to build on in the absence of a sense, and represent an important gap in understanding how unimodal areas reorganize following sensory deprivation (reviewed in Bavelier and Neville, 2002).

Despite these similarities, some notable differences between auditory and visual cross-modal reorganization exist. For example, in the blind, converging evidence from functional imaging, electrophysiological, and anatomical evidence suggests that V1 itself becomes reorganized. However, conflicting reports exist for A1, which has led to the proposal of a model in which auditory deprivation leads to deficits in the interaction of primary with higher-order cortical areas (Kral, 2007). If A1 truly does not reorganize following deafness, this would represent a fundamental difference between reorganization in the visual and auditory systems. Some of the differences in cross-modal plasticity among and between the studies of blind and deaf individuals above could be due to heterogeneity in the etiology of the deficit (Bavelier et al., 2006), and furthermore, some of the enhanced abilities documented may not be generalizable to blindness or deafness of differing etiology (Merabet and Pascual-Leone, 2010).

1.3.5 Developmental considerations

It is well-known that the visual, auditory, and somatosensory systems of mammals undergo a critical period during which typical development and maturation of the system is dependent on specific inputs received during that time window (Hensch, 2004). It is also known that functional recovery following cochlear implant in humans is affected by the length of time that lapses between the onset of hearing loss and implantation (Lee et al., 2003; Doucet et al., 2006), as well as the age of the individual at implantation (Lee et al., 2001; Harrison et al., 2005; Sharma et al., 2005). It has been suggested that the degree to which cross-modal reorganization has occurred may account for these effects, as the cortical real estate devoted to processing information from the remaining sensory modalities may limit the adaptation needed to occur following the reintroduction of auditory information (Lee et al., 2001).

While it is generally accepted that sensory deprivation that occurs early in life leads to task-specific cross-modal compensations (Kujala et al., 2000), whether such changes occur following damage to mature sensory systems remains under debate. To this end, a number of studies in humans have sought to evaluate the differences following sensory deprivation early versus later in life with ambiguous results. Some studies have reported no evidence of cross-modal plasticity in cases of late sensory deprivation (Cohen et al., 1999), while others have reported similar changes after late sensory deprivation to that observed following early (Kujala et al., 1997), and still others have reported cases of late sensory deprivation that differ from both early-deprived and control participants (Büchel et al., 1998). A number of studies in animal models support these findings, and have shown that reorganization following damage to mature sensory systems can occur (Rebillard et al., 1977; Shepherd et al., 1999; Allman et al., 2009; Park et al., 2010).

1.4 Thesis overview

This thesis aims to shed light on the structural and functional properties of DZ of cat auditory cortex in hearing and deafness. Chapters 2 through 5 chronologically outline the research questions and experiments undertaken in order to accomplish this goal.

- First, in Chapter 2, I evaluate the structural changes that occur following long-term removal of auditory input at two different stages of development. In order to achieve this, a neuronal retrograde tracer was injected into DZ of hearing, early-, and late-deafened animals, and the cortical connectivity patterns within and outside of auditory cortex were examined. Specifically, because a role in visual motion processing has been identified for DZ in congenitally deaf animals (Lomber et al., 2010), I hypothesized that changes in connectivity with cortical visual areas might be found in early-deaf animals.
- Second, I evaluate the role of DZ within the auditory cortical hierarchy in Chapter 3 by removing auditory input from A1 and PAF separately and in

combination, using reversible deactivation in combination with multiunit electrophysiology. The consequences of the short term removal of input from these areas on neuronal firing patterns in DZ are reported. As mentioned above, a major distinguishing feature of the ascending auditory pathway is the amount of parallel versus serial processing that occurs, especially in comparison to the visual pathway. Because of this, I did not expect abolition of auditory responses in DZ following cooling of either A1 or PAF; however, because it is thought that information in auditory cortex arrives first to auditory cortical areas, and is subsequently disseminated to surrounding belt and para-belt regions, and because of the strong tonotopic organization in A1, I expected reduced responses to pure tonal stimuli in DZ as a consequence of A1 deactivation.

- Third, I assess multisensory processing in DZ of hearing animals in Chapter 4, using electrophysiological recording techniques. I describe how auditory responses are modulated by the presence of visual and somatosensory stimulation, and I compare single unit, multiunit and local field potential measures of multisensory processing. Because Chapter 2 showed strong visual projections from adjacent extrastriate visual areas to DZ in hearing animals, I expected that visual stimulation might influence auditory cortical responses.
- Finally, in Chapter 5, I investigate cross-modal reorganization at the neuronal level in DZ of early-deafened animals. I compare these findings at multiple scales of activity to sensory responses in hearing animals. Again, since DZ of deaf animals has been shown to mediate enhanced visual motion processing abilities (Lomber et al., 2010), I expected that this would be reflected at the neuronal level in deaf animals – DZ neurons would have to respond to visual stimuli in order to mediate this behavioral advantage. However, because DZ is not known to receive strong projections from any region involved in tactile processing, I did not expect that DZ neurons would respond to somatosensory stimulation in deaf animals.

Together, these findings are expected to significantly advance our understanding of the structural and functional organization in area DZ of the cat. In particular, these advances may lead to the establishment of a homology between DZ and auditory cortical regions in other species, and will further provide a comprehensive description of cross-modal plasticity in a higher-order region of mammalian cortex.

1.5 References

Alary F, Duquette M, Goldstein R, Chapman CE, Voss P, La Buissonnière-Ariza V, Lepore F (2009) Tactile acuity in the blind: a closer look reveals superiority over the sighted in some but not all cutaneous tasks. Neuropsychologia 47:2037-2043.

Alary F, Goldstein R, Duquette M, Chapman CE, Voss P, Lepore F (2008) Tactile acuity in the blind: a psychophysical study using a two-dimensional angle discrimination task. Exp Brain Res 187:587-594.

Alho K, Kujala T, Paavilainen P, Summala H, Näätänen R (1993) Auditory processing in visual brain areas of the early blind: evidence from event-related potentials. Electroen Clin Neuro 86:418-427.

Allman BL, Meredith MA (2007) Multisensory processing in “unimodal” neurons: cross-modal subthreshold auditory effects in cat extrastriate visual cortex. J Neurophysiol 98:545-549.

Auer Jr. ET, Bernstein LE, Sungkarat W, Singh M (2007) Vibrotactile activation of the auditory cortices in deaf versus hearing adults. Neuroreport 18:645-648.

Banks MI, Smith PH (2011) Thalamocortical relations. In JA Winer & CE Schreiner (eds.), The Auditory Cortex (pp. 75-97). New York, NY: Springer.

Bavelier D, Dye MW, Hauser PC (2006) Do deaf individuals see better? Trends Cogn Sci 10:512-518.

Bavelier D, Neville HJ (2002) Cross-modal plasticity: where and how? Nat Rev Neurosci 3:443-452.

Bizley JK, King AJ (2008) Visual–auditory spatial processing in auditory cortical neurons. Brain Res 1242:24-36.

Bizley, JK, King AJ (2009) Visual influences on ferret auditory cortex. Hear Res 258:55-63.

Bizley, JK, Nodal FR, Bajo VM, Nelken I, King AJ (2007) Physiological and anatomical evidence for multisensory interactions in auditory cortex. Cereb cortex 17:2172-2189.

Büchel C, Price C, Frackowiak RS, Friston K (1998) Different activation patterns in the visual cortex of late and congenitally blind subjects. Brain 121:409-419.

Bullier J, Hupé JM, James AC, Girard P (2001) The role of feedback connections in shaping the responses of visual cortical neurons. Prog Brain Res 134:193-204.

Burton H, Snyder AZ, Conturo TE, Akbudak E, Ollinger JM, Raichle ME (2002) Adaptive changes in early and late blind: a fMRI study of Braille reading. J Neurophysiol 87:589-607.

Burton H, Sinclair RJ, McLaren DG (2004) Cortical activity to vibrotactile stimulation: an fMRI study in blind and sighted individuals. Hum Brain Mapp 23:210-228.

Campi KL, Bales KL, Grunewald R, Krubitzer L (2010) Connections of auditory and visual cortex in the prairie vole (Microtus ochrogaster): evidence for multisensory processing in primary sensory areas. Cereb Cortex 20:89-108.

Carrasco A, Lomber SG (2009) Evidence for hierarchical processing in cat auditory cortex: nonreciprocal influence of primary auditory cortex on the posterior auditory field. J Neurosci 29:14323-14333.

Charbonneau V, Laramée ME, Boucher V, Bronchti G, Boire D (2012) Cortical and subcortical projections to primary visual cortex in anophthalmic, enucleated and sighted mice. Eur J Neurosci 36:2949-2963.

Chen R, Cohen LG, Hallett M (2002) Nervous system reorganization following injury. Neuroscience 111:761-773.

Cohen LG, Celnik P, Pascual-Leone A, Corwell B, Faiz L, Dambrosia J, Honda M, Sadato N, Gerloff C, Catala MD, Hallett M (1997) Functional relevance of cross-modal plasticity in blind humans. Nature 389:180-183.

Cuevas I, Plaza P, Rombaux P, De Volder AG, Renier L (2009) Odour discrimination and identification are improved in early blindness. Neuropsychologia 47:3079-3083.

de la Mothe LA, Blumell S, Kajikawa Y, Hackett TA (2006) Cortical connections of the auditory cortex in marmoset monkeys: core and medial belt regions. J Comp Neurol 496:27-71.

de la Mothe LA, Blumell S, Kajikawa Y, Hackett TA (2006) Thalamic connections of the auditory cortex in marmoset monkeys: core and medial belt regions. J Comp Neurol 496:72-96.

Dormal G, Collignon O (2011) Functional selectivity in sensory-deprived cortices. J Neurophysiol 105:2627-2630.

Doron N, Wollberg Z (1994) Cross-modal neuroplasticity in the blind mole rat Spalax ehrenbergi: a WGA-HRP tracing study. Neuroreport 5:2697-2702.

Doucet ME, Bergeron F, Lassonde M, Ferron P, Lepore F (2006) Cross-modal reorganization and speech perception in cochlear implant users. Brain 129:3376-3383.

Elbert T, Sterr A, Rockstroh B, Pantev C, Müller MM, Taub E (2002) Expansion of the tonotopic area in the auditory cortex of the blind. J Neurosci 22:9941-9944.

Falchier A, Clavagnier S, Barone P, Kennedy H (2002) Anatomical evidence of multimodal integration in primate striate cortex. J Neurosci 22:5749-5759.

Fine I, Finney EM, Boynton GM, Dobkins KR (2005) Comparing the effects of auditory deprivation and sign language within the auditory and visual cortex. J Cogn Neurosci 17:1621-1637.

Finney EM, Clementz BA, Hickok G, Dobkins KR (2003) Visual stimuli activate auditory cortex in deaf subjects: evidence from MEG. Neuroreport 14:1425-1427.

Finney E M, Fine I, Dobkins K R (2001) Visual stimuli activate auditory cortex in the deaf. Nat Neurosci 4:1171-1173.

Fu K, MG, Johnston TA, Shah, AS, Arnold L, Smiley J, Hackett TA, Garraghty PE, Schroeder CE (2003) Auditory cortical neurons respond to somatosensory stimulation. J Neurosci 23:7510-7515.

Fujii T, Tanabe HC, Kochiyama T, Sadato N (2009) An investigation of cross-modal plasticity of effective connectivity in the blind by dynamic causal modeling of functional MRI data. Neurosci Res 65:175-186.

Ghazanfar AA, Schroeder CE (2006) Is neocortex essentially multisensory? Trends Cogn Sci 10:278-285.

Girard P, Lomber SG, Bullier J (2002) Shape discrimination deficits during reversible deactivation of area V4 in the macaque monkey. Cereb Cortex 12:1146-1156.shep

Girard P, Salin PA, Bullier J (1991) Visual activity in macaque area V4 depends on area 17 input. Neuroreport 2:81-84.

Goldreich D, Kanics I M (2003) Tactile acuity is enhanced in blindness. J Neurosci 23:3439-3445.

Gougoux F, Lepore F, Lassonde M, Voss P, Zatorre R J, Belin P (2004) Neuropsychology: pitch discrimination in the early blind. Nature 430:309-309.

Gougoux F, Zatorre RJ, Lassonde M, Voss P, Lepore F (2005) A functional neuroimaging study of sound localization: visual cortex activity predicts performance in early-blind individuals. PLOS Biol 3:e27.

Gross C (2000) Neurogenesis in the adult brain: death of a dogma. Nat Rev Neurosci 1:67-73.

Hackett T (2011) Information flow in the auditory cortical network. Hear Res 271:133-146.

Hall AJ, Lomber SG (2008) Auditory cortex projections target the peripheral field representation of primary visual cortex. Exp Brain Res 190:413-430.

Hamilton RH, Pascual-Leone A (1998) Cortical plasticity associated with Braille learning. Trends Cogn Sci 2:168-174.

Harrison RV, Gordon KA, Mount RJ (2005) Is there a critical period for cochlear implantation in congenitally deaf children? Analyses of hearing and speech perception performance after implantation. Dev Psychobiol 46:252-261.

Hauthal N, Sandmann P, Debener S, Thorne J D (2013) Visual movement perception in deaf and hearing individuals. Adv Cogn Psychol 9:53-61.

Hensch TK (2004) Critical period regulation. Annu Rev Neurosci 27:549-579.

Hubel DH, Wiesel TN (1970) The period of susceptibility to the physiological effects of unilateral eye closure in kittens. J Physiol 206:419-436.

Hunt DL, King B, Kahn DM, Yamoah EN, Shull GE, Krubitzer L (2005) Aberrant retinal projections in congenitally deaf mice: how are phenotypic characteristics specified in development and evolution? Anat Rec Part A 287:1051-1066.

Hunt D L, Yamoah E N, Krubitzer L (2006) Multisensory plasticity in congenitally deaf mice: how are cortical areas functionally specified? Neurosci 139:1507-1524.

Hyvärinen J, Carlson S, Hyvärinen L (1981) Early visual deprivation alters modality of neuronal responses in area 19 of monkey cortex. Neurosci Lett 26:239-243.

Hyvärinen L, Linnankoski I (1981) Modification of parietal association cortex and functional blindness after binocular deprivation in young monkeys. Exp Brain Res 42:1-8.

Izraeli R, Koay G, Lamish M, Heicklen-Klein AJ, Heffner HE, Heffner RS, Wollberg Z (2002) Cross-modal neuroplasticity in neonatally enucleated hamsters: structure, electrophysiology and behaviour. Eur J Neurosci 15:693-712.

Kaas JH, Hackett TA, Tramo MJ (1999) Auditory processing in primate cerebral cortex. Curr Opin Neurobiol 9:164-170.

Kahn D M, Krubitzer L (2002) Massive cross-modal cortical plasticity and the emergence of a new cortical area in developmentally blind mammals. PNAS 99:11429-11434.

Karlen S J, Kahn D M, Krubitzer L (2006) Early blindness results in abnormal corticocortical and thalamocortical connections. Neurosci 142:843-858.

Kayser C, Petkov CI, Augath M, Logothetis NK (2007) Functional imaging reveals visual modulation of specific fields in auditory cortex. J Neurosci 27:1824-1835.

Kayser C, Petkov CI, Logothetis NK (2008) Visual modulation of neurons in auditory cortex. Cereb Cortex 18:1560-1574.

Korte M, Rauschecker JP (1993) Auditory spatial tuning of cortical neurons is sharpened in cats with early blindness. J Neurophysiol 70:1717-1721.

Kral A (2007) Unimodal and cross-modal plasticity in the ‘deaf’ auditory cortex. Int J Audiol 46:479-493.

Kral A, Schröder JH, Klinke R, Engel AK (2003) Absence of cross-modal reorganization in the primary auditory cortex of congenitally deaf cats. Exp Brain Res 153:605-613.

Kupers R, Pappens M, de Noordhout AM, Schoenen J, Ptito M, Fumal A (2007) rTMS of the occipital cortex abolishes Braille reading and repetition priming in blind subjects. Neurology 68:691-693.

Kujala T, Alho K, Paavilainen P, Summala H, Näätänen R (1992) Neural plasticity in processing of sound location by the early blind: an event-related potential study. Electroen Clin Neuro 84:469-472.

Lakatos P, Chen CM, O'Connell MN, Mills A, Schroeder CE (2007) Neuronal oscillations and multisensory interaction in primary auditory cortex. Neuron 53:279-292.

Lambertz N, Gizewski ER, de Grieff A, Forsting M (2005) Cross-modal plasticity in deaf subjects dependent on the extent of hearing loss. Cog Br Res 25:884-890.

Lee DS, Lee JS, Oh SH, Kim SK, Kim JW, Chung JK, Lee MC, Kim CS (2001) Deafness: cross-modal plasticity and cochlear implants. Nature 409:149-150.

Lee JS, Lee DS, Oh SH, Kim CS, Kim JW, Hwang CH, Koo J, Kang E, Chung JK, Lee MC (2003) PET evidence of neuroplasticity in adult auditory cortex of postlingual deafness. J Nucl Med 44:1435-1439.

Lee CC, Winer JA (2008) Connections of cat auditory cortex: I. Thalamocortical system. J Comp Neurol 507:1879-1900.

Lee CC, Winer JA (2008) Connections of cat auditory cortex: III. Corticocortical system. J Comp Neurol 507:1920-1943.

Legge GE, Madison C, Vaughn BN, Cheong AM, Miller JC (2008) Retention of high tactile acuity throughout the life span in blindness. Percept Psychophys 70: 1471-1488.

Lessard N, Pare M, Lepore F, Lassonde M (1998) Early-blind human subjects localize sound sources better than sighted subjects. Nature 395:278-280.

Levänen S, Hamdorf D (2001) Feeling vibrations: enhanced tactile sensitivity in congenitally deaf humans. Neurosci Lett 301:75-77.

Levänen S, Jousmäki V, Hari R (1998) Vibration-induced auditory-cortex activation in a congenitally deaf adult. Curr Biol 8:869-872.

Lomber SG (1999) The advantages and limitations of permanent of reversible deactivation techniques in the assessment of neural function. J Neurosci Meth 86:109-117.

Lomber SG, Malhotra S (2008) Double dissociation of 'what' and 'where' processing in auditory cortex. Nat Neurosci 11:609-616.

Lomber SG, Meredith MA, Kral A (2010) Cross-modal plasticity in specific auditory cortices underlies visual compensations in the deaf. Nat Neurosci 13:1421-1427.

Macaluso E (2006) Multisensory processing in sensory-specific cortical areas. Neuroscientist 12:327-338.

Merabet LB, Pascual-Leone A (2010) Neural reorganization following sensory loss: the opportunity of change. Nat Rev Neurosci 11:44-52.

Meredith MA, Kryklywy J, McMillan AJ, Malhotra S, Lum-Tai R, Lomber SG (2011) Crossmodal reorganization in the early deaf switches sensory, but not behavioral roles of auditory cortex. Proc Natl Acad Sci 108:8856–8861.

Meredith MA, Lomber SG (2011) Somatosensory and visual crossmodal plasticity in the anterior auditory field of early-deaf cats. Hear Res 280:38–47.

Merzenich MM, Nelson RJ, Stryker MP, Cynader MS, Schoppmann A, Zook JM (1984) Somatosensory cortical map changes following digit amputation in adult monkeys. J Comp Neurol 224:591-605.

Miller MW, Vogt BA (1984) Direct connections of rat visual cortex with sensory, motor, and association cortices. J Comp Neurol 226:184-202.

Nishimura H, Hashikawa K, Doi K, Iwaki T, Watanabe Y, Kusuoka H, Nishimura T, Kubo T (1999) Sign language 'heard' in the auditory cortex. Nature 397:116.

Nodal FR, Bajo VM, King AJ (2012) Plasticity of spatial hearing: behavioural effects of cortical inactivation. J Physiol 590:3965-3986.

Noppeney U (2007) The effects of visual deprivation on functional and structural organization of the human brain. Neurosci Biobehav R 31:1169-1180.

Park MH, Lee HJ, Kim JS, Lee JS, Lee DS, Oh SH (2010) Cross-modal and compensatory plasticity in adult deafened cats: A longitudinal PET study. Brain Res 1354:85-90.

Petitto LA, Zatorre RJ, Gauna K, Nikelski EJ, Dostie D, Evans AC (2000) Speech-like cerebral activity in profoundly deaf people processing signed languages: implications for the neural basis of human language. PNAS 97:13961-13966.

Poirier C, Collignon O, Scheiber C, Renier L, Vanlierde A, Tranduy D, Veraart AG, De Volder AG (2006) Auditory motion perception activates visual motion areas in early blind subjects. Neuroimage 31:279-285.

Ptito M, Moesgaard SM, Gjedde A, Kupers R (2005) Cross-modal plasticity revealed by electrotactile stimulation of the tongue in the congenitally blind. Brain 128:606-614.

Rauschecker JP, Harris LR (1983) Auditory compensation of the effects of visual deprivation in the cat's superior colliculus. Exp Brain Res 50:69-83.

Rauschecker JP, Kniepert U (1994) Auditory localization behaviour in visually deprived cats. Eur J Neurosci 6:149-160.

Rauschecker JP, Korte M (1993) Auditory compensation for early blindness in cat cerebral cortex. J Neuroscience 13:4538-4548.

Rauschecker JP, Tian B (2000) Mechanisms and streams for processing of “what” and “where” in auditory cortex. PNAS 97:11800-11806.

Rebillard G, Carlier E, Rebillard M, Pujol R (1977) Enhancement of visual responses on the primary auditory cortex of the cat after an early destruction of cochlear receptors. Brain Res 129:162-164.

Röder B, Teder-Sälejärvi W, Sterr A, Rösler F, Hillyard SA, Neville HJ (1999) Improved auditory spatial tuning in blind humans. Nature 400:162-166.

Romanski LM, Tian B, Fritz J, Mishkin M, Goldman-Rakic PS, Rauschecker, JP (1999) Dual streams of auditory afferents target multiple domains in the primate prefrontal cortex. Nat Neurosci 2:1131-1136.

Sadato N, Pascual-Leone A, Grafman J, Deiber MP, Ibanez V, Hallett M (1998). Neural networks for Braille reading by the blind. Brain 121:1213-1229.

Sadato N, Pascual-Leone A, Grafman J, Ibañez V, Deiber MP, Dold G, Hallett M (1996) Activation of the primary visual cortex by Braille reading in blind subjects. Nature 380:526-528.

Sanchez-Vives MV, Nowak LG, Descalzo VF, Garcia-Velasco JV, Gallego R, Berbel P (2006) Crossmodal audio–visual interactions in the primary visual cortex of the visually deprived cat: a physiological and anatomical study. Prog Brain Res 155:287-311.

Schroeder CE, Foxe JJ (2002) The timing and laminar profile of converging inputs to multisensory areas of the macaque neocortex. Cogn Brain Res 14:187-198.

Schroeder CE, Lindsley RW, Specht C, Marcovici A, Smiley JF, Javitt DC (2001) Somatosensory input to auditory association cortex in the macaque monkey. J Neurophysiol 85:1322-1327.

Sharma A, Dorman MF, Kral A (2005) The influence of a sensitive period on central auditory development in children with unilateral and bilateral cochlear implants. Hear Res 203:134-143.

Shepherd RK, Baxi JH, Hardie NA (1999) Response of inferior colliculus neurons to electrical stimulation of the auditory nerve in neonatally deafened cats. J Neurophysiol 82:1363-1380.

Sterr A, Müller MM, Elbert T, Rockstroh B, Pantev C, Taub E (1998a) Changed perceptions in Braille readers. Nature 391:134-135.

Sterr A, Müller MM, Elbert T, Rockstroh B, Pantev C, Taub E (1998b) Perceptual correlates of changes in cortical representation of fingers in blind multifinger Braille readers. J Neurosci 18:4417-4423.

Stevens AA, Weaver KE (2009) Functional characteristics of auditory cortex in the blind. Behav Brain Res 196:134-138.

Stevens JC, Foulke E, Patterson MQ (1996) Tactile acuity, aging, and braille reading in long-term blindness. J Exp Psychol-Appl 2:91-106.

Van Boven RW, Hamilton RH, Kauffman T, Keenan JP, Pascual–Leone A (2000) Tactile spatial resolution in blind Braille readers. Neurology,54:2230-2236.

Vidyasagar, T R (1978) Possible plasticity in the rat superior colliculus. Nature 275:140-141.

Voss P, Gougoux F, Zatorre RJ, Lassonde M, Lepore F (2008) Differential occipital responses in early-and late-blind individuals during a sound-source discrimination task. Neuroimage 40:746-758.

Voss P, Lassonde M, Gougoux F, Fortin M, Guillemot JP, Lepore F (2004) Early-and late-onset blind individuals show supra-normal auditory abilities in far-space. Curr Biol 14:1734-1738.

Weeks R, Horwitz B, Aziz-Sultan A, Tian B, Wessinger CM, Cohen LG, Hallett M, Rauschecker JP (2000) A positron emission tomographic study of auditory localization in the congenitally blind. J Neurosci 20:2664-2672.

Wan CY, Wood AG, Reutens DC, Wilson SJ (2010) Early but not late-blindness leads to enhanced auditory perception. Neuropsychologia 48:344-348.

Wiesel TN, Hubel DH (1965) Comparison of the effects of unilateral and bilateral eye closure on cortical unit responses in kittens. J Neurophysiol 28:1029-1040.

Wiesel TN, Hubel DH (1965) Extent of recovery from the effects of visual deprivation in kittens. J Neurophysiol 28:1060-1072.

Wiesel TN, Hubel DH (1963) Single-cell responses in striate cortex of kittens deprived of vision in one eye. J Neurophysiol 26:1003-1017.

Winer JA, Miller LM, Lee CC, Schreiner CE (2005) Auditory thalamocortical transformation: structure and function. Trends Neurosci 28:255-263.

Wong M, Gnanakumaran V, Goldreich D (2011) Tactile spatial acuity enhancement in blindness: evidence for experience-dependent mechanisms. J Neurosci 31:7028-7037.

Yaka R, Yinon U, Rosner M, Wollberg Z (2000) Pathological and experimentally induced blindness induces auditory activity in the cat primary visual cortex. Exp Brain Res 131:144-148.

Yaka R, Yinon U, Wollberg Z (1999) Auditory activation of cortical visual areas in cats after early visual deprivation. Eur J Neurosci 11:1301-1312.

Zhang HQ, Zachariah MK, Coleman GT, Rowe MJ (2001) Hierarchical equivalence of somatosensory areas I and II for tactile processing in the cerebral cortex of the marmoset monkey. J Neurophysiol 85:1823-1835.

Chapter 2: Cross-modal reorganization of cortical afferents to dorsal auditory cortex following early- and late-onset deafness[1]

2.1 Abstract.

Cat auditory cortex is known to undergo cross-modal reorganization following deafness, such that behavioral advantages in visual motion detection are abolished when a specific region of deaf auditory cortex, the dorsal zone (DZ), is deactivated. Thus, the purpose of the present investigation was to examine the changes in connectivity that might subserve this plasticity. I deposited biotinylated dextran amine (BDA; 3,000 MW), a retrograde tracer, unilaterally into the posterior portion of the suprasylvian fringe, corresponding to area DZ of hearing, early-deafened (onset <1M) and late-deafened (onset >3M) cats to reveal cortical afferent projections. Overall, the pattern of cortical projections to DZ was similar in both hearing and deafened animals. However, there was a progressive increase in projection strength between hearing, late- and early-deafened animals from an extrastriate visual cortical region known to be involved in the processing of visual motion, the posterolateral lateral suprasylvian area (PLLS). Additionally, although no such change was documented for the posteromedial lateral suprasylvian area (PMLS), labeled neurons were present within a subregion of PMLS devoted to foveal vision in both late- and early-deafened animals, but not in hearing controls. PMLS is also an extrastriate visual motion processing area, and is widely considered to be the homolog of primate area MT. No changes in auditory cortical connectivity were observed between groups. These observations suggest that amplified cortical projections from extrastriate visual areas involved in visual motion processing to DZ may contribute to the cross-modal reorganization that functionally manifests as superior visual motion detection ability in the deaf animal.

---

[1] A version of this chapter is published as:

Kok MA, Chabot N, Lomber SG (2014) Cross-modal reorganization of cortical afferents to dorsal auditory cortex following early- and late-onset deafness. J Comp Neurol 5*22*:654-675.

2.2 Introduction

The cerebral cortex is a complex and adaptable structure that changes over the course of the lifespan. Cortical plasticity describes the changes in the structure and function of the cerebrum that occur as a consequence of experience. Most studies of cortical plasticity focus on normal adaptation to environmental input (e.g. development and maturation, learning); however, a growing body of research is focused on understanding the conditions under which the cerebrum is capable of rewiring itself following insult, injury or the lack of a specific class of inputs. Adaptive cross-modal plasticity refers to the cortical reorganization that takes place across sensory modalities following the loss or impairment of a sensory system. As suggested by the name, this process not only helps to compensate for the lost modality, but also results in the expansion or heightened ability of the remaining sensory modalities (Bavelier and Neville, 2002). The basis for this claim derives mainly from visual deprivation literature, in which numerous studies have cited superior behavioral performance in blind individuals performing auditory (Weeks et al. 2000) or tactile tasks (Grant et al., 2000; Sathian, 2000; D'Anguilli and Wairach, 2002; Sathian, 2005). This phenomenon has more recently been extended to deaf individuals performing visual or somatosensory tasks (Bavelier et al., 2000; Levanen and Hamdof, 2001; Karns et al., 2012).

While it is generally accepted that sensory deprivation that occurs early in life leads to cross-modal compensations (Kujala et al., 2000), whether such changes occur following damage to mature sensory systems remains under debate. To this end, a number of studies in humans have sought to evaluate the differences following sensory deprivation early versus later in life with ambiguous results. Some studies have reported no evidence of cross-modal plasticity in cases of late sensory deprivation (Cohen et al., 1999), while others have reported similar changes after late sensory deprivation to that observed following early (Kujala et al., 1997), and still others have reported cases of late sensory

deprivation that differ from both early-deprived and control participants (Büchel et al., 1998).

Evidence of cross-modal reorganization following deafness has also been documented in the animal literature (Hunt et al., 2006; Allman et al., 2009; Lomber et al., 2010; Meredith et al., 2011). Cat auditory cortex is known to undergo cross-modal reorganization following deafness, such that superior peripheral visual localization and visual motion detection abilities are abolished when specific regions of auditory cortex are deactivated in congenitally deaf animals: the posterior auditory field (PAF) for localization, and the dorsal zone (DZ) for motion detection (Lomber et al., 2010). Furthermore, it has been suggested that the original function of these reorganized cortical areas may be maintained following sensory deprivation, even though the sensory modality that mediates the function has changed (Lomber et al., 2010, Meredith et al., 2011). For example, PAF is known to be involved in auditory spatial localization in the hearing animal (Malhotra and Lomber, 2007; Lomber and Malhotra, 2008); while in the deaf animal, PAF is cross-modally reorganized to aid with visual peripheral localization (Lomber et al. 2010). As such, localization behavior appears to be 'supramodal' with respect to PAF, it is merely the class of inputs (auditory versus visual) that changes. However, it is unknown whether such principles hold true following damage to sensory systems later in life. The few studies in animal models that have examined differences in levels of cross-modal reorganization between the early and late deaf suggest that similar compensations can occur following damage to mature sensory systems (cat: Rebillard et al., 1977; Shepherd et al., 1999; Park et al., 2010; ferret: Allman et al., 2009).

While these experiments provide important information regarding which cortical areas undergo cross-modal reorganization in the deaf cat, the next logical step is to reveal any underlying changes in brain circuitry that might give rise to this plasticity. The plethora of studies documenting functional changes following the loss of auditory input stand in stark contrast to the paucity of studies seeking to understand the anatomical substrates of these changes. To date, at

least three studies have compared changes in corticocortical connectivity between visually impaired animals and those with normal vision (Karlen et al., 2009; Larsen et al., 2009; Charbonneau et al., 2012), whereas, to the best of our knowledge, no such comparison has been documented for hearing versus deafened animals. Thus, the current study seeks to evaluate the structural adaptations that may occur as a consequence of the removal of auditory input at different stages of developmental maturity. In order to do this, biotinylated dextran amine (BDA; 3,000 MW) was injected into the posterior portion of the suprasylvian fringe (Woolsey, 1960; Paula-Barbosa et al., 1975; Niimi and Matsuoka, 1979; Beneyto et al., 1998), corresponding to area DZ (**Figure 2.1**), a region that is known to undergo cross-modal reorganization following deafness (Lomber et al., 2010). Injections were performed on three groups: hearing, early-deafened (onset <1 month) and late-deafened (onset >3 months) animals. Our results indicate that the proportion of projections to visual cortical regions is increased in both early- and late-deafened animals compared to hearing. This increase in visual projection strength is largely due to increased connectivity with extrastriate visual cortical regions known to be involved in processing visual motion, the posterolateral lateral suprasylvian area (PLLS), and the posteromedial lateral suprasylvian area (PMLS).

2.3 Materials and Methods

Cortical connections were examined in 15 adult domestic cats that were acquired from a licensed commercial laboratory animal breeding facility (Liberty Labs, Waverly, NY) and housed in an enriched colony environment. Five mature hearing cats (>3 months) constituted the hearing group and five cats were ototoxically deafened postnatally around the time of hearing onset (<1 month) to form the early deaf group, and a third group of five cats was deafened later in life (>3 months) to form the late deaf group (**Figure 2.2**). Deafness in all cases was confirmed by the absence of stimulus-evoked activity in an auditory brainstem response (ABR). Not less than 6 months following deafening, injections of BDA were made into the left hemisphere, followed two weeks later by perfusion and

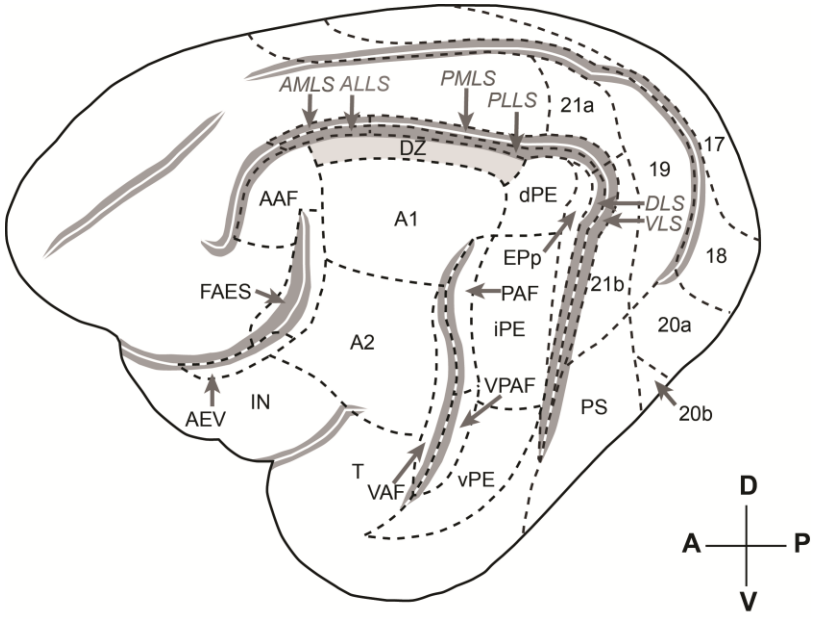

Figure 2.1 The auditory and visual cortices and sub-fields of the cat.

Lateral view of the left hemisphere of the cat depicting auditory (A1, A2, AAF, DZ, fAES, IN, PAF, dPE, iPE, vPE, T, VAF, VPAF) and visual (Areas 17, 18, 19, 20a, 20b, 21a, 21b, AEV, ALLS, AMLS, DLS, PLLS, PMLS, PS, VLS) cortical regions, bounded by dashed lines. Cortical regions lying within the banks of major sulci are depicted in dark grey with the fundus represented as a white line. Visual cortical regions lying within the middle and posterior suprasylvian sulci are indicated with gray italics. The region highlighted in light grey corresponds to the location of the area targeted in the current study, the dorsal zone of auditory cortex (DZ).

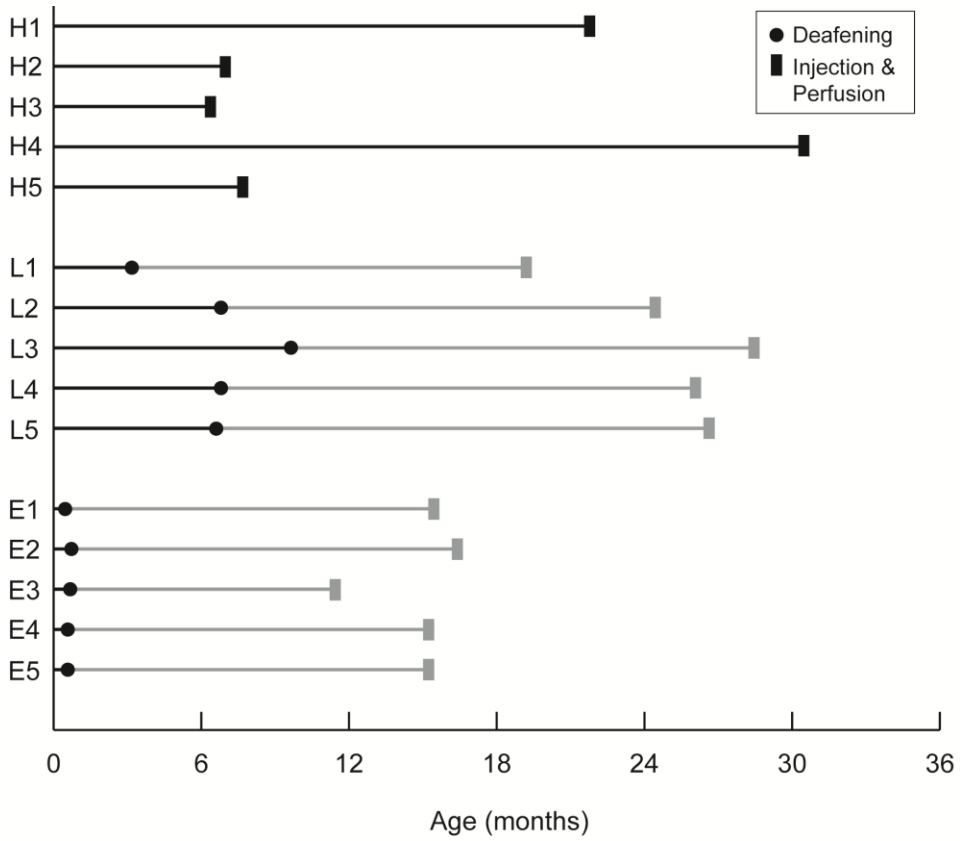

Figure 2.2 Timeline of deafening and other procedures performed on each group.

Timeline of procedures performed for each animal in the hearing (H), late- (L) and early-deafened (E) groups. Hearing experience is indicated in black; deafness in grey. Circles indicate the time of deafening; rectangles indicate the two week period during which BDA tracer injection and perfusion took place. All hearing animals had at least 6 months of hearing experience, and all animals were at least 6 months of age before perfusion. Both late- and early-deafened animals experienced at least 6 months of deafness before injection and perfusion procedures.

tissue processing. All procedures were conducted in compliance with the National Research Council's *Guidelines for the Care and Use of Mammals in Neuroscience and Behavioral Research* (2003), the Canadian Council on Animal Care's *Guide to the Care and Use of Experimental Animals* (Olfert et al., 1993) and were approved by the University of Western Ontario Animal Use Subcommittee of the University Council on Animal Care.

2.3.1 Deafening Procedures

Five cats were ototoxically deafened around the time of hearing onset (14 days postnatal; Shipley et al., 1980), or when the animal had reached 300 g, to constitute the early deaf group (**Figure 2.2**). In all cases, deafness was induced by co-administration of kanamycin and Edecrin® (ethacrynic acid; Valeant Pharmaceuticals, Laval, Quebec), which produces permanent, rapid and profound bilateral hearing loss as a result of the destruction of cochlear hair cells (Xu et al. 1993). Loop diurectics such as ethacrynic acid have been demonstrated to minimally affect vestibular end-organ function (Elidan et al., 1986); however, no obvious vestibular deficits were noted in animals in the current study. Prior to the procedure, animals were anesthetized by spontaneous inhalation of oxygen (1 L/min) and isofluorane (5% to effect for induction, then reduced to 1.5 – 2.5% to maintain). An intravenous catheter was inserted in the jugular vein at the neck. Electroencephalography (EEG) recording leads were inserted subdermally above the right and left ears, and a ground was placed on the lower back. Auditory stimuli (0.1 ms squarewave clicks; range: 0-80 dB) were delivered via speakers positioned in front of each ear. Evoked potentials in response to click presentations were recorded (Nicolet Biomedical Inc., Madison, WI). Next, animals were administered sodium edecrine, a loop diuretic (to effect: 35-60 mg/kg, i.v.), and injected with kanamycin (300 mg/kg, s.c.). Auditory brainstem responses (ABRs) to click presentations were collected at levels ranging from 0-80 dB SPL prior to, and following, deafening procedures (**Figure 2.3**). Deafness in all cases was confirmed by the absence of responses at all

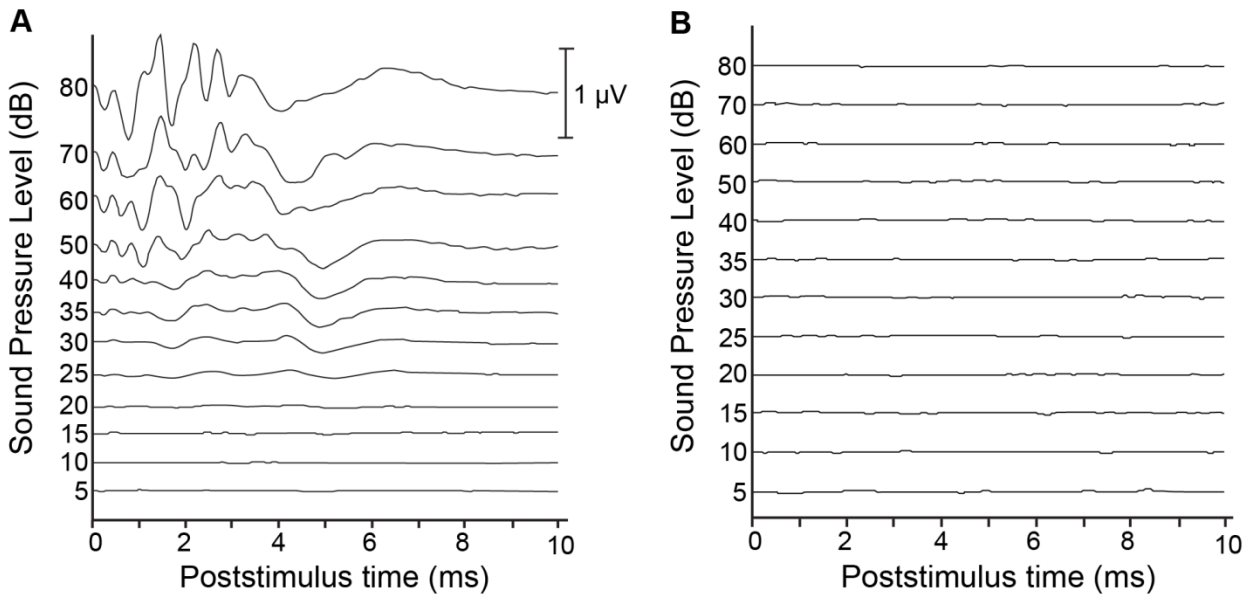

Figure 2.3 Pre- and post-deafening auditory brainstem responses.

Auditory brainstem responses (ABRs) for a late-deafened animal (L2) in response to 2,000 click presentations at sound pressure levels ranging from 5 – 80 dB SPL. All responses are scaled to 1 microvolt. **A:** Brainstem response of a late-deafened cat prior to deafening at 6 months of age. **B:** Absence of evoked responses to the same stimuli in the same cat, post-deafening. ABRs were collected for both early- and late-deafened animals in order to confirm deafness.

stimulus intensities presented (a flat ABR; **Figure 2.3B**). Diuretic infusion was then terminated and replaced by lactated Ringer's solution (4 ml/kg/h, i.v.). Following this, the catheter was removed and animals were recovered. Follow-up ABRs were conducted after 3 months to confirm deafness. The same procedures were conducted on older animals (>3 months) to constitute the late deaf group (**Figure 2.2**). All hearing animals had at least 6 months of hearing experience, and all animals were at least 6 months of age before perfusion. Both late- and early-deafened animals experienced at least 6 months of deafness before injection and perfusion procedures.

2.3.2 Tracer injections

The afternoon prior to surgery, animals were fasted and lightly anesthetized with ketamine (4 mg/kg, i.m.) and domitor (0.05 mg/kg, i.m.), in order to facilitate the insertion of an indwelling feline catheter into the cephalic vein (in preparation for the administration of i.v. anesthetic during the surgery). Each animal also received a dose of anti-inflammatory medication (dexamethasone, 0.05 mg/kg, i.v.).

On the day of surgery, animals were administered atropine (0.02 mg/kg., s.c.) to minimize respiratory and alimentary secretions, acepromazine (0.02 mg/kg, s.c.), a second dose of dexamethasone (0.5 mg/kg, i.v.), and buprenorphine (0.005 mg/kg, s.c.). Sodium pentobarbital (25 mg/kg to effect, i.v.) was then administered to induce general anesthesia. In order to inhibit the gag reflex, the mucosa of the pharynx was anesthetized with a topical anesthetic (Cetacaine, Cetylite Laboratories, Pennsauken, NJ), and the trachea was intubated with a cuffed endotracheal tube in order to ensure adequate ventilation. Respiration was unassisted. Ophthalmic ointment (Neosporin, Kirkland, Quebec) was applied to the cornea to prevent desiccation. Following this, the animal's head was placed into a stereotaxic frame (David Kopf Instruments, Tujunga, CA), and was fixed by palato-orbital restraints and blunt (non-rupture) ear bars, while the body rested on a water-filled heating pad in order to maintain core temperature at 37°C. The animal was then prepared for surgery using antiseptic

procedures. Body temperature, respiration rate, heart rate and blood pressure were monitored continuously throughout surgery.

A midline incision was made, and the temporalis muscle was reflected laterally. A craniotomy and durotomy were then performed over dorsal auditory cortex of the left hemisphere, exposing the middle suprasylvian sulcus. Biotinylated dextran amine (BDA; 3,000 MW) was pressure injected (Nanoliter 2000, World Precision Instruments, Sarasota, FL) through a glass pipette into the gyral lip of the lateral bank of the suprasylvian sulcus of the cat, at Horsley-Clarke[2] coordinates AP0, A3 and A5. At each location, two deposits were made: a volume of 1.5 µL at a depth of 1,400 µm from the cortical surface, and a volume of 2 µL at a depth of 700 µm, in order to ensure the injection spanned all cortical layers. Each brain was digitally photographed in order to provide a record of the location of the injection sites with respect to cerebral vasculature and anatomical landmarks. Following the injection, the craniotomy was closed and the animal was provided with standard postoperative care (see Malhotra et al., 2004). In all cases, recovery was uneventful.

2.3.3 Histological processing

After a survival period of two weeks, animals were deeply anesthetized using sodium pentobarbital (40 mg/kg, i.v.), and were administered an anticoagulant (heparin, 10,000 U; 1 mL) and a vasodilator (1% sodium nitrite, 1 mL). Animals were perfused intracardially through the ascending aorta with 1L physiological saline, followed by 2L fixative (4% paraformaldehyde), and finally 1L 10% sucrose solution, in order to cryoprotect the tissue. All solutions were buffered to pH 7.4 with 0.1M Sorenson's buffer and infused at a rate of 100 ml/min. The net effect of these procedures was to exsanguinate the cat, a method consistent with the recommendations of the American Veterinary Medical Association Panel on Euthanasia (Beaver et al. 2001). The brain was stereotaxically blocked in the coronal plane at Horsley-Clarke level A22,

[2] Stereotaxic coordinates were determined using the Horsley and Clarke (1908) system as described in Reinoso-Suárez (1961).

extracted from the skull and placed in 30% sucrose solution at 4^{o}C for cryoprotection, until it sunk. Following this, the brain was frozen and the portions of the brain comprising the visual, auditory and somatosensory cortices were cut in 60 µm serial sections, using either a freezing microtome or a cryostat. Six series of sections at 360 µm intervals were collected. One series was immunohistochemically processed to reveal the presence of the tracer (BDA) using the avidin-biotin peroxidase method, with nickel-cobalt intensification (Veenman, 1992). An adjacent series was processed with the monoclonal antibody SMI-32 (Covance, Princeton, NJ; Sternberger and Sternberger, 1983; van der Gucht et al., 2001; Lee and Winer, 2008a; Mellott et al., 2010). Two additional series were processed using cytochrome oxidase (Wong-Riley, 1979; Payne and Lomber, 1996) and Nissl stain (Clasca et al., 1997) in order to assist with laminar and other border distinctions. The two remaining series were retained as spares and were processed with the above methods as needed.

2.3.4 Areal border delimitation

All areal borders were delimited using cytoarchitectonic methods where possible, in addition to sulcal and gyral landmarks. SMI-32 is a monoclonal antibody that selectively binds to non-phosphorylated epitopes on the medium- and high-molecular weight subunits of neurofilament proteins (Sternberger and Sternberger, 1983). This results in robust labeling of cortical pyramidal cells and dendritic arbors, particularly in cortical layers III and V (Mellott et al., 2010; **Figure 2.4A**). Regional variation in the strength and extent of this labeling can be used to parcellate visual (van der Gucht et al., 2001) and auditory cortical areas (Lee and Winer, 2008a; Mellott et al., 2010). For example, the defining characteristic of SMI-32 labeling in DZ is heavy immunoreactivity in layers II and III (Mellott et al., 2010). While PLLS, the visual area that lies within the middle suprasylvian sulcus medial to DZ, also exhibits heavy layer III immunoreactivity, the dendritic arbors of layer III pyramidal cells extend well into layer II in DZ, but do not extend beyond the superficial half of layer III in PLLS (van der Gucht et al., 2001). Additionally, a distinguishing feature of PLLS is the very large

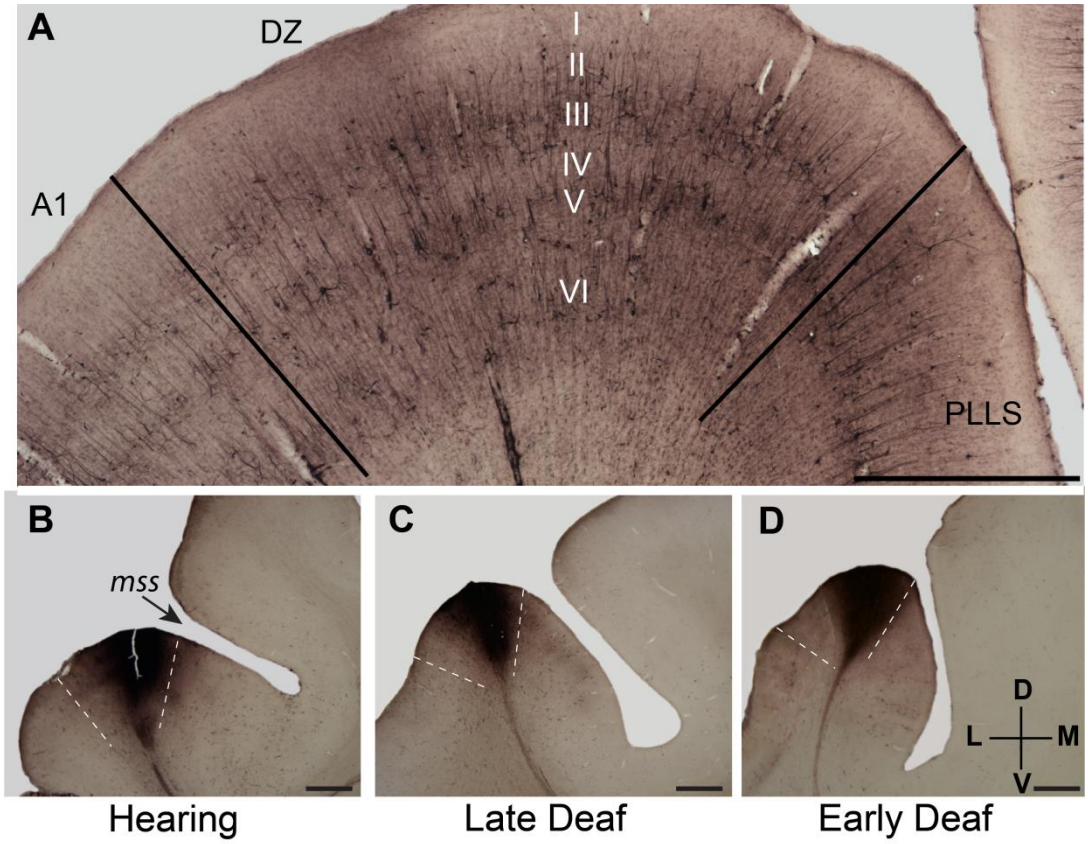

Figure 2.2.4 Cortical border delimitation.

A: Representative example of A1-DZ and DZ-PLLS borders as determined by cytoarchitecture in SMI-32 stained tissue. DZ is characterized by strong immunoreactivity in cortical layers II and III, whereas A1 is noticeably less dense, as well as lighter in appearance comparatively. Labeled dendrites typically extend well into layer II in DZ, but not in PLLS. **B-D:** Representative BDA injection sites for a single animal within each group (H2, L5, and E5) taken at similar AP coordinates (~A5). Note that in all cases, the injection site traverses all six cortical layers, and is well localized to the gyral lip of the lateral bank of the middle suprasylvian sulcus (mss), corresponding to area DZ. Dashed white lines indicate the medial and lateral borders of DZ as determined by SMI-32 labelling in adjacent sections. Scale bar: 1 mm.

immunopositive cells in layer V (van der Gucht et al., 2001); cells of this size are typically not seen in DZ. SMI-32 reactivity also readily distinguishes DZ from adjacent auditory cortical areas. Primary auditory cortex (A1), which lies immediately ventral to DZ, between the anterior and posterior ectosylvian sulci, is moderately reactive to SMI-32 and has lower labeling density in layers III and V than DZ (Mellott et al., 2010). This difference is marked enough to be visible at low magnification (Mellott et al., 2010). Furthermore, the SMI-32 staining profiles that were originally characterized in hearing cats (Mellott et al., 2010) have been shown to be conserved in both early- and late-deafened animals (Wong et al., 2013). Somatosensory borders were determined using mainly Nissl labeling profiles (Clasca et al., 1997), although somatosensory areas that bordered auditory areas were distinguishable using SMI-32, as somatosensory areas tend to react more heavily with SMI-32, and have darker staining profiles than visual (and auditory) cortical areas (van der Gucht et al., 2001). Here I have adopted the convention reported in Updyke (1986) and Rauschecker (1987), which places the borders between visual areas of the posterior lateral suprasylvian area (PLLS and PMLS, and the dorsal and ventral lateral suprasylvian areas (DLS and VLS)) on the lateral bank of the middle suprasylvian sulcus and the dorsal bank of the posterior limb of the suprasylvian sulcus, respectively, rather than at the level of the fundus, as suggested by the earliest studies of these areas (Palmer et al., 1978). Thus, both PMLS and VLS straddle the fundus, with the PMLS-PLLS border shifting toward the fundus in the posterior-to-anterior direction. This convention is supported by cytoarchitectonic border delimitation in the visual system (van der Gucht et al., 2001).

2.3.5 Data analysis

Neuronal labeling with BDA was visualized using a Nikon E600 microscope equipped with Nomarski DIC imaging and mounted with a DXM 1200 digital camera. Tissue outlines, injection sites, and labeled neurons were plotted using a PC-driven motorized stage controlled by Neurolucida software (MBF Bioscience, Inc; Williston, VT). Neurons were considered labeled only when the

entirety of the soma membrane was visible (**Figure 2.5**). Portions of cell bodies or dendritic branches alone were not counted in order to exclude artifacts of the reaction process. Labeled neurons within the injection site itself or within the lateral extent of the injection were not counted to avoid the inclusion of artifactual labeling. Focal levels throughout the z-plane of the section were taken in order to ensure the full thickness of the section was examined. When labeled cells were found on the border between two cortical areas or within a transitional zone between two areas, the total number of cells in question was equally distributed to each of the two areas. Following this, labeling profiles were constructed for each group (i.e. hearing, early deaf, late deaf), and these groups were contrasted against one another in order to evaluate any change in connectivity profiles that may have occurred as a result of cross-modal plasticity. Proportional data are reported using the total number of labeled neurons in the hemisphere ipsilateral to the injection as the denominator. All statistical analyses were done on arcsine transformed proportional data; however, the means reported in the text and in the figures reflect the original data prior to transformation for ease of comparison with the existing literature. A univariate analysis of variance was conducted on the data. Bonferroni corrections were applied to all pairwise comparisons in order to compare means between individual cortical regions.

2.4 Results

2.4.1 Tracer deposits

Injection sites spanned all six cortical layers and occupied the posterior portion of the gyral lip of the lateral bank of the middle suprasylvian sulcus (**Figure 2.4 B-D**). The volume of tracer injected ensured that the spread of injection formed a continuous band of darkly stained tissue between injection sites, as could be visualized with the naked eye in sections stained to reveal the presence of the tracer.

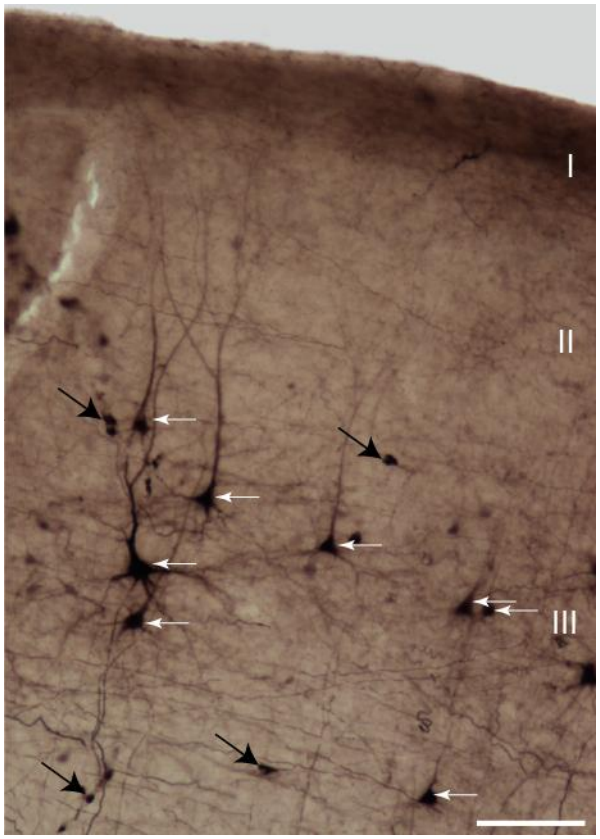

Figure 2.5 BDA-labeled neurons in A1.

Photomicrograph of retrogradely labeled neurons (white arrows) in A1 of a hearing animal (H2). The soma and dendrites of labeled neurons are easily recognizable. Cortical layers are labeled in white roman numerals. Black arrows indicate labeling artifacts or profiles not clearly identifiable as labeled neurons, which were not counted as neurons. Scale bar: 100 µm.

2.4.2 Labeling of cortical afferents

In all animals, neuronal labeling was observed in each of the thirteen regions of auditory cortex. In hearing animals, although labeling was concentrated dorso-posteriorly within auditory cortex, it extended both anteriorly and ventrally (**Figure 2.6**, sections 2-9). A high density of labeling is evident in posterior primary auditory cortex (A1; **Figure 2.6**, sections 6-7). While scattered labeling was still present in all thirteen regions of auditory cortex in both late- and early-deafened animals, it was concentrated dorso-posteriorly to a greater extent in both cases compared to hearing animals (**Figures 2.7 & 2.8**, sections 2-9;), with a corresponding paucity of labeled cells located ventrally (**Figures 2.7 & 2.8**, sections 4-7;). Illustrated cases in **Figures 2.6, 2.7 and 2.8** were matched as closely as possible for the total number of labeled neurons (range: 3122-3495), and for fidelity to the group mean of the data for cortical regions examined. Different cases from those illustrated in **Figures 2.6-2.8** are shown in **Figures 2.9, 2.10 and 2.11**, which were selected based on the same criteria, but were plotted on standardized sections to facilitate comparisons between groups. The range between the total number of labeled neurons for the cases plotted in **Figures 2.9-2.11** was 2080-2675. For both hearing and deafened animals, labeling also tended to be concentrated supragranularly, rather than infragranularly.

Figure 2.6 Injection sites and labeling in a hearing animal.

Plots of labelled neurons on coronal sections from a hearing animal (H1), with areal boundaries delimited by SMI-32 labeling profiles in adjacent sections. Injection sites are represented by dark shading with the lateral extent of the injection site represented by intermediate shading; no neurons were counted within these regions. Light shading represents tissue stained by the injection, but lying outside of the injection site and the lateral extent. Inset, lateral view, shows the position of each of the 13 coronal sections.

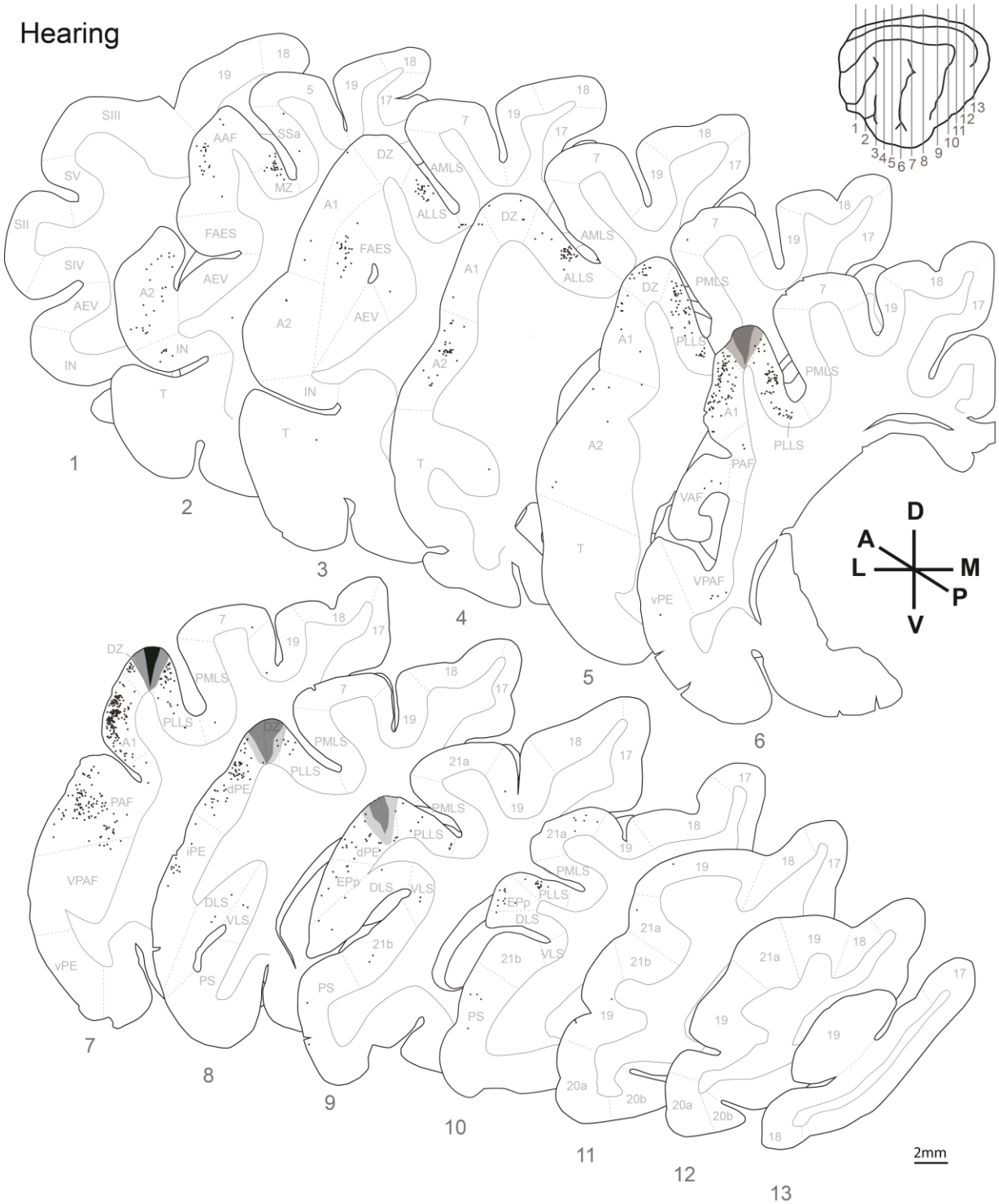
Hearing
SIII
SV
SII
SIV
AEV
IN
T
AAF
SSa
MZ
FAES
A2
A1
DZ
AMLS
ALLS
PMLS
PLLS
PAF
VAF
VPAF
vPE
dPE
lPE
EPp
DLS
VLS
PS
21a
21b
20a
20b
18
19
17
7
5
D
A
L
M
P
V
1
2
3
4
5
6
7
8
9
10
11
12
13
2mm

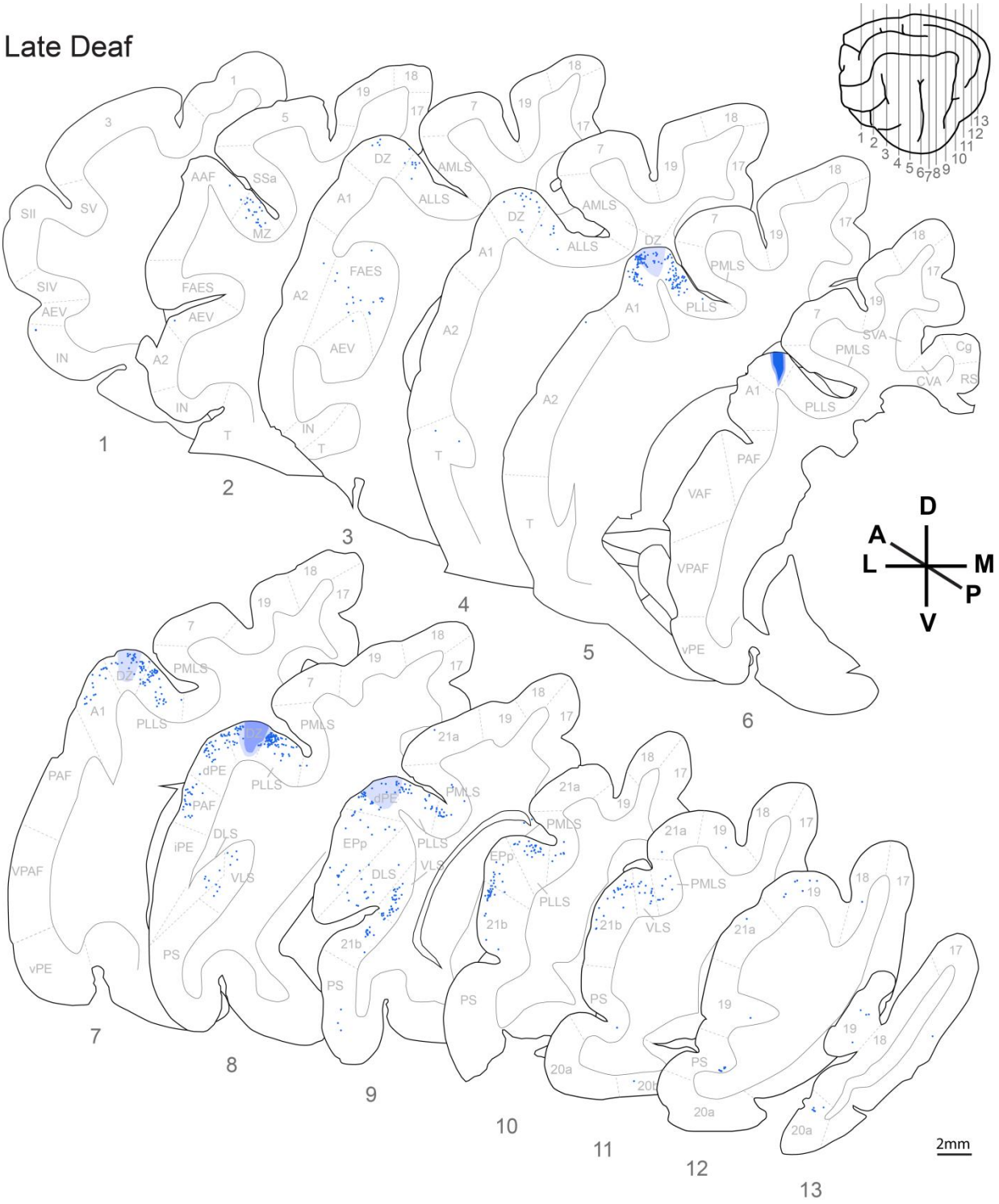

Figure 2.7 Labeled neurons and injection sites from a late-deafened animal (L4).

Areal boundaries were determined by SMI-32 labeling profiles in adjacent sections. Conventions as in Figure 2.6.

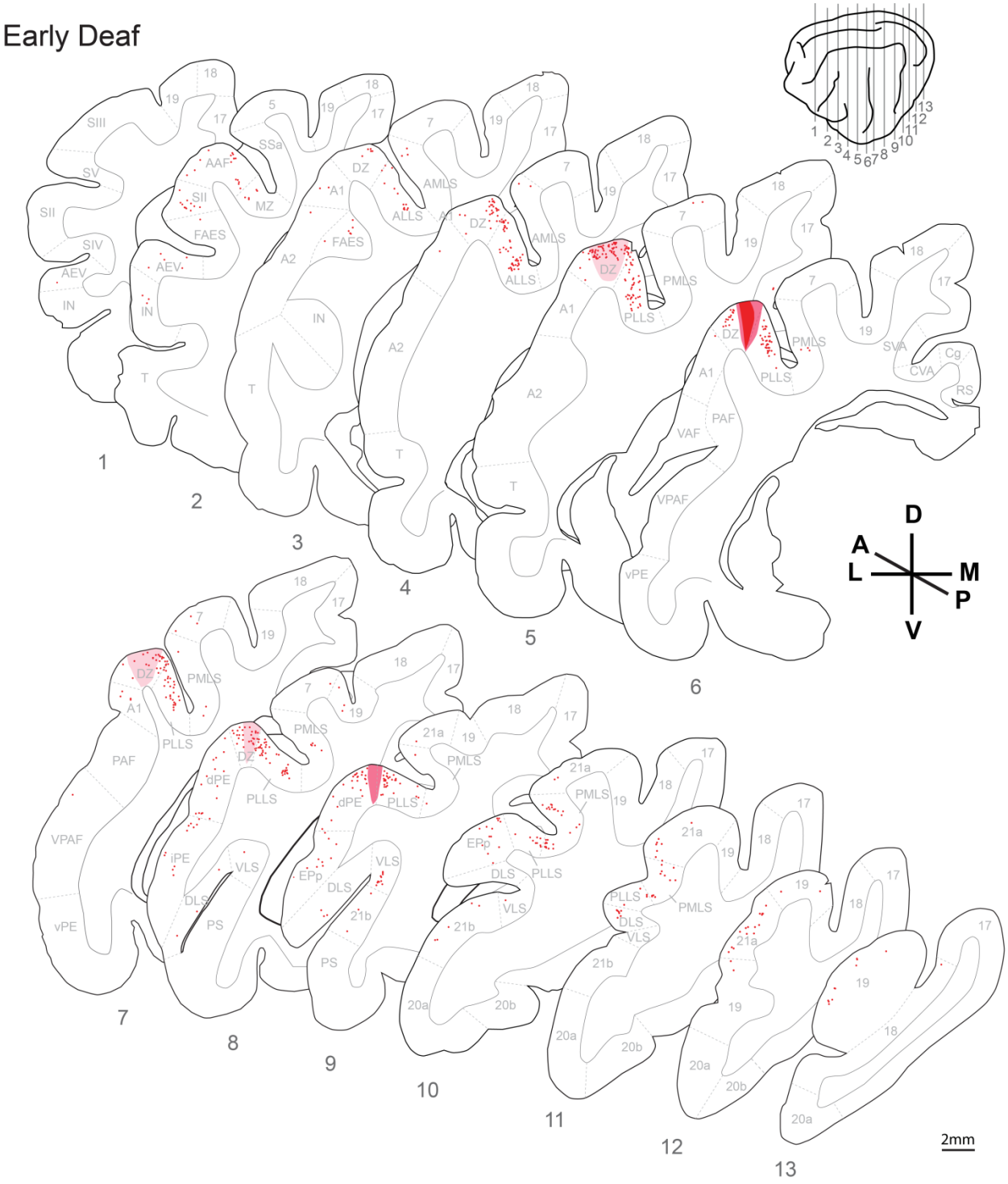

Figure 2.8 Labeled neurons and injection sites from an early-deaf animal (E2).

Areal boundaries as determined by SMI-32 labeling profiles in adjacent sections. Conventions as in Figure 2.6.

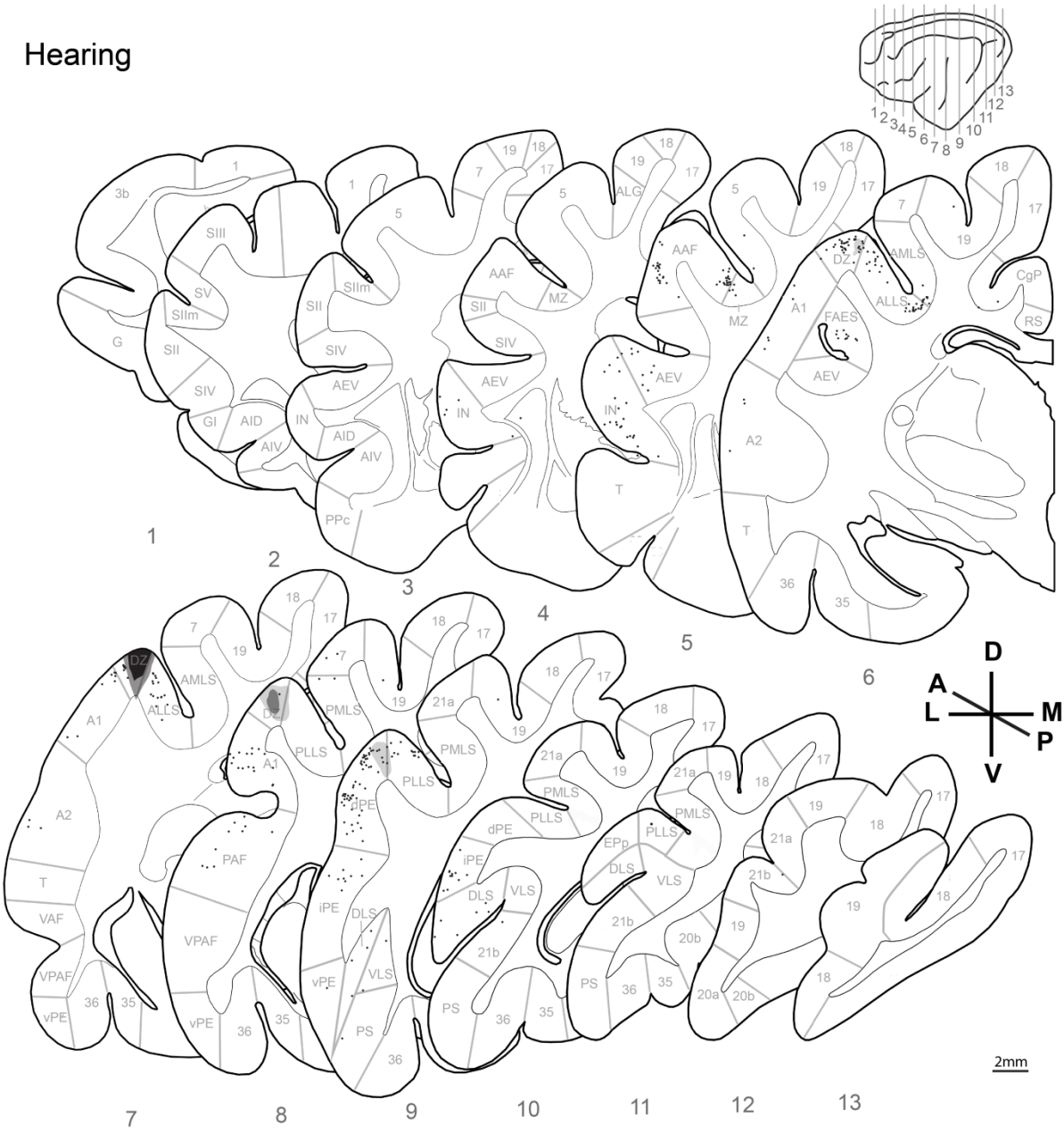

Figure 2.9 Injection sites and neuronal labeling for a hearing animal.

Representative distribution of labeled neurons throughout auditory and visual cortical areas following an injection of BDA into DZ in a hearing animal (black; H2). Labeled neurons from each case have been superimposed onto standardized sections adapted from Reinoso-Suárez (1961). Conventions as in Figure 2.6.

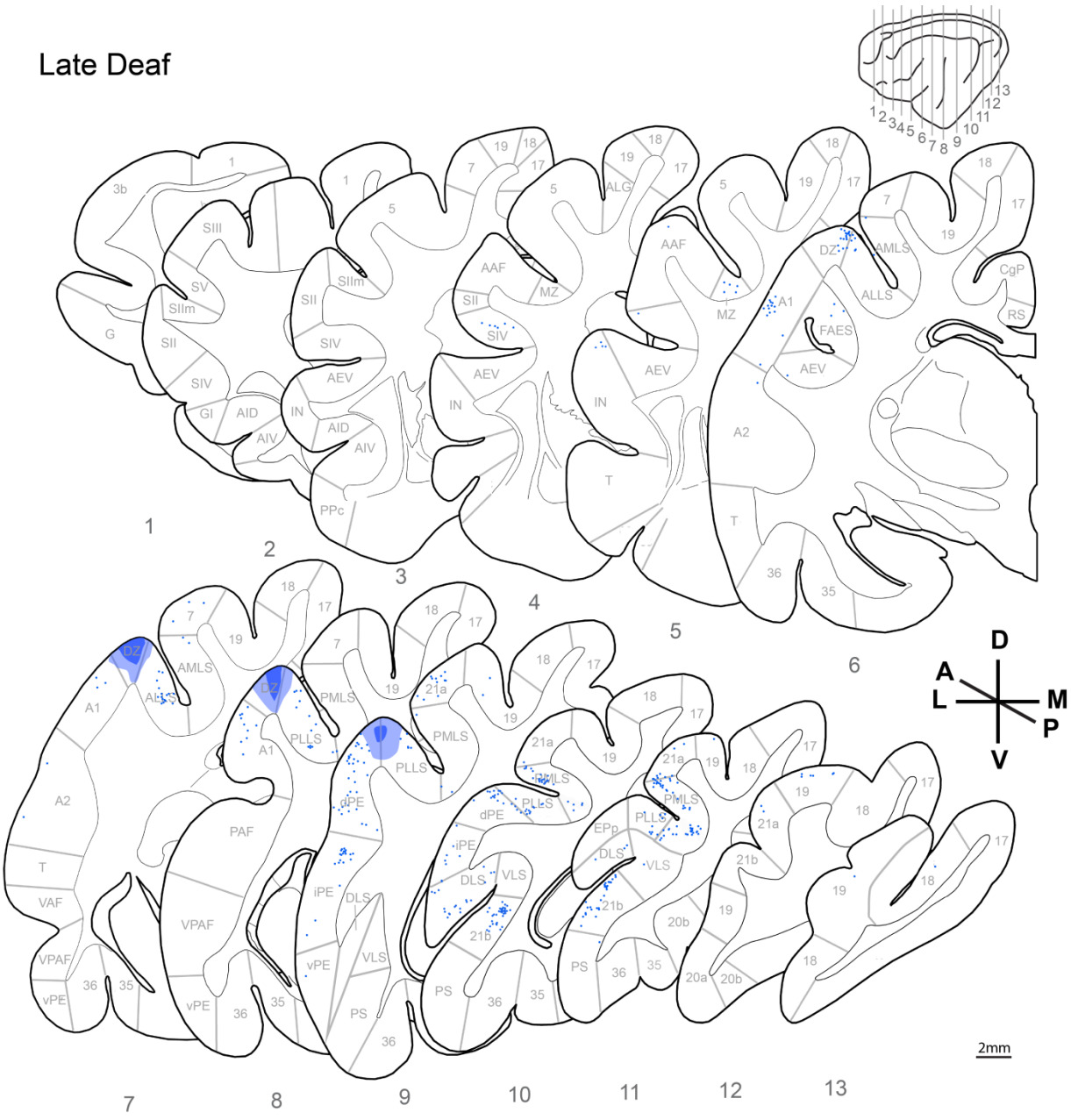

Figure 2.10 Standardized injection sites and neuronal labeling for a late-deafened animal.

Representative distribution of labeled neurons throughout auditory and visual cortical areas following an injection of BDA into DZ in a hearing animal (blue; case L3). Labeled neurons from each case have been superimposed onto standardized sections adapted from Reinoso-Suarez (1961). Conventions as in Figure 2.6.

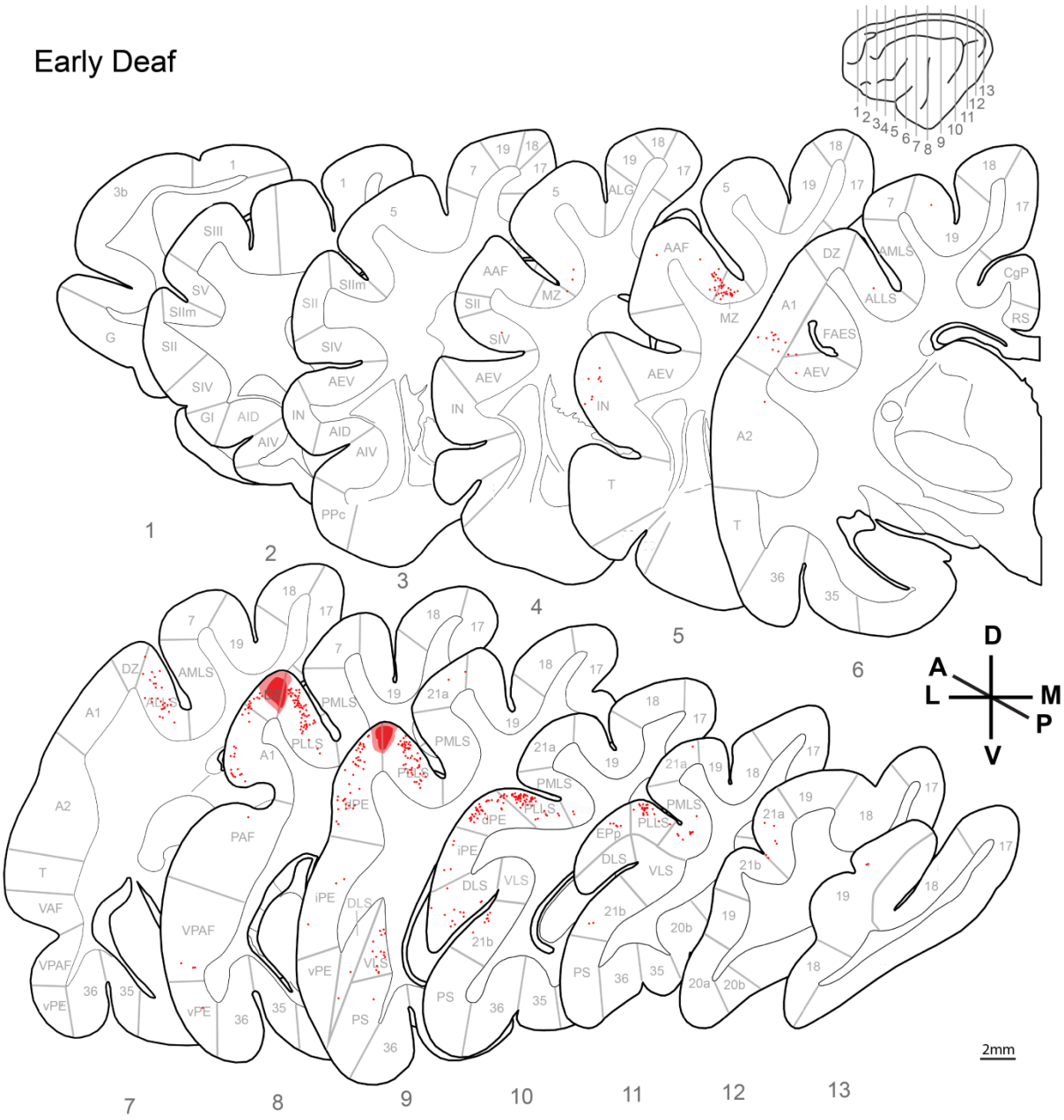

Figure 2.11 Injection sites and labeled neurons on std. sections.

Representative distribution of labeled neurons throughout auditory and visual cortical areas following an injection of BDA into DZ in a hearing animal (red; case E1). Labeled neurons from each case have been superimposed onto standardized sections adapted from Reinoso-Suárez (1961). Conventions as in Figure 2.6.

In hearing animals, although labeling was concentrated within auditory cortex, some labeling was present in visual cortical areas. The majority of this labeling tended to be localized to areas that bordered DZ; that is, the anterolateral and posterolateral lateral suprasylvian areas (ALLS and PLLS, respectively; **Figure 2.6**, sections 3-10; **Figure 2.9**, sections 6-11). Visualcortical labeling generally extended further posterior in both late- and early-deafened animals compared to hearing animals (**Figures 2.7 & 8**, sections 3-13; **Figures 2.10 & 2.11**, sections 6-11). Furthermore, within the middle suprasylvian sulcus, labeling in the fundus and on the medial bank was evident in both late- and early-deafened animals, especially in more posterior sections (**Figures 2.7 & 2.8**, sections 9-11; **Figures 2.10 & 2.11**, sections 10-11). As in auditory cortex, in both hearing and deafened animals, a greater proportion of labeling was supragranular rather than infragranular.

2.4.3 Comparisons between modalities

In order to investigate the differences in cortical connectivity between the hearing and the deaf brain, as well as any differences in the level of cross-modal plasticity observed between cats that were deafened earlier in life versus later, deposits of biotinylated dextran amine (BDA) were made into the posterior half of the suprasylvian fringe, and the extent of auditory, visual, somatosensory and multisensory projections to this area were examined. On average, auditory cortical projection strength to DZ is stronger in hearing (46.33%) than in late-deafened animals (29.91%) and early deafened animals (35.86%; **Figure 2.12A**). Conversely, both late-deafened and early-deafened animals show stronger projections from visual cortical areas (65.98% and 60.85%, respectively)) compared to hearing animals (45.55%). Somatosensory projection strength was weak and remained relatively constant between groups, on the order of less than 1% for each (H – 0.55%, L – 0.18%, E – 0.47%). Projections arising from multisensory/association areas (defined as area 7 and the multisensory zone (MZ) of the posterior limb of the rostral suprasylvian sulcus) also remained relatively constant (H – 6.78%, L – 3.36%, E – 3.05%). Collapsing individual

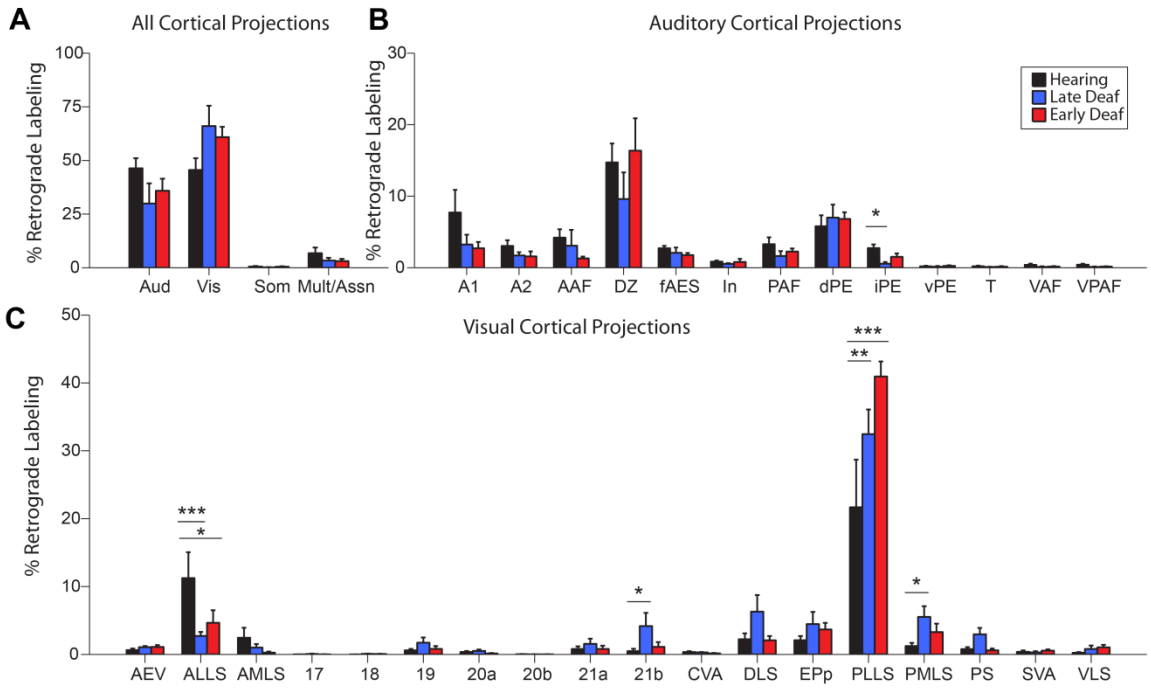

Figure 2.12 Proportion of projections by cortical area.

A: Percentage of total ipsilateral cortical projections to DZ by sensory type. **B:** Percentage of total ipsilateral projections to the DZ from auditory cortical areas. No significant changes in projection strength were observed. **C:** Percentage of total ipsilateral projections to the DZ from visual cortical areas. Significant changes between hearing and both late- and early-deafened animals included a reduction in projection strength from ALLS, and an increase in projection strength from PLLS. Significance levels are indicated by asterisks as follows: ** $p<0.01$, *** $p<0.001$.

cortical regions into groups indicated that the projection strength from auditory and visual cortical areas is roughly equal for hearing animals and relatively few sub-regions within a sensory modality appear to change following deafness, as discussed in detail below (**Figure 2.12A**). An omnibus univariate analysis of variance on individual cortical regions indicated a statistically significant interaction between the cortical area examined and group (hearing (H), late deaf (L) and early deaf (E); $F(60,372) = 2.02$, $p < 0.001$.

2.4.4 Auditory cortical projections

A statistically significant decrease in projection strength from the intermediate posterior ectosylvian area (iPE) was found for hearing (H – 2.75%) compared to late-deaf animals (LD – 0.56%, $p = 0.046$). Neither the hearing nor late-deaf group differed from the early-deaf (E – 1.51%) group for this region. No significant changes in projection strength from any of the other auditory cortical regions to DZ were found between late-deafened, early-deafened or hearing animals were observed (**Figure 2.12 B**). However, although not statistically significant, there was a trend toward slight reductions in the percentage of auditory cortical projections to DZ between groups arose from the core or primary auditory cortical areas: A1 (H – 7.72%, L – 3.23%, E – 2.73%) and the anterior auditory field (AAF; H – 4.19%, L – 3.08%, E – 1.29%). This trend was similar, but generally smaller in magnitude for the dorsal, non-primary auditory regions, which include the second auditory cortex (A2; H – 3.04%, L – 1.72%, E – 1.58%), auditory field of the anterior ectosylvian sulcus (fAES; H – 2.73%, L – 2.07%, E – 1.76%), and posterior auditory field (PAF; H – 3.29%, L – 1.64%, E – 2.26%). The dorsal posterior ectosylvian area (dPE) is the sole auditory cortical area that showed a trend toward increased projection strength between hearing and deafened animals (H – 5.80%, L – 7.01%, E – 6.83%). The ventral auditory areas (insular cortex (In), ventral posterior ectosylvian area (vPE), temporal cortex (T), ventral auditory field (VAF), and ventral posterior auditory field (VPAF)) are all remarkably consistent between groups in terms of the projection strength, and for all areas and groups, these correspond to weak projections (1% or less).

2.4.5 Visual cortical projections

Changes in the proportion of visual cortical projections to the DZ were observed for a few visual areas (**Figure 2.12C**). A progressive increase in projection strength between hearing, late- and early-deafened animals was documented from an area known to be involved in visual motion processing: PLLS (H – 21.67%, L – 32.44%, E – 40.95%). For PLLS, an increase in projection strength was found between hearing and late-deafened animals ($p = 0.002$) and hearing and early-deafened animals ($p < 0.001$ for each). The only decreases in projection strength between hearing and deafened animals arose from anterior regions thought to be involved in more complex visual motion processing, the anterolateral lateral suprasylvian area (ALLS; H – 11.25%, L – 2.71%, E – 4.66%). The reduction in ALLS projection strength was significant between hearing and late-deafened animals ($p < 0.001$), and hearing and early-deafened animals ($p = 0.015$). There was no statistical difference between late and early-deafened animals. However, statistically significant increases in projection strength were found for visual areas 21b (H – 0.49%, L – 4.17%, E – 1.11%) and PMLS (H – 1.23%, L – 5.54%, E – 3.29%) between hearing and late-deafened animals only ($p = 0.024$ and $p = 0.011$, respectively).

There were slight, but not statistically significant increases in projection strength in both early- and late-deafened animals from the visual area occupying the posterior third of the posterior ectosylvian gyrus, a region referred to in the literature as EPp was also increased (H – 2.09%, L – 4.47%, E – 3.68%). Three regions of visual cortex located within the same general area also showed slight, but not statistically significant increases in projection strength for late-deafened animals compared to hearing animals, which was not present in early-deafened animals. These three regions all comprise some portion of the gyrus occupying the posterior bank of the posterior suprasylvian gyrus (see **Figure 2.1**). These were DLS (H – 2.23%, L – 6.29%, E – 2.08%), area 21b (H – 0.49%, L – 4.17%, E – 1.11%), and posterior suprasylvian area (PS; H – 0.78%, L – 2.95%, E – 0.61%). Importantly, this 2-4% increase in projection strength in late-deafened animals could not be accounted for by a particularly strong projection present in a

single animal; that is, this trend was present in more than one of the late-deafened animals. All other visual cortical regions either provided weak (<1%) or no input to the DZ in hearing animals, and these projection strengths remained weak or non-existent in the deaf animals.

2.5 Discussion

2.5.1 Spatial processing in DZ

Although a specific, unique role in auditory cortical processing has not been identified for DZ, both behavioral (Malhotra et al. 2008) and electrophysiological (Stecker et al. 2005) evidence suggests that DZ is involved in auditory spatial perception. Cat auditory cortex has not formally been categorized into “core” and “belt” regions, as has primate auditory cortex (Read et al. 2002), but DZ has been suggested to form part of a functional “belt” auditory region because responses in DZ are more complex, non-linear, and have longer latencies and broader tuning curves (Middlebrooks and Zook 1983; He and Hashikawa,1998; Stecker et al. 2005) than the “core” regions A1 and AAF, which are characterized by simple, linear responses with short latencies and sharp tuning curves (Stecker et al. 2005). This designation is further supported by anatomical analyses of thalamocortical connectivity. Core regions typically receive projections from the ventral portion of the medial geniculate nucleus (MGN), whereas belt and parabelt regions typically receive projections from dorsal divisions of MGN (Hackett 2011). Such a designation would fit well with current models of a postero-auditory or “where” stream for spatial (Lomber and Malhotra, 2008) and even motion processing (Rauschecker and Scott, 2009). Beyond the proposed designation of DZ as a belt region, homologous structures in primate auditory cortex have not been proposed for DZ.

2.5.2 Localization of injection sites

Several criteria were used to localize the site of injections: 1) a pattern of labeling in auditory cortical areas consistent with previously published findings for hearing animals (e.g. He and Hashikawa, 1998; Lee and Winer, 2008b), 2)

stereotaxically-guided injections, 3) cytoarchitectonic analysis of adjacent SMI-32 sections, and 4) position relative to known sulcal and gyral landmarks. In this case, the location of the anterior two injection sites (at Horsley-Clarke coordinates A3 and A5), can be well localized to area DZ based on all four criteria. However, the location of the third injection site (AP 0) requires discussion. Based on the position of the injection relative to sulcal and gyral landmarks, this injection site could be classified as lying within dPE (see shaded regions on sections 8 and 9 of **Figures 2.6-12**). Cytoarchitectonic analysis of the DZ-dPE border is somewhat unreliable, given that characteristic SMI-32 patterns of labeling have not been described in detail for area dPE, as they have for the 10 more anterior areas of auditory cortex (see Mellott et al., 2010), and an SMI-32 staining gradient exists, such that the tissue is not as darkly stained in posterior DZ as it is in more anterior sections (Wong et al., 2013). Additionally, many of the boundaries of auditory cortical areas are defined as being "transitional" rather than "clear cut" (Mellott et al., 2010), suggesting that most cortical borders do not abruptly switch from one auditory cortical area to another. Thus, the pattern of projections observed might be considered the most reliable marker of injection site location. As discussed in detail below, the pattern of projections in the present study are most consistent with injections lying within DZ, based on previously published retrograde analyses of DZ injections in hearing animals (He and Hashikawa, 1998; Lee and Winer, 2008b), and compared with the published results of injections into adjacent visual and auditory cortical areas (Symonds and Rosenquist, 1984; Bowman and Olson, 1988; Scannell et al. 1995; Lee and Winer, 2008b). Thus, I have considered our injection sites as being localized to DZ based on the pattern of projections observed.

2.5.3 Auditory cortical projections to DZ in hearing animals

Overall, the pattern of auditory cortical projections to DZ in hearing animals in the present study is consistent with that reported in two previous studies (He and Hashikawa, 1998; Lee and Winer, 2008b). He and Hashikawa

(1998) found that DZ receives relatively strong projections from A1, A2, AAF and PAF, with strong corticocortical connections present within DZ itself. In a similar study, Lee and Winer (2008b) found that DZ received projections mainly from dorsal auditory regions, including A1, A2, fAES, PAF and dPE, with weaker projections from other (mainly ventral) auditory areas (AAF, In, iPE, vPE, T, VAF, VPAF), and also with strong intra-DZ connections present outside of the injection site. In support of these findings, early lesion experiments involving the superficial suprasylvian fringe (now known to be DZ) resulted in neuronal degeneration in these same auditory cortical regions (areas A1, A2, AAF, fAES, PAF and dPE; Paula-Barbosa et al., 1975). Together, these studies agree very well with the pattern of auditory cortical projections observed in the current study. That is, DZ received the strongest auditory cortical projections from dorsal auditory areas (A1, A2, AAF, fAES, PAF, dPE, iPE) with much weaker input from ventral areas (In, T, vPE, VAF, VPAF), and with strong intra-DZ connectivity. In all previous studies, the strongest non-DZ auditory cortical projection arose from A1, consistent with the findings reported in the present study (He and Hashikawa, 1998; Lee and Winer, 2008b).

2.5.4 Comparison to late- and early-deafened animals

Overall, the pattern of auditory cortical projections to DZ was conserved in both early- and late-deafened animals (**Figures 2.7, 2.8, 2.10, 2.11, 2.12**). Although there were virtually no statistically significant changes observed between groups, there was a trend indicating a progressive weakening of projection strength from A1 to DZ between hearing, late- and early-deafened animals. This may be accounted for by the fact that the medial border of A1 (the A1-DZ border) has been found to shift laterally in congenitally deaf animals (Lomber et al., 2010). More recent studies have confirmed this based on analysis with tissue stained for SMI-32, and have additionally determined that there exists a decrease in cortical volume for A1 in early-deafened animals compared to that of hearing or late-deafened animals (Wong et al., 2013). Deaf A1 has not been shown to exhibit visual cross-modal reorganization in electrophysiological

(Stewart and Starr, 1970; Kral et al., 2003) or behavioral (Lomber et al., 2010) studies in cats. Based on this observation, it has been suggested that following deafness, the absence of auditory input to A1 will affect supragranular connections between A1 and higher-order auditory cortical regions, causing A1 to become functionally decoupled from these areas (Kral, 2007). Thus, it is likely that both the decrease in A1 representation in deaf auditory cortex, accompanied by the decoupling of A1 from higher-order auditory cortical areas may account for this small reduction in cortical projection strength from A1 to deaf DZ.

Outside of A1, the dorsal auditory regions AAF, fAES and PAF have all been shown to exhibit some degree of cross-modal reorganization behaviorally and/or electrophysiologically, such that these areas respond to visual (AAF, fAES, PAF) and/or somatosensory (AAF) stimulation in early-deafened animals (Lomber et al., 2010; Meredith et al., 2011; Meredith and Lomber, 2011). Presumably, in the absence of auditory stimulation, existing visual and/or somatosensory inputs to these regions become strengthened or "unmasked" via Hebbian experience-dependent synaptic plasticity. If these "auditory" cortical regions are recruited by other sensory systems following deafness, temporally correlated activity may still occur (e.g. using existing visual inputs), which may be enough to maintain connectivity with other previously auditory regions. Although deaf auditory cortex may not function as a unit in the same way that it would in a hearing animal, these cross-modally reorganized areas might retain the need to communicate with one another, particularly if they are recruited by the same sensory modality (e.g. vision), which might account for why intra-auditory connections remained similar to those of hearing cats in the present study. As such, although the nature of communication between these areas is likely different in the absence of auditory input, the structure is retained to some degree.

2.5.5 Visual cortical projections to DZ in hearing animals

On the whole, projections to auditory cortical regions arising from areas outside of auditory cortex itself have received relatively little consideration, with

the exception of A1. Non-auditory sensory, multisensory and other non-sensory projections to A1 have been extensively documented in the rodent (Budinger et al., 2006, 2007, 2009). Additionally, Falchier et al. (2010) documented projections from select visual areas to caudal auditory cortex in the macaque. This stands in contrast to the visual system, in which a growing body of evidence supports the idea that auditory cortical regions project to both primary visual cortex (Falchier et al., 2002; Rockland and Ojima, 2003; Clavagnier et al., 2004; Hall and Lomber, 2008) and extrastriate visual cortical regions (Clemo et al. 2008; Laramee et al. 2011). Although two previous studies have characterized auditory cortical projections to DZ in hearing animals by means of retrograde tracing analysis (He and Hashikawa, 1998; Lee and Winer, 2008b), projections to DZ arising from areas outside of auditory cortex were not described in either study, despite scattered labeling being visibly present outside of auditory cortical regions in the figures (e.g. Figure 8D of Lee and Winer, 2008b). Lesions of the superficial suprasylvian fringe (now referred to as area DZ) have been reported to result in degeneration in both auditory and visual cortical regions (Paula-Barbosa et al., 1975). The pattern of visual cortical degradation is generally in good agreement with the pattern of visual cortical projections observed in the present study, although significant degradation found in area 17 might indicate that the lesions included part of visual area PLLS. An autoradiographic study also documented projections from PLLS to the suprasylvian fringe (Squatrito et al., 1981). Together, these studies support the idea that DZ receives input from visual cortical regions in the hearing animal, although the nature and strength of these projections have not previously been quantified.

Accordingly, the present study determined that a large proportion of ipsilateral cortical projections to DZ in the hearing animal arise from visual cortical areas, in addition to the auditory cortical projections previously documented. The visual projections described here arise mainly from the two visual areas abutting DZ: ALLS (>10%) and PLLS (>20%). Importantly, the projection from ALLS cannot be accounted for by encroachment of the lateral spread of the injection into ALLS itself, as the injection sites in the present study

were well posterior of ALLS. Encroachment of the injections into PLLS and dPE will be discussed in detail below (see *Technical considerations*). Electrophysiological recordings have indicated that there exist a population of bimodal neurons in PLLS at the PLLS-DZ border; that is, although most neurons in this region respond to visual stimuli alone, some can also be driven by auditory stimuli alone (Allman and Meredith, 2007). This is presumably a function of the density of auditory cortical projections to PLLS, which is high near the lateral bank of the suprasylvian sulcus, and decreases progressively toward the fundus (Clemo et al., 2008). As a result, bimodal responses give way to subthreshold auditory responses as the recording electrode travels deeper into PLLS toward the fundus. It is possible that these bimodal and subthreshold zones might exist bidirectionally, given that PLLS has been shown to project to the suprasylvian fringe (Squatrito et al., 1981). This represents an area of future study. Thus, although it is at first surprising that the proportion of auditory cortical projections is roughly equal to the proportion of visual cortical projections in the hearing animal, the vast majority of these visual projections arise from the visual areas that border DZ.

2.5.6 Comparison to late- and early-deafened animals

In all animals, labeling was strongest on the lateral bank, and decreased in density toward the fundus. In hearing animals, neuronal labeling was restricted almost exclusively to the lateral bank, with sparse labeling in the fundus between A2-A8 (**Figure 2.13 D**). Interestingly, in deafened animals, the projection strength from the anterior region of the lateral suprasylvian bank (ALLS) is reduced, while projection strength from the posterior region of the lateral suprasylvian bank (PLLS) is increased. In both early- and late-deafened animals, this manifested as an increase in labeling density in PLLS (**Figure 2.13 E, F**). In addition, labeling in deafened animals extended up the opposing medial bank, particularly at more posterior levels (A2-P3; **Figure 2.13 E, F**).

These findings were consistent across all animals in both the early- and late-deafened groups. Additionally, in deafened animals, scattered labeling was

found in the fundus and medial bank of the most posterior part of the middle suprasylvian sulcus, corresponding to the part of area PMLS in which foveal vision is represented, according to previous electrophysiological work (Palmer et al., 1978). Projections from this region were remarkably consistent and were present in every deafened animal, but were notably absent in each hearing animal. Although labeling was present in PMLS in hearing animals, it was always located near the PLLS/PMLS border, particularly at the fundus in more anterior sections. PLLS and PMLS are known to be involved in visual motion processing in the cat (Li et al., 2001; Rauschecker et al., 1987), and PMLS is widely considered to be the homolog of the middle temporal (MT)/area V5 in the primate (Payne, 1993). Congenitally deaf animals have been shown behaviorally to exhibit lower motion detection thresholds compared to hearing animals (Lomber et al., 2010). When Lomber and colleagues cortically cooled area DZ, it was shown that deactivating this region of auditory cortex abolished this behavioral

Figure 2.13 Pattern of labeling within the middle suprasylvian sulcus.

Comparison of labelled cell positions in visual cortex and characteristic visual receptive field positions. Visual representation of averaged number and density of labeled neurons within PLLS and PMLS plotted onto a flattened view of the middle suprasylvian cortex as modified from Palmer et al. (1978). **A:** Lateral view of the cat brain with a portion of the middle suprasylvian sulcus highlighted. **B:** The highlighted region of cortex in A unfolded using the fundus of the sulcus (solid black line) as a hinge. Areal boundaries are indicated with dashed lines. **C:** Representation of the visual hemifield. The horizontal meridian (HM) is indicated by a thick dashed line, whereas the vertical meridian (VM) is represented by a finely dashed line. All numbers indicate degrees of the visual field. **D-F:** Averaged representation of neuronal labeling for hearing (**D**; black), late-deafened (**E**; blue), and early-deafened (**F**; red) animals following a DZ injection. The dark grey shading corresponds to the region of PMLS where foveal vision is represented. The light grey region adjacent to the foveal representation corresponds to the portion of the visual field lying within 5 degrees of the fovea. Thick dashed lines indicate HM and areas represented parallel to HM as indicated numerically. Finer dashed lines indicate VM with parallel representations indicated numerically.

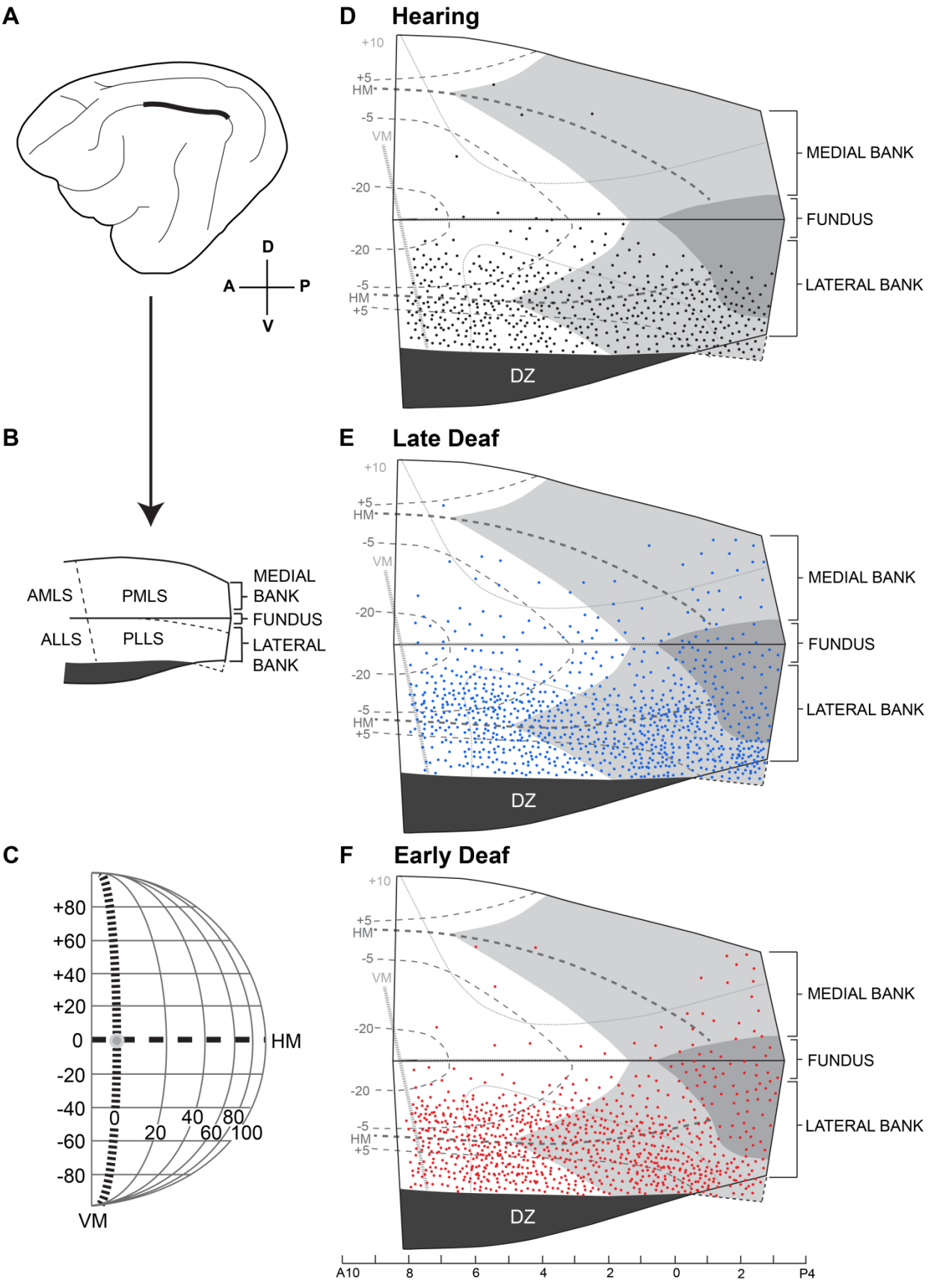
A
D
A
P
V
B
AMLS
PMLS
ALLS
PLLS
MEDIAL BANK
FUNDUS
LATERAL BANK
C
+80
+60
+40
+20
0
-20
-40
-60
-80
HM
0
20
40
60
80
100
VM
D Hearing
E Late Deaf
F Early Deaf
+10
+5
HM
-5
VM
-20
DZ
MEDIAL BANK
FUNDUS
LATERAL BANK
A10
8
6
4
2
0
2
P4

advantage. As such, it was concluded that DZ is cross-modally reorganized in deafness, such that it becomes involved in visual motion detection, and mediates the lower motion detection threshold advantage. The results of the current study suggest that the amplified projections from extrastriate visual cortical regions involved in visual motion processing may provide an anatomical basis for this cross-modal reorganization. Further, this appears to come at the cost of connectivity with anterior regions of the lateral suprasylvian area, as well as connectivity with other auditory cortical regions. These connections are not completely abolished following deafness, but they are reduced in deafened compared to hearing animals.

A number of regions located on the posterior bank of the posterior suprasylvian sulcus (area 21b, DLS, and PS) showed evidence of increases in projection strength in late-deafened animals only, when compared to early-deafened and hearing animals. It should be noted that these increases were not consistent across all late-deafened animals, but rather, seemed to be driven by very strong projections in a subset of animals. Area PS is known to send a moderate projection to dPE, and area 21b is known to weakly project to area dPE as well (Lee and Winer 2008b). Based on this, one explanation for the increase in projection strength for these areas in late-deafened animals might be that on average, the lateral extent of the injections encroached into dPE to a greater extent in the late-deafened group compared to the other groups. However, iPE is strongly connected with dPE, while areas 20a, In and vPE are moderately connected with dPE (Lee and Winer, 2008b). If it were true that this increase in projection strength were solely due to encroachment of the injection sites into dPE, I would expect that connectivity to these areas would be increased as well. This is not the case; if anything, projection strength to these areas in the late-deafened animal is actually slightly lower than in the hearing and early-deafened animals.

Similarly, a second explanation might be that the lateral extent of the injections in late-deafened animals encroached on PLLS to a greater degree than

in hearing or early-deafened animals. This is more plausible than the case for dPE encroachment, given that PLLS is known to receive strong projections from areas DLS and PS, but nothing from area 21b (Symonds and Rosenquist, 1984; Scannell et al., 1995). PLLS is additionally known to receive intermediate projections from areas ALLS, 18 and 20a (Symonds and Rosenquist, 1984; Scannell et al., 1995). I would then expect to see an increase in the projection strength to these areas in the late-deafened animals compared to the other two groups, and in fact, there are very slight, non-statistically significant increases in projection strength to areas 18 and 20a in the late-deafened animals, although in both cases, the strength of this increase is less than 0.15%. However, there is a very strong decrease in projection strength to ALLS (over 7%). Thus, I cannot claim that the increases in projection strength for area 21b, DLS and PS are a unique feature of cross-modal reorganization in the late-deafened animal; rather, it is possible that the lateral extent of the injections may have encroached into areas dPE and/or PLLS to a greater degree in some late-deafened animals.

2.5.7 Other considerations

It is not possible to expose areas occupying small regions of cortex to larger volumes of tracer without small incursions into neighboring areas (A1, AAF, dPE, PLLS). I have considered these incursions negligible because the pattern of labeling observed in the current study is most consistent with DZ injection sites. First, the profile of auditory cortical projections in hearing animals in our study was similar to that previously reported for DZ injections in two other experiments (He and Hashikawa, 1998; Lee and Winer, 2008b), and do not resemble the pattern of projections documented for other auditory cortical regions. Secondly, our results differ from the pattern of projections that would be expected with a significant encroachment into each of these areas. A1 and AAF have previously been reported to receive strong projections from VAF, and A1 is additionally known to receive strong projections from VPAF (Lee and Winer, 2008b). Our results indicate a very weak projection from both VAF and VPAF, which would be more consistent with DZ injection sites. Similarly, dPE receives

strong projections from area 7, visual areas 20a and 20b, as well as auditory areas iPE, VPAF, T and In (Scannell et al., 1995; Lee and Winer, 2008b). Very weak projections (<1%) were observed from each of these areas, which again, would be more consistent with DZ injection sites. Finally, PLLS is known to receive strong projections from the anterior ectosylvian visual area (AEV), DLS and PS (Symonds and Rosenquist, 1984; Scannell et al., 1995). In our study, projections from both of these areas amounted to less than 1% for areas AEV and PS, and 2% for DLS. Additionally, projections to PLLS have previously been reported for areas 17, 18 and 20a (Symonds and Rosenquist, 1984; Scannell et al., 1995) which are largely absent in the hearing animals in our experiment (0.00% for areas 17 and 18; <0.4% for 20a). Thus, although I cannot rule out any spread of our injections into these regions, it seems likely that any encroachment was minimal.

Similarly, it might be argued that because DZ is known to be laterally displaced in early-deafened animals (Lomber et al., 2010; Wong et al., 2013), that area PLLS was injected in the early-deafened animals, or that the lateral spread of the injection into PLLS was greater, which may account for the increased proportion of visual cortical projections to the DZ in these animals. Two lines of evidence argue against this: 1) greater encroachment into PLLS would be expected to yield increases in projection strength in the early deaf to cortical regions that PLLS is known to send strong projections to, namely, AEV, DLS and PS (Symonds and Rosenquist, 1984; Scannell et al., 1995). However, projection strength is remarkably consistent between hearing and early-deafened animals for these three regions, and is actually slightly decreased in the early deaf in DLS and PS; 2) any increases in the percentage of projections from visual cortical areas between hearing and deafened animals are fairly consistent regardless of whether the animal was early or late-deafened, and there is no evidence to suggest that DZ is shifted laterally in late-deafened animals. The same argument could be made with respect to dPE, even though any border displacement has not been documented for this area following deafness. Again, I would then expect increases in projection strength in deafened animals to

regions that dPE is known to receive strong projections from (areas 7, 20a and 20b, iPE, VPAF, T and In). Projection strength from these regions is actually decreased in both early- and late-deafened animals (except for a slight increase in area 20a in late-deafened animals only). Therefore, a greater encroachment of our injections into either PLLS or dPE in deafened animals compared to hearing does not seem to account for the changes in connectivity observed following deafness in the present study.

2.5.8 Summary and conclusions

Structural cross-modal reorganization following deafness was examined following injections of retrograde tracer into the posterior suprasylvian fringe in early and late-deafened animals, as well as hearing controls. This area corresponds to auditory cortical region DZ, which is known to undergo cross-modal reorganization in the early-deaf animal. There was a progressive increase in projection strength between hearing, late- and early-deafened from an extrastriate visual cortical region known to be involved in the processing of visual motion, the PLLS (**Figure 2.14 B, C**). Additionally, there was a corresponding decrease in projection strength from ALLS, a region thought to be involved in complex visual processing. Although no change was documented for visual area PMLS as a whole, labeled neurons were present within a subregion of PMLS devoted to foveal vision in both late- and early-deafened animals, but not in hearing controls. PMLS is also an extrastriate visual motion processing area, and is widely considered to be the homolog of primate area MT (Payne, 1993). No differences in projection strength from auditory, somatosensory, multisensory/associative, or other visual cortical regions were observed between groups (**Figure 2.14 B, C**). The results of the current study provide an anatomical basis for previously published behavioral findings indicating that deaf DZ is cross-modally reorganized to participate in visual motion processing (Lomber et al., 2010). These results are similar to those of Karlen et al. (2009), who found that primary visual cortex of bilaterally enucleated opossums retains connectivity with the same cortical areas as that of opossums with normal vision, but also receives projections from somatosensory cortex (absent in animals with normal

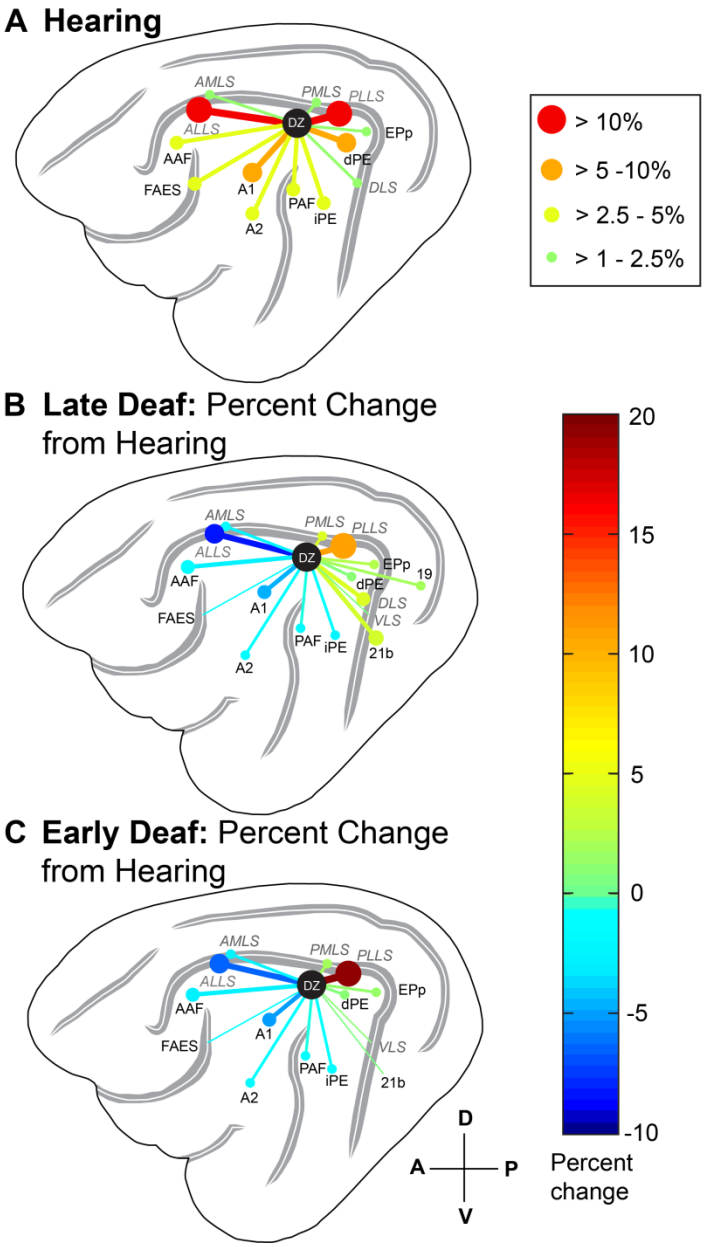

Figure 2.14 Projections present in hearing animals and change in projection strength following late- and early-deafness.

A: Summary of projection strength from auditory and visual cortical areas to DZ in the hearing animal. Only projections greater than 1% in strength are plotted, as indicated by the legend to the right. Note that DZ receives projections from all dorsal auditory cortical regions, with little input from ventral auditory cortical regions (<1%). There exist additional projections from visual cortical regions, even in the hearing animal, but these are largely limited to the regions bordering

DZ. **B-C:** Changes in projection strength to DZ between hearing and late- and early-deafened animals, respectively. Only changes greater than 0.5% in magnitude are plotted. Statistically significant changes are in bold, plotted in full contrast, and significance level is indicated with asterisks. Significance levels are indicated by asterisks as follows: ** $p < 0.01$, *** $p < 0.001$. Non-statistically significant trends are plotted in faded colours for comparison. In general, decreases in projection strength are plotted in shades of blue, whereas increases are plotted in "warmer" colours (green, yellow, orange, and red as shown in the scale on the right).

---

vision), as well as amplified projections from auditory and multimodal cortices. Taken together, these results suggest that factors both intrinsic and extrinsic to the individual play a significant role in cortical development – that there seems to be a template for cortical connectivity that is laid down independent of sensorystimulation, which is modifiable to some degree as a consequence of experience (Katz and Shatz, 1996).

The results of the current study also support previously published findings suggesting that cross-modal reorganization can occur following damage to mature sensory systems (Rebillard et al., 1977; Shepherd et al., 1999; Allman et al., 2009; Park et al., 2010). In addition, the increase in projection strength from PLLS is greater in magnitude for early-deafened animals compared to late-deafened. These results then also support the notion that the degree to which compensation can occur later in life follows the timeline of developmental plasticity constraints; that is, that plasticity of the system is generally reduced if damage to the system occurs after the closing of sensitive periods (see Hensch, 2004 for review).

Plasticity is known to be mediated synaptically, and can effect change in two ways: 1) via the strengthening of existing synapses, and/or 2) via the formation and elimination of synapses (for review see Holtmaat and Svoboda, 2009). Both types of synaptic plasticity have been demonstrated to extend into adulthood (Chen and Nedivi, 2010). The methodology of the present study

addresses the second type of synaptic plasticity; that is, the changes described above reflect the formation of new synapses. However, it is probable that both types of synaptic plasticity operate in conjunction to give rise to functional changes that are ultimately observable on a behavioral level. Given that the present study also documented existing projections from multiple extrastriate visual areas to DZ in the hearing animal, it is possible that these projections may become unmasked or receive greater functional weighting following deafness. In support of this, only 2 of more than 30 individual cortical regions examined documented statistically significant changes in projection strength between hearing and deafened animals. Similar intermodal connectivity has been documented in intact, enucleated and anophthalmic mice (Charbonneau et al., 2012). Together, these studies suggest that following sensory deprivation, both visual and auditory cortex may make use of already present cross-sensory cortical connections, which may account for the lack of widespread reorganization between groups in multiple cortical regions. However, future studies incorporating functional methodologies will be needed to confirm this.

2.6 References

Allman B, Keniston LP, Meredith MA (2009) Adult deafness induces somatosensory conversion of ferret auditory cortex. Proc Natl Acad Sci 106: 5925-5930.

Allman BL, Meredith MA (2007) Multisensory processing in “unimodal” neurons: cross-modal subthreshold auditory effects in cat extrastriate visual cortex. J Neurophysiol 98:545–549.

Bavelier D, Tomann A, Hutton C, Mitchell T, Corina D, Liu G, Neville H (2000) Visual attention to the periphery is enhanced in congenitally deaf individuals. J Neurosci 20:1-6.

Bavelier D, Neville HJ (2002) Cross-modal plasticity: where and how? Nat Rev Neurosci 3:443–452.

Barone P, Lacassagne L, Kral A. (2013). Reorganization of the connectivity of cortical field DZ in congenitally deaf cat. PLoS One 8:e60093.

Beaver BV, Reed W, Leary S, McKiernan B, Bain F, Schultz R, Bennett BT, Pascoe P, Schull E, Cork LC, Francis-Floyd R, Amass KD, Johnson RJ, Schmidt RH, Underwood W, Thorton GW, Kohn B. (2001). 2000 report of the American Veterinary Medical association Panel of Euthanasia. J Am Vet Med Assoc 218:669-696.

Beneyto M, Winer JA, Larue DT, Prieto JJ. 1998. Auditory connections and neurochemistry of the sagulum. J Comp Neurol 401:329-351.

Bowman EM, Olson CR (1988) Visual and auditory association areas of the cat's posterior ectosylvian gyrus: cortical afferents. J Comp Neurol 272:30–42.

Büchel C, Price C, Frackowiak RSJ, Friston K (1998) Different activation patterns in the visual cortex of late and congenitally blind subjects. Brain 121:409–419.

Charbonneau V, Laramee M-E, Boucher V, Bronchti G, Boire D (2012) Cortical and subcortical projections to primary visual cortex in anophthalmic, enucleated and sighted mice. Eur J Neurosci 36:2949-63.

Chen JL, Nedivi E (2010) Neuronal structural remodeling: Is it all about access? Curr Opin Neurobiol 20:557-62.

Clasca F, Llamas A, Reinoso-Suárez F (1997) Insular cortex and neighboring fields in the cat: a redefinition based on cortical microarchitecture and connections with the thalamus. J Comp Neur 384:456-82.

Clavagnier S, Falchier A, Kennedy H (2004) Long-distance feedback projections to area V1: implications for multisensory integration, spatial awareness, and visual consciousness. Cogn Affect Behav Neurosci 4:117–126.

Clemo HR, Sharma GK, Allman BL, Meredith MA (2008) Auditory projections to extrastriate visual cortex: connectional basis for multisensory processing in "unimodal" visual neurons. Exp Brain Res 191:37–47.

Cohen LG, Weeks RA, Sadato N, Celnik P, Ishii K, Hallett M (1999) Period of susceptibility for cross-modal plasticity in the blind. Ann Neurol 45:451–460.

D'Anguilli A, Waraich P (2002) Enhanced tactile encoding and memory recognition in congenital blindness. Int J Rehabil Res 25:143-145.

Elidan J, Lin J, Honrubia V (1986) The effect of loop diuretics on the vestibular system: Assessment by recording the vestibular evoked response. Arch Otolaryngol Head Neck Surg 112:836-839.

Falchier A, Clavagnier S, Barone P, Kennedy G (2002) Anatomical evidence of multimodal integration in primate striate cortex. J Neurosci 22:5749–5759.

Falchier A, Schroeder CE, Hackett TA, Lakatos P, Nascimento-Silva S, Ulbert I, Karmos G, Smiley JF (2010) Projection from visual areas V2 and prostriata to caudal auditory cortex in the monkey. Cereb Cortex 20:1529-1538.

Grant AC, Thiagarajah MC, Sathian K (2000) Tactile perception in blind Braille readers: a psychophysical study of acuity and hyperacuity using gratings and dot patterns. Percept Psychophys 62:301-312.

Hackett T (2011) Information flow in the auditory cortical network. Hear Res 271:133-146.

Hall AJ, Lomber SG (2008) Auditory cortex projections target the peripheral field representation of primary visual cortex. Exp Brain Res 190:413–430.

He J, Hashikawa T (1998) Connections of the dorsal zone of cat auditory cortex. J Comp Neurol 400:334–348.

Hensch T (2004) Critical period regulation. Ann Rev Neurosci 27: 549-79.

Holtmaat A, Svoboda K (2009) Experience-dependent structural synaptic plasticity in the mammalian brain. Nat Rev Neurosci 10:647-58.

Horsley V, Clarke RH (1908) The structure and function of the cerebellum examined by a new method. Brain 31:45-124.

Hunt DL, Yamoah EN, Krubitzer L (2006) Multisensory plasticity in congenitally deaf mice: how are cortical areas functionally specified? Neurosci 139:1507-24.

Katz LC, Shatz CJ (1996) Synaptic activity and the construction of cortical circuits. Science 274:1133-38.

Karlen SJ, Kahn DM, Krubitzer L (2006) Early blindness results in abnormal corticocortical and corticothalamic connections. Neuroscience 142:843-58.

Karns CM, Dow MW, Neville HJ (2012) Altered cross-modal processing in the primary auditory cortex of congenitally deaf adults: a visual-somatosensory fMRI study with a double-flash illusion. J Neurosci 32:6488-11.

Kral A, Schröder JH, Klinke R, Engel AK (2003) Absence of cross-modal reorganization in the primary auditory cortex of congenitally deaf cats. Exp Brain Res 153:605-13.

Kral A (2007) Unimodal and cross-modal plasticity in the “deaf” auditory cortex. Int J Audiol 46:479–493.

Kral A, Schröder J-H, Klinke R, Engel AK (2003) Absence of cross-modal reorganization in the primary auditory cortex of congenitally deaf cats. Exp Brain Res 153:605–613.

Kujala T, Alho K, Huotilainen M, Ilmoniemi RJ, Lehtokoski A, Leinonen A, Rinne T, Salonen O, Sinkkonen J, Standertskjold-Nordenstam C-G, Naatanen R (1997) Electrophysiological evidence for cross-modal plasticity in humans with early- and late-onset blindness. Psychophysiology 34:213–216.

Kujala T, Alho K, Näätänen R (2000) Cross-modal reorganization of human cortical functions. Trends Neurosci 23:115–120.

Laramee ME, Kurotani T, Rockland KS, Bronchti G, Boire D (2011) Indirect pathway between the primary auditory and visual cortices through layer V pyramidal neurons in V2L in mouse and the effects of bilateral enucleation. Eur J Neurosci 34:65-78.

Larsen DD, Luu JD, Burns ME, Krubitzer L (2009) What are the effects of severe visual impairment on the cortical organization and connectivity of primary visual cortex? Front Neuroanat 3:1-16.

Lee CC, Winer JA (2008a) Connections of cat auditory cortex: I. Thalamocortical system. J Comp Neurol 507:1879-900.

Lee CC, Winer JA (2008b) Connections of cat auditory cortex: III. Corticocortical system. J Comp Neurol 507:1920–1943.

Levanen S, Hamdof D (2001) Feeling vibrations: enhanced tactile sensitivity in congenitally deaf humans. Neurosci Lett 301:75-77.

Li BW, Chen Y, Wang LH, Diao YC (2001) Pattern and component motion selectivity in cortical area PMLS of the cat. Eur J Neurosci 14:690–700.

Lomber SG, Malhotra S (2008) Double dissociation of “what” and “where” processing in auditory cortex. Nat Neurosci 11: 609-616.

Lomber SG, Meredith MA, Kral A (2010) Cross-modal plasticity in specific auditory cortices underlies visual compensations in the deaf. Nat Neurosci 13:1421–1427.

Malhotra S, Hall AJ, Lomber SG (2004) Cortical control of sound localization in the cat: unilateral cooling deactivation of 19 cerebral areas. J Neurophys 92:1625-43.

Malhotra S, Lomber SG (2007) Sound localization during homotopic and heterotopic bilateral cooling deactivation of primary and nonprimary auditory cortical areas in the cat. J Neurophysiol 97:26–43.

Malhotra S, Stecker G, Middlebrooks J, Lomber SG (2008) Sound localization deficits during reversible deactivation of primary auditory cortex and/or the dorsal zone. J Neurophys 99:1628-42.

Mellott JG, van der Gucht E, Lee CC, Carrasco A, Winer JA, Lomber, SG (2010) Areas of cat auditory cortex as defined by neurofilament proteins expressing SMI-32. Hear Res 267:119-36.

Meredith MA, Kryklywy J, McMillan AJ, Malhotra S, Lum-Tai R, Lomber SG (2011) Crossmodal reorganization in the early deaf switches sensory, but not behavioral roles of auditory cortex. Proc Natl Acad Sci 108:8856–8861.

Meredith MA, Lomber SG (2011) Somatosensory and visual crossmodal plasticity in the anterior auditory field of early-deaf cats. Hear Res 280:38–47.

Middlebrooks JC, Zook JM (1983) Intrinsic organization of the cat's medial geniculate body identified by projections to binaural response-specific bands in the primary auditory cortex. J Neurosci 3:203-244.

Niimi K, Matsuoka H (1979) Thalamocortical organization of the auditory system in the cat studied by retrograde and axonal transport of horseradish peroxidase. Adv Anat Embryol Cell Biol 57:1-56.

Olfert E, Cross BM, McWilliam AA (1993) Guide to the Care and Use of Experimental Animals. Canadian Council on Animal Care. Ottawa, Ontario: Canadian Council on Animal Care.

Palmer LA, Rosenquist AC, Tusa RJ (1978) The retinotopic organization of lateral suprasylvian visual areas in the cat. J Comp Neurol 177:237–256.

Park MH, Lee HJ, Kim JS, Lee JS, Lee DS, Oh SH (2010) Cross-modal and compensatory plasticity in adult deafened cats: a longitudinal PET study. Brain Res 1354:85-90.

Paula-Barbosa MM, Feyo PB, Sousa-Pinto A (1975) The association connexions of the suprasylvian fringe (SF) and other areas of the cat auditory cortex. Exp Brain Res 23:535-554.

Payne BR (1993) Evidence for visual cortical area homologs in cat and macaque monkey. Cereb Cortex 3:1–25.

Payne BR, Lomber SG (1996) Age dependent modification of cytochrome oxidase activity in the cat dorsal lateral geniculate nucleus following removal of primary visual cortex. Vis Neurosci 13:805-816.

Rauschecker JP, von Grunau MW, Poulin C (1987) Centrifugal Organization of Direction Preferences in the Cat's Lateral Suprasylvian Visual Cortex and Its Relation to Flow Field Processing. J Neurosci 7:943–958.

Rauschecker J, Scott SK (2009) Maps and streams in the auditory cortex: nonhuman primates illuminate human speech processing. Nat Neurosci 12:718-724.

Read HL, Winer JA, Schreiner CE (2002) Functional architecture of auditory cortex. Curr Opinion Neurobiology 12:433-440.

Rebillard G, Carlier E, Rebillard M, Pujol R (1977) Enhancement of visual responses on the primary auditory cortex of the cat after an early destruction of cochlear receptors. Brain Res 129:162–164.

Reinoso-Suárez F (1961) Topographical atlas of the cat brain for experimental-physiological research. Darmstad, Federal Republic of Germany: Merck.

Rockland KS, Ojima H (2003) Multisensory convergence in calcarine visual areas in macaque monkey. J Psychophys 50:19–26.

Sathian K (2000) Practice makes perfect: sharper tactile perception in the blind. Neurol 54:2203-2204.

Sathian K (2005) Visual cortical activity during tactile perception in the sighted and the visually deprived. Dev Psychobiol 46:279–286.

Scannell JW, Blakemore C, Young MP (1995) Analysis of connectivity in the cat cerebral cortex. J Neurosci 15:1463–1483.

Shepherd RK, Baxi JH, Hardie NA (1999) Response of inferior colliculus neurons to electrical stimulation of the auditory nerve in neonatally deafened cats. J Neurophysiol 82:1363–1380.

Shipley C, Buchwald JS, Norman R, Guthrie D (1980) Brain stem auditory evoked response development in the kitten. Brain Res 182(2):313-26.

Squatrito S, Galletti C, Battaglini PP, Sanseverino ER (1981) An autoradiographic study of bilateral cortical projections from cat area 19 and lateral suprasylvian visual area. Arch Ital Biol 119:21-42.

Stecker G, Harrington I, Macpherson EA, Middlebrooks JC (2005) Spatial sensitivity in the dorsal zone (area DZ) of cat auditory cortex. J Neurophys 2:1267-80.

Sternberger LA and Sternberger NH (1983) Monoclonal antibodies distinguish phosphorylated and nonphosphorylated forms of neurofilaments in situ. Proc Natl Acad Sci USA 80:6126-30.

Stewart DL and Starr A (1970) Absence of visually influenced cells in auditory cortex of normal and congenitally deaf cats. Exp Neurol 28:525-8.

Symonds LL, Rosenquist AC (1984) Corticocortical connections among visual areas in the cat. J Comp Neurol 229:1–38.

Updyke B V (1986) Retinotopic organization within the cat's posterior suprasylvian sulcus and gyrus. J Comp Neurol 246:265–280.

van der Gucht E, Vandesande F, Arckens L (2001) Neurofilament Protein : A Selective Marker for the Architectonic Parcellation of the Visual Cortex in Adult Cat Brain. J Comp Neurol 441:345–368.

Veenman CL, Reiner A, Honig MG (1992) Biotinylated dextran amine as an anterograde tracer for single- and double-labeling studies. J Neurosci Methods 41:239-54.

Weeks R, Horwitz B, Aziz-Sultan A, Tian B, Wessinger CM, Cohen LG (2004) A positron emission tomographic study of auditory localization in the congenitally blind. J Neurosci 20:2664–2672.

Woolsey CN (1960) Organization of cortical auditory system: a review and synthesis. In: Rasmussen GL, Windle WF, editors. Neural Mechanisms of the Auditory and Vestibular Systems. Springfield: Thomas. pp. 165-180.

Wong C, Chabot N, Kok MA, Lomber SG (2013) Modified areal cartography in auditory cortex following early and late-onset deafness. Cereb Cortex, doi: 10.1093/cercor/bht026.

Wong-Riley, MT (1979) Changes in the visual system of the monocularly sutured or enucleated cats demonstrable with cytochrome oxidase histochemistry. Brain Res 171:11-28.

Xu SA, Shepherd RK, Chen Y, Clark GM (1993) Profound hearing loss in the cat following the single co-administration of kanamycin and ethacrynic acid. Hear Res 70:205-215.

Chapter 3: Dissociable influences of primary auditory cortex and the posterior auditory field on neuronal responses in the dorsal zone of auditory cortex[3]

3.1 Abstract.

Current models of hierarchical processing in auditory cortex have been based principally on anatomical connectivity while functional interactions between individual regions have remained largely unexplored. Previous cortical deactivation studies in the cat have addressed functional reciprocal connectivity between primary auditory cortex (A1) and other hierarchically lower-level fields. The present study sought to assess the functional contribution of inputs along multiple stages of the current hierarchical model to a higher-order area, the dorsal zone (DZ) of auditory cortex in the anaesthetized cat. Cryoloops were placed over A1 and posterior auditory field (PAF). Multiunit neuronal responses to noise burst and tonal stimuli were recorded in DZ during cortical deactivation of each field individually and in concert. Deactivation of A1 suppressed peak neuronal responses in DZ regardless of stimulus and resulted in increased minimum thresholds and reduced absolute bandwidths for tone frequency receptive fields in DZ. PAF deactivation had less robust effects on DZ firing rates and receptive fields compared to A1 deactivation, and combined A1/PAF cooling was largely driven by the effects of A1 deactivation at the population level. These results provide physiological support for the current anatomically-based model of both serial and parallel processing schemes in auditory cortical hierarchical organization.

[3] A version of this chapter is published as:

Kok MA, Stolzberg D, Brown TA, Lomber SG (2015) Dissociable influences of primary auditory cortex and the posterior auditory field on neuronal responses in the dorsal zone of auditory cortex. J Neurophysiol 113:475-486.

3.2 Introduction

The past two decades have witnessed a dramatic increase in brain connectivity studies with advances in functional imaging analysis methodology, providing the ability to non-invasively assess dependence between brain regions (Friston, 2011). While a thorough understanding of the structural connectivity of the brain is a necessary component for understanding network function (Sporns, 2012), investigations regarding the degree to which one brain region can exert influence on another are critical, as anatomical connectivity alone "is neither a sufficient nor a complete description of connectivity" (Friston, 2011). Hierarchical processing schemes for cat auditory cortex have been proposed based mainly on structural connectivity analyses between individual regions of auditory cortex (**Figure 3.1**; Rouiller et al., 1991; Lee and Winer, 2011), while the functional importance of these connections has remained largely unexplored. Using cortical cooling deactivation, previous studies have addressed functional reciprocal connectivity between primary auditory cortex (A1) and the anterior and posterior auditory fields (AAF and PAF), as well as second auditory cortex (A2; Carrasco and Lomber, 2009a, 2010). However, functional interactions for higher-order fields of the hierarchy have not been investigated to date.

The present study expanded this functional assessment of inputs along multiple stations of the proposed hierarchical scheme to a higher-order auditory area, the dorsal zone (DZ). Although a specific, unique role in auditory cortical processing has not been identified for DZ, both behavioral (Malhotra and Lomber, 2007) and electrophysiological (Stecker et al., 2005) evidence suggests that DZ is involved in auditory spatial perception, and as such, may be part of a "where" stream for auditory spatial processing in the cat. DZ has also been proposed to be involved in processing the more complex aspects of sound in the frequency and time domains based on the discovery of duration-tuned neurons in the area (He et al., 1997). Furthermore, DZ has been suggested to form part of a functional auditory belt region because responses in DZ exhibit more complex

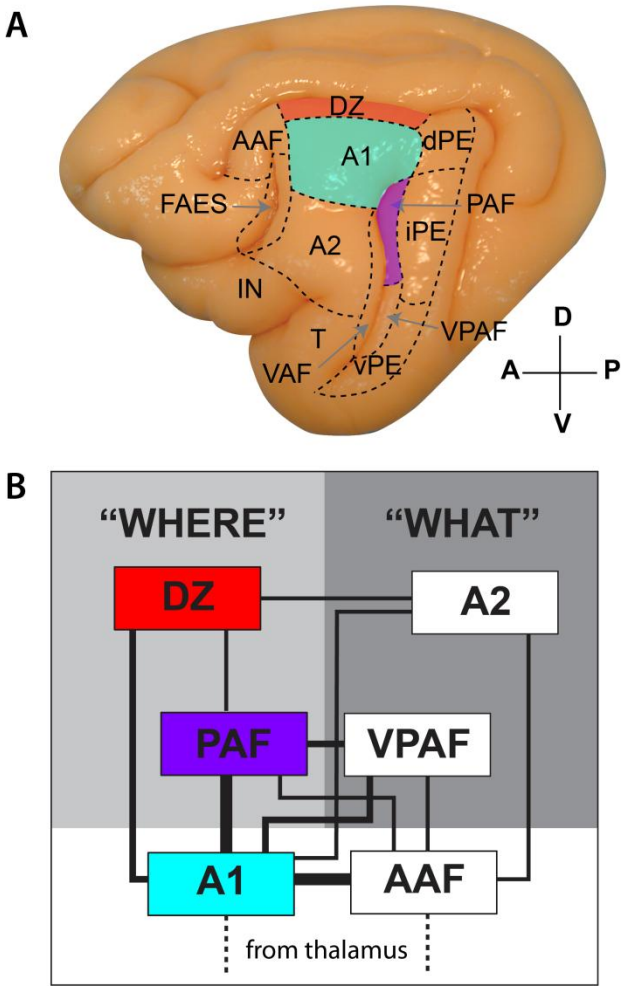

Figure 3.1 Organization and hierarchical connections of cat auditory cortex.

A: Lateral view of the left hemisphere of the cat depicting the thirteen regions of auditory cortex, bounded by dashed lines. The region highlighted in red corresponds to the location of the area targeted in the current study, the dorsal zone of auditory cortex (DZ). A1 (cyan) and PAF (purple) were reversibly deactivated in the present study because they comprise two of the largest auditory cortical inputs to DZ. **B:** Schematic view of the proposed hierarchical connections of auditory cortical areas, based on cortical and thalamic connectivity. Core regions A1 and AAF occupy the lowest region in the hierarchy, with PAF and DZ streamed into the putative "where" pathway, and occupying higher positions. Line thickness is indicative of connectional strength: strong (thick), medium, and weak (thin). Figure adapted from Lee and Winer (2011).

frequency tuning, non-monotonicity, and have longer response latencies and broader tuning curves (He et al., 1997; Middlebrooks and Zook, 1983; Stecker et al., 2005) than core regions A1 and AAF, which are characterized by simple, linear responses with short response latencies and sharp tuning curves (Carrasco and Lomber, 2011; Stecker et al., 2005; Sutter and Schreiner, 1991). Thalamocortical connectivity analyses further support this designation (He and Hashikawa, 1998), as thalamocortical projections to DZ in the cat (Lee and Winer, 2008a) match those documented for belt regions of primate auditory cortex (Kaas et al., 1999).

Because A1 and PAF comprise two of the largest anatomical auditory cortical inputs to DZ (Barone et al., 2013; He and Hashikawa, 1998; Kok et al., 2014; Lee and Winer, 2008b), and because both cortical regions are known to be involved in auditory spatial processing (**Figure 3.1**; (Malhotra and Lomber, 2007; Malhotra et al., 2008; Stecker et al., 2005)), I predicted that reversible deactivation of these areas would reduce neuronal response rates in DZ. Our results confirmed this hypothesis, providing physiological support for previously proposed anatomically-based models of auditory cortical hierarchy involving both serial and parallel processing.

3.3 Materials and Methods

3.3.1 Overview.

Neuronal responses to auditory stimuli were assessed in eight healthy adult (> 6 month old) cats of both sexes (*Felis catus*; Liberty Labs, Waverly, NY). All animals were housed in an enriched colony environment with unrestricted access to food and water. All experimental procedures were conducted in compliance with the National Research Council's *Guidelines for the Care and Use of Mammals in Neuroscience and Behavioral Research* (2003), the Canadian Council on Animal Care's *Guide to the Care and Use of Experimental Animals* (Olfert et al., 1993) and were approved by the Animal Use Subcommittee of the University Council on Animal Care at the University of

Western Ontario. Surgical procedures used in the present study have previously been described in the literature (Carrasco and Lomber, 2009a). A brief synopsis of the methodology is presented below.

3.3.2 Surgical procedures

Approximately two weeks before electrophysiological recording, animals underwent surgery to perform a craniotomy, implant a cryoloop over PAF and attach a head holder for use during electrophysiological procedures. Cryoloops were custom made for PAF according to previously published methods (Lomber et al., 1999; Malhotra et al., 2004). A heat-shielding compound was applied to the anterior surface of the loop prior to implantation in order to limit the spread of cooling to the dorsal aspect of the posterior bank of the posterior ectosylvian sulcus. This prevented any direct effect of PAF cooling on A1 (Lomber et al., 2007; see the *Data Acquisition* subsection below for more detailed information). The loops were then sterilized with ethylene oxide gas prior to implantation. On the day of surgery, animals were anesthetized using sodium pentobarbital (25 mg/kg to effect, i.v.), followed by supplemental doses as required. Animals were intubated and respiration remained unassisted throughout the surgical procedure. Body temperature, respiration rate, heart rate, blood pressure and end tidal CO2 were monitored continuously. A craniotomy was made over the left hemisphere between coordinates A2-A12 (Horsley and Clarke, 1908), in order to expose auditory cortex. The dura was opened over the posterior ectosylvian sulcus and an arachnoid hook was used to dissect the arachnoid mater over the sulcus. A custom-made cooling loop was inserted into the dorso-posterior aspect of the sulcus (corresponding to area PAF) and secured to the cranium using stainless steel bone screws and dental acrylic. The craniotomy was closed with dental cement and a head holder was attached to the frontal bone of the skull using dental acrylic and bone screws. The animal was then provided with standard postoperative care (see Malhotra et al., 2004). In all cases, recovery was uneventful.

Approximately two weeks following surgery, electrophysiological recording procedures were initiated. Animals were administered atropine (0.02 mg/kg, s.c.), dexamethasone (0.5 mg/kg, s.c.), acepromazine (0.4 mg/kg, i.m.), and sodium pentobarbital (25 mg/kg to effect, i.v.). The animal was then intubated and respiration remained unassisted for the duration of the experiment, although supplemental oxygen was supplied if blood oxygen saturation fell below 90%. Indwelling feline catheters were inserted into the saphenous vein bilaterally, as well as the left cephalic vein. The animal was secured to a stereotaxic frame using the head holder previously implanted. The dental acrylic over the craniotomy was removed and the dura was resected in preparation for recording. A layer of silicone oil was applied to the cortex to prevent desiccation. A warm water circulating pad (Gaymar, Orchard Park, NY) was used to maintain core body temperature. Animals were hydrated throughout the experiment using an infusion pump supplied with 2.5% dextrose/half-strength lactated Ringer's solution (4 ml/kg/h, i.v.). Dexamethasone (1.0 mg/kg, i.v.) and atropine (0.03 mg/kg, s.c.) were administered on a 24 hour schedule for the duration of the experiment. A digital image of the exposed cortex was taken with the aid of a surgical microscope in order to record the position of each electrode penetration relative to cerebral vasculature and cortical topography.

3.3.3 Stimulus generation and presentation

Recordings took place within a double-walled sound chamber on an electrically shielded, vibration-free table (Technical Manufacturing Corporation, Peabody, MA). Acoustic signals were generated with a 24-bit digital-to-analog converter at ~156 kHz sampling rate (Tucker-Davis Technologies, Alachua, FL) and presented open-field 15 cm from the midline of the head contralateral to the craniotomy (FF1, Tucker-Davis Technologies, Alachua, FL). There were no obstacles situated between the ear contralateral to the craniotomy (right ear) and the speaker, which was in line with the ears (i.e. at an azimuth of 90º relative to the nose). All stimuli were 25 ms in duration, had 5 ms rise and fall times, were cosine squared gated, and were presented at a rate of 2 Hz. To determine the

size and approximate boundaries of A1 and AAF based on cochleotopic organization (Merzenich et al., 1975; Knight, 1977), pure tones of varying frequency (0.5 to 64 kHz in 1/16 octave steps) and intensity (0-80 dB in 5 dB steps) were presented during cortical mapping procedures. Each frequency-intensity combination was presented once in pseudorandomized fashion. Subsequently, sites in DZ were recorded while A1 and PAF were subjected to reversible deactivation, during which three sets of acoustic stimuli were presented: 1) Noise bursts (65 dB SPL; 1-32 kHz bandwidth), 600 repetitions per cooling phase; 2) noise bursts of varying intensity (Noise rate-intensity function (RIF); 0-80 dB SPL in 10 dB steps), 100 repetitions of each sound intensity (pseudorandomized) per cooling phase; 3) pure tones of varying frequency (Tones; 0.5-64 kHz in 1/16 octave steps) and intensity (0-80 dB SPL in 10 dB steps). Each frequency-intensity combination was presented in pseudorandomized fashion five times per cooling phase.

3.3.4 Data acquisition

Neuronal responses to auditory stimuli were collected using parylene-coated tungsten microelectrodes positioned in a 2x2 configuration spaced 115µm apart (FHC, Bowdoin, ME). Impedance measures ranged from 1-2MΩ. Neuronal activity was band-pass filtered from 300-5,000 Hz. All activity was amplified (x10,000) and digitized at ~25 kHz (RZ2, Tucker-Davis Technologies; Alachua, FL). In all animals, frequency-intensity receptive fields were generated for sites spanning A1, A2 and AAF, in order to generate a map of tonotopic organization (**Figure 3.2 A**; Merzenich et al., 1975; Knight, 1977; Reale and Imig, 1980). This was used to determine the borders of A1 to guide accurate placement of the A1 cryoloop. No cortical deactivation was induced during cortical mapping procedures.

Following this, an appropriately sized and shaped cooling loop was selected for placement within the boundaries of A1 (**Figure 3.2 B**). In general, A1 cryoloops were placed over the mid- to low- frequency representations (i.e. below ~20 kHz isofrequency band) in order to ensure that cooling deactivation did not

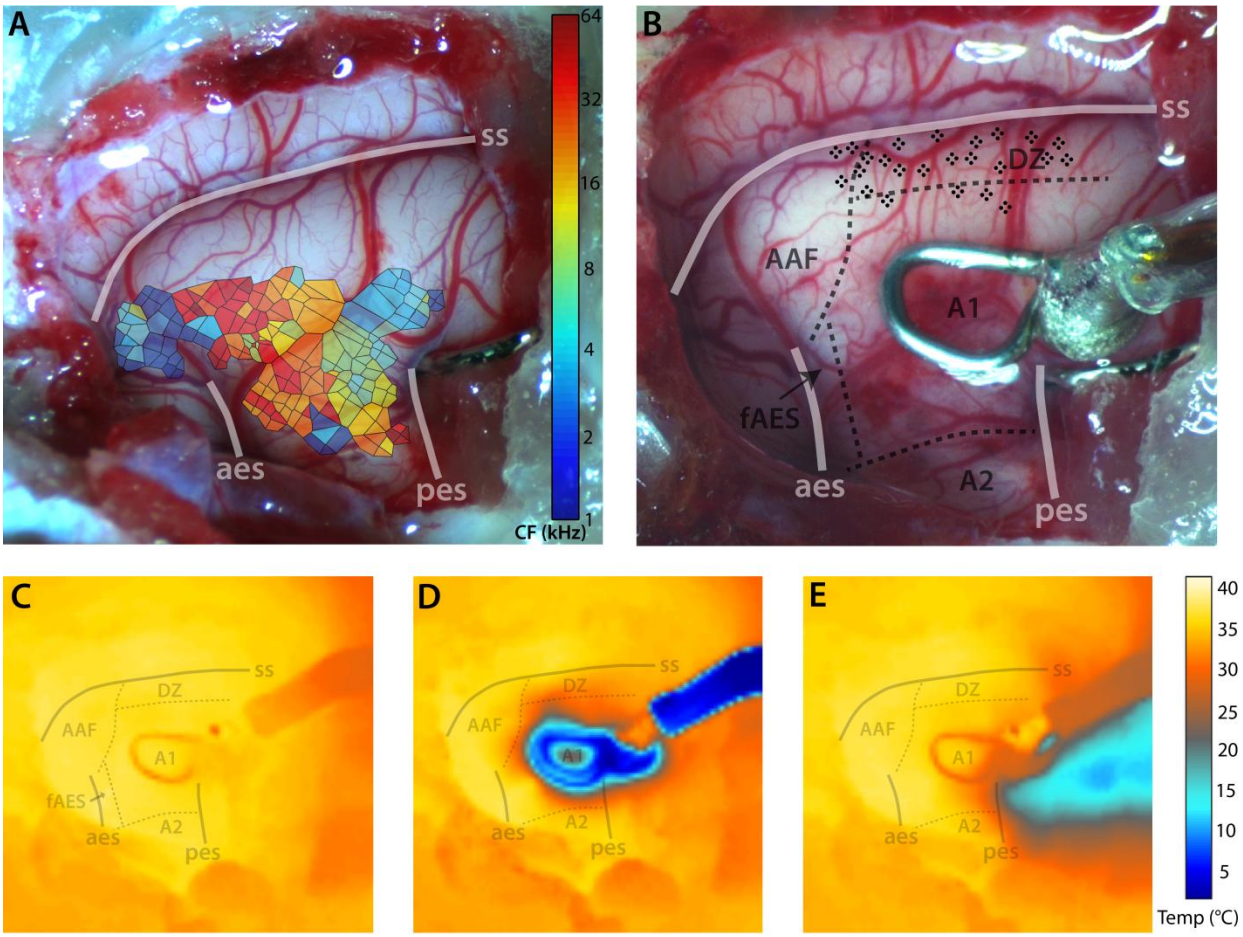

Figure 3.2 Position of cryoloops and extent of cortical deactivation.

A: Characteristic frequency (CF) map constructed using Voronoi tessellations of AAF and A1 tone responses at each recording site superimposed onto a photomicrograph of the craniotomy. This map was used to guide placement of the A1 cryoloop. **B:** Photomicrograph of the same craniotomy in A after placement the A1 cryoloop. The borders delimiting cortical field boundaries as determined by SMI-32 labeling are indicated by dashed grey lines. Each black dot indicates a recording site at which reversible deactivation of A1 and PAF were induced. **C-E:** Thermal images taken while cortex was warm (C), during A1 deactivation (D), and during PAF deactivation (E). Abbreviations as in Figure 3.1; aes, anterior ectosylvian sulcus; pes, posterior ectosylvian sulcus; ss, suprasylvian sulcus.

spread past the high-frequency reversal demarcating the A1/AAF border (**Figure 3.2 B**; see (Carrasco and Lomber, 2009 a, b, 2010). The A1/DZ border was not mapped, in order to avoid damaging potential recording sites in or near DZ. However, the A1 loop was always placed as far ventral as the A1/A2 border demarcation would allow, so as to avoid any direct cooling of tissue in DZ. The previously implanted PAF cryoloop and the A1 cryoloop were then connected to Teflon tubing, and the cooling deactivation apparatus was tested by pumping chilled methanol through the lumen of the tubing and loops according to previously published methods (Lomber et al., 1999). Thermal images of cortex were recorded using an infrared camera (FLIR SC300; Portland, OR) during both A1 and PAF cooling in order to confirm that the spread of cooling did not exceed ~1 mm from the cryoloop, in accordance with previously published work (**Figure 3.2 C-E**; Lomber et al., 1999). Loop temperatures were continuously monitored throughout all phases of cooling deactivation using a wireless thermometer (UWTC-2; Omega, Stamford, CT), and were maintained at ~2-3°C. Previous work has demonstrated that if the cryoloop is cooled to 3°C, the cortical temperature in layer VI falls below 20°C, which results in the silencing of efferent signals emanating from all layers of the cooled region (Carrasco and Lomber, 2009a, b, 2010; Lomber et al., 1999). Additionally, in two animals, mini-hypodermic probes (HYP-O; Omega, Laval, Canada) were used to corroborate temperature measures taken at the cortical surface using the infrared camera, as well as to ascertain that the tissue temperature recorded below the surface of cortex corresponded to previously published work, both within the vicinity of the cryoloop, as well as outside of it (Carrasco & Lomber, 2009a, 2009b, 2010; Lomber et al., 1999). In all cases, temperature measures in the current study were in line with previously published work.

Following A1 loop placement and testing, electrodes were lowered ~1,200 µm orthogonal to the exposed surface of DZ targeting granular layers. However, the depth of the penetration was adjusted to optimize the strength of the response across all four shanks. Multiunit neuronal responses were recorded across five phases of cortical deactivation: 1) while cortex was warm, 2) while A1

alone was cooled, 3) while A1 and PAF were cooled in concert, 4) while PAF alone was cooled, and 5) following rewarming of cortex. It should be noted that DZ straddles the ventral lip of the middle suprasylvian sulcus, and is known to extend progressively further into the sulcus as one moves from posterior to anterior. Recordings in the current experiment were limited to the ~1,200 µm directly below the gyral surface, and no recordings were made from any portion of DZ extending into the middle suprasylvian sulcus. Upon completion of a deactivation cycle, the electrodes were repositioned at a new cortical location and the same procedure was repeated. The temporal order in which loops were cooled varied between successive penetrations, so as to control for any effect of cooling order (i.e., A1 was cooled first in some penetrations, while PAF was cooled first in others). However, for ease of interpretation, the data in the current study is always presented in alphabetical cooling order, even though this was not necessarily the order in which cooling occurred for every penetration.

3.3.5 Histological procedures

After 36-100 hours of recording, animals were administered an anticoagulant (heparin, 10,000U; 1 mL), a vasodilator (1% sodium nitrite, 1 mL), and deeply anesthetized using sodium pentobarbital (40 mg/kg, i.v.). Animals were perfused intracardially through the ascending aorta at a rate of 100 mL/min with physiological saline (1 L), followed by 4% paraformaldehyde (2 L). In some animals, this was followed by 10% sucrose. The brain was stereotaxically blocked, removed and placed in 30% sucrose for cryoprotection. Once sunk, the brain was frozen and cut in 60 µm coronal sections using a cryostat (Leica CM 3050S, Wetzlar, Germany). One series was processed with the monoclonal antibody SMI-32 (Covance; Princeton, NJ), while the other was kept as a spare or stained using Cresyl Violet and used to visualize electrode tracks. SMI-32 staining profiles have been shown to effectively parcellate individual auditory cortical regions (Mellott et al., 2010), and were used to delimit borders within auditory cortex in the present study. The location of the PAF cooling loop was also verified using SMI-32 staining patterns.

3.3.6 Data analysis

Multiunit responses were de-noised and waveforms were manually inspected using Plexon Offline Sorter (Plexon, Dallas, TX). All data analysis was conducted using custom written scripts in Matlab (Mathworks, Natick, MA). For all stimuli, only neuronal responses in which the rewarm phase returned to at least 60% of the original firing rate during the warm phase were included in the analysis.

Peri-stimulus time histograms (PSTHs) for noise bursts and tones were constructed by binning neuronal responses with a time resolution of 1 ms. PSTHs were then smoothed using convolution of a 6 ms Gaussian window. Peak response rates were defined as the maximum number of spikes per second within a given PSTH. Peak response latency refers to the amount of time (in milliseconds) elapsed between stimulus onset and the peak response. Peak response onsets and offsets were defined as the first and last responses greater than the mean spontaneous rate plus 20% of the peak firing rate (Sutter and Schreiner, 1991). These measures were manually inspected with respect to the histogram, and in all cases appeared to result in correct detection of the onset and offset of the response as displayed on the PSTH. Response duration was calculated by subtracting the onset of the response from the offset of the response (i.e. the duration of the response at stimulus onset). It should be noted that in some cases, a response was also present at the offset of the stimulus. The measures calculated above were restricted to the peak response after the onset of the stimulus and were not applied to the offset responses that were present in a minority of units. Noise RIFs were constructed by computing the average firing rate over the first 50 ms for each sound intensity level. Monotonicity ratios were calculated by dividing the peak response in spikes/second at the highest sound level (80 dB SPL) by the maximum observed response at any sound level (Stecker et al., 2005; Sutter and Schreiner, 1991). Monotonicity ratios between 0.9 and 1 were classified as monotonic, as visual inspection of the data showed either a saturating response at the highest sound

levels presented, or a clear monotonic increase in response as sound level increased. Monotonicity ratios below 0.9 were classified as non-monotonic and always showed a clear peak at sound levels below 80 dB SPL.

Frequency receptive fields were generated by computing the mean firing rate during the first 50 ms post-stimulus onset over five repetitions of each frequency-intensity combination. The receptive field matrix was then smoothed using a 2-dimensional Savitzky-Golay filter. An evoked response was defined as any response exceeding one-third of the averaged maximum response of the warm and rewarm phases. The characteristic frequency (CF) was defined as the stimulus frequency which evoked a response at the lowest sound intensity level (minimum threshold). In some cases, there were multiple points which fit this definition (multi-peaked responses), in which case the peak with the strongest response was used. Bandwidths for each sound intensity level above minimum threshold were calculated by subtracting the lowest frequency at which an evoked response occurred from the highest frequency at which a response occurred, expressed in octaves. Receptive field bandwidths were subsequently analyzed in one of two ways. Absolute bandwidth refers to bandwidths measured at each individual sound intensity level (e.g. 10 dB SPL). If no evoked responses were present at a particular sound intensity level, the bandwidth was given a value of zero. Relative bandwidths refer to measurements at sound intensity levels with respect to threshold (e.g. 10 dB above threshold). For this analysis, if no evoked responses were present at a particular sound intensity level above threshold the unit was excluded from analysis. All receptive fields were individually examined after these analyses were performed, and in the vast majority of cases, the CFs, minimum thresholds, and bandwidths corresponded very well with visual inspection of the plotted receptive field.

All data were subjected to Kolmogorov-Smirnov tests and in no cases were the data normally distributed. As a result, all statistical analyses were conducted using non-parametric Friedman tests (unless otherwise stated), and were followed by post hoc Wilcoxon tests adjusted using Bonferroni's inequality

to account for multiple comparisons. All p values reported in the text are corrected for multiple comparisons. All statistical comparisons reported include the median followed by the interquartile range in square brackets. Where appropriate, the data in some figures is represented as mean ± standard error of the mean for ease of comparison with other studies, even though statistical calculations were done on ranked data.

3.4 Results

The goal of the present investigation was to evaluate the functional contribution of inputs at multiple levels of the proposed model of auditory cortical hierarchy to DZ, a higher-order region. I first compare mapping data obtained from A1 and AAF to data collected in DZ. I then go on to discuss the effects of reversible deactivation of A1 and PAF individually or in concert on neuronal responses in DZ for each of the stimuli presented.

3.4.1 Comparison of DZ responses to A1 and AAF responses

Neuronal responses to tone presentations in A1 and AAF were recorded for the purpose of mapping the A1/AAF and A1/A2 border prior to placement of the A1 cooling loop. Responses that were well localized (i.e. not lying close to a border) to A1 (n = 205) and AAF (n = 147) were compared to responses collected during tone presentation for the warm condition in DZ (n = 92). Peak response rates differed significantly between the three areas ($\chi^2(2) = 44.2$, $p < 0.001$, n = 444; Kruskal-Wallis test). Peak response rates in DZ (26.1 [15.6 49.1] spikes/s) were significantly lower than those in A1 (58.0 [29.0 82.3] spikes/s; $p < 0.001$) and AAF (47.0 [27.3 67.0] spikes/s; $p < 0.001$). Peak response latencies also differed between areas ($\chi^2(2) = 39.5$, $p < 0.001$; Kruskal-Wallis test). Peak response latencies in DZ (17.0 [16.0 21.0] ms) were significantly longer than both A1 (14.0 [13.0 17.0] ms; $p < 0.001$) and AAF (15.0 [13.0 16.0] ms; $p < 0.001$). This result agrees well with previously published work, in which latency values for DZ range from those comparable to A1 or AAF (~10-20 ms) to much longer (> 40 ms; Sutter and Schreiner, 1991; He et al., 1997).

3.4.2 Noise burst responses during cooling deactivation

Peak response rates in DZ to 65 dB noise bursts differed significantly across the phases of the cooling cycle (**Figure 3.3**; $\chi^2(4) = 222$; $p < 0.001$, $n = 123$). Post hoc comparisons indicated that peak response rates in DZ were reduced from the warm condition (233 [83.3 353] spikes/s) when A1 was cooled alone (63.3 [26.7 133] spikes/s, $p < 0.001$), when both A1 and PAF were cooled in concert (58.3 [18.3 112] spikes/s, $p < 0.001$), and when PAF alone was cooled (98.3 [40.0 190] spikes/s, $p < 0.01$). No change from the warm condition was observed after cortex was rewarmed (225 [85.0 332] spikes/s, $p = 1.00$), and there was no difference between response rates when A1 was cooled alone compared to when it was cooled in concert with PAF ($p = 0.84$). No significant differences in noise burst peak latencies or response duration were found. In addition, 11/120 units recorded in DZ exhibited both onset and offset responses, consistent with previous reports (He et al., 1997). Where offset responses were present, all responses were strongly reduced during cortical deactivation of A1, PAF or A1 and PAF together.

Analyses of the changes in firing rate at individual sites were also conducted to determine if a statistical difference at the group level was mediated by a subset of recording sites or across all units in the population (**Figure 3.4 A**). The same conventions used by Carrasco and Lomber (2010) were adopted in the present study: a reduction greater than two-thirds of the original firing rate was termed a large reduction, whereas a reduction of less than one-third of the original firing rate was classified as a small reduction. Anything in between (33-66% reduction) was regarded as moderate. When A1 was cooled either alone or in combination with PAF, the vast majority of sites (>75%) experienced either a strong or moderate reduction in firing rate (e.g. **Figure 3.4 B**). However, a small proportion of units either showed little reduction (e.g. **Figure 3.4 C**) or actually experienced an increase in firing rate while A1 was cooled (e.g. **Figure 3.4 D**). In contrast, when PAF alone was cooled, about half of DZ units experienced strong or moderate reductions in firing rate. When PAF was cooled in combination with

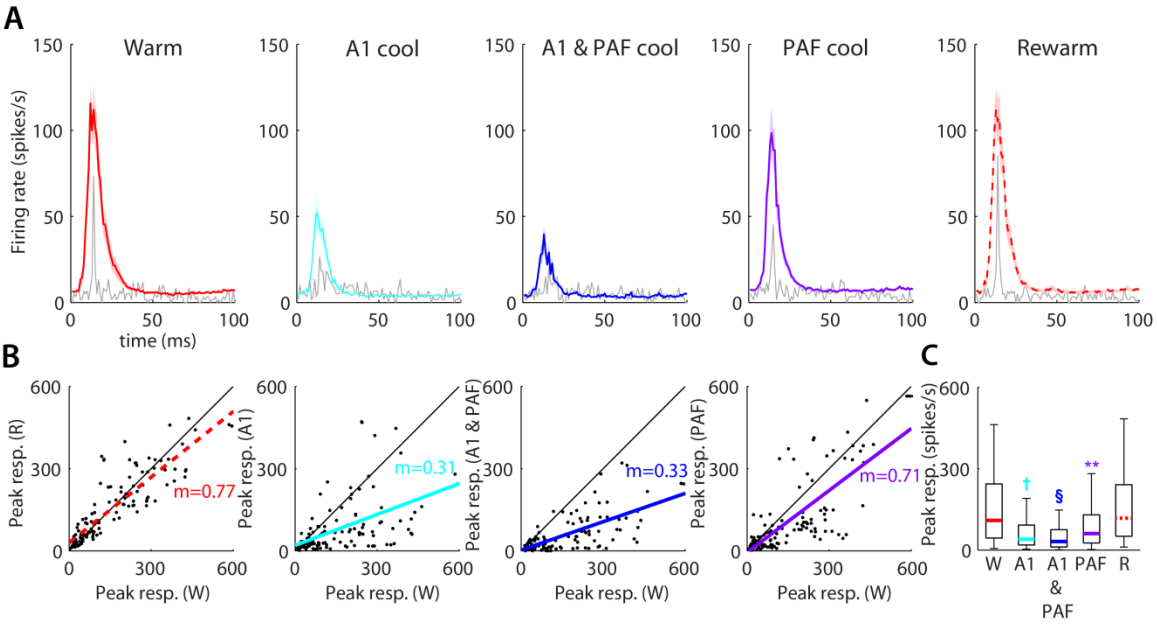

Figure 3.3 Population level effects of reversible deactivation on DZ responses to 65 dB noise bursts.

A: A representative example of a DZ recording site across deactivation phases is plotted in grey with the averaged PSTH for all DZ sites (n = 123) superimposed in color (± SEM in light shading). **B:** Peak responses in DZ (spikes/s) for the warm condition are plotted on the x-axis against peak responses for each of the other cooling conditions plotted on the y-axis. Least square regression lines for the y-axis responses are plotted in color. The slope of the regression line is also indicated in color. **C:** Box plot indicating DZ peak response rates for each of the conditions. The limits of the box indicate the upper and lower quartile range of peak response values, with the colored line indicating the median. Whiskers extend to the most extreme data points. W: Warm, A1: A1 alone cooled, A1 & PAF: both A1 and PAF cooled, PAF: PAF alone cooled, R: Rewarm. ** $p < 0.01$; † $p < 1.00 \times 10^{-5}$; § $p < 1.00 \times 10^{-10}$.

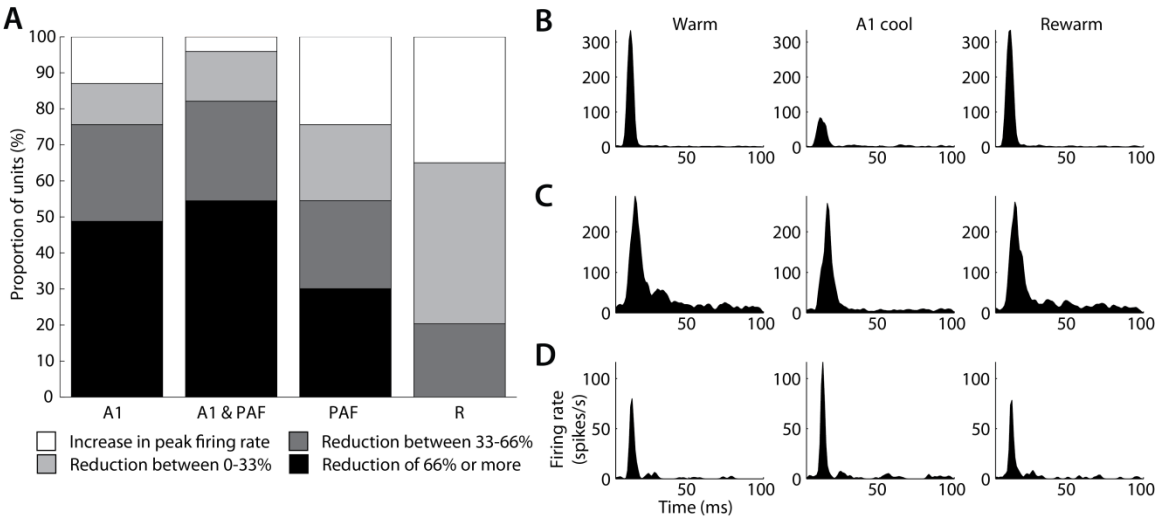

Figure 3.4 Effects of reversible deactivation during noise burst presentation on individual sites.

A: Proportion of sites showing strong (black), moderate (dark grey), or small (light grey) reductions in peak firing rate across deactivation phases. Increases in firing rate are shown in white. **B-D:** Representative examples of the magnitude of change observed at individual sites in DZ. For simplicity, only responses during the deactivation of A1 alone are shown, however, similar changes were observed during other deactivation phases as well. Abbreviations as in Figure 3.3.

A1, there was an increase in the proportion of units that showed a reduction in firing rate of any magnitude. Overall, deactivation of both A1 and PAF resulted in significant declines in neuronal activity in DZ in response to noise bursts at the population level, with A1 deactivation strongly suppressing responses in more DZ units than during PAF deactivation.

3.4.3 Noise RIF responses during cortical cooling

Response rates in DZ differed significantly across the phases of the cooling cycle during presentations of noise bursts at varying sound intensity levels ($\chi^2(4) = 557$; $p < 0.001$). Firing rates were significantly reduced in DZ across all sound levels when A1 was cooled either alone, or in concert with PAF (**Figure 3.5 A**; $p < 0.01$ for all sound intensity levels measured). Conversely, when PAF alone was deactivated, firing rates were only suppressed at sound levels greater than 50 dB SPL ($p < 0.05$ for all comparisons). In no case did the warm condition significantly differ from the rewarm condition ($p = 1.00$ for all comparisons), and there were no differences between response rates at any of the sound levels when A1 was cooled alone versus in concert with PAF ($p = 1.00$ for all). Monotonicity was evaluated and 90/105 (85.7%) of neurons in DZ were found to be monotonic (defined as having a monotonicity ratio greater than 0.9; **Figure 3.5 B**). The remainder of units were classified as non-monotonic (having monotonicity ratios of less than 0.9; **Figure 3.5 C**). These numbers correspond very closely to those reported in He et al. (1997) in which 84.7% of units were classified as monotonic (purely monotonic or saturating responses). Collectively, these results suggest that firing rates in DZ are only suppressed at high sound intensity levels during PAF deactivation, whereas A1 deactivation results in suppression at all sound intensity levels measured.

3.4.4 Responses to tones during reversible deactivation

Peak response rates to all tones presented differed significantly across the phases of the cooling cycle for sites in DZ (**Figure 3.6**; $\chi^2(4) = 233$; $p < 0.001$, $n = 92$). Post hoc comparisons indicated that peak responses were significantly

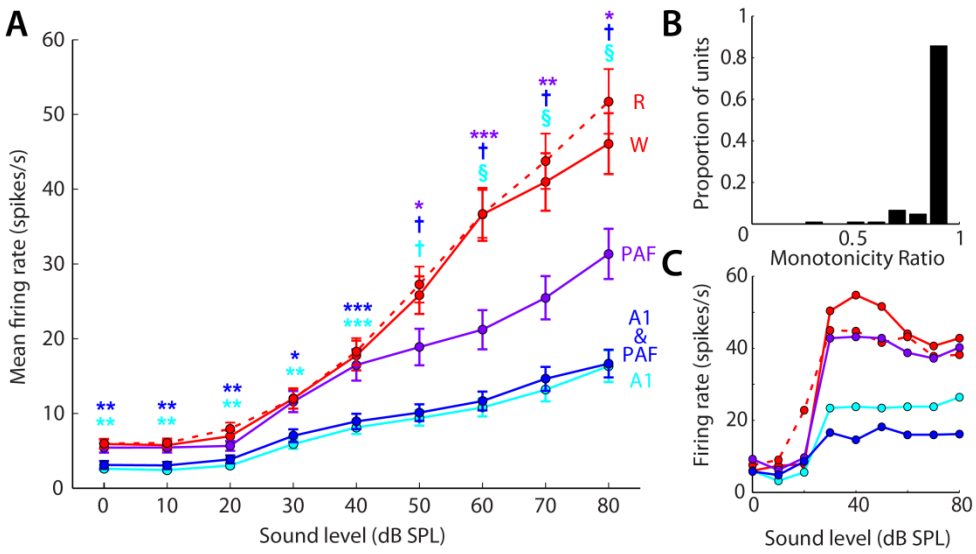

Figure 3.5 Noise Rate-intensity functions and monotonicity ratios.

A: Noise rate-intensity functions (RIFs) for DZ. RIF for DZ responses (n = 105). Each circle indicates the mean of the average firing rates of all recorded units over the first 50 ms of the response for each sound intensity level presented (± SEM). **B:** Bar graph showing the proportion of units according to monotonicity ratio. **C:** Example of a site with a non-monotonic RIF. Abbreviations as in Figure 3.3. Asterisks indicate a statistically significant change from the warm condition as follows: * $p < 0.05$; ** $p < 0.01$; *** $p < 0.001$; † $p < 1.00 \times 10^{-5}$; § $p < 1.00 \times 10^{-10}$.

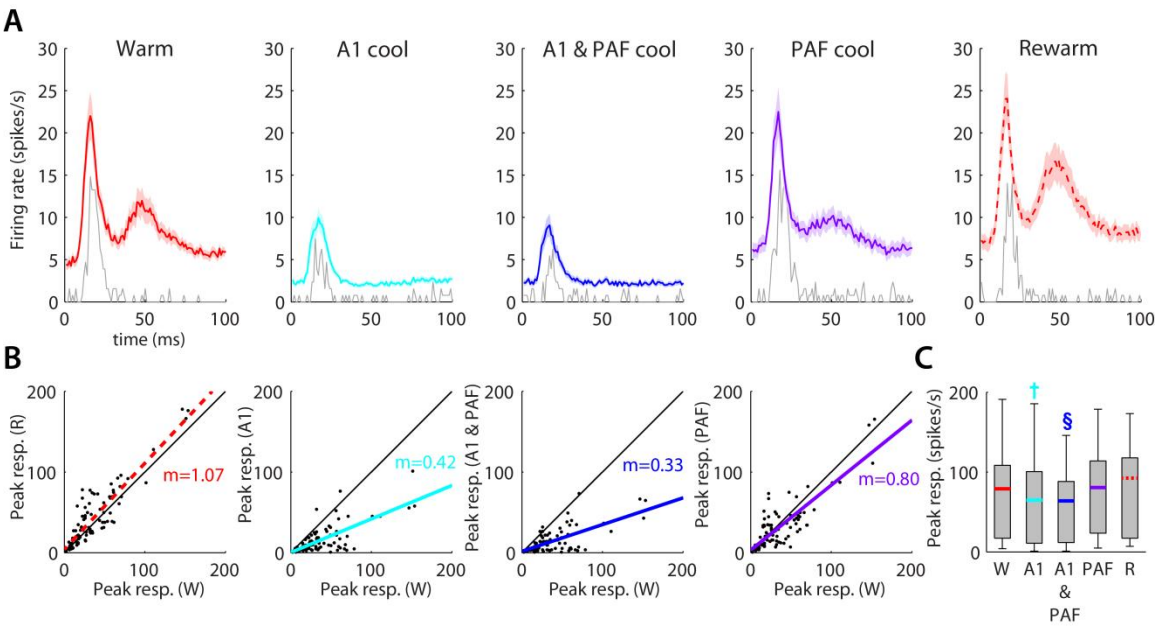

Figure 3.6 Population level effects of reversible deactivation on DZ responses to tones.

A: A representative example of a DZ recording site across deactivation phases is plotted in grey with the averaged PSTH for all DZ sites (n = 92) superimposed in color (± SEM in light shading). **B:** Peak responses in DZ (spikes/s) for the warm condition are plotted on the x-axis against peak responses for each of the other cooling conditions plotted on the y-axis. Least square regression lines for the y-axis responses are plotted in color. The slope of the regression line is also indicated in color. **C:** Box plot indicating DZ peak response rates for each of the conditions. The limits of the box indicate the upper and lower quartile range of peak response values, with the colored line indicating the median. Whiskers extend to the most extreme data points. Abbreviations as in Figure 3.3. * $p < 0.05$, ** $p < 0.01$, *** $p < 0.001$, † $p < 1.00 \times 10^{-5}$; § $p < 1.00 \times 10^{-10}$.

reduced in comparison to the warm condition (26.1 [15.6 49.1] spikes/s) when A1 was cooled alone (7.80 [4.68 18.7] spikes/s, $p < 0.001$), and when both A1 and PAF were cooled in concert (7.02 [3.90 18.7] spikes/s, $p < 0.001$). No change from the warm condition occurred when PAF was cooled alone (27.7 [9.36 42.9] spikes/s, $p = 1.00$), or when cortex was rewarmed (31.2[14.8 60.8] spikes/s, $p = 1.00$). Peak responses when A1 was cooled alone were not different from those when A1 and PAF were cooled in concert ($p = 1.00$). No differences were observed for response latencies or response durations in DZ between deactivation phases. Both an onset and an offset response were present in a minority of DZ units (7/92). Where an offset response was present, responses were either strongly or moderately reduced during A1 deactivation, either alone or in concert with PAF, and were moderately reduced when PAF alone was deactivated. As with responses to noise bursts, responses to tones were also analyzed at the unit level (**Figure 3.7 A**). These findings largely paralleled those reported for responses to noise bursts in that a large proportion (~80%) of units experienced either a strong or moderate reduction in firing rate when A1 was cooled, either alone or in combination with PAF. Conversely, when PAF alone was cooled, ~25% of units actually increased firing rate and the proportions of units that showed a strong reduction in firing rate was considerably lower (~5%) than those observed during deactivation of A1 alone (~40%). These changes in response rates were spread out across DZ, and importantly, the effects of deactivation did not vary with distance from the cooling loop (**Figure 3.7 B**), suggesting that the proximity of a recording site to the cooling loops did not account for the effects observed.

In general, receptive fields constructed for DZ units agreed well with findings reported in previous studies. Specifically, multi-peaked tuning curves were observed in 25/81 (30.9%) units (He et al., 1997; Stecker et al., 2005; Sutter and Schreiner, 1991), while the remainder were single-peaked (56/81). However, it should be noted that in some cases, well-separated peaks were observable during epochs of reversible deactivation, even though the warm and rewarm conditions did not show evidence of clear separation between peaks,

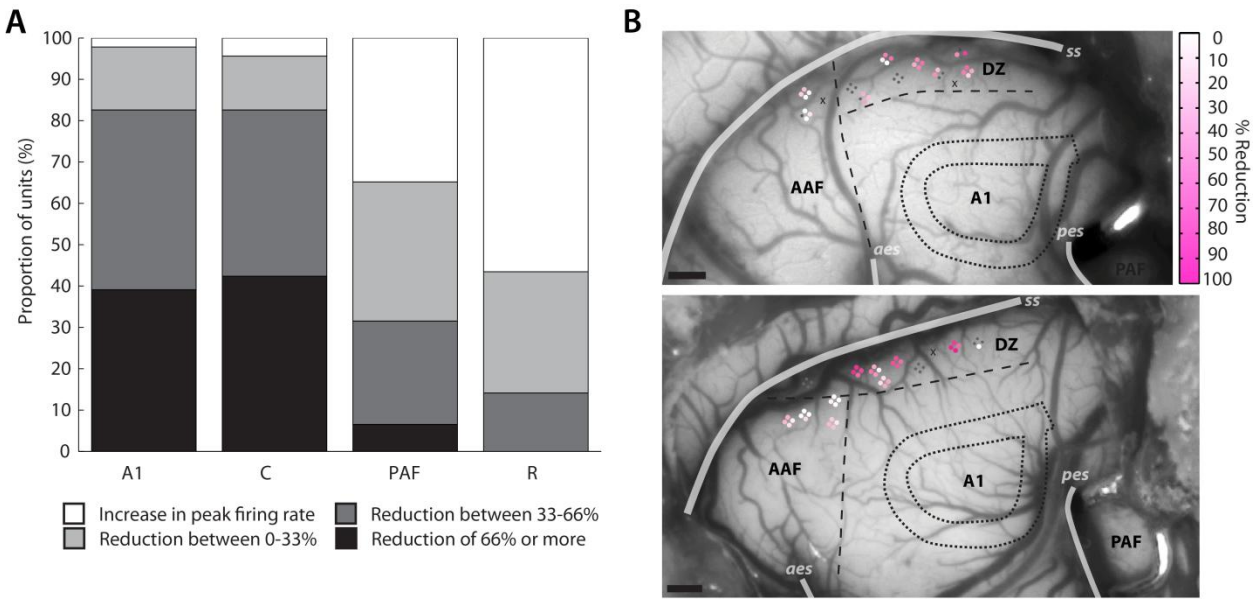

Figure 3.7 Effects of reversible deactivation during tone presentations on individual sites.

A: Proportion of sites showing strong (black), moderate (dark grey), or small (light grey) reductions in firing rate across deactivation phases. Increases in firing rate are shown in white. **B:** The magnitude of reduction in firing rate during A1 deactivation plotted on the cortical surface for two animals. The location of the A1 cooling loop is indicated by finely dashed lines. Note that the magnitude of reduction does not appear to be related to the proximity of the site to the cooling loop. Areal borders are indicated by longer dashed lines. Abbreviations as in Figure 3.3. Scale bar = 1 mm.

and thus, these sites were designated as single-peaked (e.g. **Figure 3.8**). Of the multi-peaked tuning curves, 7/25 had three peaks while the remaining 18/25 had two. Where multipeaked tuning curves were recorded, it was noted that the peaks tended to cluster in a space of less than one octave in agreement with previously published findings (Sutter and Schreiner, 1991). Isofrequency contours were also found to shift caudally at the A1/DZ border and consequently, more than 75% of CFs in DZ were tuned to frequencies higher than 20 kHz (Middlebrooks and Zook, 1983; Sutter and Schreiner, 1991). No changes in CF were observed across deactivation phases ($\chi^2(4) = 4.00$, $p = 0.41$, $n = 81$).

Receptive field bandwidths differed significantly between the phases of the cooling cycle at absolute sound intensity levels (**Figure 3.9 A**; $\chi^2(4) = 623$, $p < 0.001$, $n = 81$). However, receptive field thresholds were also increased as a consequence of reversible deactivation (**Figure 3.9 B**; $\chi^2(3) = 118$, $p < 0.001$, $n = 81$). On average, the threshold of DZ receptive fields increased by 30.0 [-40.0 -10.0] dB SPL when A1 alone was cooled ($p < 0.001$), by 20.0 [-40.0 -20.0] when both A1 and PAF were cooled together ($p < 0.001$), and by 10.0 [-30.0 0.00] when PAF alone was cooled ($p < 0.001$). No change in threshold occurred between the warm and rewarm conditions (0.00 [-10.0 0.00] dB SPL, $p = 0.23$). Because of this increase in threshold, an additional analysis of receptive field bandwidths at intensity levels relative to threshold was done in order to determine whether any reduction in bandwidth observed at absolute sound intensity levels was due to an effect of reversible deactivation on the shape of the tuning curve, or simply due to the increased threshold. However, in the majority of cases (>70%), very few evoked responses in DZ tuning curves were discernable when A1 was cooled, rendering it impossible to calculate bandwidth. If such sites are removed from consideration, it is possible to calculate bandwidth at several intensities above threshold, however, very few sites remain (**Figure 3.9 C**), making it difficult to draw a conclusion. Thus, it is not possible to conclude whether reductions in absolute bandwidth are due to elevated receptive field thresholds or reflect a sharpening of the tuning curve.

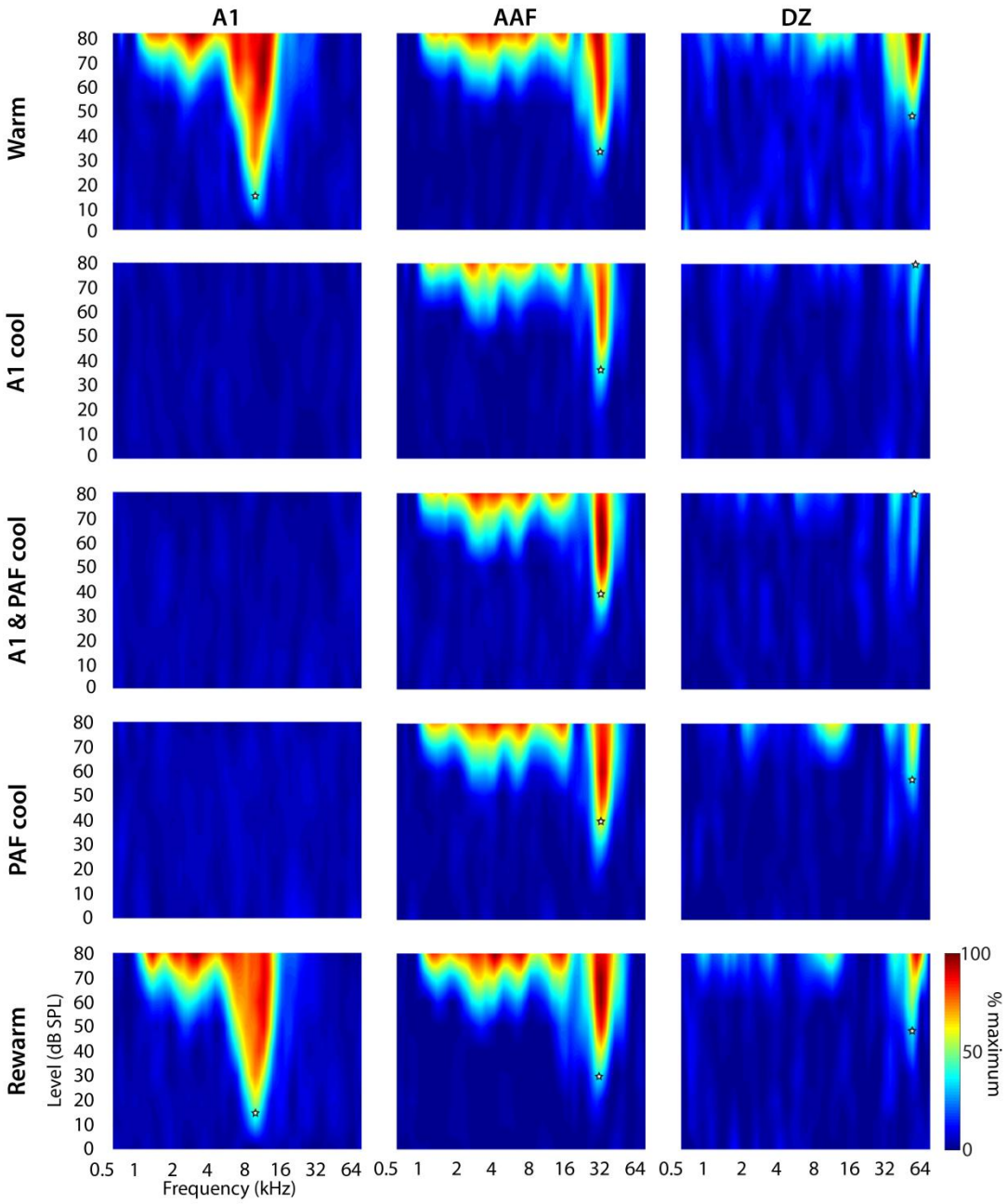

Figure 3.8 Representative example of tuning curves recorded in fields A1, AAF and DZ.

Each site was recorded over five phases of reversible deactivation (top to bottom): while cortex is warm, during A1 deactivation, while both A1 and PAF are deactivated, during PAF deactivation, and upon rewarming. White stars indicate the CF and minimum threshold for the recorded unit. Note that A1, AAF and DZ examples are considered single-peaked, because the DZ unit lacks clear separation between the peaks in the Warm and Rewarm phases.

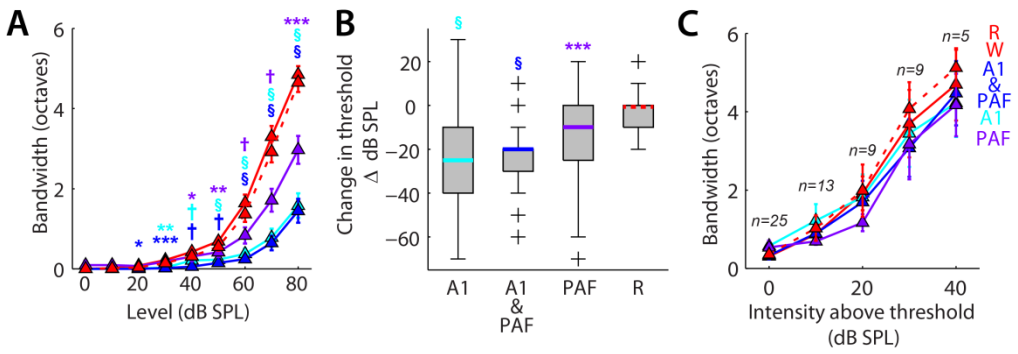

Figure 3.9 Summary of changes in DZ receptive field properties as a function of reversible deactivation.

A: Mean absolute bandwidth measures recorded at each sound intensity level presented (± SEM). **B:** Boxplot showing the magnitude of change in threshold (from the Warm condition) for each phase of reversible deactivation. **C:** Mean relative bandwidth measures recorded in 10 dB SPL steps above minimum threshold (± SEM). Abbreviations as in Figure 3.3. * $p < 0.05$, ** $p < 0.01$, *** $p < 0.001$, † $p < 1.00 \times 10^{-5}$; § $p < 1.00 \times 10^{-10}$.

Receptive field properties were also subjected to analysis at the level of individual units. When A1 was cooled either alone or in concert with PAF, ~70% of units showed an increase in threshold greater than 10 dB SPL (**Figure 3.10 A**). PAF deactivation alone also resulted in an increased threshold of more than 10 dB SPL for ~45% of units. An increase threshold during combined deactivation of A1 and PAF was observed in a greater proportion of units than during deactivation of either field alone. Across all cooling conditions, the majority of units in each case did not show any change in CF (**Figure 3.10 B**). However, some changes in CF did occur across epochs of cooling deactivation. Manual inspection of the receptive fields indicated that changes in CF of less than an octave often reflected changes in multi-peaked tuning curves (i.e. an increase in threshold for one peak but not another resulted in a change in CF from the first peak to the second peak). Changes greater than one octave appeared to be due to an increase in threshold during deactivation in which evoked activity was present at 80 dB SPL, but did not occur at the same frequency as the CF in the warm/rewarm conditions. This demonstrated that the unit still retained the ability to respond during epochs of reversible deactivation, but tuning was generally very poor, resulting in a change in CF (see the definition of CF in Materials and Methods).

Overall, the effect of A1 deactivation on PSTH measures during tonal stimulation was a reduction in peak firing rates in DZ at both the population and unit level. A1 deactivation also resulted in increased receptive field thresholds and reduced absolute bandwidths. In contrast, PAF deactivation does not reduce peak responses in DZ during tonal stimulation at the population level, at least during the early phase of the response. However, offset response rates were reduced during PAF cooling (e.g. see the second peak in **Figure 3.5 A**). With respect to individual units, cortical cooling of PAF resulted in a measurable decline in activity for more than 60% of sites, however, these reductions are far less robust than those observed during noise burst stimulation. Despite this, an

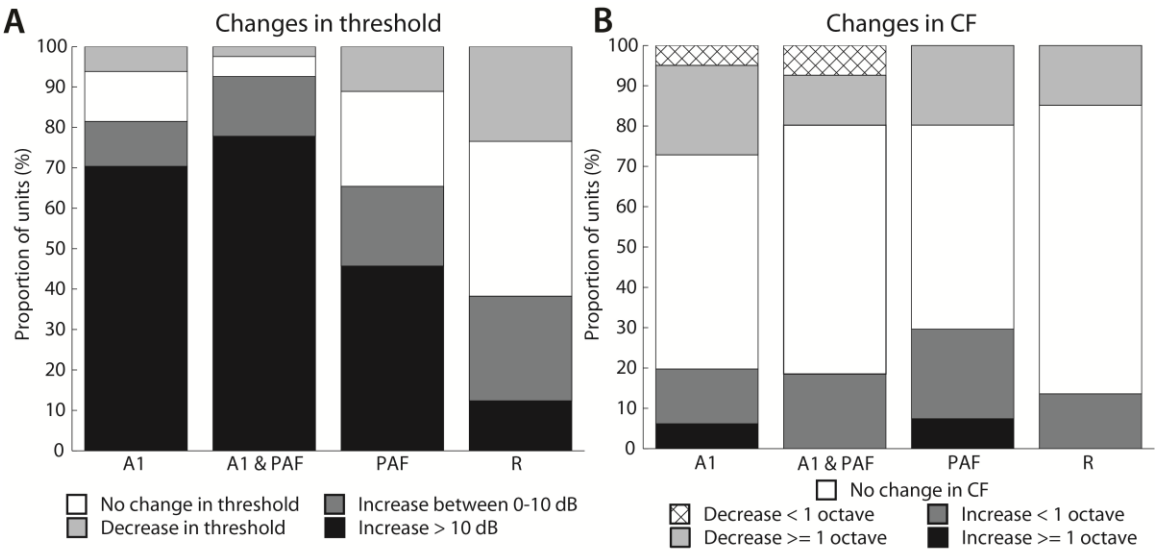

Figure 3.10 Summary of changes in threshold and CF at individual sites in DZ.

A: Proportion of units during each phase of deactivation that show changes in threshold from the warm condition. **B:** Proportion of units across cooling phases that show changes in CF (in octaves) from the warm condition. Abbreviations as in Figure 3.3.

increase in receptive field threshold is evident at both the population and individual unit level during PAF deactivation.

3.4.5 Results summary

Neuronal responses in DZ were recorded in response to noise burst and tone stimulation during reversible deactivation of A1 alone, PAF alone, or A1 and PAF combined. Reversible deactivation of A1, regardless of whether it was deactivated alone or in combination with PAF, always resulted in strong suppression of DZ responses, both at the population and individual unit level. These changes affected peak response rates as well as longer latency aspects of the response, and manifested as increased receptive field thresholds and reduced absolute bandwidths at each sound intensity level presented (**Figure 3.11 A-D**). Conversely, deactivation of PAF alone had stronger effects for noise burst than tonal stimulation, both at the population level and for individual sites. Further, cooling PAF seemed to exert the greatest effect at high sound intensity levels and affected longer latency aspects of the response. Receptive field thresholds were also increased during PAF deactivation. Overall, combined cooling of A1 and PAF together at the population level was largely driven by the effects of A1 deactivation as, in all cases, neuronal responses during deactivation of both A1 and PAF were indistinguishable from those of A1 deactivation alone. However, analysis of individual sites revealed small alterations in the proportions of neurons that showed strong reductions in firing rate and increased minimum thresholds.

3.5 Discussion

3.5.1 Comparison of DZ responses to previously published findings

These data agree well with the few studies that have characterized neuronal responses in DZ. Specifically, DZ exhibits longer response latencies than A1 and AAF (Sutter and Schreiner, 1991; Stecker et al., 2005; He et al., 1997), and receptive fields in DZ are complex and broadly tuned to higher

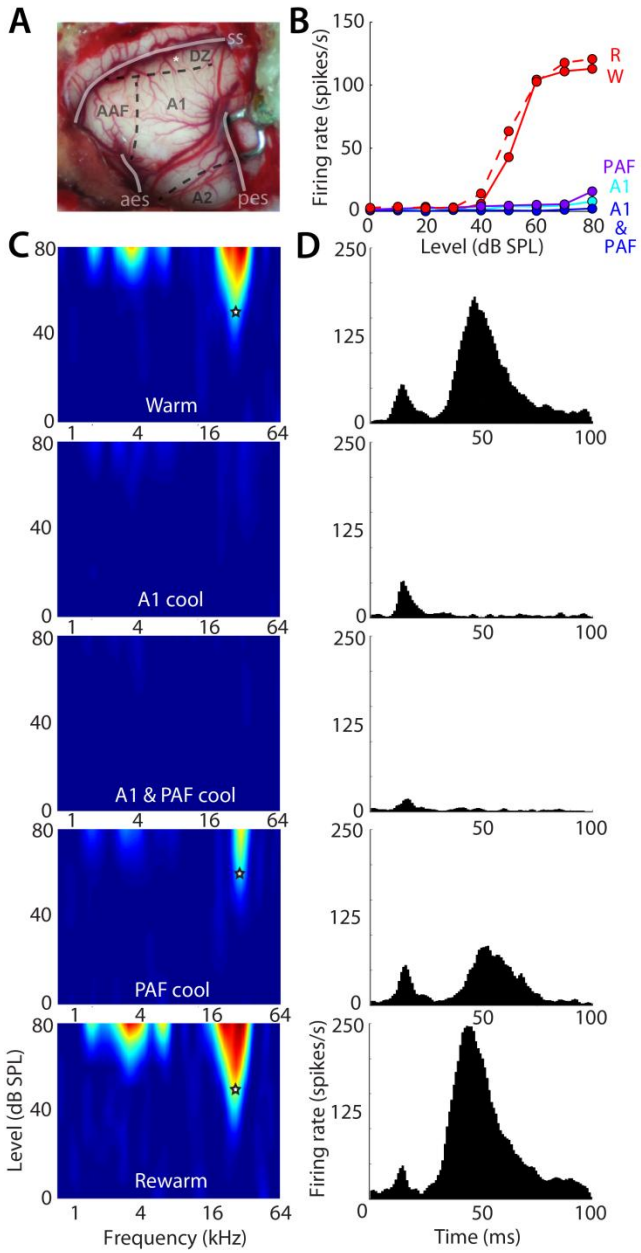

Figure 3.11 Representative example of a recording site in DZ in response to various stimuli.

A: The location of the representative site on the cortical surface of the craniotomy is indicated by a white asterisk. **B:** Noise RIF for representative site. **C:** Receptive fields for each of the five deactivation phases (indicated in white letters). **D.** PSTHs to tone stimuli for representative example during the same cooling phases as in C. Note that the data used to plot the PSTHs is the same as that used to plot the receptive fields in C. Abbreviations as in Figure 3.3.

frequencies (He et al., 1997; Middlebrooks and Zook, 1983; Stecker et al., 2005; Sutter and Schreiner, 1991). DZ responds more strongly to noise bursts than to tones, which is consistent with some reports (Sutter and Schreiner, 1991), but not others (Stecker et al., 2005). Non-primary belt areas of primate auditory cortex (have also been shown to respond better to band-passed noise than to tones (Rauschecker et al., 1995). DZ also exhibits mainly monotonic RIFs to noise bursts, in agreement with He et al. (1997), but not Stecker et al. (2005). The above discrepancies may be due to differences in anaesthetic regimes, as our data agree with measures collected under pentobarbital (He et al., 1997; Sutter and Schreiner, 1991), and differ from those collected under alpha chlorolose (Stecker et al., 2005). This is an important difference, as GABAergic inhibition has been demonstrated to affect the shape of the RIF in the bat inferior colliculus (e.g. Yang et al., 1992), and barbiturates are known to modulate post-synaptic responses to GABA (Olsen, 1981). Additionally, it is important to note that stimulus sets in the current study were not optimized for either duration or location at individual sites. Therefore, it is also possible that the discrepancies reported above may reflect differences in terms of the spatial preference of the neuron, since stimulus location was optimized in Stecker et al. (2005), but not Sutter and Schreiner (1991), He et al. (1997), or the present study. Overall, these results support the view that DZ is a higher order auditory field involved in complex sound processing (He et al., 1997; Sutter and Schreiner, 1991).

3.5.2 Effects of reversible deactivation in DZ

To date, the functional effects of the removal of auditory inputs to DZ have not been evaluated. In the present study, A1 deactivation caused a strong reduction, but not abolishment, of DZ responses irrespective of stimulus. These effects were observable across sound levels, and affected both peak response rates as well as longer-latency aspects of the response. This is consistent with what would be expected following deactivation of a major source of excitatory auditory input to DZ. These effects were evident in the majority of units, however, the proportion of neurons mediating the effect differed for noise burst versus

tonal stimulation. Over 95% of units showed a decline in response rate to tonal stimulation versus ~85% for noise burst stimulation. Interestingly, a small portion of units (5% for tones compared to 15% for noise bursts) increased firing rate as a consequence of A1 deactivation, which may reflect a release of inhibition on DZ as a consequence of A1 deactivation. Changes in receptive field properties also occurred following A1 deactivation. Specifically, receptive field thresholds were elevated, and absolute bandwidths were reduced. However, it is not clear whether bandwidth reductions reflect a narrowing of individual receptive fields, or whether these reductions occurred as a consequence of elevated threshold because in many cases, evoked responses were completely abolished following A1 deactivation.

In contrast to the strong effects of A1 deactivation irrespective of stimulus, PAF deactivation more strongly modulated DZ responses to noise bursts than tonal stimulation. Additionally, responses recorded at higher sound levels appeared to be more susceptible to modulation than those at lower sound levels. Although peak firing rates do not change dramatically during PAF deactivation for tonal stimuli, receptive field thresholds increase both at the population and unit level. This suggests that either a small modulation of peak firing rates during PAF deactivation can effect statistically significant changes in minimum threshold, or that some aspect of the response other than peak firing rate is susceptible to PAF deactivation and may be responsible for mediating the increase in minimum thresholds. Indeed, some longer-latency aspects of the response do change following PAF deactivation (e.g., see offset responses in PAF panel of **Figures 3.6 A and 3.11 D**), which is not surprising given that response latencies in PAF tend to occur later than those of DZ (Stecker et al., 2005).

When A1 and PAF are cooled in concert, responses for all measures calculated were no different at the population level from the effects of A1 deactivation. This suggests that any effect of PAF deactivation may actually be due to blocking neural activity that ultimately originates in A1, because response rates would be expected to decline beyond those observed when A1 was cooled

if PAF were contributing additional novel information (i.e. one would expect an additive effect). Modulation of DZ responses by A1 via PAF likely occurs through the most direct route, the cortico-cortical projection from A1 to PAF (Lee and Winer, 2008b). However, it is also possible that responses could be modulated via indirect cortical routes that pass through other auditory cortical structures in between A1 and PAF, such as VAF and VPAF, or through cortico-thalamo-cortical loops as the main sources of thalamic input to PAF arise from the ventral portion and dorsal superficial nucleus of the medial geniculate nucleus (MGN; Lee and Winer, 2008a), and corticofugal projections exist from A1 to both of these areas (Winer et al., 2001). Interestingly, an additive effect for the combination of A1 and PAF deactivation does occur to some extent at the level of individual units, particularly for peak response rates to noise burst stimuli and minimum thresholds (see stacked bar 'C' in Figures 4A and 10A). This suggests that not all of the information arising from PAF originates in A1. The results from this and previous experiments support a framework in which both serial and parallel processing mechanisms are at work.

It is not surprising that some responsiveness in DZ is preserved following reversible deactivation, given that DZ receives projections from cortical and thalamic sources unlikely to be disrupted by A1 or PAF deactivation. DZ receives projections from dorsal MGN (He and Hashikawa, 1998; Lee and Winer, 2008a; Barone et al., 2013), which in turn receives input from the ascending auditory tract via the inferior colliculus (Winer, 2011). Cortically, DZ receives input from AAF (Barone et al., 2013; Kok et al., 2014; Lee and Winer, 2008b), which itself receives tonotopically organized input from ventral MGN (Winer et al., 2001; Lee and Winer, 2008a). AAF receives weak input from PAF and although AAF receives strong input from A1 (Lee and Winer, 2008b), previous studies have demonstrated that it is unsusceptible to A1 deactivation (Carrasco and Lomber, 2009a). DZ similarly receives cortical input from fAES (Barone et al., 2013; Kok et al., 2014; Lee and Winer, 2008b), which is the only dorsal auditory region lacking strong projections from A1, receives weak input from PAF (Lee and Winer, 2008b) and also processes auditory spatial information (Malhotra et al.,

2004). A2 could be considered a candidate for possible sources contributing to the preservation of responses in DZ based on weak inputs from A1 and PAF with projections of moderate strength to DZ (Lee and Winer, 2008b). However, A2 neurons exhibit sustained responses with peak response latencies comparable to or longer than those of DZ (Carrasco and Lomber, 2010; Schreiner and Cynader, 1984), making it unlikely that information processed in A2 would shape DZ responses, at least during the early phases of the response. While DZ receives projections from other auditory cortical areas, most of these areas either receive strong projections from A1 and/or PAF (Lee and Winer, 2008b) or are higher order/parabelt areas known to respond to visual as well as auditory stimulation (Reale and Imig, 1980; Updyke, 1986), making it more likely that these serve as feedback projections. Any of the sources of input discussed may modulate aspects of DZ responses following deactivation via cortico-cortical connections and/or cortico-thalamo-cortical loops (Lee and Winer, 2008a; Winer et al., 2001), however, dorsal MGN, AAF and fAES are likely the primary sources of "bottom-up" auditory input to DZ that could account for the perseveration of responses following reversible deactivation of A1 and/or PAF.

These results suggest that the contributions of inputs from both A1 and PAF provide important "bottom-up" information to DZ for the stimuli used in the present study. However, future studies might further examine the functional contribution of inputs from A1 and PAF while varying either the duration or location of stimuli in order to further tease apart the hierarchical contributions of A1 and PAF to DZ using optimized stimuli at each recording site, given that individual sites in DZ have been shown to exhibit duration (He et al., 1997) and spatial (Stecker et al., 2005) tuning. Such investigations may yield additional information regarding the role that A1, PAF and DZ play in the functional hierarchy of the "where" pathway of auditory cortex, and may be particularly informative for higher-order fields such as DZ.

Overall, the present study is the first to demonstrate dissociable effects of the removal of auditory inputs from multiple levels of the auditory cortical

hierarchy on a higher-order region. These results additionally support previous anatomically-based hierarchical models involving both serial and parallel processing in auditory cortex (Lee and Winer, 2011; Rouiller et al., 1991). While A1 is a significant source of auditory information, particularly for fields in the "where" pathway, A1 does not form a bottleneck for entry of auditory information to cortex in the same way that V1 appears to for the visual system (Girard and Bullier, 1989; Girard et al., 1991).

3.6 References

Barone P, Lacassagne L, Kral A (2013) Reorganization of the connectivity of cortical field DZ in congenitally deaf cat. PLoS One 8:e60093.

Carrasco A, Lomber SG (2009a) Evidence for hierarchical processing in cat auditory cortex: nonreciprocal influence of primary auditory cortex on the posterior auditory field. J Neurosci 29:14323–14333.

Carrasco A, Lomber SG (2009b) Differential Modulatory Influences between Primary Auditory Cortex and the Anterior Auditory Field. J Neurosci 29:8350–8362.

Carrasco A, Lomber SG (2010) Reciprocal modulatory influences between tonotopic and nontonotopic cortical fields in the cat. J Neurosci 30:1476–1487.

Carrasco A, Lomber SG (2011) Neuronal activation times to simple, complex, and natural sounds in cat primary and nonprimary auditory cortex. J Neurophysiol 106:1166–1178.

Friston KJ (2011) Functional and effective connectivity: a review. Brain Connect 1:13–36.

Girard P, Bullier J (1989) Visual activity in area V2 during reversible inactivation of area 17 in the macaque monkey. J Neurophysiol 62:1287-1302.

Girard P, Salin PA, Bullier J (1991) Visual activity in areas V3a and V3 during reversible deactivation of area V1 in the macaque monkey. J Neurophysiol 66:1493-1503.

He J, Hashikawa T (1998) Connections of the dorsal zone of cat auditory cortex. J Comp Neurol 400:334–348.

He J, Hashikawa T, Ojima H, Kinouchi Y (1997) Temporal integration and duration tuning in the dorsal zone of cat auditory cortex. J Neurosci 17:2615–2625.

Horsley V, Clarke RH (1908) The structure and function of the cerebellum examined by a new method. Brain 31:45-124.

Kaas JH, Hackett TA, Tramo MJ (1999) Auditory processing in primate cerebral cortex. Curr Opin Neurobiol 9:164–170.

Kok MA, Chabot N, Lomber SG (2014) Cross-modal reorganization of cortical afferents to dorsal auditory cortex following early- and late-onset deafness. J Comp Neurol 522:654–675.

Lee CC, Winer JA (2008b) Connections of cat auditory cortex: I. Thalamocortical system. J Comp Neurol 507:1879–1900.

Lee CC, Winer JA (2008a) Connections of cat auditory cortex: III. Corticocortical system. J Comp Neurol 507:1920–1943.

Lee CC, Winer JA (2011) Convergence of thalamic and cortical pathways in cat auditory cortex. Hear Res 274:85–94.

Lomber SG, Malhotra S, Hall AJ (2007) Functional specialization in non-primary auditory cortex of the cat: Areal and laminar contributions to sound localization. Hear Res 229:31–45.

Lomber SG, Payne BR, Horel JA (1999) The cryoloop: an adaptable reversible cooling deactivation method for behavioral or electrophysiological assessment of neural function. J Neurosci Methods 86:179–194.

Malhotra S, Hall AJ, Lomber SG (2004) Cortical control of sound localization in the cat: unilateral cooling deactivation of 19 cerebral areas. J Neurophysiol 92:1625–1643.

Malhotra S, Lomber SG (2007) Sound localization during homotopic and heterotopic bilateral cooling deactivation of primary and nonprimary auditory cortical areas in the cat. J Neurophysiol 97:26–43.

Malhotra S, Stecker GC, Middlebrooks JC, Lomber SG (2008) Sound localization deficits during reversible deactivation of primary auditory cortex and/or the dorsal zone. J Neurophysiol 99:1628–1642.

Mellott JG, van der Gucht E, Lee CC, Carrasco A, Winer J a, Lomber SG (2010) Areas of cat auditory cortex as defined by neurofilament proteins expressing SMI-32. Hear Res 267:119–136.

Merzenich MM, Knight PL, Roth GL (1975) Representation of Cochlea Within Primarv Auditory Cortex in the Cat. J Neurophysiol:231–249.

Middlebrooks JC, Zook JM (1983) Intrinsic organization of the cat's medial geniculate body identified by projections to binaural response-specific bands in the primary auditory cortex. J Neurosci 3:203–224.

Olfert ED, Cross BM, McWilliam AA eds. (1993) Guide to the Care and Use of Experimental Animals.

Rauschecker JP, Tian B, Hauser M (1995) Processing of Complex Sounds in the Macaque Nonprimary Auditory Cortex. Science (80-) 268:111–114.

Reale RA, Imig TJ (1980) Tonotopic organization in auditory cortex of the cat. J Comp Neurol 192:265–291.

Rouiller EM, Simm GM, Villa AEP, de Ribaupierre Y, de Ribaupierre F (1991) Auditory corticocortical interconnections in the cat: evidence for parallel and hierarchical arrangement of the auditory cortical areas. Exp Brain Res 86:483–505.

Schreiner CE, Cynader MS (1984) Basic Functional Second Auditory Organization of Cortical Field (AII) of the Cat. J Neurophysiol 51:1284–1305.

Stecker GC, Harrington IA, Macpherson EA, Middlebrooks JC (2005) Spatial sensitivity in the dorsal zone (area DZ) of cat auditory cortex. J Neurophysiol 94:1267–1280.

Sutter ML, Schreiner CE (1991) Physiology and topography of neurons with multipeaked tuning curves in cat primary auditory cortex. J Neurophysiol 65:1207–1226.

Updyke B V (1986) Retinotopic organization within the cat's posterior suprasylvian sulcus and gyrus. J Comp Neurol 246:265–280.

Winer JA, Diehl JJ, Larue DT (2001) Projections of auditory cortex to the medial geniculate body of the cat. J Comp Neurol 430:27–55.

Yang L, Pollak GD, Resler C (1992) GABAergic circuits sharpen tuning curves and modify response properties in the mustache bat inferior colliculus. J Neurophysiol 68:1760-74.

Chapter 4: Diametric modulation of early and late components of acoustically-evoked activity in the dorsal zone of auditory cortex by visual and tactile stimulation

4.1 Abstract

Recently, the view that sensory systems operate as independent modules has been challenged by numerous studies demonstrating multisensory interactions in brain regions that have traditionally been thought of as unisensory. Despite functional imaging evidence of tactile or visual modulation of auditory cortical activity, single unit investigations in auditory cortex have only evaluated the influence of either modality on auditory responses, not both. Here I provide evidence that auditory-evoked activity in a higher-order area of cat auditory cortex, the dorsal zone (DZ), is modulated by both visual and somatosensory signals. I show that roughly half of the neurons in DZ are either bimodal audio-visual neurons, or are modulated by the presence of visual or somatosensory stimuli. These bimodal and integrative neurons do not appear to show any evidence of topographic organization within area DZ. I further demonstrate that visual and somatosensory inputs can have differing modulatory effects on independent portions of the auditory response. Specifically, the short-latency, high-amplitude neuronal response that occurs just after stimulus onset is suppressed following pairing of the auditory stimulus with somatosensory and/or visual stimuli, whereas longer-latency aspects of the sustained response to the stimulus are enhanced. Finally, the proportion of sites responsive to, or modulated by, more than one sensory modality is substantially higher using multiunit or local field potential (LFP) techniques compared to single unit recordings. This suggests that LFP and multiunit techniques, as well as other population-based measures of neuronal activity, may significantly overestimate the degree of multisensory processing in a given cortical area.

4.2 Introduction

Traditionally, cortical sensory organization has been viewed as a modular system in which specific regions of the brain are specialized for processing information from a particular sense (Jones & Powell, 1970). Multisensory processing was hypothesized to be the domain of polysensory areas that respond to multiple sensory modalities, such as parietal (e.g. Hyvarinen & Shelepin, 1979) or frontal cortex (e.g. Bignall, 1970). While much evidence supports this hypothesis, the concept of unisensory brain regions is increasingly challenged by behavioral, functional imaging and electrophysiological investigations indicating that these areas are susceptible to modulation by other senses (see reviews of Shimojo and Shams, 2001; Ghazanfar and Schroeder, 2006; Macaluso, 2006). Neuroanatomical connectivity studies across multiple species and cortical areas support this notion, with an increasing number of studies documenting projections from other senses to 'unisensory areas', even at the level of primary sensory cortices (Falchier et al., 2002; Schroeder and Foxe, 2002; Budinger et al., 2006; Bizley et al., 2007). Sensory deprivation studies have provided additional evidence challenging the sensory modularity hypothesis, demonstrating that other sensory modalities appear to compensate for the impaired modality by recruiting the deprived region for the processing of other sensory information (for review, see Bavelier and Neville, 2002; Merabet and Pascual-Leone, 2010).

Despite mounting evidence from the imaging literature that responses in auditory cortex can be modulated by visual and/or somatosensory stimuli (see Calvert 2001 for review), few studies have evaluated multisensory integration in auditory cortex at the single neuron level (ferret: Bizley et al., 2007; Bizley and King, 2008, 2009; Meredith and Allman, in press; macaque: Kayser et al., 2008). Even fewer studies have evaluated tactile influences on auditory responses, even though auditory-somatosensory interactions have been demonstrated using imaging, EEG, multiunit and field potential activity (Foxe et al., 2000, 2002; Lakatos et al., 2007). None of these studies have investigated the influence of

more than one other sensory modality on auditory cortical responses. Additionally, despite well-documented multisensory interactions in the imaging literature, only one study has directly compared integration at the single unit level to that of local field potentials (LFP; Kayser et al., 2008). Thus, there is a dearth of assessment of cortical modular functionality using comprehensive multisensory approaches.

Recently, two studies have documented visual projections to a higher-order region of cat auditory cortex, the dorsal zone (DZ; Barone et al., 2013; Kok et al., 2014). This region has also been shown behaviorally to exhibit visual cross-modal reorganization following deafness (Lomber et al., 2010), making DZ a prime candidate for investigations of multisensory processing. Thus, the present study sought to evaluate the influence of visual and tactile stimulation on auditory processing in DZ at multiple scales of neuronal activity (LFP, multiunit and single unit activity). Our results demonstrate both visual and somatosensory modulation of auditory responses distributed widely across DZ, with notably different modulatory effects during different portions of the response. Furthermore, the current study shows that LFP and multiunit techniques may significantly overestimate the degree of multisensory processing in a cortical area.

4.3 Materials and Methods

4.3.1 Overview

Multisensory neuronal responses were assessed in six adult domestic cats (*felis catus;* Liberty Labs, Waverly, NY). All animals were housed in an enriched colony environment. All experimental procedures were conducted in compliance with the National Research Council's *Guidelines for the Care and Use of Mammals in Neuroscience and Behavioral Research* (2003), the Canadian Council on Animal Care's *Guide to the Care and Use of Experimental Animals* (Olfert et al., 1993) and were approved by the Animal Use

Subcommittee of the University Council on Animal Care at the University of Western Ontario.

4.3.2 Surgical Preparation

Approximately 1-2 weeks before electrophysiological recording, animals underwent surgery to attach a head holder to the frontal bone, perform the craniotomy and build up a recording well over DZ and surrounding auditory, visual and somatosensory cortices using dental acrylic. The afternoon prior to surgery, animals were fasted and lightly anesthetized with ketamine (4mg/kg, i.m.) and Dexdomitor (0.05mg/kg, i.m.), in order to facilitate the insertion of an indwelling feline catheter into the cephalic vein for intravenous anesthetic administration during the surgery. Each animal also received a dose of anti-inflammatory medication (dexamethasone, 0.05 mg/kg, i.v.) to reduce post-surgical inflammation.

4.3.3 Surgical Procedures

On the day of surgery, animals were administered atropine (0.02 mg/kg., s.c.) to minimize respiratory and alimentary secretions, acepromazine (0.02 mg/kg, s.c.), buprenorphine (0.01 mg/kg, s.c.), Cefazolin (35 mg/kg, i.v.), and dexamethasone (0.5 mg/kg, i.v.). Sodium pentobarbital (25 mg/kg to effect, i.v.) was then administered to induce general anesthesia, followed by supplemental doses as needed. In order to inhibit the gag reflex, the mucosa of the pharynx was anesthetized with a topical anesthetic (Cetacaine; Cetylite Laboratories, Pennsauken, NJ), and the trachea was intubated with a cuffed endotracheal tube in order to ensure adequate ventilation. Respiration was unassisted. Ophthalmic ointment (Neosporin; Kirkland, Quebec) was applied to the cornea to prevent desiccation. The animal was positioned into a stereotaxic frame (David Kopf Instruments; Tujunga, CA), and the head was fixed by palato-orbital restraints and blunt (non-rupture) ear bars, while the body rested on a water-filled heating pad in order to maintain core temperature at 37°C. The animal was then prepared for surgery using antiseptic procedures. Body temperature, respiration

rate, heart rate, blood pressure and end tidal CO_2 were monitored continuously throughout surgery. A midline incision was made in the scalp, and the right temporalis muscle was detached medially and reflected laterally. A craniotomy was made over the right hemisphere between Horsley-Clarke (1908) coordinates A0-A15, in order to expose auditory cortex, the middle suprasylvian sulcus, as well as anterior somatosensory areas (**Figure 4.1 A**). Following this, an acrylic recording well was built up around the craniotomy and sealed closed with dental cement. A head holder was attached to the frontal bone of the skull using bone screws and dental acrylic. The animal was then provided with standard postoperative care (see Malhotra et al. 2004). In all cases, recovery was uneventful.

4.3.4 Preparation for recording

Approximately 1-2 weeks later, electrophysiological recording procedures were initiated. Animals were administered atropine (0.02 mg/kg, s.c.), dexamethasone (0.5 mg/kg, s.c.), acepromazine (0.4 mg/kg, i.m.), and ketamine (35 mg/kg, i.m.). The trachea was intubated with a cuffed endotracheal tube in preparation for ventilation. Indwelling feline catheters were inserted into the saphenous vein bilaterally, as well as the right cephalic vein. Phenylephrine and atropine drops were administered to each eye, a clear feline contact lens with an optimal focal distance of 25 cm was inserted into the left eye (contralateral to craniotomy), and an opaque lens was inserted into the right (ipsilateral) eye. The left eye was sutured open in order to ensure the eye remained open for the duration of recording procedures. Expandable foam ear buds were inserted bilaterally within the ear canals in close proximity to the tympanic membrane. Next, the ears canals and pinna were packed with Otoform (Betavox, Sherbrooke, QC) to dampen/block any acoustic noise exterior to the earbuds. The animal was then secured to a stereotaxic frame using the previously implanted head holder. As ketamine is the preferred anesthetic for multisensory

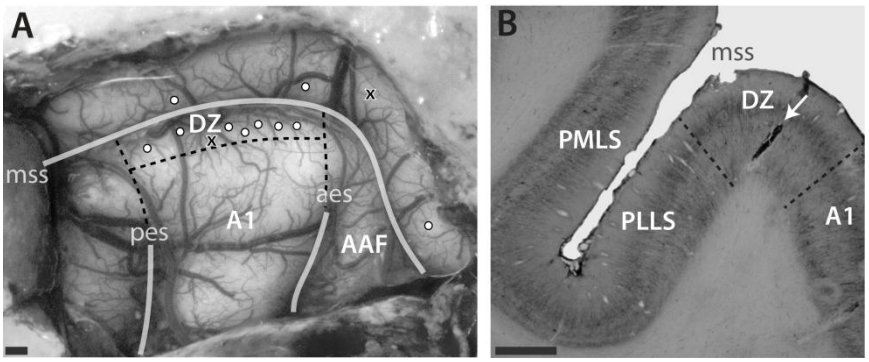

Figure 4.1 Location of recording sites within DZ.

A: Photomicrograph of the craniotomy and electrode penetration sites (white circles) in the dorsal zone of auditory cortex (DZ). Sites at which evoked responses were not reliably elicited are denoted with a black 'x'. Note that a few recording sites lie outside of auditory cortex, in known visual and somatosensory areas, served as verification that visual and somatosensory stimuli reliably elicited responses. Right is anterior. **B:** Photomicrograph of a coronal section stained with SMI-32 showing an electrode track in DZ. Borders between auditory cortical areas (as determined by SMI-32 labelling profiles) are indicated by dashed black lines. Right is lateral. Abbreviations: A1 – primary auditory cortex; AAF – anterior auditory field; aes – anterior ectosylvian sulcus; mss – middle suprasylvian sulcus; pes – posterior ectosylvian sulcus; PLLS – posterolateral lateral suprasylvian area; PMLS – posteromedial lateral suprasylvian area. Scale bars: 1 mm.

recording in cats (e.g. Allman and Meredith, 2007; Carriere et al., 2007; Wallace and Stein, 2007), ketamine (8-10 mg/kg/h) and acepromazine (0.04-0.05 mg/kg/h) were continuously infused. The craniotomy was unsealed and the dura was resected in preparation for recording. A layer of silicone oil was applied to the cortex to prevent dessication. Baseline respiratory and physiological measures were recorded and the animal was placed on a ventilator. Expired CO_2 was monitored and maintained at ~4-5%. The animal was then paralyzed with Nimbex (cistracurium besylate; induction: 1.5 mg/kg, i.v., constant infusion: 1.5 mg/kg/h, i.v.), in order to prevent ocular drift and movement of the limbs away from the somatosensory stimulators. A warm water circulating pad (Gaymar, Orchard Park, NY) was used to maintain core body temperature. Animals were hydrated with constant infusions of anesthetic and paralytic in 2.5% dextrose/half-strength lactated Ringer's solution. Dexamethasone (1.0 mg/kg, i.v.) and atropine (0.03 mg/kg, s.c.) were administered on a 24 hour schedule for the duration of the experiment. Finally, a digital image of the exposed cortex was taken with the aid of a surgical microscope in order to record the position of each electrode penetration relative to cerebral vasculature and cortical topography.

4.3.5 Stimulus generation and presentation

Electrophysiological recordings were conducted within a double-walled sound chamber on an electrically shielded, vibration-free table (Technical Manufacturing Corporation, Peabody, MA). Animals were exposed to auditory, visual and somatosensory stimuli, presented both alone (A, S, V) and in combination (AS, AV, ASV) in pseudo-random order. Auditory stimuli (white noise bursts, 1-32 kHz, 500 ms duration, 65 dB SPL) were presented binaurally via the earbuds using closed-field transducers (EC1; Tucker Davis Technologies, Alachua, FL), and were digitally generated with a 24-bit digital-to-analog converter at 156 kHz (RX6; Tucker-Davis Technologies). Acoustic signals had 5 ms rise and fall times and were cosine squared gated.

Somatosensory stimuli were presented using all-ceramic bender actuators (PL140.10; PI Ceramic, Auburn, MA) with a displacement distance of 1 mm.

Three stimulators were placed in contact with the animal's body, in order to stimulate three distinct sensory nerves: 1) contralateral vibrissae (contralateral trigeminal nerve), 2) ipsilateral vibrissae (ipsilateral trigeminal nerve), and 3) contralateral forepaw (radial nerve). Somatosensory stimulation sites on the head and forepaw were chosen, as previous research in two other species have shown auditory-somatosensory (AS) interactions in auditory cortex using tactile stimulation on these regions of the body (Fu et al., 2003; Meredith and Allman, 2012). It should also be noted that the AS condition involved pairing the auditory stimulus with tactile stimulation of the contralateral vibrissae, whereas the AVS condition paired auditory stimulation with all three stimulators.

Visual flashes (80 lux, 500 ms duration) were programmed in Adobe Flash and presented using a 17 inch liquid crystal monitor placed ~25 cm in front of the animal. The timing of stimulus presentation was designed such that neuronal responses to each type of sensory stimulus occurred at approximately the same time, in order to account for differences in cortical response latencies. Previous studies have demonstrated that audiovisual interactions are strongest when the visual stimulus precedes the auditory stimulus (Meredith et al., 1987; Bizley et al., 2007; Kayser et al., 2008), and cortical response latencies for the visual system are typically longer than those for the auditory system, particularly for non-primary regions (Bullier and Nowak, 1995; Carrasco and Lomber, 2011). Additionally, because previous research has demonstrated that maximal response enhancement occurs when the peak responses to individual sensory modalities are overlapped (e.g. Meredith et al., 1987), stimulus onset asynchronies in the present study were set such that the cortical responses to stimulus onset occurred at roughly the same time. To this end, auditory and somatosensory stimuli were programmed in temporal register, while the visual stimulus was programmed to precede each of them by ~65 ms, consistent with previous investigations of higher-order cortical regions (Allman and Meredith, 2007; Kayser et al., 2008; Foxworthy et al., 2013). Although previous research has identified fairly consistent levels of multisensory integration when the visual

stimulus precedes the auditory by 0-50 ms in the ferret (Bizley et al., 2007) and 20-80 ms in the macaque (Kayser et al., 2008), in order to rule out an effect of the timing of the visual stimulus on the level of integration observed, responses in two animals to the same set of stimuli presented above were analyzed while the timing of the visual stimulus varied within a small window around 40 ms (between 70 and 20 ms) prior to the onset of the auditory and somatosensory stimuli.

4.3.6 Data acquisition

Neuronal responses to multisensory stimuli were collected using an iridium axial array microelectrode (AM-002, 200 µm diameter; FHC, Bowdoin, ME), on which twelve electrode sites are spaced linearly 150 µm apart. Impedance measures ranged from 1-3MΩ. Neuronal activity was classified based on band-pass filtering as either spikes (300-5000Hz) or local field potentials (LFP; 1-200Hz). All activity was amplified (x10,000) and digitized at 25,000 Hz (RZ2; Tucker-Davis Technologies). Electrodes were lowered ~1,800-2,000 µm orthogonal to the exposed surface of dorsal auditory cortex (Fig. 1A). Care was taken not to lower the electrode further as extrastriate visual areas, the anterolateral and posterolateral lateral suprasylvian areas (ALLS and PLLS), occupy the lateral bank of the middle suprasylvian sulcus, directly beneath DZ, which straddles the lip of the middle suprasylvian sulcus. The degree to which DZ extends into the middle suprasylvian sulcus is known to increase in the posterior-to-anterior direction. Recording sessions ranged in duration from 71-97 hours.

4.3.7 Histological Procedures

At the end of the experiment, animals were administered an anticoagulant (heparin, 10,000U; 1 mL) and a vasodilator (1% sodium nitrite, 1 mL), and overdosed with Euthanol (sodium pentobarbital, 50 mg/kg, i.v.). Animals were perfused intracardially through the ascending aorta with physiological saline (0.01 M PBS), followed by fixative (4% paraformaldehyde) and 10% sucrose. The brain was stereotaxically blocked, removed, photographed, and placed in

30% sucrose until it sunk. The brain was frozen and cut in 60 µm coronal sections using a cryostat. Every second section was processed with the monoclonal antibody SMI-32 (Covance; Princeton, NJ) in order to determine auditory and visual cortical borders (van der Gucht et al., 2001; Mellott et al., 2010). The remaining sections were either re-stained for SMI-32 reactivity (if the first round of staining was too faint) or stained with cresyl violet and used to visualize electrode tracks (Fig. 1B). Only sites that could be identified as lying within DZ were analyzed.

4.3.8 Data Analysis

All units were de-noised and waveforms were sorted in 3-D principal component space using Offline Sorter (Plexon, Dallas, TX). Only units which achieved statistically significant levels of separation in principal component space and showed a clear refractory period were classified as single units, and only one single unit was ever isolated at a given recording site. When a single unit was isolated, the remainder of the de-noised waveforms were classified as multiunit activity for that site (**Figure 4.2**). Where no single unit was clearly discernable in principal component space, all de-noised waveforms were classified as multiunit activity for that site. All data analysis was performed in Matlab (Mathworks, Natick, MA) using custom-written scripts. Peri-stimulus time histograms (PSTHs) were constructed using 10 ms bins. DZ units often displayed a “typical” large-magnitude, short-duration auditory response to the onset of stimulation, followed by a period of response suppression, after which a sustained response of varying magnitude was usually present (**Figure 4.2**). Visual inspection of the data indicated that there might be differential effects of auditory stimulation when combined with another sensory modality during these two response epochs. As a result, the onset response (0-100 ms) was calculated separately from the sustained portion of the response (101-700 ms).

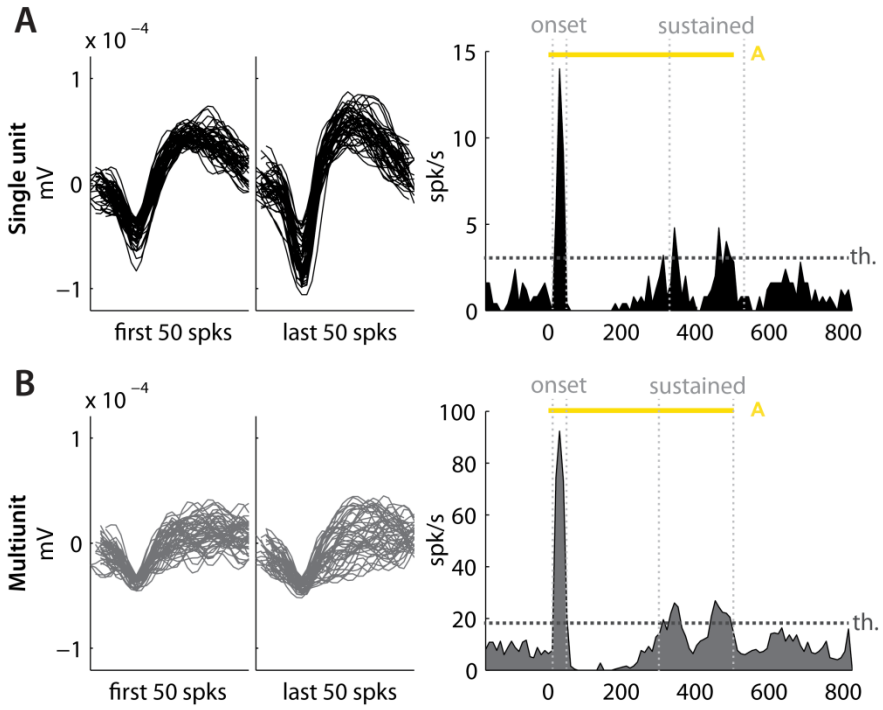

Figure 4.2 Waveforms and typical profile of single unit and multiunit activity at a representative site following auditory noise burst stimulation

A: The first 50 and last 50 waveforms for a representative single unit. The distinctive shape of the waveforms indicate this is likely a pyramidal cell. To be considered a response, neuronal activity had to exceed a threshold (th.) of 3 standard deviations beyond the mean of the spontaneous firing rate (see Methods). Virtually every neuron recorded showed a strong response after the onset of the auditory stimulus (yellow bar), which typically lasted for about 30 ms, followed by a period of suppression, after which sustained activity of variable duration and amplitude was often present. Sustained activity usually ceased at stimulus offset. **B:** Multiunit waveforms from the same site as in A, are plotted separately in grey at the same scale. Note the much smaller amplitude of the waveforms. The PSTH shows a similar pattern of activation to the noise burst stimulus. The criteria for determining a response was the same for multiunit activity as for single unit activity.

Previously published methods were used to analyze single unit data and were adapted where necessary (Meredith et al., 1987; Wallace et al., 2004; Stanford et al., 2005; Allman and Meredith, 2007; Kayser et al., 2008; Foxworthy et al., 2013; Sarko et al., 2013). A response to stimulation was determined to have occurred if the weighted sum of the number of spikes/trial during a 30 ms window centered around the peak response exceeded 3 standard deviations (SD) of that of spontaneous activity. This method prevented spurious activity that exceeded the 3 SD threshold from being classified as a response, while still correctly picking up neurons with very narrow onset response durations (e.g. 10 ms). PSTHs for all single units were visually inspected, and paired t-tests comparing the number of spikes per trial that occurred during a response window to spontaneous activity confirmed that the algorithm was able to correctly distinguish neuronal responses from spontaneous activity. Because cortical borders are often transitional, rather than clear-cut designations, analysis of sites located near the DZ-PLLS border was restricted to cells where auditory-evoked activity was greater than or equal to that of visually-evoked activity, in order to ensure that neurons in PLLS were excluded from analysis. Following this, a repeated-measures ANOVA followed by Dunnett's post hoc testing was used to compare the mean number of spikes per trial for the most effective unimodal response (A, V, or S) to that of combined modality stimulation (AS, AV, or AVS) that contained the unimodal response. For example, if the most effective unimodal stimulus was V, then V was compared to AV and AVS, but not AS, since the AS response did not contain visual stimulation. When statistically significant differences between responses during combined modality stimulation (AS, AV, or AVS) and the most effective single modality response (A, V, or S) occurred, the neuron was classified as integrative.

Each neuron could then be assigned to one of four categories based on the stimuli that evoked a response as well whether the neuron exhibited multisensory interaction: 1) Unimodal – responsive to only one stimulus modality with no multisensory integration, 2) Subthreshold – only one sensory modality is capable of eliciting a response, but the neuron exhibits integration when

presented with combined modality stimulation, 3) Bimodal non-integrative – responsive to more than one stimulus modality with no multisensory integration, and 4) Bimodal integrative – more than one modality elicits a response, and a multisensory interaction occurs following combined modality stimulation. The degree to which the response to stimulation by a single modality is enhanced or suppressed by the presence of a stimulus of another modality can be quantified using the interactive index (Meredith and Stein, 1983):

$$\left[\frac{CM\ -SMmax}{SMmax}\right] \times\ 100\ =\ \%\ interaction$$

where *CM* is the response to combined modality stimulation and *SMmax* is the response to the most effective single modality. A score of zero would indicate that the response does not change following combined modality stimulation. A positive number indicates that the response is enhanced when stimulation is paired with more than one sensory modality, while a negative number indicates suppression of the response during multisensory stimulation. In all cases, the most effective single modality for the onset portion of the response was the auditory stimulus. However, particularly in bimodal AV neurons, the visual stimulus was sometimes most effective for the sustained portion of the response. There were no overt responses to somatosensory stimulation in any neurons during any portion of the response.

Response additivity was also calculated in order to determine whether response enhancement following combined modality stimulation could be characterized as a linear summation of the responses to single modality auditory and visual stimulation. This was done using a bootstrapping procedure in which the baseline normalized response to combined modality stimulation is compared to all possible summations of the baseline normalized auditory and visual responses (Stanford et al., 2005). A significant deviation from the predicted sum is then classified as either sub-additive or supra-additive. This deviation from additivity can be quantified using the additivity index (Kayser et al., 2008):

$$\frac{CM - (A + V)}{CM + (A + V)} * 100$$

In this case, a score of zero indicates that the response to combined stimulation is equivalent to the sum of the auditory and visual responses (i.e. it is linear or additive), a score greater than zero indicates supra-additivity, and a score below zero indicates sub-additivity.

The above analyses were repeated for multiunit and LFP responses. For LFP responses, the area under the curve for each trial was calculated instead of the mean number of spikes per trial. Because multiunit activity reflects the spiking activity of multiple neurons in the vicinity of the recording electrode, and LFP activity reflects the local synaptic processing activity surrounding the recording electrode (Katzner et al., 2009), comparisons between these measures and single unit activity are referred to as comparisons between different scopes of neuronal activity in the current study. To differentiate between these multiunit/LFP measures and those of multisensory *integration* determined at the single unit level, the term 'multisensory *interaction*' is used here to denote a statistically significant change between the response during single modality stimulation (A,V,S) and combined modality stimulation (AS, AV, AVS) for multiunit and LFP responses. In order to assess possible differences in time course of the cross-modal interaction, the response difference between combined-sensory stimulation and single-modality stimulation was calculated for each recording site. Confidence intervals were constructed using the 100 ms prior to the onset of the visual stimulus, and any response that exceeded the 95% confidence interval was considered statistically different from zero.

4.4 Results

4.4.1 Overview

The goal of the present investigation was to evaluate whether auditory responses in DZ were modulated by individual or combined visual or tactile

stimuli, and to compare the findings at the single unit level to that of multiunit and LFP activity. Responses were collected from 176 single units, and from 390 multiunit and 407 LFP sites. Each site was presented with auditory, visual and somatosensory stimuli, both alone and in combination. I first report in detail the multisensory properties of single neurons in DZ, and then I go on to compare integration at the single unit level to multisensory processing at the level of multiunit and LFP activity.

4.4.2 Multisensory integration in DZ neurons

All DZ neurons identified as single units responded vigorously to auditory stimulation, and the majority were influenced exclusively by auditory stimulation (51.1%; 90/176) where non-auditory cues had no significant effect (either alone or in combination) on auditory responses, as depicted in **Figure 4.3 A-B**. No units were identified to be responsive to visual or somatosensory stimulation alone. A subset of neurons was found to be activated by auditory and by visual stimulation (33.5%; 59/176), termed bimodal multisensory neurons. Of these bimodal neurons, many (24/59) exhibited significant activity changes in response to multisensory stimulation, as illustrated in **Figure 4.3 G-H**; although most (n=35/59) did not (**Figure 4.3 E-F**). In addition, a small proportion of neurons were activated exclusively by auditory stimulation, but those auditory responses were significantly modulated by the presence of a visual and/or a somatosensory cue (15.4%; 27/117; **Figure 4.3 C-D**); termed subthreshold multisensory neurons (Dehner et al., 2004; Allman and Meredith 2007). In general, these findings agree well with previous studies documenting a higher prevalence of auditory-responsive than visually-responsive or bimodal neurons near the cortical surface of the ventral lip of the middle suprasylvian sulcus (Yaka et al., 2002; Allman and Meredith, 2007).

Overall, DZ neurons responded most strongly to the onset of the auditory stimulus, although a long-latency response to the sustained stimulus (500 ms duration) was also evident in most units. The duration of the sustained response was variable, ranging from 30 to 410 ms, with a mean duration of 174 ms. The

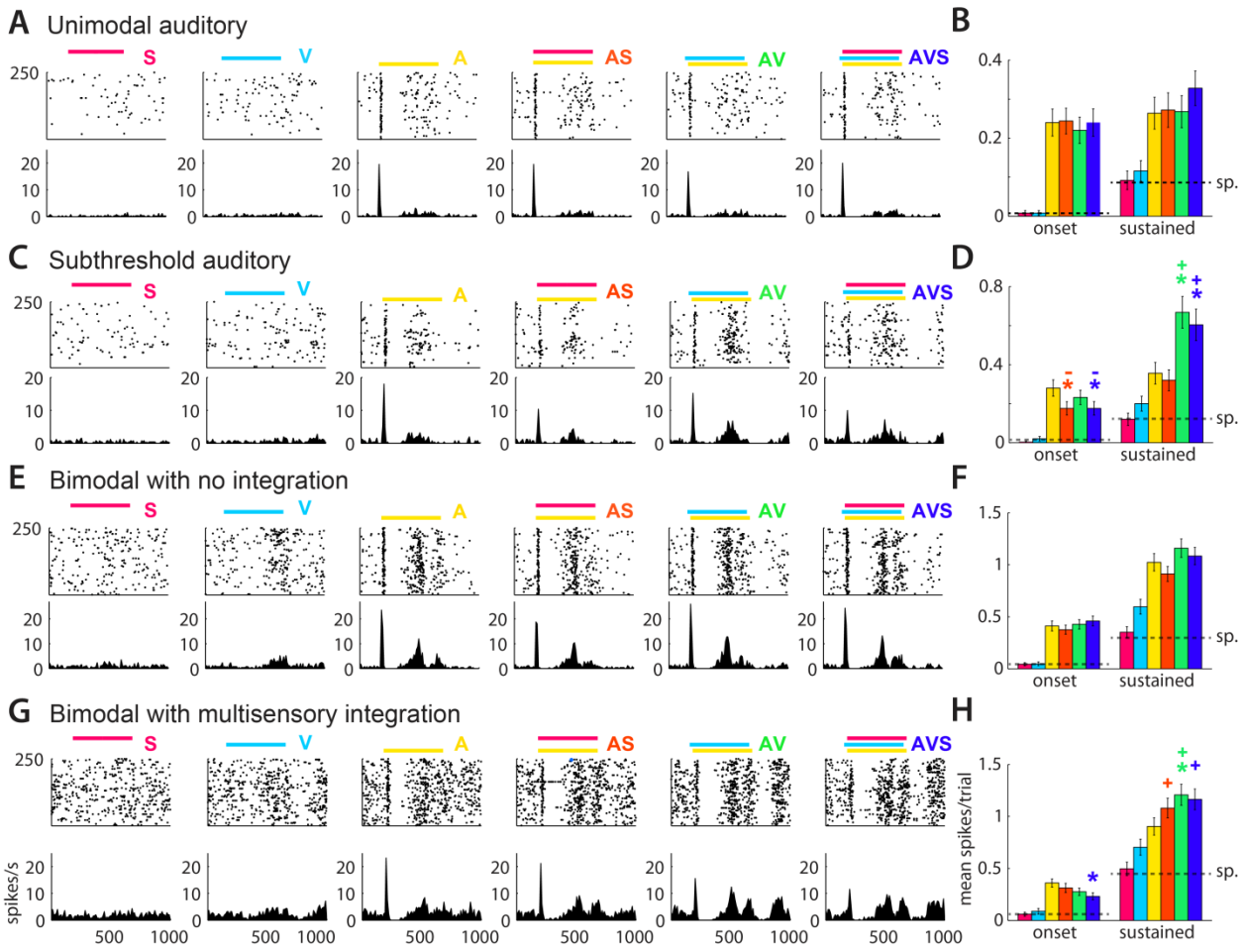

Figure 4.3 Representative examples of rasters, PSTHs and bar graphs of single unit responses for the four classes of neurons recorded in DZ.

The colored bars over each graph indicate the length and modality of the stimulus (S = somatosensory, V = visual, A = auditory). Note that regardless of class, there always exists a strong response of short duration to the onset of the stimulus, followed by a period of suppression, followed by a weaker response that is sustained until stimulus offset. Statistically significant enhancement or suppression is designated with an asterisk (*), while statistically significant sub/supra additivity is indicated by a minus (-) or plus (+) sign, respectively; $p < 0.05$ for both. **A:** A unimodal auditory neuron. This neuron showed no multisensory integration. The sustained response is still evident, but does not show any enhancement in combined modality stimulus conditions **B:** Bar graph showing mean spikes per trial recorded for both the onset portion of the response and the sustained portion of the response. The auditory response does not significantly differ from the responses during combined modality stimulation. **C:** A subthreshold auditory neuron. This unit shows sub-additive suppression of the

onset response on both the raster and PSTH (**C**) and the adjacent bar graph (**D**). The sustained portion of the response shows supra-additive enhancement of the response. **E:** A non-integrative bimodal neuron. No response enhancement or depression appears noticeable in the rasters and PSTHs, and no differences in response are evident on the accompanying bar graph (**F**). Note that the mean number of spikes/trial during the sustained portion of the response now well exceeds the spontaneous firing rate (sp.) **G:** A bimodal neuron showing multisensory integration during both the onset and sustained portions of the response. Note that the response at onset is depressed when all three modalities are stimulated (AVS), and the sustained response is enhanced whenever a visual stimulus accompanies the auditory stimulus (AV or AVS). All PSTHs were binned at a resolution of 10 ms. All error bars plotted indicate standard error of the mean.

---

mean peak of this response occurred at 382 ms relative to the onset of the auditory stimulus. In bimodal AV neurons, the response to the visual stimulus typically occurred just prior to the offset of the visual stimulus – in the vast majority of cases, there was no distinguishable response to visual stimulation at onset (e.g. **Figure. 4.3 E,G**). The direction of response modulation by visual and/or somatosensory stimulation differed for the different portions of the auditory response. The numbers of individual neurons showing response enhancement or suppression during each type of combined-modality stimulation are summarized in **Figure 4.4**. A greater proportion of neurons showed suppression of the onset response during combined modality stimulation, whereas the opposite was true for the sustained portion of the response, with the greatest number of neurons showing enhanced responses. Where enhancement was observed, it often exceeded the predicted sum of the responses to auditory and visual stimulation alone (i.e. enhanced responses tended to be supra-additive). These opposing effects observed between onset and sustained responses were generally observed for both bimodal and subthreshold multisensory neurons. Furthermore, the same neuron could be modulated by both visual and somatosensory stimulation, suggesting neuronal convergence (Meredith, 2002). This also indicates that multisensory DZ neurons are not

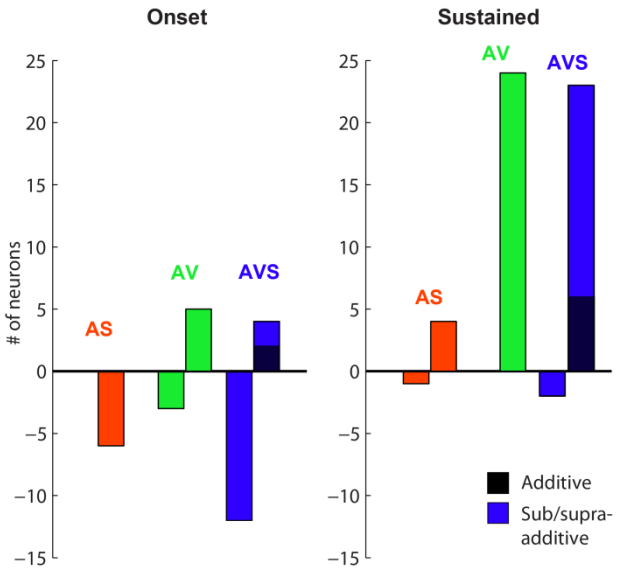

Figure 4.4 Summary of multisensory integration for individual single units.

Each bar indicates the number of neurons showing response enhancement (above zero) or depression (below zero) for each combined-modality stimulus (AS, AV, and AVS), for the onset portion of the response (left) as well as for the sustained portion of the response (right). Additionally, the enhanced neurons are subdivided into responses that are consistent with a linear sum of the unimodal response to auditory and visual stimulation (additive, black) or supra-additive (color).

comprised of independent populations of visually-modulated cells and somatosensory-modulated cells.

At a population level, although roughly a third of single units were bimodal and responded to both auditory and visual stimulation, there were significant differences in the level of spiking activity evoked by single modality stimulation ($F(2,244) = 109$, $p < 0.001$, $n = 123$). Post hoc Dunnett tests indicated that auditory stimulation ($m = 0.381$ spikes/trial) always evoked a greater number of spikes than somatosensory ($m = 0.020$ spikes/trial; $p < 0.001$) or visual stimulation ($m = 0.137$ spikes/trial, $p < 0.001$; **Figure 4.5 A**). The integrative effects observed at the population level also mirrored the findings for individual neurons. It should be noted that because no significant interaction was observed between the response to single modality stimulation (A, V, S) and response window (onset, sustained), the effects reported above are true for both portions of the response.

However, a statistically significant interaction between sensory condition (A, AS, AV, AVS) and response window (onset, sustained) was observed for the population of DZ neurons ($F(1.66, 208) = 38.3$; $p < 0.001$, Greenhouse-Geisser corrected). Across all single units, there were significant differences between the response to the auditory stimulus alone compared to that of combined modality stimulation for both the onset portion of the response ($F(3, 492) = 8.70$, $p < 0.001$; $n = 165$), as well as for the sustained portion of the response ($F(3, 396) = 37.6$, $p < 0.001$; $n = 133$). Post-hoc Dunnett tests determined that the mean number of spikes in the AVS condition ($m = 0.169$ spikes/trial) were lower than that of the A condition ($m = 0.183$ spikes/trial) for the onset portion of the response ($p < 0.01$; **Figure 4.5 B**). For the sustained portion of the response, the mean number of spikes per trial for both the AV ($m = 0.264$ spikes/trial) and AVS ($m = 0.259$ spikes/trial) conditions were increased compared to that of the A condition ($m = 0.170$ spikes/trial, $p < 0.001$ for both; **Fig. 4.5 B**).

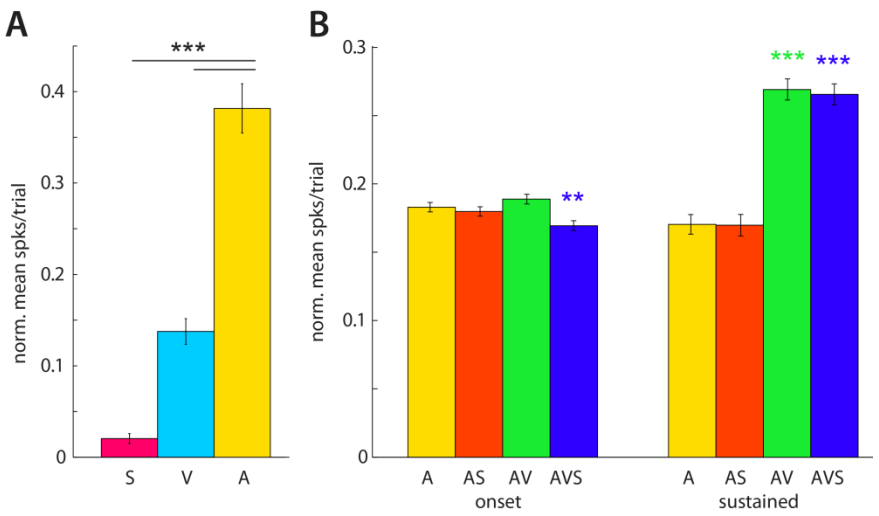

Figure 4.5 Summary of multisensory integration across the population of single units.

A: Auditory (A) stimulation over the entire response always evoked a greater response than visual (V) or somatosensory (S) stimulation. **B:** The onset portion of the response was suppressed during co-stimulation by all three modalities (AVS). The sustained portion of the response was enhanced during audiovisual (AV) stimulation as well as during co-stimulation by all three modalities (AVS). *p < 0.05; ***p < 0.001.

Unlike some previous reports (Allman and Meredith, 2007), no clear evidence of segregation of auditory versus bimodal sites at the single unit level was found. Rather, bimodal AV and integrative sites seemed to be scattered throughout DZ (**Figure 4.6 A**). Weighted linear regression analyses showed slight but non-significant trends for more bimodal cells located posteriorly in DZ (**Figure 4.6 B**), and more integrative cells located more deeply in DZ (**Figure 4.6 C**). However, overall, neither bimodal nor integrative neurons showed any statistically significant evidence of organization in either the rostrocaudal or mediolateral direction.

Collectively, these results are the first to demonstrate that almost half of the neurons in DZ are influenced by non-auditory stimuli, and that these multisensory neurons show no evidence of rostrocaudal or mediolateral organization. The modulatory effects reported above are evident at the neuronal level, as well as for the entire population of DZ neurons.

4.4.3 Response characteristics of single units in DZ

The auditory response characteristics for each class of neuron recorded in DZ (unimodal, subthreshold, bimodal non-integrative, and bimodal integrative) were also compared (**Figure 4.7**). No differences in peak response latencies for either the onset or sustained portion of the response were found between the classes of neurons recorded. Overall, the mean peak response latency of the auditory response was 20.7 ms. This corresponds well with previous studies that have documented longer onset response latencies in DZ compared to core areas of auditory cortex, namely the primary auditory cortex (A1) and the anterior auditory field (AAF; (Sutter and Schreiner, 1991; He et al., 1997; Stecker et al., 2005; Kok et al., 2015). One-way ANOVA tests showed that the response characteristics of the classes of neurons recorded were found to differ for peak firing rate ($F(3,162) = 6.77$, $p < 0.001$, $n = 166$) and spontaneous firing rate ($F(3,172) = 4.18$, $p < 0.01$, $n = 176$). Post hoc testing (Tukey's HSD) showed that bimodal integrative neurons had higher peak firing rates (26.3 spks/s) than

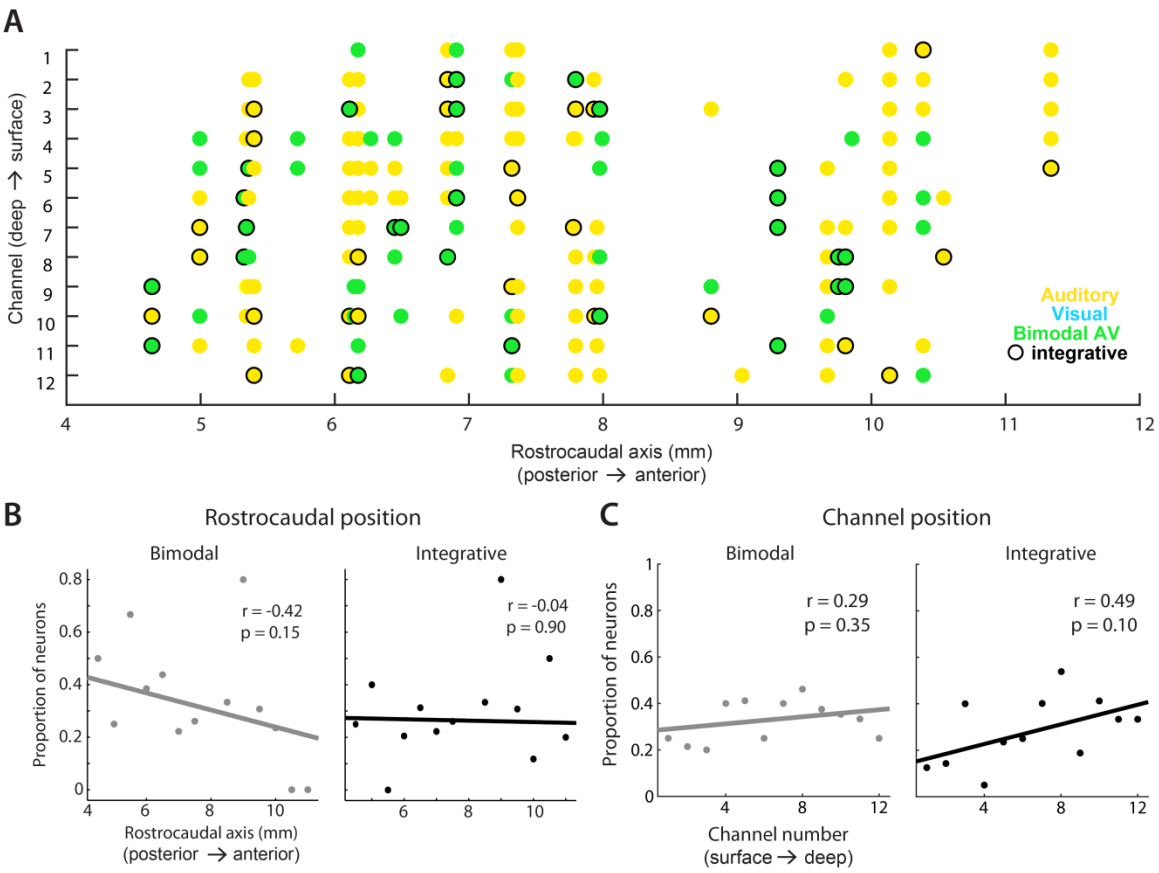

Figure 4.6 Location of bimodal and integrative neurons in DZ.

A: Location of neurons in DZ that responded only to auditory stimulation (yellow), or to both auditory and visual stimulation (bimodal; green) across all animals. There were no neurons in DZ responsive to visual stimulation alone. The channel location is plotted on the y-axis (1 is near the surface of cortex, 12 is deep), and rostrocaudal axis is plotted on the x-axis (the number in mm indicates the approximate A-P level in Horsley-Clarke coordinates). A black outline indicates a neuron that was either significantly suppressed or enhanced (i.e. an integrative neuron). **B:** Relationship between rostrocaudal position and incidence of bimodal (left; grey) or integrative (right; black) neurons in DZ. There is a non-significant trend towards more bimodal neurons posteriorly compared to anteriorly. **C:** Relationship between channel position and proportion of bimodal (left; grey) or integrative (right; black) neurons in DZ. Overall, DZ neurons do not show any apparent organization, either on the surface of cortex, or in terms of depth.

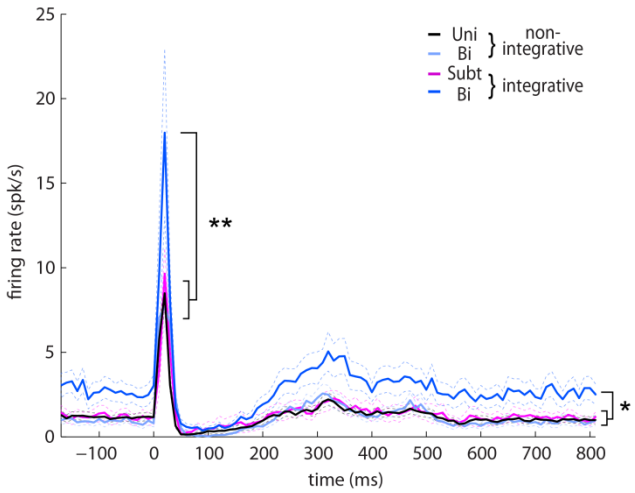

Figure 4.7 Summary of differences in response characteristics among classes of neurons in DZ.

Bimodal integrative neurons have higher peak and spontaneous firing rates than unimodal, subthreshold or bimodal non-integrative neurons. No differences in peak response latencies were found for either the onset or sustained portion of the response. For simplicity, only the minimum significant difference is shown here.

unimodal (10.9 spks/s, $p < 0.001$), subthreshold (12.0 spks/s, $p < 0.01$) or bimodal non-integrative (14.6 spks/s, $p < 0.05$) neurons. Bimodal integrative neurons also had higher spontaneous firing rates (2.6 spks/s) than unimodal (1.10 spks/s, $p < 0.01$), subthreshold (1.23 spks/s, $p < 0.05$) or bimodal non-integrative neurons (0.90 spks/s, $p < 0.05$). This supports previous research that has also documented higher spontaneous firing rates in bimodal compared to unimodal neurons in ferret parietal cortex (Foxworthy et al., 2013).

Response enhancement and additivity index distributions for each type of neuron and each portion of the response are depicted in **Figure 4.8**. The populations of subthreshold (med = -26.5%) and unimodal auditory (med = -11.5%) neurons appear to be responsible for mediating the suppression of the onset response in the AVS condition. This suggests that responses of unimodal auditory neurons also show evidence of suppression in the AVS condition, however, the suppression was not statistically significant at the level of individual neurons. Similarly, while the enhancement of the sustained portion of the response in the AV and AVS conditions is mediated by the populations of each class of neurons, the strongest levels of enhancement can be found amongst the subthreshold (med_{AV} = 57.7%; med_{AVS} = 49.9%) and integrative bimodal (med_{AV} = 40.3%; med_{AVS} = 28.8%) neurons. These findings are not particularly surprising given that both classes of integrative neuron are defined by a statistically significant modulation of the response. By comparison, all neuron classes are sub-additive for the onset portion of the response in the AVS condition. For the sustained portion of the response, both classes of integrative neurons (subthreshold and bimodal) are both supra-additive for the AV response, while in the AVS condition, only subthreshold neurons are supra-additive.

Together, these results suggest that bimodal integrative neurons as a class exhibit different response properties than other classes of neurons identified in DZ. Furthermore, subthreshold neurons show the highest proportional changes for onset response suppression as well as sustained response enhancement and additivity.

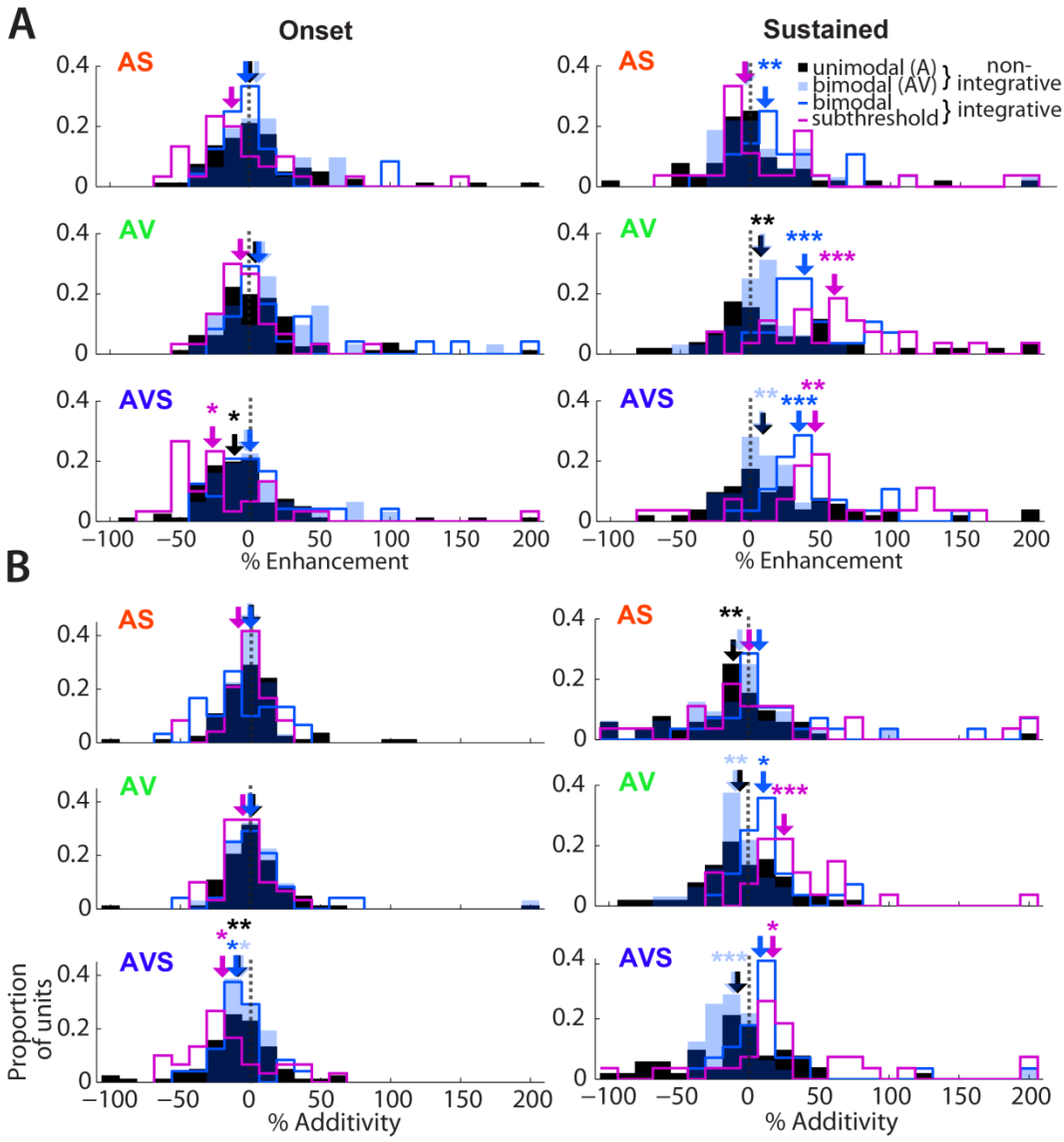

Figure 4.8 Distributions showing the enhancement and additivity indices for responses to combined-modality stimulation for each class of neuron encountered.

The enhancement (**A**) and additivity (**B**) indices for the onset and sustained portions of the response. Unimodal auditory (Uni) – black; non-integrative bimodal (Bi) – light blue; subthreshold (Subt) – magenta outline; and integrative bimodal (Bi) – blue outline. The arrows above each plot represent the median value for that distribution, and asterisks represent distributions with a median that differs significantly from a continuous distribution with a median of zero (two-sided sign test). The dashed black line indicates zero, while the solid red line indicates the mean of all classes of neurons. *p < 0.05; **p < 0.01; ***p < 0.001.

4.4.4 Timing of the visual stimulus

As with previous measures, an interaction between stimulus condition (A, AS, AV, AVS) and response window (onset, sustained) was found ($F(3,1048) = 44.4$, $p < 0.01$). Auditory peak responses were found to be modulated by combined-modality stimulation for both the onset ($F(3,524) = 11.5$, $p < 0.001$) and sustained ($F(3,524) = 68.0$, $p < 0.001$) response windows. Post hoc testing confirmed that auditory responses were suppressed during AVS stimulation ($p < 0.05$; **Figure 4.9 A**) during the onset portion of the response, but were enhanced following AV and AVS stimulation ($p < 0.001$ for both) during the sustained portion of the response. Both normalized peak firing rate and normalized area were tested within each condition containing a visual stimulus (V, AV, AVS) to determine if responses differed as a function of the timing of the visual stimulus. No significant differences were found as the timing of the visual stimulus varied for any of the conditions containing a visual stimulus.

However, these different measures of response activity (and multisensory integration) did not always exhibit the same effects at the same site. Figure 10 shows an example of one recording site at which the single unit responds only to auditory stimulation (**Figure 4.10 A**), whereas the multiunit site shows bimodal responses to auditory and visual stimulation (**Figure 4.10 B**), and the LFP site is trimodal, responding to auditory, visual and somatosensory stimulation (**Figure 4.10 C**). Differences in the proportion of units or sites responsive to auditory versus somatosensory or visual stimulation across DZ occur as the scope of neuronal activity increases from single unit to multiunit to LFP responses. The The averaged PSTH for each of the AV and AVS conditions are plotted over the auditory response in **Figure 4.9 B**. Note that although there is some variability in the response, both the shape of the PSTHs as well as the effects of combined stimulation are fairly consistent regardless of the timing of the visual stimulus relative to the auditory stimulus. The onset response is always suppressed, while the sustained portion of the response is always enhanced during combined-modality stimulation paradigms. Therefore, the timing of the visual stimulus

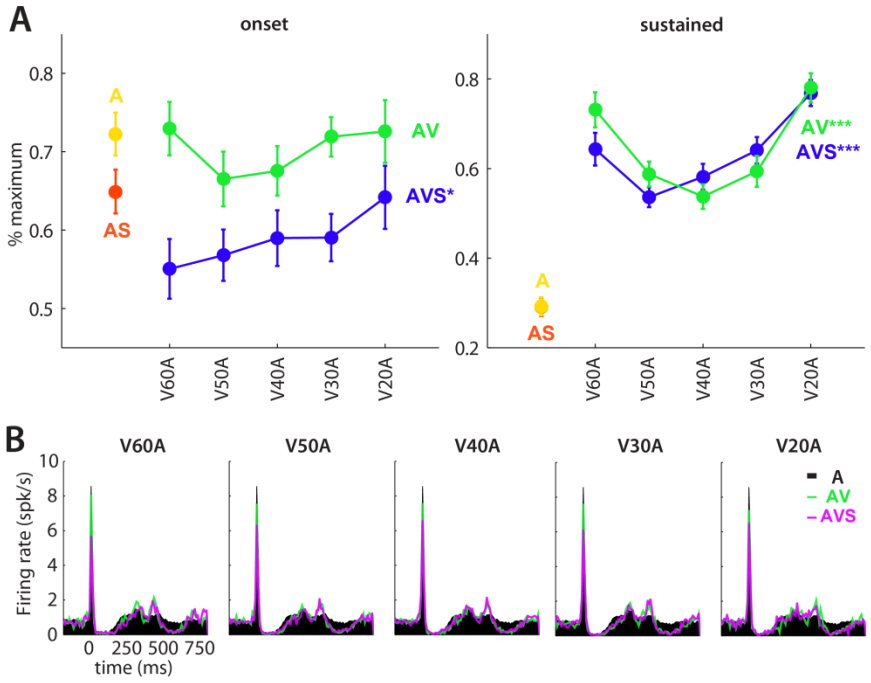

Figure 4.9 Analysis of visual onset asynchronies.

A: Mean normalized peak firing rate (expressed as a percentage of the maximum firing rate for a particular block of trials) for A and each of the combined-modality multisensory stimulus conditions (AS, AV, AVS) for each stimulus onset asynchrony. Note that the effects reported here are remarkably similar to those reported above, regardless of the timing of the visual stimulus relative to the auditory stimulus. Onset responses to all three conditions are suppressed, whereas sustained responses to AV and AVS are enhanced. Asterisks indicate a statistical difference compared to the auditory stimulus; *$p < 0.05$, ***$p < 0.001$. **B:** Averaged PSTHs for each of the visual onset asynchronies. The response to A is plotted in black, with the responses to AV (green) and AVS (magenta) superimposed. Histograms are plotted with 10 ms bins.

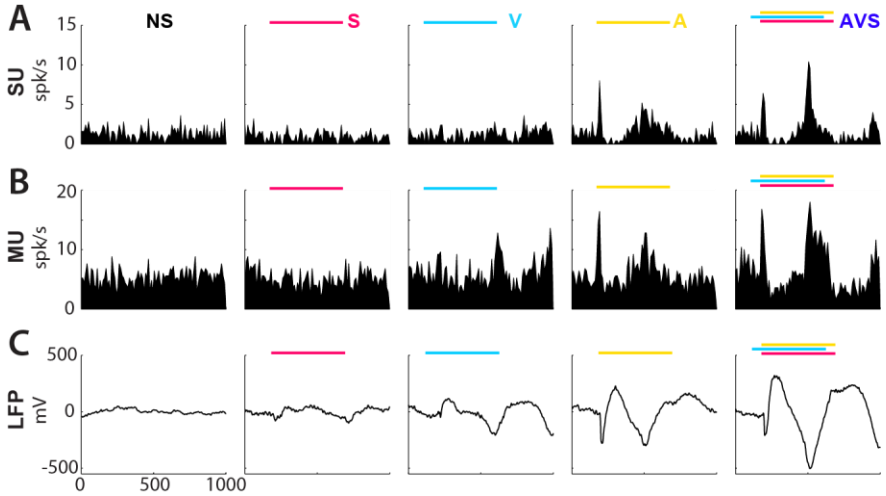

Figure 4.10 Representative site showing neuronal responses at different scales of activity

PSTHs and mean LFP response are shown for spontaneous activity (NS), each unimodal stimulus (S, V, A), and combined stimulation (AVS). For simplicity, only the AVS combined stimulation paradigm is shown. **A:** The single unit shows no discernable response to S or V stimulation, but robust activity to A stimulation. This spiking activity is increased during the sustained portion of the response to AVS stimulation. This unit would therefore be classified as a subthreshold multisensory neuron. **B:** In the multiunit activity, a response to the visual stimulus is now evident. Again, spiking activity is increased during the sustained portion of the response. This site would therefore be classified as bimodal with a multisensory interaction. **C:** Onset and offset responses to somatosensory stimulation are evident in the LFP trace. The area under the curve for the sustained portion of the response is increased following AVS stimulation. Therefore, this site is classified as trimodal with a multisensory interaction.

relative to the auditory stimulus does not alter the pattern of integrative effects observed in the present study.

4.4.5 Comparison of SU data with MU and LFP activity

The present study examined not only the effects of non-auditory stimulation on identified single units in DZ, those same recordings also revealed multiunit responses at the same time that local field potentials were recorded. The proportion of bimodal AV responses increases from 33.5% (59/176) at the single unit level to 74.6% (291/390) at the multiunit level and 53.8% (219/407) for field potentials (**Figure 4.11 A-C**). However, bimodal AS and trimodal AVS responses are additionally present in the field potentials, but are not observed in the spiking responses of single or multiunit activity. These field potential responses to somatosensory stimuli were observed in all animals but one, and tended to represent contralateral space (45.5% contralateral vibrissae, 43.6% contralateral forepaw, 10.9% bilateral vibrissae). These somatosensory responses were found at sites throughout DZ, with no apparent organization or differences in distribution. When all field potential sites that show bimodal or trimodal influences (AV, AS, or AVS) are considered, this proportion (78.6% or 320/407) is very similar to that observed for bimodal AV responses in the multiunit activity (74.6%; 291/390 sites).

Differences between the proportion of single units that showed multisensory integration and the proportion of sites that showed multisensory interactions for multiunit and LFP activity were observed. The total number of single units that showed multisensory integration was 51/176 (29.0%). In comparison, a higher proportion of multiunit (252/390 or 64.6%) and local field potential sites (239/407 or 58.7%) showed multisensory interactions.

The mean response profile for each scope of activity shows a number of similarities as well as some key differences. AVS responses during the onset portion of the response are smaller in magnitude than A responses for all three

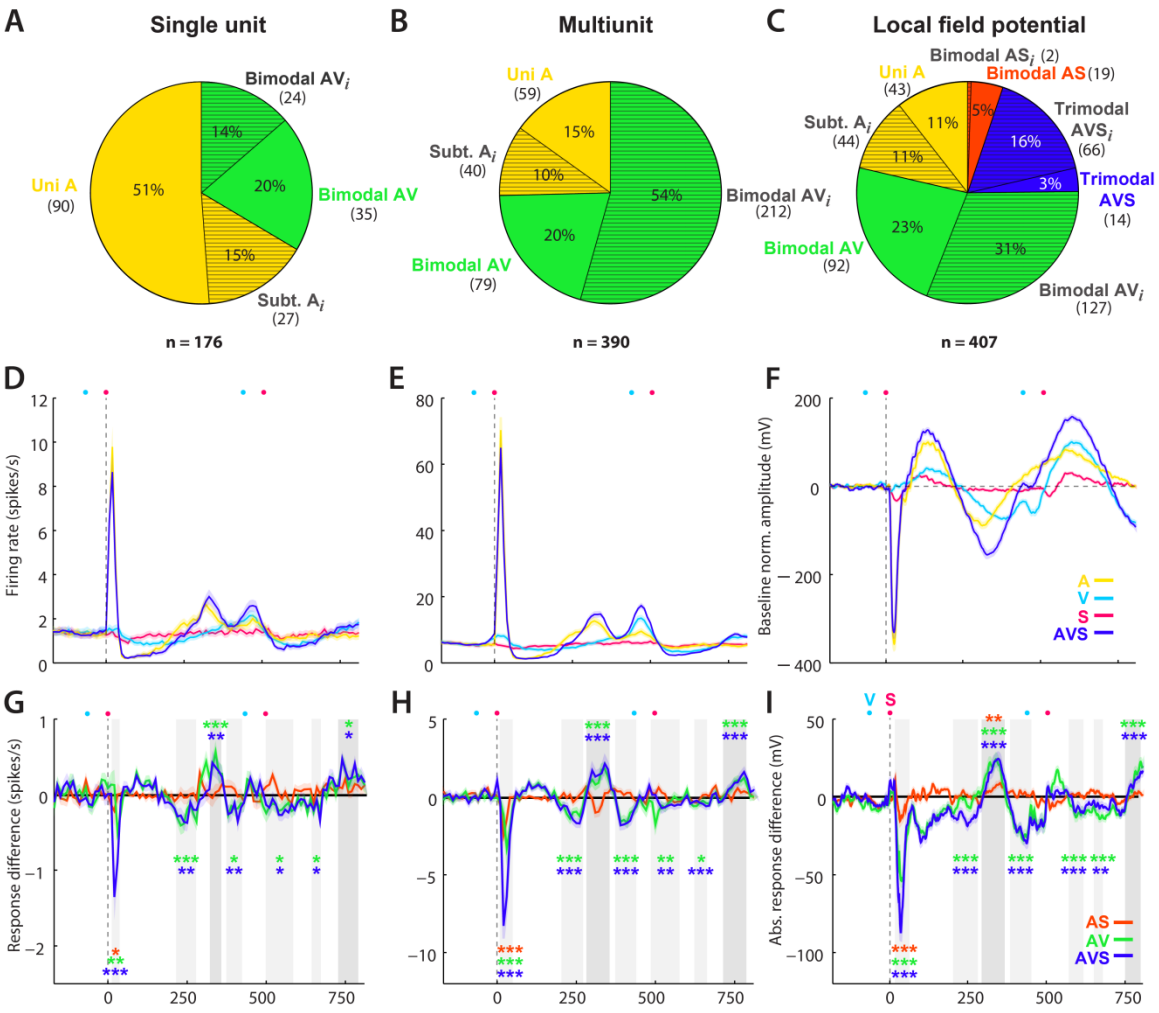

Figure 4.11 Summary of results for single unit (SU), multiunit (MU) and local field potential (LFP) responses.

A-C: Proportion of each type of response recorded for SU, MU and LFP recordings. The number of units for each type of response is also indicated in parentheses. **D-F:** Grand average responses over all recorded sites for SU, MU and LFP recordings, respectively. The onset of the auditory stimulus is indicated by a vertical dashed line, with the onset and offset of the visual (blue) and somatosensory (pink) stimuli indicated by colored circles. **G-I:** The time course of the cross-modal interaction. For each graph, the plotted line represents the difference between responses to multi-modal stimulation and single modality stimulation (e.g. AVS here represents AVS-A-V-S), leaving the resultant cross-modal interaction. Confidence intervals were calculated for the baseline response 100 ms prior to the onset of the visual stimulus. Grey boxes indicate regions of similarity between the three scopes of neuronal activity that are statistically different from baseline, with the magnitude of the difference for each line

indicated by asterisks (*p < 0.05, **p < 0.01, ***p < 0.001). Dark grey boxes indicate regions where the response is lower than baseline, whereas lighter grey boxes indicate regions where the response is greater than baseline.

---

measures (SU, MU, LFP; **Fig. 4.11 D-F**). Responses to single modality auditory and visual stimulation are both evident during the sustained portion of the response at all three scopes of activity, with the response to AVS stimulation exceeding the response to either modality presented alone at multiple timepoints. In contrast, there are somatosensory responses to stimulus onset and offset present in the LFP activity, which are entirely absent in the single and multiunit spiking responses.

A comparison of the time course of the cross-modal interaction between all three scopes also yields very similar findings (**Figure 4.11 G-I**). Again, at all three scopes of activity, the response during AVS stimulation was suppressed during the onset portion of the response. However, both the AS and AV conditions show the same trend, albeit smaller in magnitude. The sustained portion of the response is modulated in an interesting way across all three scopes of activity for the AV and AVS conditions as well. A period of increased suppression is evident starting around 200 ms, followed by the response enhancement previously mentioned, after which suppression is again evident around 500 ms in the single unit and multiunit plots, and 400-500 ms in the LFP. Finally, after the offset of all stimulus modalities, there is again suppression of the response around 650 ms in the single and multiunit plots, and at 750 ms in the LFP plot. This agrees well with what appears to be a “sharpening” of the sustained response in during combined-modality stimulation in the rasters and PSTHs of individual units (**Figure 4.3 C,G**). This is immediately followed by enhancement during the last 100 ms of the response across all three scopes of neuronal activity in the AV and AVS conditions. Together, these results indicate a much larger proportion of sites responsive to more than one stimulus modality,

as well as a higher proportion of sites with multisensory interactions for multiunit and LFP activity compared to single unit activity.

4.4.6 Summary of findings

At the single unit level, the majority of DZ neurons are vigorously responsive to auditory stimulation and are not modulated by the presence of a stimulus from another sensory modality. However, nearly half are multisensory neurons that are influenced by non-auditory stimuli and are present in bimodal or subthreshold forms. Both bimodal and subthreshold neurons exhibited multisensory integration when auditory cues were combined with non-auditory stimuli, which suppressed auditory onset responses while enhancing sustained auditory activity. This finding was true for individual neurons, as well as for the entire population of neurons recorded. These bimodal and integrative neurons also appeared to be scattered throughout DZ, with no apparent organization. Finally, I demonstrate that, compared with single unit measures, multiunit and LFP activity in DZ show increased evidence of multisensory processing. This is manifested in two ways. First, multiunit and LFP recordings have a higher incidence of bimodal and/or trimodal sites than do single neurons. In both cases, roughly three-quarters of multiunit and LFP sites showed overt responses to more than one stimulus modality, compared to about one-third of single units. Second, more than half of multiunit and LFP sites demonstrated multisensory interactions, compared to less than one-third of single units. Together, these findings suggest that studies of multisensory integration at the multiunit and field potential level may over-represent the multisensory properties of single units.

4.5 Discussion

The present study demonstrates clear evidence of both visual and somatosensory modulation of auditory reponses at multiple scopes of neuronal activity, showing that regions of the cerebrum often considered ‘unimodal’ can be modulated by other senses. These results are supported by a growing body of literature documenting multisensory integration in ‘unisensory’ cortices (see

reviews of Shimojo and Shams, 2001; Ghazanfar and Schroeder, 2006; Macaluso, 2006). However, although functional imaging research has demonstrated multisensory audio-visual and audio-tactile interactions in auditory cortex (for review, see Calvert, 2001), electrophysiological investigations in auditory cortex have tended to focus on either visual or somatosensory influences, not both.

Anatomical, behavioral and electrophysiological studies have demonstrated that DZ is a higher-order area of cat auditory cortex known to play a role in auditory localization (He et al., 1997; Stecker et al., 2005; Lee and Winer, 2008; Malhotra et al., 2008; Kok et al., 2015). Our findings support previous studies which have demonstrated that higher-order regions of cortex typically show increased incidence of multisensory interactions compared to core regions (Ghazanfar et al., 2005; Kayser et al., 2008; Bizley and King, 2009). Additionally, the proportion of visually-modulated neurons in DZ is comparable to that of higher-order regions of ferret auditory cortex (Bizley et al., 2007; Bizley and King, 2009), and the proportion of subthreshold neurons is comparable to that of adjacent extrastriate visual cortex (Allman and Meredith, 2007).

Larger proportions of multisensory neurons are also known to be found at the borders between sensory modalities (Meredith, 2004; Wallace et al., 2004). Presumably, this phenomenon results from modality-specific projections that extend beyond the areal limits of a particular modality. DZ represents the dorsal limit of auditory cortex (Middlebrooks and Zook, 1983), and is bordered by an extrastriate visual area, from which it receives projections that become strengthened following deafness (Barone et al., 2013; Kok et al., 2014). DZ has also been shown to confer compensatory visual motion processing capabilities following deafness (Lomber et al., 2010), suggesting behavioral functional relevance of these visual inputs. Therefore, the unique position of DZ at the border of the auditory and visual cortices, as well as known interconnectivity with visual cortex and visual reorganization following deafness would suggest a proclivity towards multisensory processing, which is confirmed in the present

study. Interestingly, neither the bimodal nor the integrative populations are organized rostrocaudally or mediolaterally within DZ. A gradient for bimodal responses in either direction could have been expected, given the position of DZ at the interface of the auditory and visual cortices, as well as the known connectivity of DZ with extrastriate visual cortex discussed above.

Although auditory-tactile interactions have been shown using imaging and EEG (Foxe et al., 2000, 2002) as well as field potential and neuronal analyses (Fu et al., 2003; Lakatos et al., 2007), only recently has somatosensory modulation of single unit auditory responses been shown in A1 of the ferret (Meredith and Allman, in press). Our results also document suppressive somatosensory modulation of auditory responses at the single unit level. This finding was somewhat unexpected, given the low proportion of ipsilateral projections DZ receives from somatosensory (<1%) and associative (~5%) cortical regions, and auditory cortical fields with known somatosensory influences (AAF and fAES) that become responsive to somatosensory stimulation following deafness (Lee and Winer, 2008; Meredith and Lomber, 2011; Meredith et al., 2011; Barone et al., 2013; Kok et al., 2014). While these weak cortico-cortical projections could account for the few neurons that showed audio-tactile enhancement of the sustained response, I consider them unlikely to be responsible for the tactile-related suppression of the onset response, because of the short latency with which the onset modulation occurred. Previous investigations in macaque A1 have suggested that somatosensory modulation of auditory LFPs occurs via non-specific thalamic afferents, based on the supragranular location and short latency of the somatosensory activation (Lakatos et al., 2007). Auditory responses in DZ are largely dependent on information arising from A1 (Kok et al., 2015), and although the bulk of thalamo-cortical projections to DZ are from dorsal medial geniculate nucleus (MGN), strong projections from medial MGN also exist (Winer et al., 2001), which itself is known to become activated by a combination of vestibular and tactile stimulation (Wepsic, 1966; Blum et al., 1979). Therefore, the somatosensory modulation of auditory onset responses in DZ are likely the result of subcortical modulation;

however, it remains unknown whether this modulation arrives via direct thalamo-cortical projections to DZ, or via A1.

The present study is the first to document diametric integrative effects (i.e. opposite in direction) during different portions of the spiking response to a stimulus, although similar effects have been reported previously for visually-modulated field potentials in rat primary somatosensory cortex (Sieben et al., 2013). One reason for this might be that the duration of the stimuli used here were considerably longer than those typically used in studies of multisensory integration. This meant I considered neuronal responses to longer stimuli over a longer period of time than is typical for single unit investigations. In fact, the sustained response to auditory stimulation didn't come online until ~200 ms after the onset of the auditory stimulus, and the sustained response seems particularly susceptible to modulation by visual stimulation, accounting for the majority of integrative DZ neurons reported above.

A number of factors are known to affect the direction of multisensory interactions, namely, the timing (Meredith et al., 1987), location (Meredith and Stein, 1986), and efficacy (Meredith and Stein, 1983) of the stimuli. Although stimulus onset asynchronies were programmed to produce maximal response enhancement, onset responses were typically suppressed during combined modality stimulation in the present study. This suppression does not appear to be related to the timing of the visual stimulus (**Figure 4.9**). The location of the stimulus in space has also been shown to affect the direction of multisensory interactions: responses tend to be suppressed when presented in ipsilateral space, but enhanced when presented in contralateral space (Meredith and Stein, 1986; Lakatos et al., 2007). With the exception of one somatosensory stimulator in ipsilateral space, the visual stimulus and the two other somatosensory stimulators were presented in contralateral space. The lack of field potential responses to ipsilateral stimulation would suggest that the position of this stimulator is unlikely to account for the suppression seen here. Finally, the efficacy of stimulation is known to affect levels of multisensory integration –

weakly effective stimulation has been shown to yield larger response enhancements than strongly effective stimulation (Meredith and Stein, 1983). In the present study, the same, simple stimulus set of auditory noise bursts, diffuse light flashes, and light tactile stimulation were used at each site. Because individual neurons in DZ are known to show spatial (Stecker et al., 2005) and duration (He et al., 1997) tuning, the stimulus set used here is likely sub-optimal for many of the neurons recorded. Therefore, none of the factors that have been shown to affect multisensory integration appear to be wholly responsible for the opposing effects documented in the present study.

However, peak auditory-evoked spiking responses were also suppressed during audio-visual stimulation in macaque auditory cortex (Kayser et al., 2008), and both visual and tactile stimulation have been shown to reset the phase of ongoing oscillatory activity in auditory cortex, affecting the direction of response modulation (Lakatos et al., 2007; Kayser et al., 2008). I suggest the same mechanisms could be responsible for the visual- or tactile-induced onset suppression observed here. In contrast, the longer-latency enhancement of the sustained response could be mediated by strong cortico-cortical projections from PLLS (Kok et al., 2014), however, further experimentation will be needed to definitively elucidate the timing and contribution of these direct lateral projections from extrastriate visual cortex to DZ.

While an increasingly large number of behavioral, imaging and EEG/MEG studies have documented multisensory interactions across multiple species and brain regions (see review of Driver and Noesselt, 2008), it is unclear what such interactions reflect in terms of the multisensory processing capabilities of the actual neurons that comprise these regions. For example, LFP activity is known to correlate with the hemodynamic signal of fMRI analyses, as well as EEG/MEG measures (see Buzsáki et al., 2012 for review). Because methodologies like functional imaging, along with MU and LFP measures, reflect the aggregate activity of a population of neurons, it is difficult to discern what types of neurons are present in the population signal. This issue is compounded for LFP and

functional imaging methodologies as activity at these levels reflect neuronal input to a population of cells within a region of cortex, as opposed to neuronal output (e.g. Stevenson et al., 2014). However, direct comparisons of multisensory processing at different scales of neuronal activity are generally lacking, despite the preponderance of research findings using each technique. To date, only one study has previously compared integration at the neuronal level to that of field potentials (Kayser et al., 2008). Here I provide additional evidence to bridge this gap by comparing single unit, multiunit and LFP responses.

The present study documents a disparity in terms of the level of multisensory processing recorded at multiple scopes of neuronal activity. Higher proportions of bimodal and trimodal units, as well as a higher incidence of multisensory interactions were documented for field potential responses compared to single unit responses. Similar increases in multisensory response sites have been reported for field potentials compared to single and multiunit activity in the belt regions of macaque auditory cortex (Kayser et al., 2009). Together, these findings suggest that auditory and somatosensory influences are present in population signals (e.g. MU, LFP) in auditory cortex across multiple species, and may over-represent the level of integration present in single neurons. Ultimately, these findings indicate that visual and somatosensory influences are present in the processing of sensory signals in auditory cortex, and, thereby, further challenges the notion of cortical modality-specific modularity.

4.6 References

Allman BL, Meredith MA (2007) Multisensory processing in “unimodal” neurons: cross-modal subthreshold auditory effects in cat extrastriate visual cortex. J Neurophysiol 98:545–549.

Barone P, Lacassagne L, Kral A (2013) Reorganization of the connectivity of cortical field DZ in congenitally deaf cat. PLoS One 8:e60093.

Bavelier D, Neville HJ (2002) Cross-modal plasticity: where and how? Nat Rev Neurosci 3:443–452.

Bizley JK, King AJ (2008) Visual-auditory spatial processing in auditory cortical neurons. Brain Res 1242:24–36.

Bizley JK, King AJ (2009) Visual influences on ferret auditory cortex. Hear Res 258:55–63.

Bizley JK, Nodal FR, Bajo VM, Nelken I, King AJ (2007) Physiological and anatomical evidence for multisensory interactions in auditory cortex. Cereb Cortex 17:2172–2189.

Blum PS, Abraham LD, Gilman S (1979) Vestibular, auditory, and somatic input to the posterior thalamus of the cat. Exp Brain Res 34:1–9.

Budinger E, Heil P, Hess A, Scheich H (2006) Multisensory processing via early cortical stages: Connections of the primary auditory cortical field with other sensory systems. Neuroscience 143:1065–1083.

Bullier J, Nowak LG (1995) Parallel versus serial processing: New vistas on the distributed organization of the visual system. Curr Opin Neurobiol 5:497–503.

Buzsáki G, Anastassiou CA, Koch C (2012) The origin of extracellular fields and currents--EEG, ECoG, LFP and spikes. Nat Rev Neurosci 13:407–420.

Calvert GA (2001) Crossmodal processing in the human brain: insights from functional neuroimaging studies. Cereb Cortex 11:1110–1123.

Carrasco A, Lomber SG (2011) Neuronal activation times to simple, complex, and natural sounds in cat primary and nonprimary auditory cortex. J Neurophysiol 106:1166–1178.

Driver J, Noesselt T (2008) Multisensory interplay reveals crossmodal influences on “sensory-specific” brain regions, neural responses, and judgments. Neuron 57:11–23.

Falchier A, Clavagnier S, Barone P, Kennedy H (2002) Anatomical evidence of multimodal integration in primate striate cortex. J Neurosci 22:5749–5759.

Foxworthy WA, Allman BL, Keniston LP, Meredith MA (2013) Multisensory and unisensory neurons in ferret parietal cortex exhibit distinct functional properties. Eur J Neurosci 37:910–923.

Fu KG, Johnston TA, Shah AS, Arnold L, Smiley J, Hackett TA, Garraghty PE, Schroeder CE (2003) Auditory cortical neurons respond to somatosensory stimulation. J Neurosci 23:7510–7515.

Ghazanfar AA, Maier JX, Hoffman KL, Logothetis NK (2005) Multisensory integration of dynamic faces and voices in rhesus monkey auditory cortex. J Neurosci 25:5004–5012.

Ghazanfar AA, Schroeder CE (2006) Is neocortex essentially multisensory? Trends Cogn Sci 10:278–285.

He J, Hashikawa T, Ojima H, Kinouchi Y (1997) Temporal integration and duration tuning in the dorsal zone of cat auditory cortex. J Neurosci 17:2615–2625.

Horsley V, Clarke RH (1908) The structure and function of the cerebellum examined by a new method. Brain 31:45-124.

Katzner S, Nauhaus I, Benucci A, Bonin V, Ringach DL, Carandini M (2009) Local origin of field potentials in visual cortex. Neuron 61:35–41.

Kayser C, Petkov CI, Logothetis NK (2008) Visual modulation of neurons in auditory cortex. Cereb Cortex 18:1560–1574.

Kayser C, Petkov CI, Logothetis NK (2009) Multisensory interactions in primate auditory cortex: fMRI and electrophysiology. Hear Res 258:80–88.

Kok MA, Chabot N, Lomber SG (2014) Cross-modal reorganization of cortical afferents to dorsal auditory cortex following early- and late-onset deafness. J Comp Neurol 522:654–675.

Kok MA, Stolzberg D, Brown TA, Lomber SG (2015) Dissociable influences of primary auditory cortex and the posterior auditory field on neuronal responses in the dorsal zone of auditory cortex. J Neurophysiol 113:475–486.

Lakatos P, Chen C-M, O'Connell MN, Mills A, Schroeder CE (2007) Neuronal oscillations and multisensory interaction in primary auditory cortex. Neuron 53:279–292.

Lee CC, Winer JA (2008) Connections of cat auditory cortex: III. Corticocortical system. J Comp Neurol 507:1920–1943.

Lomber SG, Meredith MA, Kral A (2010) Cross-modal plasticity in specific auditory cortices underlies visual compensations in the deaf. Nat Neurosci 13:1421–1427.

Macaluso E (2006) Multisensory processing in sensory-specific cortical areas. Neurosci 12:327–338.

Malhotra S, Hall AJ, Lomber SG (2004) Cortical control of sound localization in the cat: unilateral cooling deactivation of 19 cerebral areas. J Neurophysiol 92:1625–1643.

Malhotra S, Stecker GC, Middlebrooks JC, Lomber SG (2008) Sound localization deficits during reversible deactivation of primary auditory cortex and/or the dorsal zone. J Neurophysiol 99:1628–1642.

Mellott JG, van der Gucht E, Lee CC, Carrasco A, Winer J a, Lomber SG (2010) Areas of cat auditory cortex as defined by neurofilament proteins expressing SMI-32. Hear Res 267:119–136.

Merabet LB, Pascual-Leone A (2010) Neural reorganization following sensory loss: the opportunity of change. Nat Rev Neurosci 11:44–52.

Meredith MA (2002) On the neuronal basis for multisensory convergence: A brief overview. Cogn Brain Res 14:31–40.

Meredith MA (2004) Cortico-cortico connectivity of cross-modal circuits. In: Handbook of multisensory processing (Calvert G, Spence C, Stein BE, eds), pp 343-358. Cambridge: MIT Press.

Meredith MA, Allman BL (2012) Early hearing-impairment results in crossmodal reorganization of ferret core auditory cortex. Neural Plast 2012:601591.

Meredith MA, Kryklywy J, McMillan AJ, Malhotra S, Lum-Tai R, Lomber SG (2011) Crossmodal reorganization in the early deaf switches sensory, but not behavioral roles of auditory cortex. Proc Natl Acad Sci 108:8856–8861.

Meredith MA, Lomber SG (2011) Somatosensory and visual crossmodal plasticity in the anterior auditory field of early-deaf cats. Hear Res 280:38–47.

Meredith MA, Nemitz JW, Stein BE (1987) Determinants of multisensory integration in superior colliculus neurons. I . Temporal factors. J Neurosci 7:3215–3229.

Meredith MA, Stein BE (1983) Interactions among converging sensory inputs in the superior colliculus. Science (80-) 221:389–391.

Meredith MA, Stein BE (1986) Spatial factors determine the activity of multisensory neurons in cat superior colliculus. Brain Res 365:350–354.

Meredith MA, Allman BL (in press) Single-unit analysis of somatosensory processing in the core auditory cortex of hearing ferrets. Eur J Neurosci.

Middlebrooks JC, Zook JM (1983) Intrinsic organization of the cat's medial geniculate body identified by projections to binaural response-specific bands in the primary auditory cortex. J Neurosci 3:203–224.

Olfert ED, Cross BM, McWilliam AA eds. (1993) Guide to the Care and Use of Experimental Animals. Ottawa, Ontario: Canadian Council on Animal Care.

Sarko DK, Ghose D, Wallace MT (2013) Convergent approaches toward the study of multisensory perception. Front Syst Neurosci 7:81.

Schroeder CE, Foxe JJ (2002) The timing and laminar profile of converging inputs to multisensory areas of the macaque neocortex. Cogn Brain Res 14:187–198.

Shimojo S, Shams L (2001) Sensory modalities are not separate modalities: plasticity and interactions. Curr Opin Neurobiol 11:505–509.

Sieben K, Röder B, Hanganu-Opatz IL (2013) Oscillatory entrainment of primary somatosensory cortex encodes visual control of tactile processing. J Neurosci 33:5736–5749.

Stanford TR, Quessy S, Stein BE (2005) Evaluating the operations underlying multisensory integration in the cat superior colliculus. J Neurosci 25:6499–6508.

Stevenson RA, Ghose D, Fister JK, Sarko DK, Altieri NA, Nidiffer AR, Kurela LR, Siemann JK, James TW, Wallace MT (2014) Identifying and quantifying multisensory integration: A tutorial review. Brain Topogr 27:707-730.

Stecker GC, Harrington IA, Macpherson EA, Middlebrooks JC (2005) Spatial sensitivity in the dorsal zone (area DZ) of cat auditory cortex. J Neurophysiol 94:1267–1280.

Sutter ML, Schreiner CE (1991) Physiology and topography of neurons with multipeaked tuning curves in cat primary auditory cortex. J Neurophysiol 65:1207–1226.

van der Gucht E, Vandesande F, Arckens L (2001) Neurofilament protein: A selective marker for the architectonic parcellation of the visual cortex in adult cat brain. J Comp Neurol 441:345–368.

Wallace MT, Ramachandran R, Stein BE (2004) A revised view of sensory cortical parcellation. Proc Natl Acad Sci U S A 101:2167–2172.

Wepsic JG (1966) Multimodal sensory activation of cells in the magnocellular medial geniculate nucleus. Exp Neurol 15:299–318.

Winer JA, Diehl JJ, Larue DT (2001) Projections of auditory cortex to the medial geniculate body of the cat. J Comp Neurol 430:27–55.

Yaka R, Notkin N, Yinon U, Wollberg Z (2002) Visual , auditory and bimodal activity in the banks of the lateral suprasylvian sulcus in the cat. Neurosci Behav Physiol 32:103–108.

Chapter 5: Visual and somatosensory cross-modal reorganization in the dorsal zone of auditory cortex following perinatal deafness

5.1 Abstract

Recently, it was shown that a specific region within cat auditory cortex, the dorsal zone (DZ), becomes reorganized following perinatal deafness to confer superior visual motion detection ability compared to hearing animals (Lomber et al., 2010). Subsequently, an increase in projection strength from extrastriate visual motion processing areas to DZ in deaf animals was also demonstrated (Kok et al., 2014). Thus, the goal of the present study was to investigate the neural basis for this reorganization in perinatally-deafened cats by electrophysiologically recording from DZ. These results were compared to those of hearing animals previously reported in Chapter 4. In hearing animals, the majority of neurons responded to auditory stimulation alone, whereas in deaf animals, the findings were markedly different, with the majority of neurons responding exclusively to visual stimulation. Additionally, one-third of neurons responded bimodally to visual and tactile stimulation in deaf animals. This ratio was consistent for multiunit and local field potential (LFP) activity as well, and is similar to the proportion of sites that showed somatosensory responses in hearing animals in Chapter 4. These results are consistent with previous behavioral and connectional findings demonstrating that DZ is cross-modally reorganized following deafness for the processing of visual stimuli. When considered in conjunction with previous anatomical and multisensory recording data, the data suggest that the somatosensory reorganization observed in the present study reflects the unmasking of previously silent synapses, whereas the visual reorganization is likely due to both unmasking as well as the formation of new synapses.

5.2 Introduction

The remarkable ability of the human brain to adapt to sensory loss has been reported anectodally for over a century, however, only recently have these claims been substantiated in the laboratory. For example, in humans, an increasing number of studies have documented superior performance of blind individuals compared to sighted controls during the performance of tactile discrimination tasks (e.g. Stevens et al., 1995, Goldreich & Kanics, 2003, Alary et al. 2008), as well as auditory spatial (e.g. Lessard et al., 1998) and pitch discrimination tasks (Gougoux et al, 2004; Wan et al., 2010), and even odor discrimination (Cuevas et al., 2010). Similarly, deaf individuals have shown evidence of enhanced tactile sensitivity (Levanen & Hamdorf, 2001), visual motion perception (Hauthal et al., 2013) and peripheral visual processing (see review of Bavelier et al., 2006).

It is generally accepted that following the loss of one sense, the brain reorganizes to compensate for this loss by recruiting the areas of the brain that would normally process the lost sense for other sensory functions. This principle has been documented in both human and animal models. A host of functional imaging studies attest to the recruitment of visual cortex during auditory and tactile taks in the blind (e.g. Sadato et al., 1996; Büchel et al., 1998), as well as the recruitment of auditory cortex in the deaf during tactile and visual tasks (e.g. Levanen et al., 1998; Finney et al., 2001). In animals, blind visual cortical regions have been shown to respond to auditory and/or somatosensory stimulation in the mouse (Kahn & Krubitzer, 2002), hamster (Izraeli et al., 2002), cat (Yaka et al., 1999), and opossum (Karlen et al., 2006). Electrophysiological evidence of auditory cortical reorganization following deafness has been shown in the mouse (Hunt et al., 2006), ferret (e.g. Allman et al., 2009), and cat (Meredith and Lomber, 2011; Meredith et al., 2011).

Recently, enhanced abilities in visual motion detection in deaf mammals were localized to the dorsal zone, a region of cat auditory cortex (Lomber et al.,

2010). Subsequently, anatomical evidence of increased projections from extrastriate visual cortical areas involved in motion processing were found in deaf cats compared to hearing controls (Kok et al., 2014). Thus, the purpose of the present study was to investigate the neural basis of these findings using electrophysiological recording techniques to compare neuronal responses to auditory, visual and somatosensory stimulation in area DZ of hearing and deaf animals (**Figure 5.1**). Our results demonstrate that DZ is cross-modally reorganized following deafness for the processing of visual stimuli. In addition, I also found that roughly one-quarter of the single unit, multiunit and local field potential sites responded bimodally to both visual and somatosensory stimulation.

5.3 Materials and methods

Neuronal responses in the dorsal zone of auditory cortex were collected from ten adult domestic cats. These animals were acquired from a licensed commercial breeding facility (Liberty Labs, Waverly, NY) and were housed in an enriched colony environment. The hearing group consisted of six mature, hearing cats (> 6 months), and the deaf group was comprised of four cats that had undergone perinatal ototoxic deafening (< 1 month). Multisensory responses in the hearing group have been reported previously in Chapter 4. All experimental procedures were conducted within the parameters outlined in the National Research Council's *Guidelines for the Care and Use of Mammals in Neuroscience and Behavioral Research* (2003), the Canadian Council on Animal Care's *Guide to the Care and Use of Experimental Animals* (Olfert et al., 1993) and were approved by the Animal Use Subcommittee of the University Council on Animal Care at the University of Western Ontario.

5.3.1 Deafening procedures

Ototoxic deafening procedures were conducted on four animals around the time of hearing onset (14 days postnatally; Shipley et al., 1980). Deafness was induced by the coadministration of kanamycin and ethacrynic acid, which is

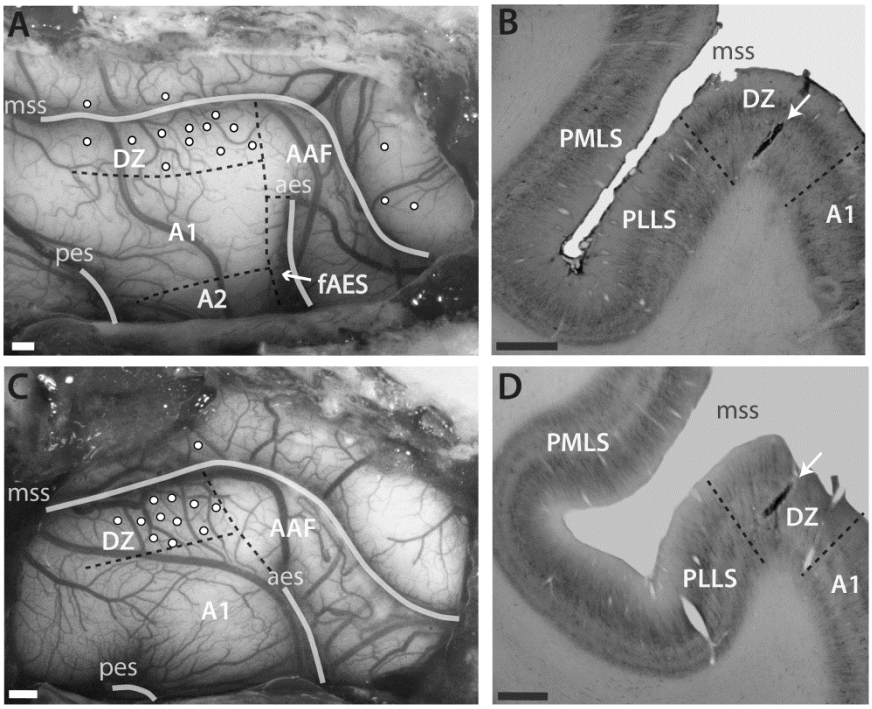

Figure 5.1 Photomicrographs of the craniotomy, electrode penetrations and SMI-32 stained sections in hearing and deafened animals

A: Photomicrograph of the craniotomy and electrode penetration sites for a hearing animal. Sites that did not reliably evoke responses are denoted with a black 'x'. Penetrations outside of auditory cortex were used to verify that visual and somatosensory stimuli evoked responses in known regions of visual and somatosensory cortex. Areal borders as determined by SMI-32 staining are indicated by dashed black lines. Right is anterior. **B:** Photomicrograph of an SMI-32 stained section from a hearing animal with an electrode track in DZ. Right is lateral. **C:** Photomicrograph of the craniotomy and electrode penetration sites for a deaf animal. **D:** Photomicrograph of an SMI-32 stained section from a deaf animal with an electrode track in DZ. Abbreviations: A1 – primary auditory cortex; AAF – anterior auditory field; aes – anterior ectosylvian sulcus; mss – middle suprasylvian sulcus; pes – posterior ectosylvian sulcus; PLLS – posterolateral lateral suprasylvian area; PMLS – posteromedial lateral suprasylvian area. Scale bars: 1 mm.

known to destroy cochlear hair cells (Xu et al., 1993), producing rapid, profound, bilateral hearing loss. Loop diurectics such as ethacrynic acid have also been shown to minimally affect vestibular end-organ function (Elidan et al., 1986); however, animals in the current study showed no obvious vestibular deficits. A detailed account of deafening procedures has been described in Chapter 2. Briefly, animals were injected with kanamycin (300 mg/kg, s.c.) and were presented with auditory stimulation while ethacrynic acid was administered (35-60 mg/kg, i.v., to effect) until auditory brainstem responses (ABRs) showed no acoustically evoked activity (i.e. a flat ABR). Follow-up ABRs were conducted three to six months later to confirm deafness (**Figure 5.2**).

5.3.2 Electrophysiological recordings

All preparatory, electrophysiological recording procedures, and data analysis in the current study were identical to those reported in Chapter 4, the only difference being the hearing status of the animal. Briefly, 1-2 weeks prior to electrophysiological recording, animals were implanted with a head holder attached to the frontal bone and a craniotomy was opened over the right auditory cortex and adjacent regions of visual and somatosensory cortex under pentobarbital anesthesia. A recording well was built up around the craniotomy and sealed closed with dental cement. Some of the deaf animals also received tracer injections into second auditory cortex of the opposite hemisphere at the same time. Standard postoperative care was provided to the animal during surgical recovery (see Malhotra et al., 2004). In all cases, recovery was uneventful.

Approximately 1-2 weeks later, electrophysiological recording procedures were initiated. Animals were anesthetized using ketamine (35 mg/kg, i.m.) and acepromazine (0.4 mg/kg, i.m.), and were intubated with a cuffed endotracheal tube in preparation for mechanical ventilation. Phenylephrine and atropine drops were administered to each eye, and a clear contact lens was inserted into the eye contralateral to the craniotomy, while an opaque lens was inserted into the

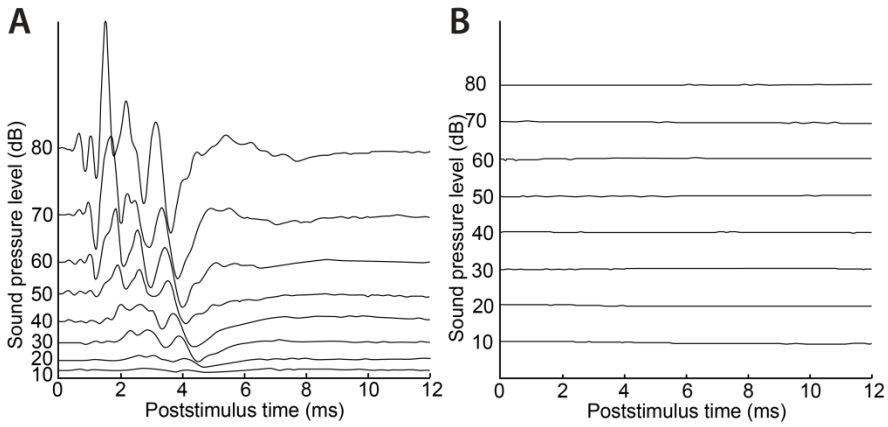

Figure 5.2 Auditory brainstem responses (ABRs) for a hearing and a deaf animal.

A: Brainstem responses to auditory click stimuli ranging in intensity from 10-80 dB SPL in a representative hearing animal. **B:** Responses to the same set of stimuli are absent in a representative deaf animal. All responses are scaled to 1 mV.

ipsilateral eye. The animal was placed into a stereotaxic frame using the previously implanted head holder and the craniotomy was unsealed and the dura resected in preparation for recording. The animal was continuously monitored while baseline respiratory and physiological measures were collected. The animal was then ventilated and a continuous infusion of ketamine (8-10 mg/kg/h) and acepromazine (0.04-0.05 mg/kg/h) was started. Following this, the animal was paralyzed with Nimbex (cistracurium besylate, induction: 1.5 mg/kg, i.v., constant infusion: 1.5 mg/kg/h, i.v.) to prevent eye and limb movement.

5.3.3 Data acquisition and stimulus presentation

Twelve channel iridium axial array microelectrodes were lowered ~1,800-2,000 µm into the dorsal zone of auditory cortex orthogonal to the exposed surface of cortex (**Figure 5.1 A, C**). Because the anterolateral and posterolateral lateral suprasylvian areas (ALLS and PLLS, respectively) of extrastriate visual cortex lie deep to DZ in the lateral bank of the middle suprasylvian sulcus, care was taken not to lower the electrode beyond 2,000 µm. A battery of auditory (A), visual (V) and somatosensory (S) stimuli were presented alone and in combination (AS, AV, VS, AVS) in pseudo-random order. Auditory stimulation consisted of white noise bursts (1-32 kHz; 500 ms duration) presented at 65 dB SPL binaurally via earbuds. Ceramic bender actuators delivered somatosensory stimulation to three locations on the animal's body, in order to stimulate three separate nerves: 1) contralateral vibrissae (contralateral trigeminal nerve), 2) ipsilateral vibrissae (ipsilateral trigeminal nerve), and 3) contralateral forepaw (radial nerve). Visual flashes (500 ms duration, 80 lux) were programmed in Adobe Flash and delivered via a monitor placed ~25 cm in front of the animal. Auditory and somatosensory stimulation were delivered at the same time, while visual stimulation was delivered ~65 ms earlier, in order to compensate for differences in cortical response latencies. Recording sessions ranged in duration from 22-124 hours.

5.3.4 Histological procedures

Following recording procedures, animals were overdosed with sodium pentobarbital and perfused intracardially through the ascending aorta with physiological saline (0.01 M PBS), then fixative (4% paraformaldehyde), and finally 10% sucrose solution. The brain was stereotaxically blocked, removed from the skull, photographed and placed in 30% sucrose solution until it sunk. The brain was then frozen and sectioned coronally using a cryostat at 60 µm intervals. Every other section was processed using the monoclonal antibody SMI-32 (Covance, Princeton, NJ), which can be used to parcellate visual (van der Gucht et al., 2001) and auditory (Mellott et al., 2010) cortical regions in the cat. The remaining sections were either re-processed for SMI-32 reactivity (if the first reaction produced faint results) or were stained with cresyl violet and used to visualize electrode tracks. The position and depth of electrode tracks were visible in the tissue, which were analyzed relative to the border of the auditory and visual cortices between DZ and ALLS/PLLS. Only electrode tracks that could clearly be determined to lie in DZ were analyzed.

5.3.5 Data analysis

All recordings were denoised and sorted in 3-D principal componenet space using Offline Sorter (Plexon, Dallas, TX). Only units showing a clear refractory period and that achieved statistically significant separation in principal component space were classified as single units (**Figure 5.3**). Once a single unit had been isolated, the remainer of the denoised waveforms were classified as multiunit activity for that site. If no single unit was clearly identifiable at a given site, all of the denoised waveforms were classified as multiunit activity.

Custom-written scripts in Matlab (Mathworks, Natick, MA) were used to analyze the data. A site was considered responsive if the weighted sum of the number of spikes/trial during a 30 ms window centered around the peak response exceeded 3 standard deviations of the mean spontaneous activity,

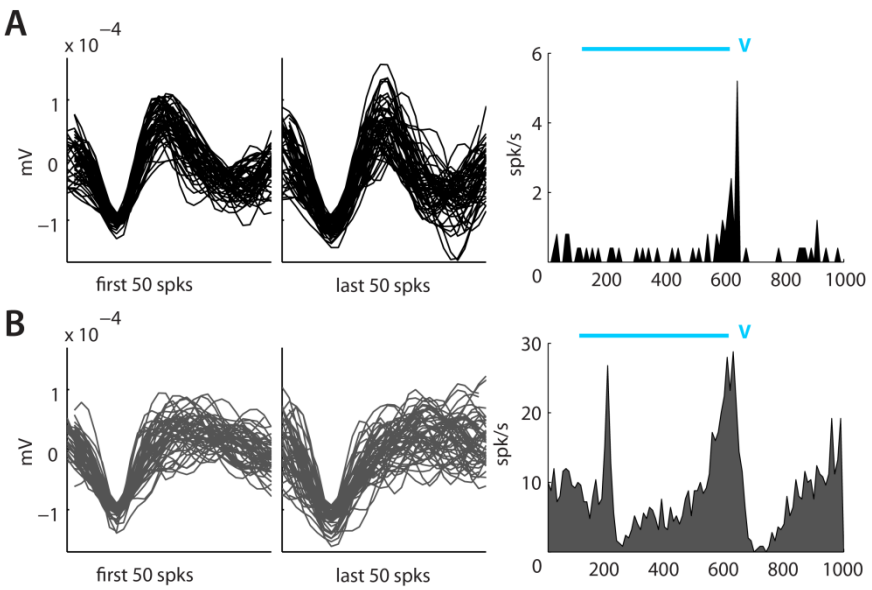

Figure 5.3 Single unit and multiunit waveforms for a representative site in DZ following visual flash stimulation.

A: The first 50 and last 50 waveforms for a representative single unit, as well as the PSTH for that unit. PSTHs have a resolution of 10 ms bins, with the visual stimulus (blue bar) superimposed. **B:** Multiunit waveforms and PSTH from the same site as in A are plotted separately in grey at the same scale.

followed by a significant paired t-test between the number of spikes per trial that had occurred within the response window following stimulation compared to that of spontaneous activity. Neurons were then classified as either unimodal (responsive to one sensory modality) or bimodal (responsive to more than one sensory modality).

These analyses were then repeated for multiunit and LFP sites. However, the area under the curve within the response window for each trial was used instead of the number of spikes per trial for LFP analyses. As in Chapter 4, comparisons between population-based measures (multiunit and LFP responses) and single units are referred to as comparisons between different scopes of neuronal activity. Proportional data were normalized by an arcsine transformation prior to analysis.

5.4 Results

5.4.1 Area DZ identification.

Consistent with previous findings (Wong et al., 2014), the auditory cortical tissue of early-deaf animals did not show any obvious morphological changes compared to that of hearing animals. The SMI-32 neurofilament stain reacted robustly in both hearing and deaf animals (**Figure 5.1 B, D**) and allowed for parcellation of the auditory and visual cortices as well as delineation of the border between DZ and adjacent extrastriate visual areas ALLS and PLLS. Characteristic SMI-32 staining patterns have been previously been described in detail for these areas (van der Gucht et al., 2001; Mellott et al., 2010), but in general, two distinguishing features could be readily observed. 1) The neuropil staining of layer VI in lateral suprasylvian visual areas (i.e. ALLS, AMLS, PLLS, PMLS) is characteristically dark, whereas the layer VI neuropil is considerably lighter in DZ. This difference is visible even at low magnification (see **Figure 5.1 B, D**). 2) DZ has a greater incidence of labeled somata and apical dendrites in layer II than do the lateral suprasylvian visual areas.

Responses to auditory, visual and somatosensory stimulation in area DZ were compared in hearing and early-deafened animals in order to determine whether cross-modal reorganization of DZ occurred at a neuronal level. Responses were collected from 115 single units and from 189 multiunit and 286 LFP sites in deaf animals (n = 4). These were compared to data from 191 single units, and from 391 multiunit and 407 LFP sites from hearing animals (n = 6). Multisensory responses have previously been described in these animals in Chapter 4. I first report comparisons between hearing and deaf animals at the single unit level, then go on to compare multiunit and LFP sites.

5.4.2 Single unit responses

In deaf animals, DZ neurons responded either solely to visual stimulation (58.7%; 64/109; e.g. **Figure 5.4 C**) or bimodally to visual and somatosensory stimulation (25.7%; 28/109; e.g. **Figure 5.4 D).** Less than one-fifth of the neurons in deaf animals were unresponsive to any of the stimulation presented in the current study (15.6%; 17/109), and no neurons responsive to auditory stimulation were found. In comparison, DZ neurons in hearing animals tested with the same battery of auditory, visual and somatosensory stimuli were mainly responsive to auditory stimulation alone (61.3%;117/191; e.g. **Figure 5.4 A**), although a fairly large proportion of neurons respond bimodally to auditory and visual stimulation (30.9%; 59/191; e.g. **Figure 5.4 B**). There was a smaller proportion of unresponsive neurons in hearing animals (7.8%; 15/191). No neurons responsive exclusively to somatosensory or visual stimulation were found in hearing animals.

As in hearing animals, bimodal neurons did not show any organization within DZ of deaf animals (**Figure 5.5 A**). Bimodal cells were found in deep and superficial layers alike, and could also be found posteriorly as well as anteriorly in DZ. Bimodal VS responses might have been expected to lie anteriorly in DZ, in closer proximity to auditory regions known to undergo tactile cross-modal

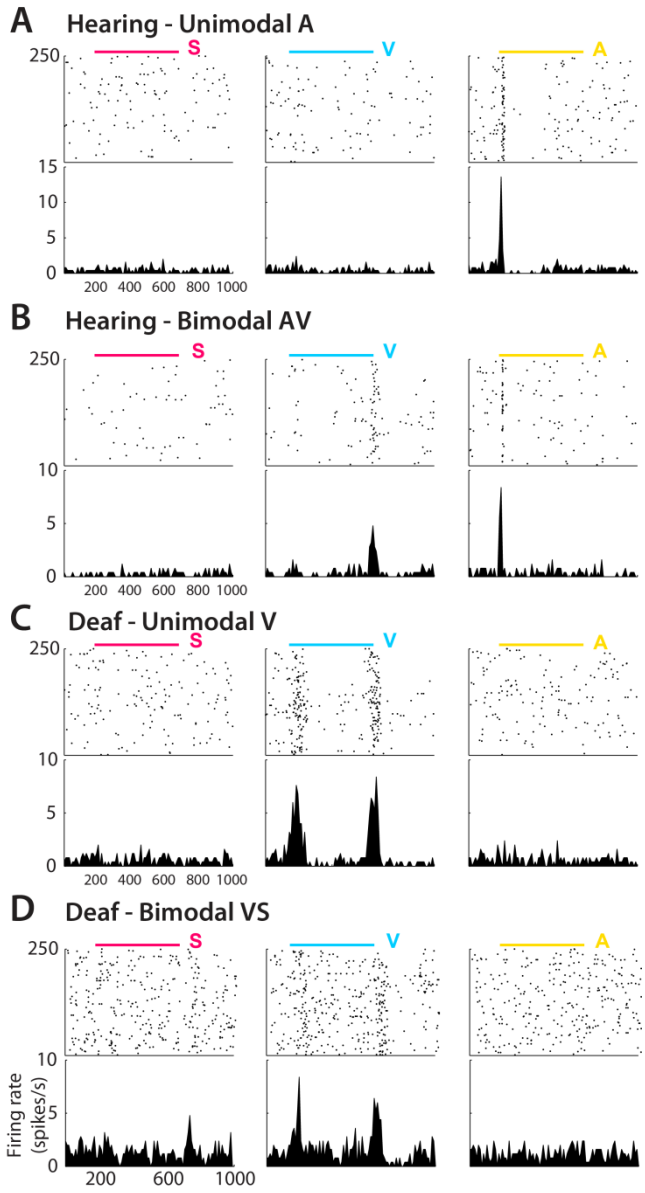

Figure 5.4 Representative examples of sensory neurons recorded in DZ of hearing and deaf animals.

A: A unimodal auditory neuron. This neuron responded vigorously to auditory stimulation, but not to somatosensory or visual stimulation. **B:** A bimodal audio-visual (AV) neuron. This neuron responded to both auditory and visual stimulation, but not somatosensory. The neurons in A and B were only encountered in hearing animals. **C:** A unimodal visual neuron. This neuron responds to visual stimulation exclusively. **D:** A bimodal visual-somatosensory (VS) neuron. The neurons in C and D were only encountered in deaf animals. Note that in the deaf animals, a vigorous onset response to visual stimulation is often present.

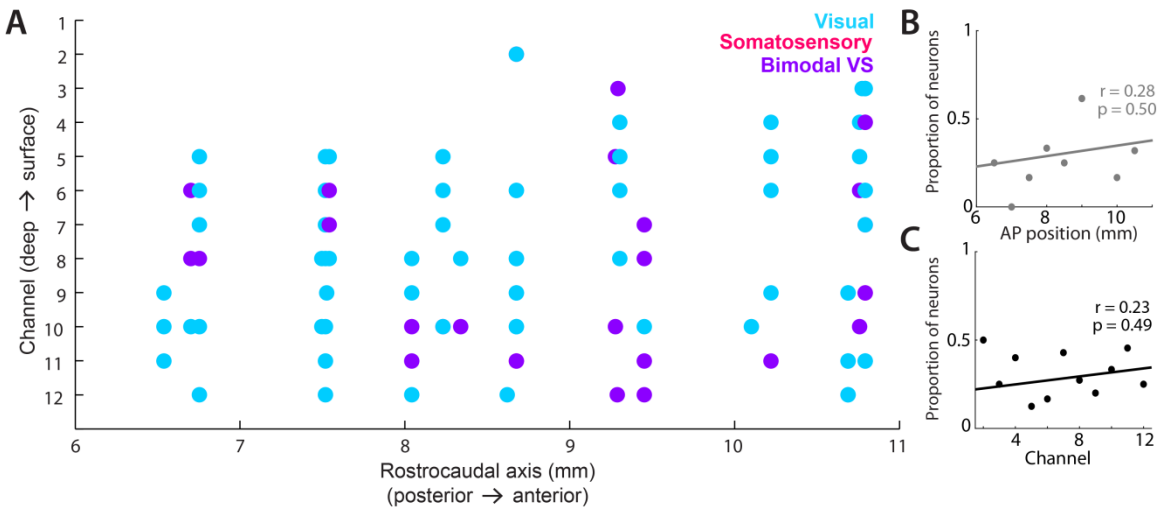

Figure 5.5 Organization of bimodal versus unimodal neurons in DZ of deaf animals

A: Location of neurons in DZ that responded exclusively to visual stimulation (blue) or to both visual and somatosensory stimulation (purple). There were no neurons in DZ that exclusively responded to somatosensory stimulation. The x-axis indicates the approximate A-P location in Horsley-Clarke (1908) coordinates. **B:** Relationship between rostrocaudal position and incidence of bimodal VS neurons (grey). **C:** Relationship between channel position and proportion of bimodal VS neurons (black).

reorganization following deafness (e.g. AAF, Meredith and Lomber, 2011; fAES, Meredith et al., 2011). However, weighted regression analyses showed no evidence for rostrocaudal (**Figure 5.5 B**) or mediolateral (**Figure 5.5 C**) organization within DZ.

5.4.3 Comparison to multiunit responses and LFP activity

A cursory examination of the differences between hearing and deafened animals at the single unit level shows similar proportions of unimodal compared to bimodal responses (**Figure 5.6 A**). At the multiunit level, 74.1% of sites in deaf DZ were responsive only to visual stimulation (140/189), whereas 25.9% of sites were bimodal and responded to both visual and somatosensory stimulation (49/189). Conversely, in hearing animals, 25.3% of sites in DZ responded only to auditory stimulation (99/391), and 74.4% responded bimodally to auditory and visual stimulation (291/391). A single site in the hearing animals was unresponsive to any stimulation (0.26%; 1/391).

The proportions of visual and bimodal VS LFP sites were similar in deafened animals to that of SU and MU activity. LFP sites mainly responded to visual stimulation alone (64.7%; 185/286), with about a third of sites showing bimodal VS responses (35.3%; 101/286). LFPs in hearing animals showed mainly responses bimodal or trimodal stimulation (AV – 53.8%, 219/407; AS – 5.16%, 21/407; AVS – 19.6%, 80/407). Roughly one-fifth of LFP sites in the hearing animal reflected exclusively auditory inputs (21.4%, 87/407).

A 3-way ANOVA was used to compare the proportion of neurons for each scale of activity (SU, MU, LFP), at unimodal vs. multimodal sites between hearing and deaf animals. No significant 3-way interaction was found. However, a significant interaction was found for hearing animals for the proportion of unimodal vs. multimodal sites at each scale of activity ($F(2,10) = 6.84$, $p = 0.013$). Differences between the proportion of neurons at each scale of activity were found for unimodal ($F(2,10) = 6.84$, $p = 0.013$) and multimodal ($F(2,10) = 4.58$, p

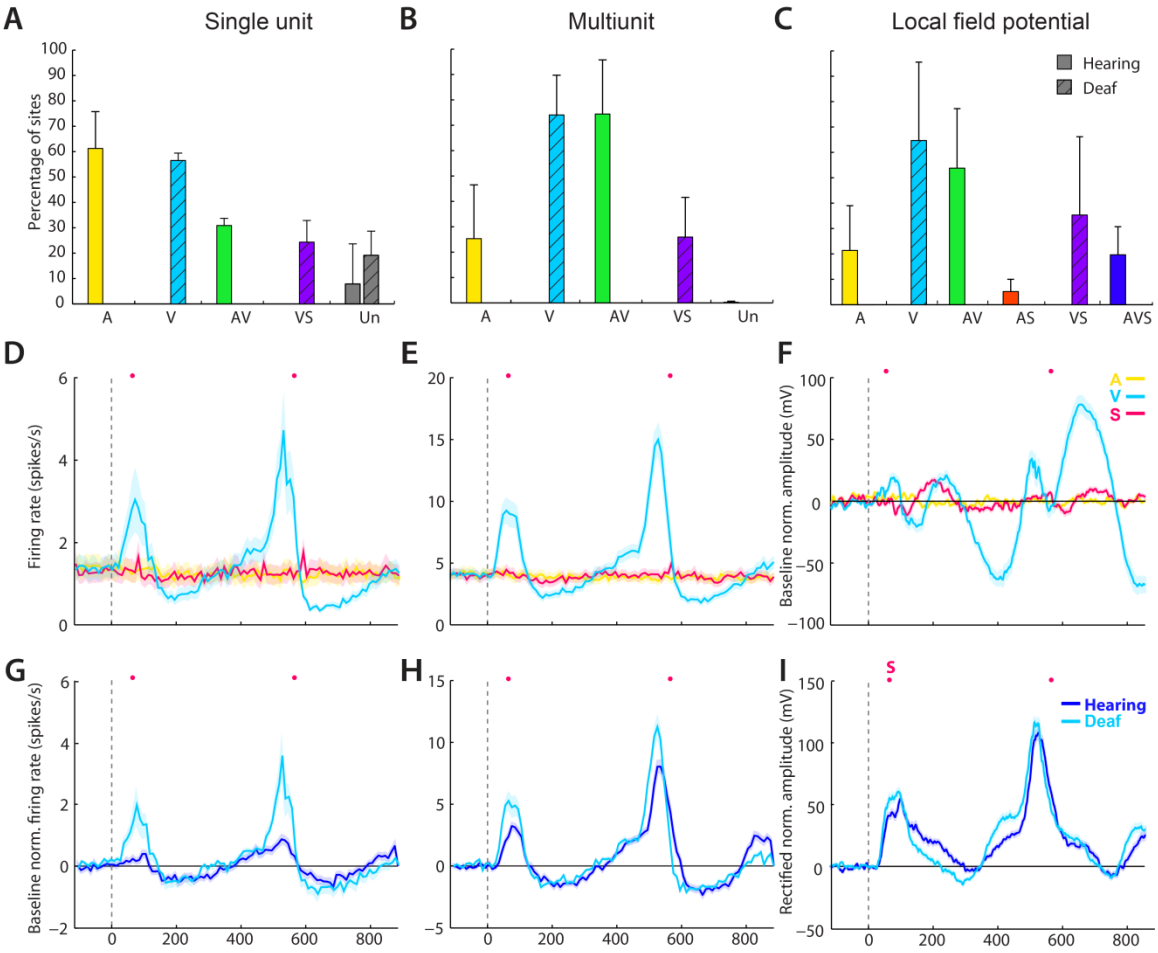

Figure 5.6 Comparison of single unit, multiunit and LFP responses in DZ of hearing and deafened animals

A-C: Percentages of responding sites for each type of sensory neuron encountered in hearing (solid bars) and deaf animals (hatched bars). **D-F:** Grand averaged responses over all recorded sites for SU, MU and LFP recordings in deaf animals, respectively. The grey dashed line indicates the onset of the visual stimulus, with the onset and offset of the somatosensory stimulus indicated by pink colored circles. **G-I:** Comparison of the baseline normalized firing rate between hearing (dark blue) and deaf (light blue) animals. The peak firing rate of SU and MU sites is increased in deaf animals compared to hearing animals at stimulus onset and offset. The LFP signal (I) was rectified at each site to control for differences in the direction of the signal.

= 0.039) sites. Post hoc Tukey-Kramer tests indicated a significant decrease in the proportion of unimodal SU compared to LFP sites ($p < 0.01$), with a corresponding increase in the proportion of multimodal sites between SU and LFP sites ($p < 0.05$). Neither the proportion of unimodal nor multimodal MU sites were different from those of SU or LFP sites. A similar comparison was run separately for deaf animals. There was no significant interaction between the proportion of unimodal vs. multimodal (in this case bimodal VS) sites for each scale of activity (SU, MU, LFP) in the deaf animals. However, a main effect was found between unimodal and multimodal sites ($F(1,8) = 11.2$, $p = 0.01$, $n = 9$), indicating the number of unimodal V sites was higher than the number of bimodal VS at each scale of activity.

As in hearing animals, while some visually-responsive sites in deaf animals showed considerably stronger responses to stimulus offset than onset (e.g. see hearing example in middle panel of **Figure 5.4 B**), many sites showed strong responses to visual stimulation at stimulus onset, which is reflected in the mean activity over all sites (**Figure 5.6 D-E**). This effect is also visible in the mean visual response profiles in hearing compared to deaf animals for single unit, multiunit and LFP activity (**Figure 5.6 G-I**). Statistical comparisons between the baseline normalized peak response in hearing and deaf animals for each response epoch (onset, offset) yielded no significant interaction for any of the scales of activity (SU, MU, LFP). However, visual peak responses at the single unit level in deaf animals (5.56 spikes/s) are higher than those of hearing animals (3.16 spikes/s; $p < 0.01$). The same holds for multiunit activity (deaf: 8.75 spikes/s; hearing: 5.58 spikes/s; $p < 0.001$), however, no change in peak LFP responses were found between hearing and deafened animals.

5.5 Discussion

The purpose of this study was to compare DZ responses to a battery of auditory, visual and somatosensory stimuli in hearing cats to those in deaf cats, in order to evaluate the neuronal properties of the behavioral (Lomber et al.,

2010) and structural (Kok et al., 2014) cross-modal reorganization previously uncovered in area DZ. A large proportion of sites responsive exclusively to visual stimulation, and a smaller proportion of bimodal sites that responded both to visual and somatosensory stimulation were observed across single unit, multiunit and LFP measures. These results stand in contrast what has been observed previously in hearing animals – while single units responded mainly to auditory stimulation, and a small proportion of bimodal auditory and visually responsive neurons were encountered, multiunit and LFP sites showed the opposite trend, namely, a high proportion of bimodal AV sites and a small proportion of sites that responded exclusively to auditory stimulation.

It is challenging to untangle what these changes mean in terms of the reorganization that has gone on at the cellular level. For example, is it merely the case that the population of bimodal AV cells in the hearing animal, once deprived of auditory input, simply become visually responsive neurons? I consider this possibility unlikely, since of 191 neurons sampled in hearing cats, 59 showed overt responses to visual stimulation. In comparison, in the deaf animal, 92 of 109 neurons sampled showed overt responses to visual stimulation. This indicates a higher absolute number of visually responsive neurons in a smaller sample of cells for the deaf animals. It is additionally unlikely that all of the neurons responsive exclusively to auditory stimulation in hearing animals become unresponsive following deafness, as although the proportion of unresponsive neurons in the deafened animal is increased, it is important to note that in terms of absolute numbers, this represents a total of two more unresponsive neurons (15 in hearing animals compared to 17 in the deaf).

Additionally, a proportion of sites were found to be responsive to both visual and somatosensory stimulation. Although at first this may seem surprising, given that no cells responded overtly to tactile stimulation in the hearing animal, the same population of DZ neurons were previously shown to be modulated by somatosensory stimulation in hearing animals in Chapter 4, and 24.8% of LFP

responses (101/407) show a response to somatosensory stimulation. Because LFP activity reflects the local synaptic processing in the vicinity of the electrode, I can conclude that there are active inputs transmitting somatosensory information to DZ. These inputs are not strong enough to cause action potentials in DZ neurons of hearing animals, but they can modulate ongoing activity. This would therefore support a competition-based model, whereby the removal of auditory input results in the unmasking of these previously 'silent' synapses (see Merabet et al., 2008 for a discussion on unmasking). Since the major driving auditory input is not present to drive these cells in the deaf animal, visual and tactile influences are free to compete with one another, and the inputs become strengthened in an activity-dependent fashion. Interestingly, the proportion of sites responsive to somatosensory stimulation in the deaf at the single and multiunit levels are remarkably consistent at ~25%, and the proportion of LFP sites responsive to somatosensory stimulation in the deaf animal (35.3%) only slightly increases. This is consistent with the unmasking hypothesis, since previous anatomical studies failed to show any increase in somatosensory inputs to DZ following deafness (Barone et al., 2013; Kok et al., 2014).

The same studies showed an increase in projection strength from PLLS in deaf animals (Kok et al., 2014), which may be responsible for the increase in the number of visually responsive single units reported here. As both overt visual responses and subthreshold visual modulation was previously reported in DZ of hearing animals in Chapter 4, I suggest that both unmasking of latent inputs as well as the formation of new connections with PLLS neurons are responsible for increase in visually-responsive neurons following deafness. Such a hypothesis would dovetail nicely with the finding that DZ becomes behaviorally reorganized following deafness to mediate enhanced visual motion perception (Lomber et al., 2010). Since PLLS is also a visual motion processing region, these results provide functional evidence of visual cross-modal reorganization in DZ following deafness, in addition to the existing structural and behavioral evidence.

These results are generally the opposite of what was reported in the anterior auditory field of deaf animals (Meredith and Lomber, 2011), where most of the neurons in the deaf animals responded exclusively to tactile stimulation, and similar to what was found in the auditory field of the anterior ectosylvian sulcus (fAES) of early-deaf animals (Meredith et al., 2011). DZ and fAES are both higher-order areas of cat auditory cortex that are involved in sound localization in the hearing cat, comprising the auditory 'where' pathway along with A1 and PAF, whereas AAF is involved in auditory identification or 'what' processing (Malhotra and Lomber, 2007; Lomber and Malhotra, 2008; Malhotra et al., 2008; Lee and Winer, 2011). It has previously been suggested that sensory-deprived brain regions may be recruited by spared modalities for the processing of homologous functions (Lomber et al., 2010; Meredith et al., 2011). For this reason, it is possible that the parallels in cross-modal reorganization of areas DZ and fAES following deafness may reflect the similar spatial processing functions present in hearing animals.

There is now behavioral (Lomber et al., 2010), anatomical (Barone et al., 2013; Kok et al., 2014), and electrophysiological evidence of cross-modal reorganization in DZ following deafness. Additionally, a thorough understanding of the multisensory processing capabilities of DZ in hearing animals reported in Chapter 4 allows for unique insights into the basis of the reorganization found in deaf animals in the present study. Collectively, these studies comprise the most extensive documentation of cross-modal plasticity in mammalian cortex to date.

5.6 References

Alary F, Duquette M, Goldstein R, Chapman CE, Voss P, La Buissonnière-Ariza V, Lepore F (2009) Tactile acuity in the blind: a closer look reveals superiority over the sighted in some but not all cutaneous tasks. Neuropsychologia 47:2037-2043.

Allman BL, Keniston LP, Meredith MA (2009) Adult deafness induces somatosensory conversion of ferret auditory cortex. Proc Natl Acad Sci 106:5925–5930.

Barone P, Lacassagne L, Kral A (2013) Reorganization of the connectivity of cortical field DZ in congenitally deaf cat. PLoS One 8:e60093.

Bavelier D, Dye MWG, Hauser PC (2006) Do deaf individuals see better? Trends Cogn Sci 10:512–518.

Büchel C, Price C, Frackowiak RS, Friston K (1998) Different activation patterns in the visual cortex of late and congenitally blind subjects. Brain 121:409-419.

Cuevas I, Plaza P, Rombaux P, De Volder AG, Renier L (2009) Odour discrimination and identification are improved in early blindness. Neuropsychologia 47:3079-3083.

Elidan J, Lin J, Honrubia V (1986) The effect of loop diuretics on the vestibular system: Assessment by recording the vestibular evoked response. Arch Otolaryngol Head Neck Surg 112:836-839.

Finney E M, Fine I, Dobkins K R (2001) Visual stimuli activate auditory cortex in the deaf. Nat Neurosci 4:1171-1173.

Goldreich D, Kanics I M (2003) Tactile acuity is enhanced in blindness. J Neurosci 23:3439-3445.

Gougoux F, Lepore F, Lassonde M, Voss P, Zatorre R J, Belin P (2004) Neuropsychology: pitch discrimination in the early blind. Nature 430:309-309.

Hauthal N, Sandmann P, Debener S, Thorne J D (2013) Visual movement perception in deaf and hearing individuals. Adv Cogn Psychol 9:53-61.

Horsley V, Clarke RH (1908) The structure and functions of the cerebellum examined by a new method. Brain 31:45-124.

Hunt D L, Yamoah E N, Krubitzer L (2006) Multisensory plasticity in congenitally deaf mice: how are cortical areas functionally specified? Neurosci 139:1507-1524.

Izraeli R, Koay G, Lamish M, Heicklen-Klein AJ, Heffner HE, Heffner RS, Wollberg Z (2002) Cross-modal neuroplasticity in neonatally enucleated hamsters: Structure, electrophysiology and behaviour. Eur J Neurosci 15:693–712.

Kahn D M, Krubitzer L (2002) Massive cross-modal cortical plasticity and the emergence of a new cortical area in developmentally blind mammals. PNAS 99:11429-11434.

Karlen S J, Kahn D M, Krubitzer L (2006) Early blindness results in abnormal corticocortical and thalamocortical connections. Neurosci 142:843-858.

Kok MA, Chabot N, Lomber SG (2014) Cross-modal reorganization of cortical afferents to dorsal auditory cortex following early- and late-onset deafness. J Comp Neurol 522:654–675.

Levänen S, Hamdorf D (2001) Feeling vibrations: enhanced tactile sensitivity in congenitally deaf humans. Neurosci lett 301:75-77.

Levänen S, Jousmäki V, Hari R (1998) Vibration-induced auditory-cortex activation in a congenitally deaf adult. Curr Biol 8:869-872.

Lee CC, Winer JA (2011) Convergence of thalamic and cortical pathways in cat auditory cortex. Hear Res 274:85-94.

Lomber SG, Malhotra S (2008) Double dissociation of 'what' and 'where' processing in auditory cortex. Nature Neurosci 11:609-616.

Lomber SG, Meredith MA, Kral A (2010) Cross-modal plasticity in specific auditory cortices underlies visual compensations in the deaf. Nat Neurosci 13:1421–1427.

Malhotra S, Lomber SG (2007) Sound localization during homotopic and heterotopic bilateral cooling deactivation of primary and nonprimary auditory cortical areas in the cat. J Neurophys 97:26-43.

Malhotra S, Stecker GC, Middlebrooks JC, Lomber SG (2008) Sound localization deficits during reversible deactivation of primary auditory cortex and/or the dorsal zone. J Neurophys 99:1628-1642.

Mellott JG, van der Gucht E, Lee CC, Carrasco A, Winer J a, Lomber SG (2010) Areas of cat auditory cortex as defined by neurofilament proteins expressing SMI-32. Hear Res 267:119–136.

Merabet LB, Hamilton R, Schlaug G, Swisher JD, Kiriakopoulos ET, Pitskel NB, Kauffman T, Pascual-Leone A (2008) Rapid and reversible recruitment of early visual cortex for touch. PLoS One 3:e3046.

Meredith MA, Kryklywy J, McMillan AJ, Malhotra S, Lum-Tai R, Lomber SG (2011) Crossmodal reorganization in the early deaf switches sensory, but not behavioral roles of auditory cortex. Proc Natl Acad Sci 108:8856–8861.

Meredith MA, Lomber SG (2011) Somatosensory and visual crossmodal plasticity in the anterior auditory field of early-deaf cats. Hear Res 280:38–47.

Olfert ED, Cross BM, McWilliam AA eds. (1993) Guide to the Care and Use of Experimental Animals. Ottawa, Canada: Canadian Council on Animal Care.

Röder B, Teder-Sälejärvi W, Sterr A, Rösler F, Hillyard SA, Neville, HJ (1999) Improved auditory spatial tuning in blind humans. Nature 40:162-166.

Sadato N, Pascual-Leone A, Grafman J, Ibañez V, Deiber MP, Dold G, Hallett M (1996) Activation of the primary visual cortex by Braille reading in blind subjects. Nature 380:526-528.

Shipley C, Buchwald JS, Norman R, Guthrie D (1980) Brain stem auditory evoked response development in the kitten. Brain Res 182:313-326.

Stevens JC, Foulke E, Patterson MQ (1996) Tactile acuity, aging, and braille reading in long-term blindness. J Exp Psychol-Appl 2:91-106.

van der Gucht E, Vandesande F, Arckens L (2001) Neurofilament protein : A selective marker for the architectonic parcellation of the visual cortex in adult cat brain. J Comp Neurol 441:345–368.

Wan CY, Wood AG, Reutens DC, Wilson SJ (2010) Early but not late-blindness leads to enhanced auditory perception. Neuropsychologia 48:344-348.

Wong C, Chabot N, Kok MA, Lomber SG (2014) Modified areal cartography in auditory cortex following early- and late-onset deafness. Cereb Cortex 24:1778–1792.

Xu SA, Shepherd RK, Chen Y, Clark, GM (1993) Profound hearing loss in the cat following the single co-administration of kanamycin and ethacrynic acid. Hear Res 70:205-215.

Yaka R, Yinon U, Wollberg Z (1999) Auditory activation of cortical visual areas in cats after early visual deprivation. Eur J Neurosci 11:1301-1312.

Chapter 6: General Discussion

6.1 Main findings and conclusions

6.1.1 DZ receives strong projections from visual cortex in hearing animals

Although the connectivity of DZ with other auditory cortical regions in hearing cats had been documented in two previous studies (He and Hashikawa, 1998; Lee and Winer, 2008), neither study commented on projections from regions outside of auditory cortex. The results presented in Chapter 2 show that a substantial body of projections from visual regions outside of auditory cortex to DZ exist. The vast majority of these projections are from ALLS and PLLS, visual motion processing regions of extrastriate visual cortex that lie very near to DZ in the banks of the middle suprasylvian sulcus. A separate study conducted around the same time confirmed these findings (Barone et al., 2013). These data clearly demonstrate that DZ of hearing animals is well-connected with visual cortical regions. However, these findings also raise two interesting, but related questions regarding the functional relevance of these auditory and visual cortical projections to DZ. The first is regarding what kinds of auditory information are being relayed by the major sources of auditory cortical projections to DZ, which is directly addressed in Chapter 3. The second is whether this large body of visual cortical projections has any overt effect on the behavior of neurons in DZ, which is directly addressed in Chapter 4.

6.1.2 The strength of visual cortical projections to DZ is increased in deaf animals

Chapter 2 further demonstrated that DZ of deaf auditory cortex retains the same pattern of connectivity as that of DZ in hearing cats. That is, I did not observe any novel projections in deaf animals originating from areas that did not show any connectivity with DZ in hearing animals. However, I did observe that the strong projection from PLLS noted in hearing animals was increased in the deaf animals. Given that DZ is known to become cross-modally reorganized in deaf animals to mediate enhanced motion detection (Lomber et al., 2010), it is

probable that this amplified projection strength from motion processing regions of visual cortex to DZ provides an anatomical basis for the supra-normal visual motion detection behavior identified in deaf animals.

6.1.3 DZ neurons rely on input from A1, whereas PAF may modulate DZ responses

To date, the most current model of auditory cortical hierarchy has relied largely on information gleaned from anatomical connectivity studies (Lee and Winer, 2011). While connectivity studies clearly provide important information regarding the structure of a particular brain region, functional insights from electrophysiological or behavioral investigations are required to understand how these connections subserve the region of study. The results of Chapter 3 indicate that DZ responses to noise bursts and tones are largely dependent on information originating in A1. Although DZ peak responses are significantly reduced following A1 deactivation, they are not completely abolished. These results are similar to those observed for area MT in the primate following inactivation of V1 (Girard et al., 1992; Moore et al., 2001), and dissimilar to those observed for early visual cortical regions in the object recognition, or 'what' pathway in visual cortex (Girard et al., 1991a, 1991b). As such, these results provide additional evidence for a spatial processing pathway in auditory cortex of the cat involving A1, DZ and PAF (Stecker et al., 2003, 2005; Lomber and Malhotra, 2008; Malhotra et al., 2008) that is analogous to the dorso-parietal 'where' pathway in visual cortex involving area MT (Mishkin et al., 1983). In contrast, neuronal responses were preserved for the most part when PAF was deactivated.

6.1.4 Almost half of DZ neurons are multisensory

In Chapter 4, I show that a large proportion of neurons in DZ are multisensory, and either respond bimodally to auditory and visual stimulation, or are modulated by the presence of visual or somatosensory stimuli. I specifically demonstrate that this modulation can occur in opposing directions during different epochs of the auditory response. I suggest that the modulation that

occurs early on in the response may arise sub-cortically, from non-specific thalamic afferents, as has been suggested by other researchers (Lakatos et al., 2007; Kayser et al., 2008), whereas multisensory enhancement of the longer-latency aspects of the auditory response could be mediated by the large proportion of visual cortical projections revealed in Chapter 2. However, further experimentation will be required to elucidate whether these projections play a definitive role in multisensory processing in DZ. Combining the methodology of Chapters 3 and 4 to reversibly deactivate PLLS while recording from DZ using multisensory stimulation would clearly demonstrate the role of these projections, and represents an interesting avenue of future investigation.

6.1.5 Population-based measures of neural activity may overestimate the degree of multisensory processing in a cortical area

An ever-increasing number of studies using many different techniques are documenting modulation of 'unisensory' cortical areas by other senses (e.g. review of Driver and Noesselt, 2008). In Chapter 4, I directly compare single-unit activity with population-based measures of neural activity, specifically multiunit and LFP recordings. I show that multiunit and LFP activity may significantly overestimate both the proportion of multisensory neurons, as well as the level of multisensory integration occurring in a cortical area. I further suggest that since LFP signals are known to correlate with other population-based measures of neural activity, such as fMRI, EEG and MEG (Buzsáki et al., 2012), that these findings may serve as a cautionary note for the interpretation of multisensory integration using population-based measures.

6.1.6 DZ neurons in deaf animals respond mainly to visual stimulation

In Chapter 5, I demonstrate that DZ becomes cross-modally reorganized at a neuronal level following early deafness. Specifically, I show that most neurons in deafened DZ respond to visual stimulation exclusively, but that a population of bimodal neurons responsive to both visual and tactile stimulation also exists. These findings support previous behavioral evidence that DZ

becomes visually reorganized following deafness to process visual motion (Lomber et al., 2010), as well as anatomical evidence showing an increase in projection strength from visual motion processing regions of the brain (Kok et al., 2014). When these studies are considered in conjunction with the multisensory processing capabilities of area DZ presented in Chapter 4, I suggest that the visual cross-modal reorganization of area DZ is likely mediated by both the unmasking of previously silent synapses, as well as by increased connectivity with visual regions of the brain, whereas the somatosensory cross-modal reorganization of DZ is more likely to be due to unmasking alone.

6.2 Conclusions

6.2.1 DZ may be homologous to caudal auditory fields in the primate

Although parcellation of auditory cortical areas into core versus belt regions has been proposed and generally accepted in the primate literature (Hackett et al., 2001), no such formal separation has been proposed for auditory cortical regions in the cat (Read et al., 2001). It has been suggested that DZ forms part of a functional belt region of auditory cortex because of the complexity and longer latency of responses in DZ in comparison to core fields A1 and AAF, as well as evidence that DZ plays a role in temporal (He et al., 1997) and spatial auditory processing (Stecker et al., 2005; Malhotra et al., 2008). However, no homologous structure in primate auditory cortex has previously been proposed for DZ. In the past, homology between cat and macaque visual systems has been suggested using a set of criteria including behaviorally determined function, cortical position, electrophysiological responses, and anatomical cortical and thalamic connectivity (Payne, 1993).

On the basis of these criteria, many parallels can be drawn between DZ in the cat and caudal regions of primate auditory cortex. Behaviorally, “what” and “where” auditory processing streams have previously been identified for both the cat (Lomber and Malhotra, 2008) and the primate (Romanski et al., 1999; Rauschecker and Tian, 2000). In the primate, the caudolateral (CL) and

caudomedial (CM) areas are known to be involved in processing auditory spatial information (Rauschecker, 1998; Rauschecker and Tian, 2000; Recanzone, 2000a; Woods et al., 2006; Kusmierek and Rauschecker, 2014), as is DZ (Stecker et al., 2005; Malhotra et al., 2008). In terms of cortical position, caudal fields CM and CL in the monkey are located dorso-posteriorly to core fields A1 and the rostral field (R). DZ is also located dorso-posteriorly to A1 and AAF in the cat, and AAF of the cat is considered to be homologous to primate field R (Rauschecker et al., 1997).

Electrophysiologically, response properties in caudal fields of the primate share a number of similarlities with DZ. Receptive fields in CM are more broadly tuned than the sharp frequency tuning found in core areas A1 and R; (Merzenich and Brugge, 1973; Morel et al., 1993; Kosaki et al., 1997)), with neurons in CM responding better to noise than to tone stimuli (Recanzone, 2000b), and neurons in CL responding better to band-passed noise than to pure tones (Rauschecker et al., 1995). Monotonic rate-level functions were also identified in CM of primate auditory cortex, with the vast majority characterized as monotonic or saturating (Kajikawa et al., 2005). Additionally, Woods et al. (2006) have shown that both CM and CL neurons respond most strongly at the highest sound intensity level presented. Similarly, Chapter 3 showed that DZ neurons respond better to noise than to tones, and also showed a dominance of monotonic rate-level functions. Perhaps most convincing is the effect of A1 ablation on neuronal responses in R and CM (Rauschecker et al., 1997). A1 ablation had no effect on neuronal responses in R, but abolished pure tone responses in CM, while responses to more complex stimuli were preserved, albeit weaker in magnitude. These results correspond well with those of Chapter 3 in which A1 deactivation strongly reduces receptive field bandwidths and increases neuronal thresholds in DZ, but has no effect on peak responses in AAF (Carrasco and Lomber, 2010). Finally, visual modulation of auditory responses in CM and CL have been shown using functional imaging (Kayser et al., 2007) and electrophysiological recordings (Kayser et al., 2008). While auditory-somatosensory integration has not been

demonstrated in either of these fields, somatosensory inputs capable of eliciting responses to median nerve stimulation have been documented in this area (Schroeder and Foxe, 2002). Again, these results correspond well with the visual and somatosensory modulation of auditory responses in DZ in Chapter 4.

Finally, both DZ (Lee and Winer, 2008a) and CM/CL (Rauschecker et al., 1997; de la Mothe et al., 2012) receive input from mainly dorsal regions of auditory thalamus. These data stand in stark contrast to the strong projections from ventral regions of auditory thalamus to A1 and AAF in the cat (Lee and Winer, 2008a) and A1 and R in the primate (Molinari et al., 1995; Rauschecker et al., 1997). Furthermore, A1 shares dense, reciprocal connectivity with fields CM and CL (Kaas and Hackett, 2000), as does DZ (Lee and Winer, 2008a).

Despite these similarities, a few discrepancies between caudal areas in the primate and DZ in the cat should be noted. Response latencies of neurons in CM and CL, for example, have been shown to be shorter or similar to those of A1 (Camalier et al., 2012; Kusmierek and Rauschecker, 2014), whereas in the cat, only AAF neurons have shorter response latencies than neurons in A1 (Carrasco and Lomber, 2009). CM is also roughly tonotopically organized in the primate (Morel et al., 1993), whereas DZ is traditionally considered to be non-tonotopic (Lee and Winer, 2011). While it could be argued that PAF and fAES may also be considered as candidates for homology with CM based on the behavioral similarity of their spatial processing roles (Malhotra et al., 2007), fAES and PAF both violate some of the above-metioned criteria for the establishment of homology. fAES violates the cortical position criterion, being located antero-ventrally to A1 and AAF, as well as the anatomical cortical connectivity criterion, as it does not receive a strong projection from A1 (Lee and Winer, 2008a). PAF violates thalamic connectivity criterion, as the strongest auditory thalamic projection it receives is from the ventral division of MGN, and as such, has been considered homologous with core regions of primate auditory cortex (Hackett et

al., 2011). Furthermore, neither fAES or PAF neurons have been shown to be modulated by either visual or somatosensory stimuli.

Therefore, the work presented in this thesis adds to a body of literature documenting shared behavioral, topographic, electrophysiological and anatomical similarities with caudal fields CM/CL of the primate, and as such, fulfil the criteria outlined above for possible homology with these fields.

6.2.2 DZ is the most extensively-documented model of cross-modal plasticity in mammalian cortex to date

In addition to the previously published behavioral evidence of cross-modal reorganization in DZ (Lomber et al., 2010), this thesis adds a number of novel insights which together make this region the most comprehensive model of cross-modal plasticity in mammalian cortex. This thesis documents anatomical changes in connectivity in deaf animals (Chapter 2) which corroborate previous behavioral findings (Lomber et al., 2010), electrophysiological evidence of cross-modal plasticity (Chapter 5), and evidence of multisensory processing in DZ at multiple scales of neuronal activity, which allow for unique insights into the cross-modal reorganization that takes place following deafness (Chapter 4).

While some neuroimaging studies have documented behavioral evidence of superior performance in blind or deaf individuals, and have located brain regions involved in mediating these enhanced abilities (e.g. Sadato et al., 1996), changes in the functional connectivity of the cerebral cortex following blindness or deafness have not been documented, and as such, the mechanisms that give rise to this plasticity remain murky. With respect to V1, some anatomical changes have been documented in the opossum (Karlen et al., 2006); however it remains unknown whether these changes are generalizable to species phylogenetically more closely related to humans.

Similarly, in the animal literature, while some studies have demonstrated a behavioral improvement in the performance of a task in sensory-deprived

animals and have correlated it with electrophysiological evidence of cross-modal plasticity (e.g. Izraeli et al. 2002), only Lomber and colleagues (2010) have conclusively localized enhanced ability to a particular brain region. Aside from this, although a few studies in cat cortex have correlated behavioral enhancements with electrophysiological findings (Korte and Rauschecker, 1993; Rauschecker and Korte, 1993; Rauschecker and Kniepert, 1994, Meredith et al., 2011), again, the connectional changes that give rise to this plasticity remain undetermined. Furthermore, the multisensory processing capabilities of these areas remain largely uninvestigated and could provide important information regarding the influence of other sensory modalities on the area of interest in non-deprived animals, particularly in the absence of documented connectional changes following deprivation.

Together, this thesis provides original insights into the structure and function of DZ in both hearing and deafened animals. These findings conclusively demonstrate that DZ receives active visual inputs in hearing animals that are strengthened following deafness to contribute to the reorganization of DZ as a region involved in visual motion processing. This research has spawned a number of interesting avenues for future experimentation to further elucidate our understanding of the principles underlying basic sensation as well as cross-modal plasticity.

6.3 Future directions

In addition to the logical extension of the findings in Chapters 2 through 4 suggested in section 6.1.4, a number of potential experiments could build on the findings reported in this thesis. For example, in Chapter 3 I recorded from anesthetized animals using fairly simple stimulus sets (noise bursts and tones). However, given the existence of a large projection from PLLS in the hearing animal found in Chapter 2, as well as the long-latency bimodal responses to auditory and visual stimulation found in Chapter 4, combined with the known spatial (Stecker et al., 2005) and duration (He et al., 1997) tuning properties of DZ, it would be interesting to record from DZ neurons while presenting auditory

and visual stimuli that varied in location and duration. Evaluation of the responses of DZ neurons to congruent and incongruent audio-visual stimuli within space could yield insights into the behavioral and functional relevance of the multisensory integration and interactions reported in this thesis.

An extension of the findings of Chapter 5 would be to evaluate the response properties of the visually-responsive neurons in hearing and deaf DZ. Do they respond to visual motion? If so, do they show direction selectivity? What is the receptive field of these neurons? Is there a difference between responses to actual motion and apparent motion? The answers to these questions could provide valuable clues to the missing pieces of the cross-modal puzzle, such as why some sub-regions of sensory-deprived cortices become reorganized and others do not.

6.4 References

Barone P, Lacassagne L, Kral A (2013) Reorganization of the connectivity of cortical field DZ in congenitally deaf cat. PLoS One 8:e60093.

Buzsáki G, Anastassiou CA, Koch C (2012) The origin of extracellular fields and currents--EEG, ECoG, LFP and spikes. Nat Rev Neurosci 13:407–420.

Camalier CR, D'Angelo WR, Sterbing-D'Angelo SJ, de la Mothe LA, Hackett TA (2012) Neural latencies across auditory cortex of macaque support a dorsal stream supramodal timing advantage in primates. Proc Natl Acad Sci 109:18168–18173.

Carrasco A, Lomber SG (2009) Differential Modulatory Influences between Primary Auditory Cortex and the Anterior Auditory Field. J Neurosci 29:8350–8362.

Carrasco A, Lomber SG (2011) Neuronal activation times to simple, complex, and natural sounds in cat primary and nonprimary auditory cortex. J Neurophysiol 106:1166–1178.

De la Mothe LA, Blumell S, Kajikawa Y, Hackett TA (2012) Thalamic connections of auditory cortex in marmoset monkeys: lateral belt and parabelt regions. Anat Rec 295:822–836.

Driver J, Noesselt T (2008) Multisensory interplay reveals crossmodal influences on “sensory-specific” brain regions, neural responses, and judgments. Neuron 57:11–23.

Girard P, Salin PA, Bullier J (1991a) Visual activity in areas V3a and V3 during reversible inactivation of area V1 in the macaque monkey. J Neurophysiol 66:1493–1503.

Girard P, Salin PA, Bullier J (1991b) Visual activity in macaque area V4 depends on area 17 input. Neuroreport 2:81–84.

Girard P, Salin PA, Bullier J (1992) Response selectivity of neurons in area MT of the macaque monkey during reversible inactivation of area V1. J Neurophysiol 67:1437–1446.

Hackett TA (2011) Information flow in the auditory cortical network. Hear Res 271:133–146.

Hackett TA, Preuss TM, Kaas JH (2001) Architectonic Identification of the Core Region in Auditory Cortex of Macaques, Chimpanzees, and Humans. J Comp Neurol 441:197–222.

He J, Hashikawa T (1998) Connections of the dorsal zone of cat auditory cortex. J Comp Neurol 400:334–348.

He J, Hashikawa T, Ojima H, Kinouchi Y (1997) Temporal integration and duration tuning in the dorsal zone of cat auditory cortex. J Neurosci 17:2615–2625.

Izraeli R, Koay G, Lamish M, Heicklen-Klein AJ, Heffner HE, Heffner RS, Wollberg Z (2002) Cross-modal neuroplasticity in neonatally enucleated hamsters: structure, electrophysiology and behaviour. Eur J Neurosci 15:693-712.

Kaas JH, Hackett TA (2000) Subdivisions of auditory cortex and processing streams in primates. PNAS 97:11793-11799.

Kajikawa Y, de La Mothe LA, Blumell S, Hackett TA (2005) A comparison of neuron response properties in areas A1 and CM of the marmoset monkey auditory cortex: tones and broadband noise. J Neurophysiol 93:22–34.

Karlen S J, Kahn D M, Krubitzer L (2006) Early blindness results in abnormal corticocortical and thalamocortical connections. Neurosci 142:843-858.

Kayser C, Petkov CI, Augath M, Logothetis NK (2007) Functional imaging reveals visual modulation of specific fields in auditory cortex. J Neurosci 27:1824-1835.

Kayser C, Petkov CI, Logothetis NK (2008) Visual modulation of neurons in auditory cortex. Cereb Cortex 18:1560–1574.

Kok MA, Chabot N, Lomber SG (2014) Cross-modal reorganization of cortical afferents to dorsal auditory cortex following early- and late-onset deafness. J Comp Neurol 522:654–675.

Korte M, Rauschecker JP (1993) Auditory spatial tuning of cortical neurons is sharpened in cats with early blindness. J Neurophysiol 70:1717-1721.

Kosaki H, Hashikawa T, He J, Jones EG (1997) Tonotopic organization of auditory cortical fields delineated by parvalbumin immunoreactivity in macaque monkeys. J Comp Neurol 386:304–316.

Kusmierek P, Rauschecker JP (2014) Selectivity for space and time in early areas of the auditory dorsal stream in the rhesus monkey. J Neurophysiol 111:1671–1685.

Lakatos P, Chen C-M, O'Connell MN, Mills A, Schroeder CE (2007) Neuronal oscillations and multisensory interaction in primary auditory cortex. Neuron 53:279–292.

Lee CC, Winer JA (2008a) Connections of cat auditory cortex: III. Corticocortical system. J Comp Neurol 507:1920–1943.

Lee CC, Winer JA (2008b) Connections of cat auditory cortex: I. Thalamocortical system. J Comp Neurol 507:1879–1900.

Lee CC, Winer JA (2011) Convergence of thalamic and cortical pathways in cat auditory cortex. Hear Res 274:85–94.

Lomber SG, Malhotra S (2008) Double dissociation of "what" and "where" processing in auditory cortex. Nat Neurosci 11:609–616.

Lomber SG, Meredith MA, Kral A (2010) Cross-modal plasticity in specific auditory cortices underlies visual compensations in the deaf. Nat Neurosci 13:1421–1427.

Malhotra S, Lomber SG (2007) Sound localization during homotopic and heterotopic bilateral cooling deactivation of primary and nonprimary auditory cortical areas in the cat. J Neurophysiol 97:26–43.

Malhotra S, Stecker GC, Middlebrooks JC, Lomber SG (2008) Sound localization deficits during reversible deactivation of primary auditory cortex and/or the dorsal zone. J Neurophysiol 99:1628–1642.

Meredith MA, Kryklywy J, McMillan AJ, Malhotra S, Lum-Tai R, Lomber SG (2011) Crossmodal reorganization in the early deaf switches sensory, but not behavioral roles of auditory cortex. Proc Natl Acad Sci 108:8856–8861.

Meredith MA, Lomber SG (2011) Somatosensory and visual crossmodal plasticity in the anterior auditory field of early-deaf cats. Hear Res 280:38–47.

Merzenich MM, Brugge JF (1973) Representation of the cochlear partition on the superior temporal plane of the macaque monkey. Brain Res 50:275–296.

Mishkin M, Ungerleider LG, Macko KA (1983) Object vision and spatial vision: Two cortical pathways. Trends Neurosci 6:414–417.

Molinari M, Dell'Anna ME, Rausell E, Leggio MG, Hashikawa T, Jones EG (1995) Auditory thalamocortical pathways defined in monkeys by calcium-binding protein immunoreactivity. J Comp Neurol 362:171-194.

Moore T, Rodman HR, Gross CG (2001) Direction of motion discrimination after early lesions of striate cortex (V1) of the macaque monkey. PNAS 98:325-330.

Morel A, Garraghty PE, Kaas JH (1993) Tonotopic organization, architectonic fields, and connections of auditory cortex in macaque monkeys. J Comp Neurol 335:437–459.

Payne BR (1993) Evidence for visual cortical area homologs in cat and macaque monkey. Cereb Cortex 3:1–25.

Rauschecker JP (1998) Parallel processing in the auditory cortex of primates. Audiol Neurootol 3:86–103.

Rauschecker JP, Kniepert U (1994) Auditory localization behaviour in visually deprived cats. Eur J Neurosci 6:149-160.

Rauschecker JP, Korte M (1993) Auditory compensation for early blindness in cat cerebral cortex. J Neuroscience 13:4538-4548.

Rauschecker JP, Tian B (2000) Mechanisms and streams for processing of “what” and “where” in auditory cortex. Proc Natl Acad Sci U S A 97:11800–11806.

Rauschecker JP, Tian B, Hauser M (1995) Processing of Complex Sounds in the Macaque Nonprimary Auditory Cortex. Science (80-) 268:111–114.

Rauschecker JP, Tian B, Pons T, Mishkin M (1997) Serial and parallel processing in rhesus monkey auditory cortex. J Comp Neurol 382:89–103.

Read HL, Winer JA, Schreiner CE (2001) Modular organization of intrinsic connections associated with spectral tuning in cat auditory cortex. Proc Natl Acad Sci U S A 98:8042–8047.

Recanzone GH (2000a) Spatial processing in the auditory cortex of the macaque monkey. Proc Natl Acad Sci 97:11829–11835.

Recanzone GH (2000b) Response profiles of auditory cortical neurons to tones and noise in behaving macaque monkeys. Hear Res 150:104–118.

Romanski LM, Tian B, Fritz J, Mishkin M, Goldman-Rakic PS, Rauschecker JP (1999) Dual streams of auditory afferents target multiple domains in the primate prefrontal cortex. Nat Neurosci, 2:1131-1136.

Sadato N, Pascual-Leone A, Grafman J, Ibañez V, Deiber MP, Dold G, Hallett M (1996) Activation of the primary visual cortex by Braille reading in blind subjects. Nature 380:526-528.

Schroeder CE, Foxe JJ (2002) The timing and laminar profile of converging inputs to multisensory areas of the macaque neocortex. Cogn Brain Res 14:187-198.

Stecker GC, Harrington IA, Macpherson EA, Middlebrooks JC (2005) Spatial sensitivity in the dorsal zone (area DZ) of cat auditory cortex. J Neurophysiol 94:1267–1280.

Stecker GC, Mickey BJ, Macpherson EA, Middlebrooks JC (2003) Spatial sensitivity in field PAF of cat auditory cortex. J Neurophysiol 89:2889–2903.

Woods TM, Lopez SE, Long JH, Rahman JE, Recanzone GH (2006) Effects of stimulus azimuth and intensity on the single-neuron activity in the auditory cortex of the alert macaque monkey. J Neurophysiol 96:3323–3337.

Appendix A

Western

AUP Number: 2009-016
PI Name: Lomber, Stephen
AUP Title: Plasticity In Auditory Cortex

Approval Date: 04/16/2013

Official Notice of Animal Use Subcommittee (AUS) Approval: Your new Animal Use Protocol (AUP) entitled "Plasticity In Auditory Cortex

" has been APPROVED by the Animal Use Subcommittee of the University Council on Animal Care. This approval, although valid for four years, and is subject to annual Protocol Renewal.2009-016::5

This AUP number must be indicated when ordering animals for this project.
Animals for other projects may not be ordered under this AUP number.
Purchases of animals other than through this system must be cleared through the ACVS office.
Health certificates will be required.

The holder of this Animal Use Protocol is responsible to ensure that all associated safety components (biosafety, radiation safety, general laboratory safety) comply with institutional safety standards and have received all necessary approvals. Please consult directly with your institutional safety officers.

Submitted by: Copeman, Laura
on behalf of the Animal Use Subcommittee
University Council on Animal Care

Curriculum Vitae

MELANIE A. KOK

EDUCATION

2007	B.A., Psychology, Biology minor University of Virginia, Charlottesville, Virginia, USA
2010	M.Sc., Neuroscience McMaster University, Hamilton, ON, CAN
2015	Ph.D., Neuroscience The University of Western Ontario, London, ON, CAN

RESEARCH EXPERIENCE

2006-2007	Research assistant, Neurolab University of Virginia, Charlottesville, VA, USA
2009-2010	Graduate student, Sensorimotor Neuroscience Lab McMaster University, Hamilton, ON, CAN
2010-present	Graduate student, Cerebral Systems Lab University of Western Ontario, London, ON, CAN

HONORS & AWARDS

2003-2007	Full athletic scholarship, University of Virginia
2006	Dean's List, University of Virginia
2006, 2007	Honor Roll, Atlantic Coast Conference
2009	McMaster University Graduate Research Scholarship
2010	Synapse Award Nominee, CIHR
2010-2012	Western University Graduate Research Scholarship
2012	Travel Award ($500), Association for Research in Otolaryngology
2013	Nominated for Graduate Student Teaching Award
2013-2014	Ontario Graduate Scholarship ($15,000)

TEACHING EXPERIENCE

2009	*Teaching Assistant* Life Science 2C03 (McMaster): Neural Communication
2010-2011	*Teaching Assistant* Psychology 1000 (UWO): Introduction to Psychology
2011-2013	*Teaching Assistant* Physiology 4710 (UWO): Physiology of the Senses
2013	*Teaching Assistant* Psychology 2220 (UWO): Intro to Behavioural and Cognitive Neuroscience

PUBLICATIONS

Accepted, in press, or published:

Carrasco A, Brown TA, **Kok MA**, Chabot N, Kral A, Lomber SG. (2013). Influence of core auditory cortical areas on acoustically-evoked activity in contralateral primary auditory cortex. *Journal of Neuroscience,* 33: 776-789. PMID: 23303954.

Kok MA, Chabot N, Lomber SG. (2014). Cross-modal reorganization of cortical afferents to dorsal auditory cortex following early- and late-onset deafness. *Journal of Comparative Neurology,* 522: 654-675. PMID: 23897533.

Wong C, Chabot, N., **Kok, MA**, Lomber SG. (2014). Modified areal cartography in auditory cortex following early- and late-onset deafness. *Cerebral Cortex,* 24: 1778-1792. PMID: 23413302.

Carrasco A, **Kok MA**, Lomber SG. (2015). Effects of core auditory cortex deactivation on neuronal response to simple and complex acoustic signals in the contralateral anterior auditory field. *Cerebral Cortex*, 25: 84-96. PMID: 23960202.

Kok MA, Stolzberg D, Brown TA, Lomber SG. (2015). Dissociable influences of primary auditory cortex and the posterior auditory field on neuronal responses in the dorsal zone of auditory cortex. *Journal of Neurophysiology,* 113(2): 475-486. PMID: 25339709

Wong C, Chabot N, **Kok MA**, Lomber SG. (accepted). Amplified somatosensory and visual cortical projections to a core auditory area, the anterior auditory field, following early- and late-onset deafness. *Journal of Comparative Neurology*.

INVITED PRESENTATIONS

"The consequences of the removal of auditory input on the dorsal zone of auditory cortex." Systems Neuroscience mini-symposium. Robarts Research Institute, London, Ontario, Canada. (Nov. 2014).

CONFERENCE PRESENTATIONS

International:

1. **Kok MA**, Chabot N, Lomber SG. Amplified extrastriate visual cortical projections to auditory cortical regions following deafness. *Association for Research in Otolaryngology Mid-winter Meeting*, San Diego, USA. February 2012.

2. **Kok MA**, Chabot N, Lomber SG. Visual cross-modal reorganization observed in auditory cortical regions following early and late-onset deafness. *4th International Conference on Auditory Cortex*, Lausanne, SUI. September 2012.

3. Chabot N, **Kok MA**, Lomber SG. Amplified somatosensory and visual cortical projections to the anterior auditory field of early- and late-deaf cats. *4th International Conference on Auditory Cortex*, Lausanne, SUI. September 2012.

4. Carrasco A, Brown T, **Kok MA**, Chabot N, Kral A, Lomber SG. Influence of core auditory cortical areas on acoustically-evoked activity in contralateral primary auditory cortex. *4th International Conference on Auditory Cortex*, Lausanne, SUI. September 2012.

5. **Kok MA**, Chabot N, Lomber SG. Visual cross-modal reorganization observed in auditory cortical regions following early and late-onset deafness. *International Multisensory Research Forum*, Jerusalem, ISR. June 2013.

6. Chabot N, **Kok MA**, Lomber SG. Amplified somatosensory and visual cortical projections underlie crossmodal plasticity in the anterior auditory field of the early-deaf*. Society for Neuroscience Annual Meeting,* San Diego, USA. Nov. 2013.

7. **Kok MA,** Stolzberg D, Brown TA, Lomber SG. (2014). Dissociable influences of the primary auditory cortex and the posterior auditory field on neuronal responses in the dorsal zone of auditory cortex. *5th International Conference on Auditory Cortex*, Magdeburg, GER. Sept. 2014.

8. Stolzberg D, Butler BE, **Kok MA,** Lomber SG. (2014). Cortical modulation of spike-time precision in the medial geniculate body of the thalamus during

reversible deactivation of primary auditory cortex in cats. *5th International Conference on Auditory Cortex*, Magdeburg, GER. Sept. 2014.

9. Carrasco A, **Kok MA,** Meredith MA, Lomber SG. (2014). Neuronal basis for visual and tactile processing in cat primary auditory cortex. *5th International Conference on Auditory Cortex*, Magdeburg, GER. Sept. 2014.

National:

1. Wong C, Chabot N, **Kok MA**, Lomber SG. Modified Areal Cartography In Auditory Cortex Following Early- And Late-Onset Deafness. *Canadian Association for Neuroscience Annual Meeting*, Vancouver, CAN. May 2012.
2. Carrasco A, **Kok MA**, Lomber SG. Effects of core auditory cortex deactivation on neuronal response to simple and complex acoustic signals in the contralateral anterior auditory field. *Canadian Association for Neuroscience Annual Meeting*, Toronto, CAN. June 2013.
3. Chabot N, **Kok MA**, Lomber SG. Amplified cortical, but not thalamic, somatosensory and visual projections to the anterior auditory field following early- or late-onset deafness. *Canadian Association for Neuroscience Annual Meeting*, Toronto, CAN. June 2013.
4. **Kok MA**, Brown TA, Carrasco A, Lomber SG. Influence of primary auditory cortex and the posterior auditory field on neuronal responses in the dorsal zone of cat auditory cortex. *Canadian Association for Neuroscience Annual Meeting*, Toronto, CAN. June 2013.
5. **Kok MA,** Stolzberg D, Brown TA, Lomber SG. Individual and combined influences of primary auditory cortex and the posterior auditory field on neuronal responses in the dorsal zone of auditory cortex. *Southern Ontario Neuroscience Association Annual Meeting*, London, CAN. May 2014.

ACTIVITIES & OUTREACH

2009	McMaster Science and Engineering Olympics volunteer and keynote speaker
2009-2010	Let's Talk Science Partnership Program volunteer
2010	Judge, Bay Area Science and Engineering Fair (BASEF) Judge
2010	Alzheimer's Society volunteer
2012-2013	Neuroscience representative, Schulich School of Medicine & Dentistry Graduate Students Council
2013-2014	Animal Care and Use Committee (ACUC) at UWO
2014	Adjudicator, University Science Case Competition, University of Western Ontario